

Biomechanical Analysis of Assisted Sit to Stand

by

Jeswin Jeyasurya

B.Eng., Memorial University, 2008

A THESIS SUBMITTED IN PARTIAL FULFILLMENT OF
THE REQUIREMENTS FOR THE DEGREE OF

MASTER OF APPLIED SCIENCE

in

THE FACULTY OF GRADUATE STUDIES

(Mechanical Engineering)

THE UNIVERSITY OF BRITISH COLUMBIA

(Vancouver)

April 2011

© Jeswin Jeyasurya, 2011

Abstract

A significant number of non-institutionalized older adults have difficulty rising from a chair. Although there exist several assistive devices to aid with sit to stand, there is a lack of research that compares and analyzes various modes of assisted sit to stand to characterize their relative effectiveness in terms of biomechanical metrics. In addition, few existing assistive devices have been designed specifically to share between the user and the device the force required to rise, an approach that has the benefit of maintaining both the mobility and muscular strength of the user.

This thesis advances our understanding of different modes of load-sharing sit to stand through empirical quantification. A specially-designed sit-to-stand test bed with load sharing capabilities was fabricated for human-subjects experiments. In addition to an unassisted rise and a static assist using a grab bar, three mechatronic modes of assist, at the seat, waist and arms, were implemented. The test bed employs a closed-loop load-sharing control scheme to require a user to provide a portion of the effort needed for a successful rise motion.

Experiments were performed with 17 healthy older adults using the five aforementioned modes of rise. Force and kinematic sensor measurements obtained during the rise were used as inputs into a biomechanical model of each subject, and each mode of rise was evaluated based on key biomechanical metrics extracted from this model relating to stability, knee effort reduction, and rise trajectory. In addition, a questionnaire was administered to determine subjective response to and preference for each rise type.

Results show that the seat and waist assists provide statistically significant improvements in terms of stability and knee effort reduction, while the arm and bar assists do not provide any biomechanical improvement from the unassisted rise. The assists most preferred by the subject were the seat and bar assists. Because of subject preference and biomechanical improvements, of the modes tested, the seat assist was determined to be the best mode of providing assistance with sit to stand.

Preface

This thesis is submitted in partial fulfillment of the requirements for a Masters of Applied Science in Mechanical Engineering at the University of British Columbia. It contains work done from September 2008 to April 2011, in the Collaborative Advanced Robotics and Intelligent Systems Laboratory.

The initial test bed design presented in Section 5.4 of Chapter 5 is based on work completed by a team of undergraduate students (Tony Chen, Dan Cho, Jason Chu, Marco Mak, Steven Quan, and Raymond So) for a senior design project with the author in the role of client representing the sponsor, the CARIS Lab. The author completed the final test bed design through several additions and modifications to the work completed by the student team. The research contributions of the student team are described in Section 5.4 and the written contributions of the students are reported in Appendix A and Appendix B. Design calculations completed by the student team are reported in their entirety in Appendix A and an excerpt from the undergraduate team project report is provided in Appendix B.

The work presented in Chapter 5 has been accepted for publication. J.Jeyasurya, T.Lai, O. Patil, E. Pospisil, E. Croft, A. Hodgson, M. Van der Loos (2010) Design of a Load Sharing Sit-to-Stand Assistive Test Bed. To appear in the 3rd International Conference on Technology and Aging (ICTA). Toronto, Canada. June 5-8, 2011.

The experiment described in Chapter 6 has been approved by the University of British Columbia Research Ethics Board (UBC Clinical Research Ethics Board number H10-00563).

Table of Contents

Abstract	ii
Preface.....	iii
Table of Contents	iv
List of Tables	xi
List of Figures.....	xii
Nomenclature.....	xvi
Acknowledgements	xix
Chapter 1 Introduction	1
1.1 The case for assistive robotics.....	1
1.2 Case for sit-to-stand (STS) assistance	2
1.3 Scope and objective.....	3
1.4 Outline of thesis	4
Chapter 2 Related Work	6
2.1 Introduction.....	6
2.2 STS characterization.....	6
2.3 Subject-related contributing factors to STS failure and corresponding assistive device evaluation criteria.....	8
2.4 The case for load sharing	9
2.5 Commercial devices	10
2.6 Research and development devices	13
2.7 Rationale for proposed test bed.....	15
Chapter 3 Validation Experiment	16
3.1 Experiment introduction	16
3.2 Experimental procedure.....	16
3.2.1 Subjects	16
3.2.2 Setup and procedure.....	16
3.2.3 Data collection.....	18
3.2.4 Data analysis.....	19
3.3 Results	21

3.3.1 Force-plate data	21
3.3.2 Joint kinematics	21
3.3.3 Joint dynamics	22
3.3.4 Torque variability	23
3.3.5 Discussion	25
3.3.6 Conclusion.....	27
Chapter 4 Simulation Study.....	29
4.1 Simulation introduction	29
4.2 Simulation model	29
4.3 Control of model	30
4.3.1 Feedforward component.....	31
4.3.2 Feedback component	31
4.3.3 Simulation model with weakness	32
4.3.4 Control of weakened model.....	33
4.3.5 Weakness component.....	33
4.3.6 Assist component.....	33
4.4 Simulation experiments and cost function	34
4.4.1 Simulation validation experiment.....	34
4.4.2 STS assist modes experiment	34
4.4.3 Stability cost	34
4.4.4 Assistance cost.....	35
4.4.5 Joint torque cost.....	36
4.4.6 Total cost.....	37
4.5 Results	37
4.6 Discussion.....	40
4.6.1 Simulation results	40
4.6.2 Expert opinion	40
4.6.2.1 Buttocks and waist assist	40
4.6.2.2 Arm assist	41
4.7 Conclusion	41
Chapter 5 Test Bed Design.....	43
5.1 Introduction.....	43

5.2 Test bed functional design requirements	44
5.3 Critical function prototype experiment.....	45
5.3.1 Introduction	45
5.3.2 Experimental procedure	46
5.3.2.1 Test subjects.....	46
5.3.2.2 Test equipment.....	46
5.3.2.3 Experimental setup and STS modes	48
5.3.2.4 Set-up and procedure.....	49
5.3.2.5 Data collection and post processing	51
5.3.2.6 Data analysis.....	52
5.3.2.6.1 Waist and seat force data averaging	52
5.3.2.6.2 Waist and seat force data scaling	53
5.3.2.6.3 Elbow trajectory calculation	53
5.3.3 Results.....	53
5.3.3.1 Assist force results	53
5.3.3.2 Assist trajectory results.....	54
5.3.4 Discussion and outcomes	55
5.4 Initial test bed design.....	56
5.4.1 Test bed frame	56
5.4.2 Seat assist mechanism.....	57
5.4.3 Waist assist mechanism.....	58
5.4.4 Arm assist mechanism	59
5.4.4.1 Four-bar linkage.....	60
5.4.4.2 Four-bar linkage adjustability.....	61
5.4.4.3 Arm cradles.....	62
5.5 Test bed final design.....	63
5.5.1 Test bed actuation system.....	63
5.5.2 Test bed modified arm cradle	65
5.5.3 Modified arm guidance mechanism trajectory	66
5.5.4 Test bed entry	67
5.5.5 Test bed force measurement.....	68
5.6 Test bed control overview.....	69

5.6.1 PXI Test Bed Control Program and Windows Data Collection Program	70
5.6.1.1 PXI Test Bed Control Program.....	70
5.6.1.2 Windows Data Collection Program.....	71
5.6.2 Motion controller	71
5.6.3 Amplifier and motor	73
5.6.4 Switches and encoder.....	73
5.6.4.1 Limit switches.....	73
5.6.4.2 Emergency stop switch.....	74
5.6.4.3 Deadman and reset switches.....	75
5.6.4.4 Encoder.....	76
5.6.4.5 Assist mechanism and sensor measurements.....	76
5.6.5 Torque regulation control scheme	77
5.6.5.1 Knee torque monitor.....	77
5.6.5.2 Velocity limiter	78
5.6.5.3 Initial non-load-sharing assistance phase	79
5.7 Data synchronization	80
5.7.1 Data collection overview.....	80
5.7.2 Synchronization problem and experiment.....	81
5.7.3 Synchronization results and analysis	81
5.8 FMEA based on safety review	84
5.9 Test bed functional design requirements validation	84
5.9.1 Pilot test results.....	84
5.9.2 Validation of design requirements.....	85
Chapter 6 Test Bed Experiment	87
6.1 Introduction.....	87
6.2 Experiment procedure.....	87
6.2.1 Subjects	87
6.2.2 Experimental design.....	89
6.2.2.1 Test bed assists.....	89
6.2.2.2 Test bed data collection.....	90
6.2.2.3 Key biomechanical metrics.....	90
6.2.2.4 Experiments	92

6.2.3 Protocol	92
6.2.3.1 Data collection procedure	96
6.2.4 Data analysis.....	97
6.2.4.1 Model	97
6.2.4.2 Extended model	100
6.2.4.3 Treatment of data	100
6.2.4.4 Data anomalies.....	102
6.3 Results	102
6.3.1 Static stability	103
6.3.2 Dynamic stability results.....	105
6.3.3 Knee extensor effort results.....	107
6.3.4 Momentum transfer strategy adherence results	110
6.3.5 Questionnaire results.....	112
6.3.5.1 Pre-experiment questionnaire results	112
6.3.5.2 Post-experiment questionnaire results.....	112
6.4 Discussion	113
6.4.1 Static stability discussion	113
6.4.2 Dynamic stability discussion.....	113
6.4.3 Knee extensor effort discussion.....	114
6.4.4 Momentum transfer strategy adherence discussion	114
6.4.5 Hypothesis discussion	115
6.4.6 Post-experiment questionnaire discussion.....	115
6.5 Summary.....	116
Chapter 7 Conclusions and Recommendations.....	117
7.1 Conclusions.....	117
7.2 Recommendations	120
7.2.1 Test bed design recommendations.....	120
7.2.1.1 Load sharing	120
7.2.1.2 Arm guidance mechanism	121
7.2.2 Recommendations for further research	121
7.2.2.1 Experiments with older adults who have STS difficulties.....	121
7.2.2.2 Commercial STS assistive device	121

7.2.2.3 Rehabilitation applications	122
Bibliography	124
Appendix A : Appendix from Student Report – Design Calculations	130
Appendix B : Student Report Excerpt – Arm Linkage Adjustability and Buttocks (Seat) and Waist Assist Descriptions.....	143
Buttocks and Waist Assist Mechanism	148
Moment Transfer Lever-Arm.....	148
Motor and Transmission	150
Range of Adjustment.....	151
Appendix C : Test Bed Operation Manual	152
Overview	154
Windows Program.....	154
PXI Program	155
Test Bed Operation	156
Data Entry.....	156
Calibration Trials	157
Assistance Trials	158
Detailed Description of PXI GUI.....	160
Run “Off” State	160
Run “On” State.....	161
Real Time Load Sharing/Speed Settings	162
Test Bed Configuration	163
Test Bed Entry	163
Setting up For Arm Assist	164
Setting up For Buttocks Assist.....	168
Setting up For Waist Assist	170
Switches.....	171
Checklists:	173
Appendix D : Failure Modes and Effects Analysis	174
Appendix E : Test Bed Safety Checklist	181
Appendix F : Pre-experiment Questionnaire	182
Appendix G : Post-Experiment Questionnaire	183

Appendix H : Experiment Script.....	185
Safety Protocol Instructions:.....	185
Experiment Instructions:.....	185
Appendix I : Experiment Checklist.....	187
Appendix J : Static Stability Results and ANOVA.....	193
Appendix K : Dynamic Stability Results and ANOVA	195
Appendix L : STS Knee Extensor Effort Results and ANOVA	197
Appendix M : STS Torque Ratio Results and Paired T-Tests	199
Appendix N : Momentum Transfer Results and ANOVA	201
Appendix O : Pre-Experiment Questionnaire Results.....	203
Appendix P : Post-Experiment Questionnaire Results and Statistical Tests	204
Appendix Q : Post-Experiment Questionnaire Comments	209
Appendix R : Single Subject (Subject 4) Multiple Trial Data Plots.....	211
Appendix S : Multiple Subjects (16 Subjects) Single Trial Data Plots	216

List of Tables

Table 3.1: Average peak joint torques for three subjects.	24
Table 3.2: Comparison of normalized peak joint torques between inverse dynamics analysis and literature values.	26
Table 4.1: Root Mean Squared Error of Body Segment Angle Trajectory.....	38
Table 4.2: Root Mean Squared Error of Joint Torque Trajectory.	39
Table 5.1: STS trials and modes.	50
Table 5.2: Measured anthropometric data.	51
Table 5.3: Measured orientation sensor and force plate data.....	52
Table 5.4: Measured maximum assist forces for each of the waist-assisted and seat-assisted trials...	53
Table 5.5: Maximum assist forces required for seat-assisted STS.....	54
Table 5.6: Maximum assist forces required for waist-assisted STS.....	54
Table 5.7: Average peak trunk flexion during each mode of STS trial in the critical function prototype experiment (standard deviation).	67
Table 5.8: Description of load measuring devices in test bed.....	68
Table 5.9: Force delay characterization.....	83
Table 5.10: Trunk flexion and knee torque results from pilot tests with six subjects.	84
Table 6.1: Summary of data from 17 healthy older adult subjects.....	88
Table 6.2: Post-experiment questionnaire.	91
Table 6.3: Summary of results from key biomechanical metrics and post-experiment questionnaire from all subjects for the five modes of STS (standard deviation)..	103
Table A.1: Linkage adjustment range corresponding to the trajectory graphs.	132
Table B.1: Maximum and minimum linkage lengths.....	144
Table B.2: Adjustment range for waist and buttocks component – final.	151

List of Figures

Figure 2.1: The four phases of STS motion [24].	6
Figure 2.2: The three strategies of STS motion [25].	7
Figure 2.3: From left to right: wall grab bars, ceiling pole grab bar, bedrail [35].	11
Figure 2.4: From left to right: lift cushion, lift chair, powered stand assist device [35].	11
Figure 2.5: Left image: intelligent walking aid with STS assistance [16]. Right image: bed and bar system [20].	14
Figure 3.1: Experiment setup.	17
Figure 3.2: The 4-link rigid biomechanical model and a representative body segment used in the inverse dynamics model.	19
Figure 3.3: Foot center of pressure location.	20
Figure 3.4: Vertical reaction forces from chair force plate and foot force plate during a representative STS trial.	21
Figure 3.5: Body segment rotation angles during a representative STS trial from a single subject.	22
Figure 3.6: Normalized joint torques during a representative STS trial.	23
Figure 3.7: Joint torques during four STS trials of a single subject.	24
Figure 3.8: Normalized joint torques during representative STS trials for each subject.	25
Figure 4.1: Simulation model.	30
Figure 4.2: Control system of joints.	30
Figure 4.3: Locations of applied assistance on weakened model.	32
Figure 4.4: Control system of joints for weakened model.	33
Figure 4.5: Diagram of foot with reaction force locations.	35
Figure 4.6: Cost functions for stability, assistance, and torque evaluation.	36
Figure 4.7: Comparison of body segment angles between simulation and reference trajectories for an unassisted STS trial.	37
Figure 4.8: Comparison of joint torque trajectories between simulation and reference trajectories for an unassisted STS trial.	38
Figure 4.9: Cost function results for three modes of STS assisted transfer.	40
Figure 5.1: Schematic of the test bed design process.	43
Figure 5.2: Locations at which test bed must provide assistance.	45

Figure 5.3: Left image: force transmitting cradle. Right Image: test frame with force transmitting cradle attached and configured for seat assist.	46
Figure 5.4: Left image: Orientation sensor locations on subject. Sensors attached to shank, thigh and trunk (thigh and trunk sensors not visible). Right Image: Orientation sensor on force transmitting cradle.	47
Figure 5.5: Four modes of STS.....	49
Figure 5.6: Trajectory of the elbow as the subject rises to a standing position for each assisted motion.....	55
Figure 5.7: Initial sit-to-stand test bed design [60].	56
Figure 5.8: Side view of original test bed solution [60].	57
Figure 5.9: Diagram of seat assist mechanism [60].	58
Figure 5.10: Diagram of waist assist mechanism [60].	59
Figure 5.11: Diagram of arm assist mechanism [60].	60
Figure 5.12: Trajectory of 4-bar linkage mechanism.....	61
Figure 5.13: Length adjustable linkages and locking pins.....	62
Figure 5.14: Adjustability of the mounting position of the linkage ends.	62
Figure 5.15: Arm cradle right and left side assemblies [60].....	63
Figure 5.16: Test bed diagram showing actuation methods.....	64
Figure 5.17: Rear view of test bed showing motor assembly and jack shaft system for arm assistance.	65
Figure 5.18: Modified arm cradle.	66
Figure 5.19: Test bed arm linkage lengths.....	67
Figure 5.20: Test bed entry.....	68
Figure 5.21: Load cell configuration.	69
Figure 5.22: General diagram of test bed control scheme.	70
Figure 5.23: NI UMI-7764 motion interface.	72
Figure 5.24: Motor position control diagram.....	73
Figure 5.25: Electrical schematic showing e-stop, limit switch and motion switch wiring.....	74
Figure 5.26: Control box.	75
Figure 5.27: From left to right: Seat/waist deadman switch, arm cradle deadman switch, reset switch.	76
Figure 5.28: Augmented motor control system.	77

Figure 5.29: Data collection diagram.....	80
Figure 5.30: Synchronization experiment.....	81
Figure 5.31: Graph showing five lever arm drops onto load cell (drop number indicated on top of graph).....	82
Figure 6.1: Sit-to-stand test bed.....	89
Figure 6.2: Experiment setup.....	93
Figure 6.3: Still frame animation of three modes of STS.....	95
Figure 6.4: Still frame animation of two modes of STS.....	96
Figure 6.5: The 4-link rigid biomechanical model and a representative body segment used in the inverse dynamics model.....	98
Figure 6.6: Average distance of the horizontal projection of the total CoM from the ankle at seat-off.	104
Figure 6.7: Trajectory of the horizontal projection of the total body CoM of a representative subject for five modes of STS.....	105
Figure 6.8: Average displacement of the foot CoP from the foot center at seat-off.	106
Figure 6.9: Trajectory of the foot CoP of a representative subject for five modes of STS.....	107
Figure 6.10: Average peak knee torque for each of the five modes of STS.	108
Figure 6.11: Knee torque trajectories of a representative subject for five modes of STS.	109
Figure 6.12: Ratio of average peak knee torque of each of the assisted rises to the average peak torque of the unassisted rise.	110
Figure 6.13: Average peak trunk flexion for each of the five modes of STS.	111
Figure 6.14: Trunk angle trajectories of a representative subject for five modes of STS.	111
Figure 6.15: Average scores for each assist in the post-experiment questionnaire.....	112
Figure A.1: Subject elbow position trajectories – minimum height.....	130
Figure A.2: Subject elbow position trajectories – medium height.....	131
Figure A.3: Subject elbow position trajectories – maximum height.....	131
Figure A.4: 4-bar linkage mechanism and linkage naming references.	132
Figure A.5: 4-bar linkage force application.....	137
Figure A.6: Linkage free body diagrams.....	138
Figure A.7: Waist assist free body diagram.....	140
Figure A.8: Buttocks assist free body diagram.....	141
Figure B.1: Mechanical model of the 4-bar linkage system.....	143

Figure B.2: Linkage layout and reference names.....	143
Figure B.3: Reference trajectories vs. achieved 4-bar linkage trajectories.....	145
Figure B.4: Achieved trajectory for arm guidance.....	145
Figure B.5: Achieved trajectory for waist assist.	146
Figure B.6: Achieved trajectory for buttocks guidance.....	146
Figure B.7: Achieved trajectory for general sit-to-stand motion.	147
Figure B.8: Revised implementation for buttocks assist.	148
Figure B.9: Revised implementation for waist assist.	149
Figure B.10: Winch cable and lever arm.	150
Figure B.11: Transmission - motor and winch setup.	151
Figure C.1: Windows program.	154
Figure C.2: PXI program.	155
Figure C.3: Data entry.	156
Figure C.4: Calibration trials.	158
Figure C.5: Assistance trial Windows setting.	159
Figure C.6: Assistance trial PXI setting.	159
Figure C.7: PXI GUI details.	161
Figure C.8: Left image: End linkage connected. Right image: End linkage retracted.	163
Figure C.9: Rear view of test bed showing labeled arm assist mechanism components.....	164
Figure C.10: Left image: Rear view of test bed showing disconnected waist and buttocks assist sling hooks. Center image: Front view of test bed showing locked waist assist. Right image: Close-up of waist assist locking cable.	164
Figure C.11: Left image: Side view of test bed. Right image: Top view close-up of end linkage connection point.	165
Figure C.12: Left image: rear view of test bed. Right image: Close-up of right side of motor mounting plate with connection bolt highlighted.	165
Figure C.13: Left image: Side view of test bed showing motor and jack shaft sprockets and loosened drive chain. Right image: Side view of test bed showing motor and jack shaft sprockets and tightened drive chain.....	166
Figure C.14: Left image: Close-up of arm cradle attachment point. Right image: Rear view of test bed showing attached arm cradles.	166

Figure C.15: Left image: Right arm cradle in rest position. Center image: Close-up of right arm cradle handle highlighting the adjustable thumbscrew. Right image: Close-up of right arm cradle highlighting deadman switch connection point..... 167

Figure C.16: Subject seated in test bed ready for arm assisted rise. 167

Figure C.17: Left image: Arm assist deadman switch. Center image: Buttocks/waist assist deadman switch. Right image: Rear view of test bed with arm cradles removed. 168

Figure C.18: Left image: Rear view of test bed showing disconnected waist assist sling hook and disconnected drive chain. Right image: Front view of test bed showing locked waist assist. 168

Figure C.19: Left image: Rear view of test bed highlighting buttocks assist cable attachment point. Center image: Close up of buttocks assist cable sling hook attachment point. Right image: Top view of test bed showing seat adjustability..... 169

Figure C.20: Subject seated in test bed ready for buttocks assisted rise. 169

Figure C.21: Left image: Rear view of test bed highlighting waist assist cable attachment point. Center image: Close up of waist assist cable sling hook attachment point. Right image: Front view of test bed showing locked waist assist. 170

Figure C.22: Left image: Side view of test bed showing lowered waist assist lever arm. Center image: Image of subject attaching waist assist belt. Right image: image of subject tightening waist assist strap..... 170

Figure C.23: Subject seated in test bed ready for waist assisted rise. 171

Figure C.24: Test bed control box..... 171

Figure C.25: Left image: Side view of test bed showing arm assist limit switches. Center image: Front view of test bed seat showing buttocks assist limit switches. Right image: Front view of test bed waist assist lever arm showing waist assist limit switches. In all images the limit switch locations are identified by the red circles..... 172

Figure C.26: Left image: Buttocks/waist deadman switch. Center image: Arm cradle deadman switch. The deadman switches are used to move the assists forward. Right image: Reset switch. The reset switch is used to move the assists backwards and is located on the right hand side of the test bed..... 172

Nomenclature

Assist End: the point in time at which the subject loses contact with either the seat or waist assist mechanism

Biomechanical Metric: One of five measures based on the kinematics or dynamics of the sit-to-stand motion used to evaluate the effectiveness of sit-to-stand assists.

CoM: Center of Mass

CoP: Center of Pressure

DVR: Dominant Vertical Rise. This STS strategy is characterized by a lowering of upper body anterior momentum at liftoff along with a cessation of forward trunk flexion, followed by knee extension and dominantly vertical momentum.

ETF: Exaggerated Trunk Flexion. This STS strategy is characterized by deep trunk flexion prior to seat-off that places the center of mass over the feet and results in a delay of trunk extension during the transition to an erect position.

Load Sharing: The concept of sharing the knee extensor effort required for sit-to-stand between the user and the assist when rising with assistance.

Movement End: The time at which the motion of the user ends (the time at which thigh extension angular velocity reduces below 0.1 rad/s).

Movement Start: The time at which the subject initiates trunk flexion (the time at which trunk angular velocity exceeds 0.1 rad/s).

MT: Momentum Transfer. This STS strategy is characterized by a smooth transition of upper body anterior momentum at liftoff to total body vertical momentum with continued anterior momentum,

RMSE: Root Mean Squared Error

Sagittal Plane: a vertical plane passing from front to rear that divides the body into right and left sections.

Seat-off: The point in time in the sit-to-stand motion at which the user loses contact with the chair.

Sit to Stand Trial: A single sit-to-stand motion

Sit to Stand: The process of rising from a seated to a standing position.

STS Mode: the particular method of chair rise, either unassisted, bar-assisted arm-assisted, seat-assisted or waist-assisted

STS: Sit to Stand

Acknowledgements

I would like to thank my supervisors, Dr. Elizabeth Croft, Dr. Machiel Van der Loos, and Dr. Antony Hodgson for their motivation, encouragement, and valuable guidance. I would like to extend my gratitude to the many fellow graduate and undergraduates students who have provided invaluable assistance along the way.

Thanks also to Dr. Jean-Sébastien Blouin, Dr. David Sanderson, and Dr. Peter Cripton, for generously lending me their equipment to use for my experiments.

I am grateful to Joey Lijauco and the other physiotherapists and clinicians who helped with my background research, and to all the people who volunteered as subjects for my experiments.

I would also like to acknowledge the financial support of the Natural Sciences and Engineering Research Council of Canada.

Finally, I would like to specially thank my parents for their support throughout my education and for teaching me to always strive for excellence.

Chapter 1 Introduction

1.1 The case for assistive robotics

Advancements in health related infrastructure, safety technology, health awareness and medical technologies among other factors over the past century have enabled North Americans to live longer lives. As a result, Canada has an aging population with projections indicating that by 2026 one in five Canadians will be 65 or older, an increase from one in eight in 2001 [1]. The 2009 Statistics Canada Year Book has indicated that aging Canadians require assistance in activities of daily living¹ (ADLs) and that a significant portion of this assistance is currently being provided by people over the age of 45 [2]. Over the next twenty years, these aging caregivers will make up a proportionally much larger group of seniors, and this will result in a lack of people able to provide care for older persons [3].

In addition to Canadian statistical surveys, the AARP (American Association of Retired Persons) completed a national survey on independent living and disability in 2003 [4]. Their principal finding was that persons 50 years and older with disabilities strongly prefer to live independently in their own homes over other alternatives. It was also noted that many persons with disabilities have unmet needs requiring long term support services and assistive equipment in their homes. With the increasing number of elderly people, and the shortage of health care dollars and workers to provide needed support, alternate means must be examined in order to provide the necessary care for elderly people.

There is an ongoing worldwide interest in creating technologies that can assist people with ADLs, enabling them to: maintain their independence at home, reduce their dependence on caregivers, function independently, and increase their quality of life, while reducing the financial burden associated with in-home personal care. The use of assistive devices has numerous general benefits. Studies have shown that persons using assistive devices have greater self-reliance and are less likely to depend on externally provided personal care [5] [6]. It has also been determined that providing equipment assistance is a more efficacious strategy for reducing and resolving limitations in comparison to personal assistance [7].

¹ Basic ADLs consist of self-care tasks, including: personal hygiene and grooming, dressing and undressing, feeding oneself, functional transfers, elimination, ambulation [68].

1.2 Case for sit-to-stand (STS) assistance

Identifying unmet needs for personal assistance with activities of daily living among community-dwelling non-institutionalized persons aged 70 years and older was the focus of a study [8] that examined data from the 1994 National Health Interview Survey's Supplement on Aging. The results showed that 20.7 % of those needing help to perform one or more activities of daily living (an estimated 629,000 persons) reported inadequate assistance. For specific activities of daily living, the prevalence of unmet need ranged from 10.2% for eating to 20.1% for transferring from a bed or chair, thus inferring that transferring is the activity of daily living with proportionally the greatest unmet need.

Difficulty in transferring, namely rising from a chair, is common among elderly people, affecting more than 6% of community dwelling older adults [9] and over 60% of nursing home residents [10]. Rising from a chair is thought to be the most biomechanically challenging functional task because of the high hip contact pressure and large knee torques produced during the chair rise motion [11]. Consequently, ailments that commonly affect older adults such as pain, reduced joint range of motion, stiffness, arthritis, and muscle weakness often limit the ability to rise to a standing position [12]. An inability to rise, especially quickly, has been linked to an increased risk of falling [13] and hip fracture [14]. Falls can result in hospitalization or institutionalization, causing people to lose the independent lifestyle they previously maintained.

Rising from a chair is one of the most important requirements of maintaining an independent lifestyle [15]. Accordingly, research into assisting people with sit to stand (STS) will have a high impact in enabling seniors to maintain their independence, and will help alleviate a problem that affects this significant and growing segment of the population.

Presently there are a number of assistive devices for independent STS both available commercially and in research and development. Commercial devices include passive supports such as grab bars and standing frames that provide stability as users rise, and active supports such as lift cushions, lift chairs, and powered standing devices that provide all of the force necessary to rise to a standing position. In the research and development phase, design configurations include STS aids that combine walker systems with powered standing aids [16] [17] [18], an assistance system consisting of a powered handrail [19] and a force assist system consisting of a moveable bed system and support bar [20].

Although there are a variety of research and commercial devices available for STS, there are few that have been designed specifically to share the load of standing between the user and the device. Passive assist devices such as grab bars and standing frames require upper body strength from users, which may be difficult for frail elders [21]. Commercially-available active assist devices such as lift cushions reduce the knee strength required by the user to rise [22] and thus may risk promotion of a decrease in user strength and mobility over time. Maintaining mobility by physical exercise is important among mobility-impaired people as it has the potential to prevent further disability and mortality [23]. Thus, a device that engages the user's available strength in the STS motion by sharing the load required to rise has the benefit of maintaining both the mobility and muscular strength of the user.

The design of a new generation of STS assistive devices with load sharing capabilities requires significant analytical and experimental work to determine the best method of assisting persons to a standing position. Unfortunately, there is a lack of research that analyzes and compares various modes of assistance in existing STS devices in order to characterize their effectiveness. The benefit of such a comparative analysis is that it would permit better understanding of the biomechanics of assisted STS and empirically characterize the optimal mode of assisting a person to a standing position. This information would help drive the design of new STS assistive devices, specifically those that share the load required for standing.

1.3 Scope and objective

In view of the concerns and needs raised in Section 1.2, the overall objective of this dissertation is to provide an empirical quantification of different modes of load-sharing STS to determine the best mode. The hypothesis to drive this objective is that there is a single mode of load-sharing STS assistance that is better than all other modes in terms of the biomechanics of the motion and user preference. To determine if this hypothesis is true, this thesis proposes the development of a STS test bed with load sharing capabilities that characterizes the biomechanics of different modes of STS assistance. Human subject experiments with the test bed can provide both a biomechanical and qualitative analysis of the STS process for healthy older subjects and can be used to determine the best mode of STS assistance.

To develop the test bed and identify of the best mode of STS assistance, the following sub-objectives were proposed:

1. Based on a review of the difficulties that older adults currently face when rising from a chair, establish evaluation criteria to address the effectiveness of STS assistive devices in addressing these difficulties.
2. Identify which modes of STS assistance to test and compare, based on research on the main modes of STS assistance currently in use.
3. Design and build a STS test bed that provides the identified modes of assistance.
4. Specify biomechanical metrics to quantitatively evaluate the test bed assist modes based on the established evaluation criteria.
5. Using the test bed, perform experiments with older adults to collect data for analysis based on the specified biomechanical metrics and subject feedback.
6. Analyze the outcome of these experiments to determine the best mode of STS assistance.

Ultimately, the information from these analyses can be used to direct the development of new institutional and consumer load-sharing STS assistive devices as well as to provide guidance in developing STS procedures.

Based on this process the contributions of this work are: (i) the development of an assistive STS test bed with load-sharing capabilities that can accommodate multiple assist load locations and trajectories, (ii) a scheme for assessing the success of a particular mode of assisted STS based on biomechanical load and motion analysis and qualitative user feedback, (iii) a characterization of each mode of assist based on the developed scheme of assessing the success of STS assist modes, and (iv) a conclusion on the best mode of providing assistance with STS from the modes tested.

1.4 Outline of thesis

Chapter 1, Introduction: Discusses the motivation for this work and presents the objectives of the thesis.

Chapter 2, Related Work: Characterizes the different strategies of STS and describes the specific difficulties with STS experienced by older adults. It also presents an overview of existing STS assistive devices and identifies the need for a biomechanical and qualitative comparison of different modes of load-sharing STS assistance.

Chapter 3, Validation Experiment: Details the development of the experiment methodology through a biomechanical analysis of unassisted STS in healthy young adults.

Chapter 4, Simulation Study: Presents simulation work and discussions with physiotherapists that resulted in the selection of the arms, waist and seat as the key locations for the test bed to provide assistance with STS.

Chapter 5, Test Bed Design: Describes the four test bed design stages: the specification of functional design requirements; experiments with a critical function prototype to help quantify the force and trajectory specifications listed in the functional design requirements; the design of the test bed; and the validation of the functional design requirements based on pilot studies with the test bed.

Chapter 6, Test Bed Experiment: Details the experiment with the test bed, including sections describing subjects, experiment design, data collection and analysis, results, discussion of results, and a summary of the key findings of the experiment.

Chapter 7, Conclusions and Recommendations: Presents a synopsis of the work completed in the thesis and conclusions based on the key experiment findings. Recommendations are then proposed for future work with the test bed and for the development of new STS assistive devices.

Chapter 2 Related Work

2.1 Introduction

Based on the need to study the biomechanics of assisted STS and develop new STS assistive devices established in Chapter 1, this chapter discusses existing literature pertaining to STS function in older persons and to current STS assistive devices. To develop the criteria used to determine better modes of assisting older persons to a standing position, it is necessary to first characterize STS in terms of the biomechanics of the motion, including the identification of the difficulties experienced in performing the motion. In addition, it is necessary to determine the main modes of assist based on the existing published and practiced modes so that a test bed can be developed to study these modes of assist. The biomechanics of STS in older persons is presented first, followed by a discussion on existing modes of assisting persons to a standing position.

2.2 STS characterization

There is a significant amount of existing literature that characterizes STS in functionally impaired and healthy older persons. Schenkman et al. [24] completed a quantitative characterization of STS in older adults with functional limitations by examining body segment motions and determined that the standing process consists of four phases, as illustrated in Figure 2.1. Phase I (flexion momentum phase) starts with initiation of movement and ends just prior to the buttocks being lifted from the seat. Phase II (momentum-transfer phase) begins with the buttocks rising from the chair and ends at the moment of maximum ankle dorsiflexion. Phase III (extension phase) starts just after maximum ankle dorsiflexion and is completed when the hip finishes extension. Phase IV (stabilization) commences with the end of hip extension and ends when the motions associated with stabilization from rising are completed.

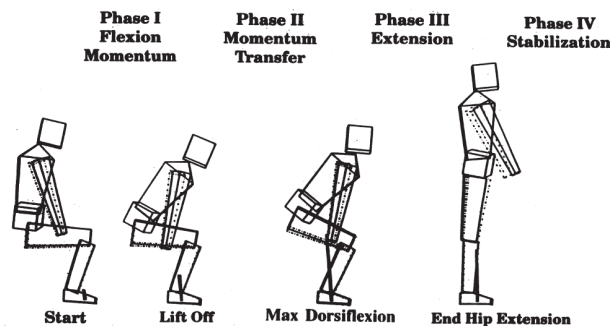


Figure 2.1: The four phases of STS motion [24].

The STS motion in older adults has been characterized into three categories based on observation of 3-D android representations of subjects during STS [25]. These categories, illustrated in Figure 2.2, consist of Dominant Vertical Rise (DVR), which has a lowering of upper body anterior momentum at liftoff along with a cessation of forward trunk flexion, followed by knee extension and dominantly vertical momentum; Momentum Transfer (MT), which involves a smooth transition of upper body anterior momentum at liftoff to total body vertical momentum with continued anterior momentum; and Exaggerated Trunk Flexion (ETF), which consists of deep trunk flexion prior to seat-off that places the center of mass (CoM) over the feet and results in a delay of trunk extension during the transition to an erect position. The study concluded that MT is the safest and most preferable strategy for STS in older adults because of extra movement timing and torque demands imposed by the other strategies. The study also showed that peak trunk flexion can be used to characterize STS rise strategy with the MT strategy characterized by a peak trunk flexion of 51° (SD 3.8°).

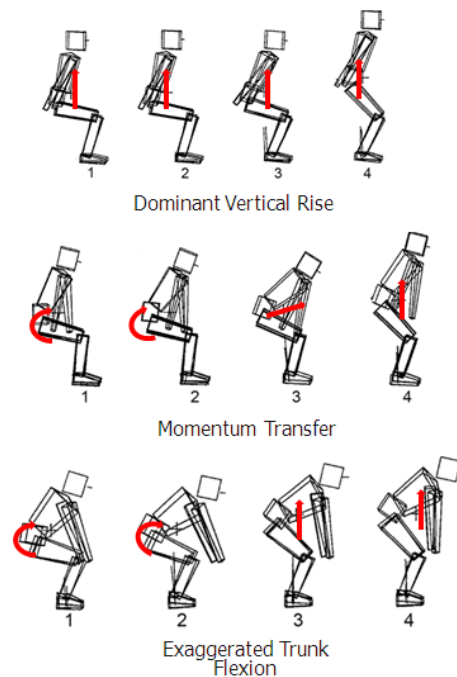


Figure 2.2: The three strategies of STS motion [25]. The arrows on each figure show the direction of motion during each phase of the rise. Phases of each rise are separated by numbered time events as follows: 1 - Lift off, 2 – maximum anteroposterior linear momentum, 3 – maximum trunk flexion, 4 – maximum vertical linear momentum. Arrows show the direction of motion during each phase of the rise.

2.3 Subject-related contributing factors to STS failure and corresponding assistive device evaluation criteria

Bernardi et al. [26] determined that STS movement among healthy seniors depends largely on three factors, namely: trunk bending momentum, center of mass position at seat-off, and lower limb extensor muscle strength. Studies in STS among functionally impaired older persons have shown that failure in STS is also related to these factors.

A study in the biomechanics of failed STS in impaired elderly [27] indicated two types of failure in STS: a sitback failure, occurring when a subject rises only slightly off the chair and then sits back down; and a step failure, which occurs when subjects are unable to stop at the end of the STS motion and take a step to stabilize themselves. The study concluded that both types of failure are a result of poor momentum control, resulting from inadequate postural coordination, and from weakness, manifested in the form of insufficient momentum and lower body torque generation.

Schultz et al. [21] determined that among functionally impaired seniors, STS strategy is such that emphasis is placed on achieving postural stability during the rise instead of minimization of joint torques. Hughes et al. [28] examined rise time, hip flexion velocity, and center of mass/base of support (CoM/BoS) separation in functionally impaired older persons rising from chairs of varying heights. Results showed that subjects attempt to increase stability by increasing rise time and decreasing the CoM/BoS separation at liftoff. For lower chair heights, which increase the difficulty of rise, subjects attempt to compensate by increasing momentum generation by increasing hip flexion velocity while maintaining the stabilizing strategy. Since increased momentum generation and increased stability are generally at odds, this results in an inefficient and difficult STS strategy leading to decreased success in rising from a chair. In concurrence with Schultz et al. [21], it appears that subjects choose this strategy of STS because they place more value on stability than on successfully rising from a chair. Deshpandi et al. [29] associated poor STS performance with fear of falling, thus fear of falling may be a contributor to the more conservative and less efficient STS strategies noted by Schultz et al. [21] and Hughes et al. [28]. Two biomechanical measures are primarily used to measure the stability of a STS rise: the displacement of the whole body Center of Mass (CoM) is used to measure static stability (postural balance) [28], and the displacement of the foot Center of Pressure (CoP) from the foot center at seat-off is used to measure dynamic stability (postural stability) [21].

Muscle strength has also been studied in the context of STS. Hughes et al. [15] determined that in functionally impaired older persons, at lower chair heights the knee extensor strength required to rise reaches 97% of the available strength, indicating that strength is a limiting factor in determining the lowest chair height from which functionally impaired persons can rise. A study evaluating the relative importance of balance and strength in STS [30] concluded that lower extremity strength is a greater predictor of STS performance in functionally impaired seniors. Concerning upper body loads, Schultz et al. [21] found that the largest mean value of shoulder torque for chair rise using armrests to assist the motion began to approach the maximum voluntary strength for elderly females. This suggests that lack of upper extremity strength can be a limitation for chair rise using upper body support. Knee torque is the biomechanical measure predominantly used to measure strength in STS and was used in the above mentioned studies by Schultz et al. [21], Hughes et al. [15], and Riley et al [27].

In summary, the literature on STS in seniors indicates that STS difficulty can be causally related to insufficient and or uncontrolled upper body momentum generation, weakness in the knee extensor muscles and shoulders, instability, improper coordination of motion, and fear of falling. The recommended strategy for STS is MT because it imposes less movement timing and torque demands than the other STS strategies. Accordingly, the design of STS assistive devices should be evaluated by how well they adhere to the following three criteria: i) reduction of the knee extensor effort required for standing, ii) guidance through a MT STS motion so that motion and momentum can be properly coordinated, and iii) provision of a sense of stability and support throughout the motion. The biomechanical measures of peak knee torque, peak trunk flexion, and CoM and CoP displacement at seat-off can be used to quantitatively evaluate adherence to the above three criteria. These measures are discussed again in Chapter 6 and used in the context of an experiment with different modes of assisted STS.

2.4 The case for load sharing

While it is important that STS assistive devices help reduce the required knee extensor strength for standing, concerns exist among rehabilitation professionals that habitual use of standing assistance, mainly through lift chairs, may contribute to accelerated muscular degeneration due to muscle disuse [32]. Although these concerns of disability from long-term lift chair use have not been studied in the literature, it is known that physical exercise among mobility-impaired people can help prevent further disability and mortality [23]. Consequently, an assistive STS device that shares with the user the load required to rise can be a means of exercise in older adults to help prevent further disability and

mortality. Repeated STS has been studied as a resistance-training stimulus for home exercise using the GrandStand System, a pressure cushion with a biofeedback monitor attached [33]. Six weeks of daily home exercise in which participants performed repeated STS motion using this system resulted in an improvement in subject balance as reported by the Berg Balance Scale [34], a scale used to measure balance in older people with impairment in balance function. The results of this study indicate that performing STS motions as a functional task based exercise can help improve balance in older subjects. Thus creating an STS device that provides load sharing instead of simply reducing the required knee extensor effort, in addition to the previously outlined design features of trajectory guidance and stability, could prove beneficial by helping maintain strength and balance.

2.5 Commercial devices

Presently there are numerous commercially available devices to assist with rising from a seated position for persons with a wide range of functional ability. Passive devices (devices without mechanical assistance) include wall grab bars for toilets, ceiling pole grab bars for multi-purpose locations, and bedrails for support when rising from a bed (Figure 2.3). These devices are stability and support devices, enabling a person to use upper body strength to aid in the standing process. Furniture risers represent another low-tech stand-assist device category. They are used to elevate the height of furniture to make it easier to shift weight forward when rising, providing a lifting advantage [35]. Omera et al. [36] studied the effects of unilateral grab rail assistance on STS performance of older adults. The use of unilateral grab rail assistance provided propulsion and safety during STS but also introduced systematic asymmetric changes to net joint moments and powers, resulting in assistance to the ipsilateral ankle and hip joints and contralateral knee joint but greater loading to the ipsilateral knee joint and contralateral hip joint. The concerns of asymmetric loading and also the lack of upper body strength discussed in Section 2.3 are the primary limitations of commercial stability devices.

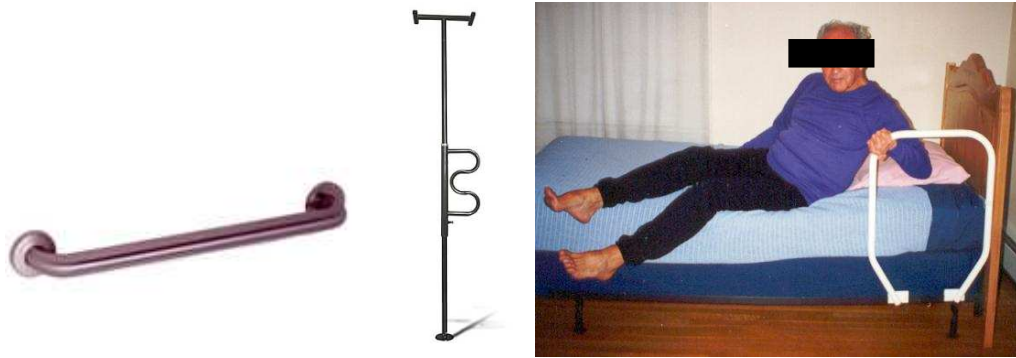


Figure 2.3: From left to right: wall grab bars, ceiling pole grab bar, bedrail [35].

In addition to passive STS assist there are also commercially available active STS assistive (devices that provide mechanical assistance). These devices consist of lift cushions, lift chairs, and powered stand assist devices (Figure 2.4) and provide mechanical assistance by raising the user close to the standing position. Lift cushions are devices placed in the chair in which the user sits. When the user stands up, a lever rotates the cushion about a pivot point at the front of the cushion and pushes the person to a standing position. Lift chairs are powered recliners that lift and tilt forward to help transfer users from a seated to standing position. Powered stand assist devices typically have a U-shaped base with leg supports, a waist harness and a lever arm to lift the harness. Assistance is provided by strapping the waist harness around the user and raising the lever arm to assist the user to a standing position. Powered stand assist devices are used mainly as assistive devices in care homes to raise residents who have some weight bearing capacity to a standing position for transfers, personal care tasks, and dressing [35].



Figure 2.4: From left to right: lift cushion, lift chair, powered stand assist device [35].

Studies have been completed on the use of lift chairs for assisting people with STS. These studies have shown that lift chairs do not destabilize users during the assisted rise [37] [38] as evident by a peak horizontal CoM velocity during the assisted rise which is similar to the peak horizontal CoM velocity during the unassisted rise. However, no research was located that established the level of assist force required to facilitate individual rising. In addition, conflicting reports have been published on the effects of lift chairs on knee loading, as Wretenberg et al. [22] reported that knee loads are reduced while rising with a lift chair compared to unassisted rising but Munroe [39] reported that knee loads are similar or greater when rising with lift chair assistance compared to unassisted rising. Hence, further investigation of the effects of lift chairs on knee joint loading can help quantify the benefit of rising with assistance from such devices.

Ruszala and Musa [40] evaluated four types of commercially available equipment that assist patient STS activities in physiotherapy. Equipment evaluated included a lift chair, a stand-and-turn aid, a stand-and-walk aid, and a walking harness. The study determined that the equipment that enabled independent transfer (stand-and-turn aid and lift chair) was beneficial in that it preserved dignity and allowed the patient to control the activity. One of the concerns raised in the study was that none of the movements generated by the equipment was able to reproduce normal STS movement adequately. However, the overall conclusion was that equipment use provides greater consistency of patient movement and is preferable to caregivers who use incorrectly performed manual techniques for STS assistance. Thus, equipment use has the potential to replace manual lifting techniques, which would help reduce the high incidence of caregiver work-related back pain and injuries resulting from manual assist of STS.

In summary, the literature on commercial devices shows that passive assists can facilitate STS, but there are concerns of asymmetric loading and excessive loading of the upper body. The powered devices facilitate stable rising, but the level of assist force required to facilitate individual rising has not been investigated, and conflicting reports are present on the effectiveness of lift chairs in reducing the knee loading as a person rises. These concerns motivate the need to further study the biomechanics of assisted STS to quantify the loads placed on joints and the stability and trajectory of the user.

2.6 Research and development devices

Most powered STS assist devices current in research and development are walkers with STS assist functionality. Mederic et al. [16] developed an intelligent walking aid with STS assistance that is provided by a two degree of freedom mechanism mounted on an active mobile platform (Figure 2.5). The mechanism controls a pair of handles that slowly pull the user from a seated to a standing position. The handle trajectory follows a natural pattern that was generated to adapt to the personal feeling and strategy of STS transfer motion of each user. In addition to maintaining a natural trajectory of the user, the device provides an assistive force to maintain the stability of the user based on a zero moment point calculation. Although this walker addresses the requirements of stability and trajectory guidance in assisted STS, it does not address the important assistance requirement of load compensation, as there was no information in the study regarding joint load reductions during the assisted STS motion. Conversely, a walker system with STS assist developed by Chuy et al. [17] did focus on knee load reduction but was not able to guide the STS motion of the user or examine the stability of the user during the rise.

Two STS assist systems that focused on all three criteria of stability, trajectory guidance, and load sharing were developed by Chugo et al. One system consists of a walker with a chest pad that provides load assist [41]. This system is able to guide the user in a trajectory close to a natural physiotherapist assisted trajectory as well as reduce the knee load to a level that maintains user strength. The force assistance is derived from a control scheme that provides assistive load based on the Zero Moment Point position of users as they rise. Thus, the system is also able to maintain the stability of the user. The drawback of this system is that the assist load is placed on the chest of the user. This has the potential to inhibit breathing, cause discomfort, and harm users who have conditions such as osteoporosis. The other system developed by Chugo et al. consists of a bed that moves up and down and provides force assistance to the user at the buttocks (Figure 2.5), and a two degree of freedom support bar that stabilizes and guides the user through a natural trajectory [20]. A control scheme was developed that combines position control and force control to guide the rise trajectory and share the load. Simulations were completed using the control scheme and showed that the system provides force assistance by reducing the load on the knees while allowing subjects to use their own physical strength. This system showed that a seat based assist can prove beneficial for load assist and an arm mechanism can help provide stability and trajectory guidance. The limitation of this device is that it requires a special bed with actuation in the vertical plane.

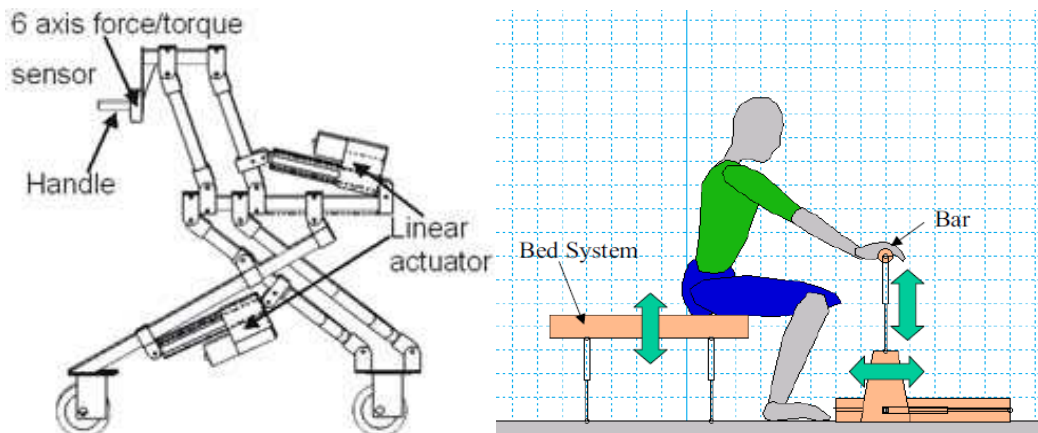


Figure 2.5: Left image: intelligent walking aid with STS assistance [16]. Right image: bed and bar system [20].

Takahashi et al. [19] developed a STS assistance system consisting of a moveable handrail that leads the user to a standing position. Experiments were completed on individuals with Parkinson's disease using three different handrail trajectories. The study concluded that a handrail trajectory that is based on the shoulder trajectory of a normal healthy individual in the process of standing up can successfully provide assistance as individuals move from a seated to a standing position. The drawback of this system is that any assist force applied by the system would be translated through one shoulder of the user, thus making the handrail system not very suitable for force assistance because of large loads transferred through the shoulder.

In summary, a review of the literature on R&D devices reveals multiple modes of STS assistance. Each assists aids with force compensation, stabilization, and trajectory guidance to different extents. The seat based and chest assist systems are generally good for load compensation while some of the arm guidance mechanisms are beneficial for trajectory guidance. A comparative evaluation of the different modes of STS in research and development as well as those available commercially can help quantify the best mode of assisting with STS.

2.7 Rationale for proposed test bed

Research on STS as a functional task based exercise in older persons [33] and the importance of physical exercise in functionally impaired people [23] as well as the load-sharing STS assistive devices developed by Chuy et al. [17] and Chugo et al. [20] have identified the need of providing load-sharing assistance to help maintain strength and balance in older adults. Few existing assistive devices incorporate load sharing. In addition, each STS assistive device has strengths and weaknesses, but a comparison of the different modes of assisting users to a standing position to determine the best mode was not found after a thorough review of the literature. Such a comparative analysis would provide empirical data on the best mode of assisting a user to a standing position.

Both of these problems can be solved by evaluating the main modes of STS assistance in a shared load paradigm. This can be completed by developing an assistive STS test bed with load-sharing capabilities that will allow an investigation into different modes of STS assistance. Incorporating load sharing in each mode of assistance will help with the development of load-sharing assistance in STS devices.

Evaluation with the test bed should examine how well each mode of assist meets the needs of older persons who experience difficulty with standing. The literature concerning subject related factors that contribute to STS failure suggests that the main contributors to failure are weakness, instability, fear of falling, and poor coordination. Biomechanical metrics developed from the evaluation criteria of knee extensor effort reduction, trajectory guidance, and stability can be used to evaluate the ability of each assist mode in the test bed to compensate for these difficulties. Using the test bed to empirically determine the best mode of assisting a person from a seated to standing position while incorporating user strength in each mode will help give baseline design criteria for the development of new STS assistive devices and will thus help provide assistance with a challenging function experienced by a significant population of older adults.

Before developing the test bed and evaluating the main modes of STS assistance, it is necessary to establish a valid method of evaluating the biomechanics of STS. The next chapter (Chapter 3) presents a validation experiment that was conducted to establish and validate an experimental procedure and data analysis procedure to evaluate the biomechanics of STS.

Chapter 3 Validation Experiment

3.1 Experiment introduction

In the last chapters the motivation for a study of assisted STS motion in older adults was presented, leading to the proposal to develop a test bed to study different modes of assisted STS. This chapter develops a method of collecting data and evaluating the biomechanics of STS in the context of a validation experiment with young healthy adults performing unassisted STS. The chapter describes the following details of the experiment: collection of STS data, evaluation of the data in terms of joint torques and motions based on a rigid body biomechanical model and Newton-Euler analysis, and a discussion of the validity of this experimental approach based on results. The experimental procedure and biomechanical model were developed similarly to other studies that analyzed the biomechanics of STS [42] [43] [44]. Whereas most experiments on the biomechanics of STS used video or motion analysis systems to obtain kinematic data [45], kinematic data in this experiment were obtained using inertial orientation trackers attached to the shank, thigh, and trunk of subjects. The outcomes of this study will be used in the following chapter to develop a STS simulation model. Furthermore, the procedure and the method of analysis developed will be used in the STS experiments described in Chapter 5 and Chapter 6.

3.2 Experimental procedure

3.2.1 Subjects

Three healthy male adults with a mean age of 21.3 years (SD, 2.4 years, range 18-23 years) took part in the experiments. The average mass was 66.3 kg (SD 8.96 kg, range 54-75 kg) and the average height was 175 cm (SD 6.5 cm, range 166-182 cm)

3.2.2 Setup and procedure

The equipment for the experiment consisted of two 6-axis AMTI (Advanced Medical Technology Incorporated) force platforms, three orientation sensors (Xsens Motion Technologies) and a height adjustable stool. The orientation sensors (5 x 3.5 x 2 cm size) were first zeroed to the world coordinate frame and then attached to a standing subject using tensor bandages. Sensors were attached to the shank, thigh, and chest at the CoM of each segment. CoM location was determined using approximate anthropometric coefficients based on segment lengths [46]. The subjects were then seated on the stool, which rested on the surface of the force platform. The seat height was

adjusted so that the subject sat with thighs approximately parallel to the ground, and feet positioned on the second force plate. Foot position was similar for all subjects and was symmetrical about the longitudinal force plate axis. Figure 3.1 shows the equipment and experiment setup.

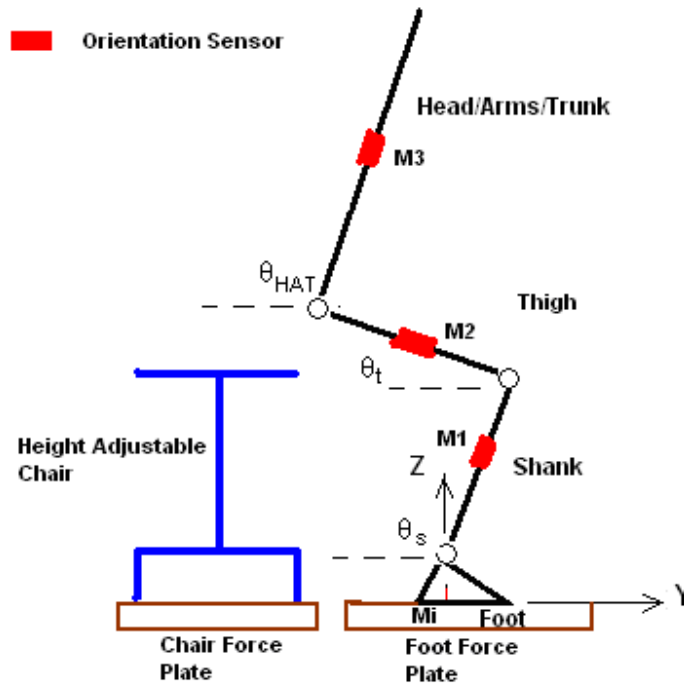


Figure 3.1: Experiment setup. θ_s is trunk angle, θ_t is thigh angle, θ_{HAT} is head/arm/trunk angle. Body segment angles are measured with respect to horizontal plane.

Subjects sat with an erect trunk and arms folded across their chest. Folding the arms across the chest was a simplification included to prevent unmeasured forces from arm usage during the rise. This simplification is consistent with experiment protocol in other STS studies [42] [43].

Subjects waited for a verbal cue before starting the STS movement. After the verbal cue, the subject rose at a self selected speed and, once standing, maintained a still upright position until asked to be seated again. Subjects performed five trials in which force plate and orientation sensor data were acquired. Before the start of the trials the force plates were zeroed to correct for long-term drift and the weight of the chair on the force plate. To ensure synchronization between force plate and

orientation sensor data collection, a countdown timer was programmed into the force plate data collection program Graphical User Interface (GUI) in LabVIEW. When the start button on the LabVIEW GUI was clicked, a five second count down was initiated, and at the zero point, a green indicator was lit and data collection started. At the same time the green indicator came on, the experimenter clicked the start data collection button on the orientation sensor data collection GUI so that both programs would start data collection at the same time.

3.2.3 Data collection

Anthropometric data were first collected from subjects. Subject weight was obtained from force plate measurements and the subject height, shank length (Femoral condyles / medial malleolus), thigh length (greater trochanter / femoral condyles), and head/arms/torso length (greater trochanter/ glenohumeral joint) were measured. Body segment lengths were found by palpation at joints to find the point of rotation and measured using a measuring tape and ruler which were used to an accuracy of 0.5 cm (0.1 cm resolution each for tape and ruler). The anthropometric data were keyed into a spreadsheet to calculate body segment mass, CoM location, and moments of inertia.

The force plate and orientation sensor data collection was initiated two seconds before the verbal rise cue and lasted approximately five seconds for each trial. Reaction forces were collected from both platforms at a frequency of 100 Hz and were digitally filtered with a zero-delay, bi-directional, fourth-order, low pass Butterworth filter at a cut-off frequency of five Hz. This type of filter was chosen to eliminate noise without any phase delay in filtering. The 6-axis AMTI force plates each have a resolution of 0.1 N and are accurate within 2.4% of the maximum load (2% inaccuracy based on crosstalk, 0.2% based on hysteresis, 0.2% based on non-linearity).

The orientation sensor measured three dimensional linear acceleration and angular velocity of the motion. The sensor program automatically integrated angular velocity to provide sensor orientation data in the form of rotation matrices with rotation relative to the zeroed position of the orientation sensor (sensor zeroed at start of trials). The orientation data provided by the sensor has an angular resolution of 0.05° Root Mean Square (RMS) and a dynamic accuracy of 2° RMS. Orientation sensor data were also collected at a frequency of 100 Hz and filtered in the same way as the force plate data. The accelerometer data were gravity compensated to negate the gravity force readings on the sensors. All data filtering and gravity compensation calculations were computed offline in Matlab after the trials were completed.

3.2.4 Data analysis

A four-link rigid body biomechanical model was created to determine the joint torques during the STS motion as advocated by Mak et al. [42] and Kuo [44]. The model consisted of four rigid body linked segments representing the feet, lower legs (shank), upper legs (thigh), and Head/Arms/Trunk (Figure 3.2).

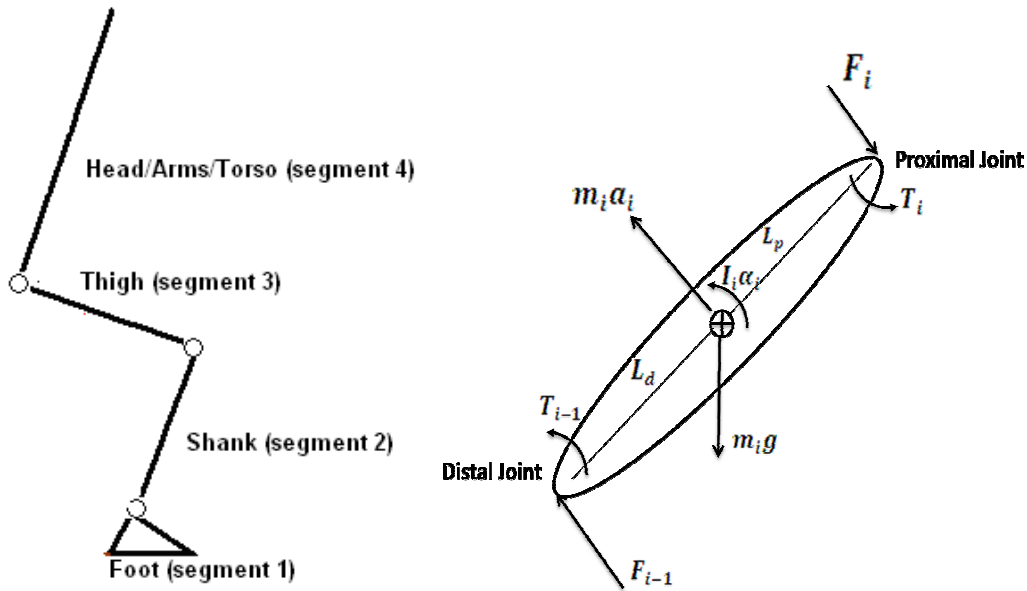


Figure 3.2: The 4-link rigid biomechanical model and a representative body segment used in the inverse dynamics model. The body consists of 4 segments connected by three joints. L_d is the distance to the distal joint from the CoM and L_p is the distance to the proximal joint from the CoM. T_{i-1} and F_{i-1} represent the joint torque and force acting on the distal joint of the current body segment (segment i) from the proximal joint of the previous body segment (segment $i-1$). Gravity force ($m_i g$) and acceleration force ($m_i a_i$) act at the CoM. T_i and F_i represent the joint torque and force acting on the proximal joint of the current body segment.

Symmetry across the mid-sagittal plane (plane dividing the body in half longitudinally) was assumed and therefore the model was created in a two dimensional plane. Using the body segment kinematic data, force plate dynamic data, and subject anthropometric data, the joint forces and torques were calculated recursively using the Newton-Euler inverse dynamic analysis.

$$\sum Forces = m_i a_i \quad i = 1, \dots, 4 \quad (3.1)$$

$$\sum Moments = I_i \alpha_i \quad i = 1, \dots, 4 \quad (3.2)$$

$$F_i = F_{i-1} - m_i g - m_i a_i \quad (3.3)$$

$$T_i = (L_d \times F_{i-1}) + (L_p \times F_i) + T_{i-1} - I_i \alpha_i \quad (3.4)$$

The Newton-Euler analysis is based on computing the dynamic equilibrium of body segments using the Newton-Euler equations of translation and angular motion (Equations 3.1 and 3.2). Figure 3.2 shows a representative body segment of the biomechanical model used in the study, with forces and torques labeled. The joint forces and torques were calculated using Equations 3.3 and 3.4 starting from the foot segment and working upwards. The vertical ground force and CoP underneath the foot was determined from force plate data. The force plate directly gave the magnitude of the vertical ground force (F_z) and horizontal ground force (F_y) and the CoP was determined using the moment about the center of the force plate (M_x) and the vertical ground force (Figure 3.3). Using this force and CoP data, the joint forces and torque at the ankle were calculated through Equations 3.3 and 3.4. Working upwards, the remainder of the joint forces and torques were also calculated using Equations 3.3 and 3.4. A trajectory profile of the net joint moments on each body segment for the duration of STS were calculated and then normalized with respect to body mass times body height ($Nm/(Kg*m)$). Peak values from these curves were extracted and compared to literature peak values.

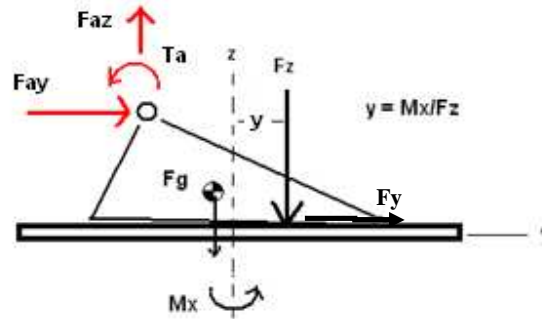


Figure 3.3: Foot center of pressure location.

3.3 Results

3.3.1 Force-plate data

Figure 3.4 shows a time history of the vertical reaction forces of both chair force plate and foot force plate. At the start of the motion, the subject leaned forward, resulting in a slight increase and decrease in chair and foot forces, respectively. This increase/decrease in force plate forces was used to determine the time of the start of the motion. Once momentum was generated through the lean forward motion, the subject started rising from the chair, as indicated by the rapid drop in chair force. The time at which seat off occurred was determined by finding the time when chair contact force reached zero. The end of the motion occurred when the chair vertical reaction stabilized to a steady state value equaling the weight of the subject. This point was determined as the time at which the thigh segment first became perpendicular to the ground (shown in Figure 3.5), that is at 90° .

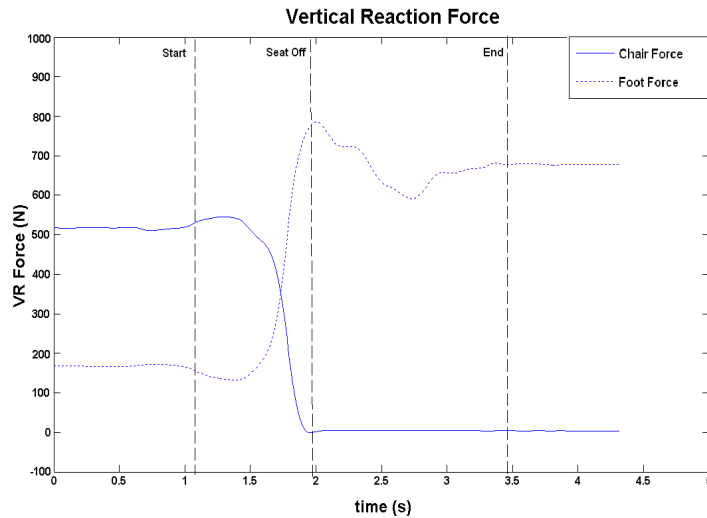


Figure 3.4: Vertical reaction forces from chair force plate and foot force plate during a representative STS trial.

3.3.2 Joint kinematics

A plot of angular displacements of body segments (measured from the horizontal plane) vs. time during the STS movement is shown in Figure 3.5. Forward flexing of the torso occurred at the start of the movement at an angle around 92° , extending to an angle of 124° at seat off, and descending to

81° after the end of the motion. Motion of the thigh and shank began at seat-off, with the thigh extending from 3° at seat off to 100° at the motion end and the shank flexing forward from 103° at seat off to a maximum angle of 118° and back to 98° at the end of the motion.

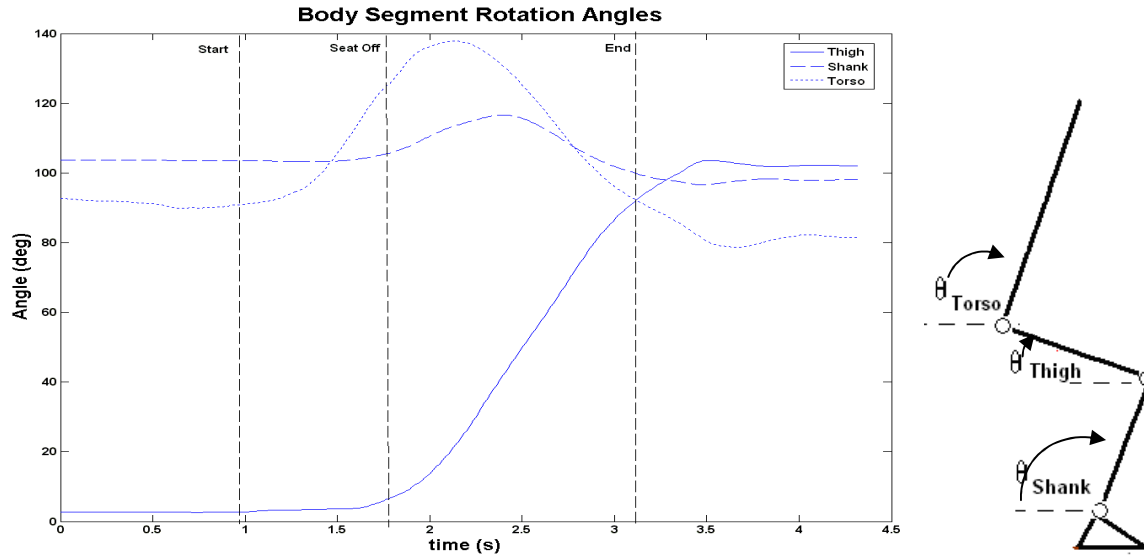


Figure 3.5: Body segment rotation angles during a representative STS trial from a single subject. Body segment angles are measured from the horizontal as shown in the illustration on the right hand side of the figure.

3.3.3 Joint dynamics

Figure 3.6 shows a plot of normalized joint torques for a representative STS motion. The torque is normalized with respect to the subject body mass multiplied by subject height, so that comparisons can be made between subjects. Positive torques indicate that the joint is being extended. At the start of the motion there was dorsiflexion in the ankle joint, with maximum dorsiflexion occurring at seat-off. This maximum ankle dorsiflexion was concurrent with the peak hip and knee maximum extension torques. From seat-off onwards the ankle went through a plantarflexion movement with maximum plantarflexion torque occurring close to the end of the movement, and a steady state torque at the Movement End higher than the initial torque. The hip and knee extension torques decreased from the maximum value at seat-off till they reached a minimum steady state value at the STS Movement End.

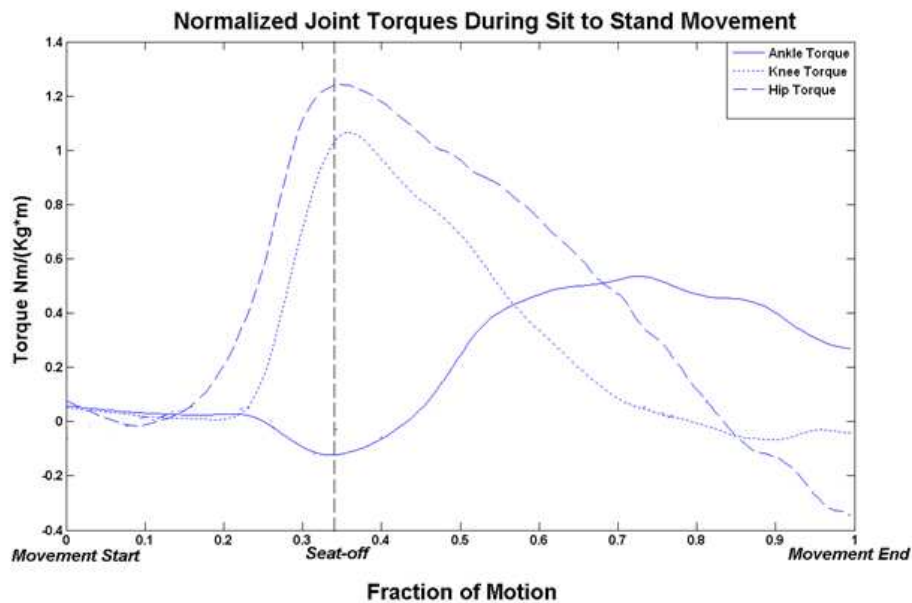


Figure 3.6: Normalized joint torques during a representative STS trial. Torques are normalized to body-mass times height. Positive torques act to extend joints. Torques are plotted with respect to the fraction of completion of the STS movement.

3.3.4 Torque variability

Figure 3.7 shows a plot of joint torques from four STS trials of a single subject to show intra-subject variability. The plot shows that joint torque trajectories are similar between trials for all three joints. The average peak joint torques and standard deviation across trials are summarized for each subject in Table 3.1. Joint torques are averaged across four trials for subject 1 and five trials for subject 2 and 3. Figure 3.8 shows representative plots of the normalized joint torques for each of the three subjects to show inter-subject variability. The average peak joint torques and standard deviation across the three subjects are summarized in Table 3.1.

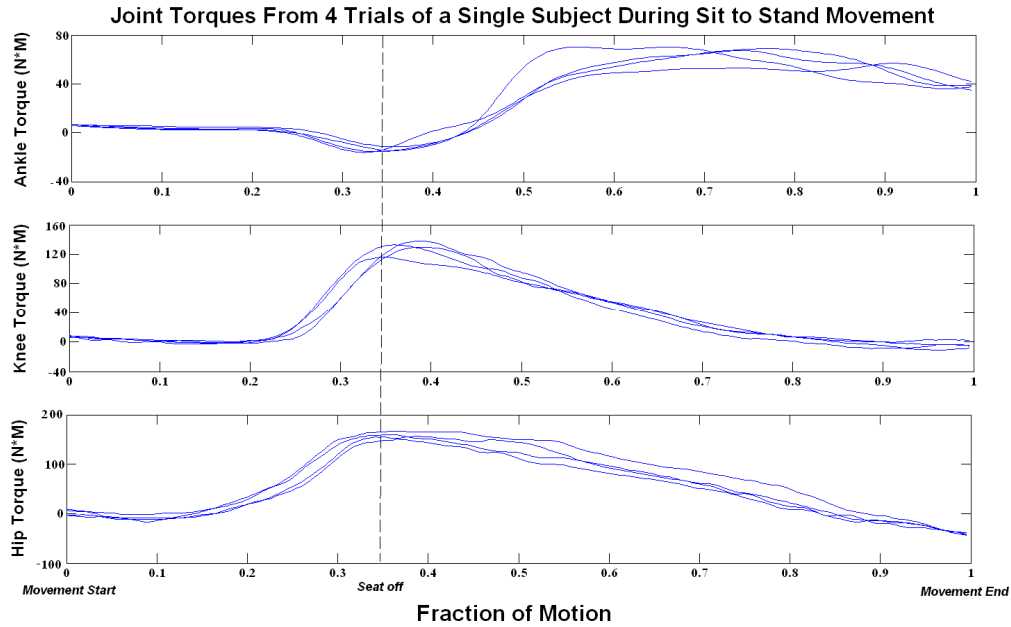


Figure 3.7: Joint torques during four STS trials of a single subject. Positive torques act to extend joints. Torques are plotted with respect to the fraction of completion of the STS movement.

Table 3.1: Average peak joint torques for three subjects.

	Ankle Torque (Nm)	Knee Torque (Nm)	Hip Torque (Nm)
Subject1 (n=4)	65.2 (4.8)	127.6 (7.7)	163.6 (11.8)
Subject2 (n=5)	32.0 (12.4)	110.2 (7.2)	133.6 (20.8)
Subject3 (n=5)	48.8 (8.4)	159.6 (16.2)	189.6 (21.0)

Values shown are means (standard deviations)

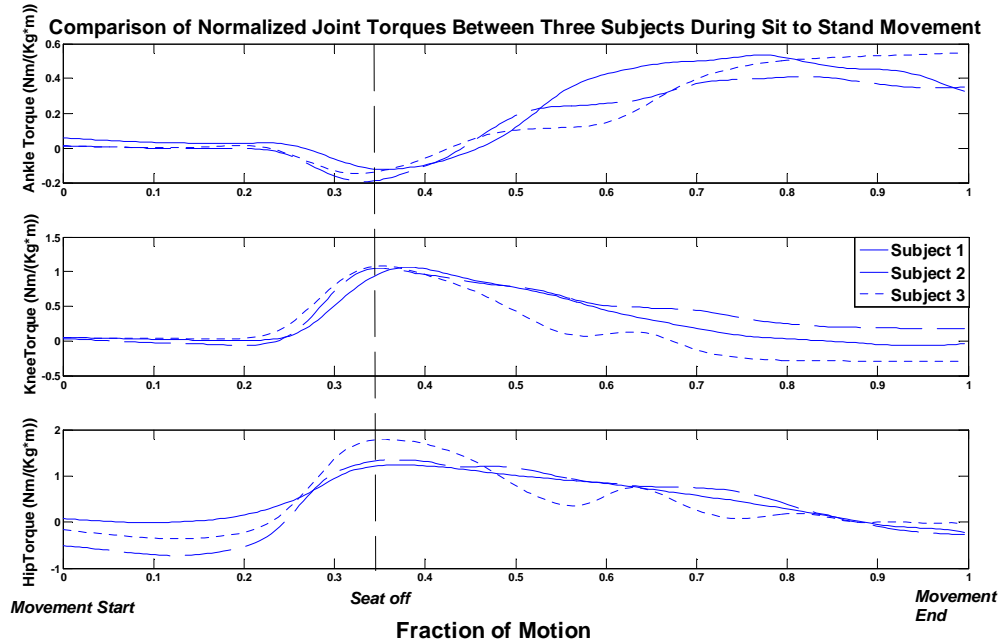


Figure 3.8: Normalized joint torques during representative STS trials for each subject. Torques are normalized to body-mass times height. Positive torques act to extend joints. Torques are plotted with respect to the fraction of completion of the STS movement.

3.3.5 Discussion

The purpose of this study was to demonstrate that the experimental procedure, biomechanical model, and Newton-Euler analysis used in the validation experiment provide a reasonably accurate analysis of the STS motion. The accuracy of the analysis was validated through a comparison of the maximum normalized joint torques calculated in this analysis to the maximum normalized joint torques calculated in a study of the STS biomechanics in healthy older adults [42], shown in Table 3.2. The peak ankle torque is $0.41 \text{ Nm kg}^{-1}\text{m}^{-1}$, which is lower than the $0.64 \text{ Nm kg}^{-1}\text{m}^{-1}$ reported in the literature but within one standard deviation ($\text{SD} = 0.14$). The peak knee torque is $1.14 \text{ Nm kg}^{-1}\text{m}^{-1}$, which is very similar to the literature value of $1.17 \text{ Nm kg}^{-1}\text{m}^{-1}$; and the peak hip torque is $1.39 \text{ Nm kg}^{-1}\text{m}^{-1}$, which is high compared to the literature value of $0.91 \text{ Nm kg}^{-1}\text{m}^{-1}$. This heightened hip peak torque could be the result of exaggerated hip flexion by the subjects in the present study. The average hip flexion of the three subjects in this study was 48° while the average hip flexion of the six healthy

subjects in Mak et al. [42] was 30°. Since hip torque is primarily used to counter the moment resulting from the gravity load on the HAT segment, the difference of 18° between peak hip flexion in the present study and the comparison study is a significant contributor to the heightened hip torque value. Another source for the discrepancy between torques obtained in this study and torques obtained in the literature may be the age differences in the subjects between the present study (mean age 23 years, SD 2.4 years) and the literature study [42] (mean age 69 years, SD 4 years).

Table 3.2: Comparison of normalized peak joint torques between inverse dynamics analysis and literature values. Torque is normalized to body mass*body height.

Peak Torque Nm/(kg*m)	Model Analysis (n = 3)	Literature (n=6) [42]
Ankle	0.41 (0.09)	0.64 (0.14)
Knee	1.14 (0.11)	1.17 (0.27)
Hip	1.39 (0.09)	0.91 (0.17)

Values shown are means (standard deviations)

The shape of the joint torques graphs (Figure 3.6) is similar to the shapes of the corresponding graphs in literature [42]. This shows that this study provides an accurate method of obtaining a time history of joint torque variations relative to the start, seat off, and end phases of the STS motion. In addition, the graphs showing chair foot plate force (Figure 3.4) and body segment angles (Figure 3.5) have similar shapes to the corresponding graphs in literature [42]. This shows that the data acquisition in this study is accurate.

The model used in this study assumed bilateral symmetry of joint torques and joint motions. The validity of this bilateral symmetry assumption has previously been investigated by Lundin [47]. The study determined that there are joint moment asymmetries during the STS task but concluded that these differences, although statistically significant, may have small biomechanical significance. To keep analyses relatively simple most studies, including studies by Mak et al. [42] and Schultz et al. [21], assume bilateral symmetry in their analyses of the STS task.

With regards to force plate accuracy, the across-subject average joint torques are the important force-plate related measures in this experiment and in the experiment described in Chapter 6. Table 3.2 shows that the standard deviation of the across-subject average peak ankle torque is 22% (0.14 Nm/(kg*m)/ 0.64 Nm/(kg*m)) of average peak ankle torque reported in the literature study [42]. The accuracy of the AMTI force plate is within 2.4% of the load on the plate (Section **Error! Reference source not found.**). Thus the accuracy of the force plate is shown to be sufficient for this experiment since the variability of the load on the plate (2.4% of peak load) is much lower than the standard deviation of the average peak ankle torque (22% of peak ankle torque) in the literature study [42]. The force plate load variability can be directly compared to the ankle torque variability since ankle torque (T_{ankle}) is directly proportional to the force plate load ($F_{ForcePlate}$) ($T_{ankle} = F_{ForcePlate} * d_{ankle}$, where d_{ankle} is the distance from the foot CoP to the ankle joint).

With regard to orientation sensor accuracy, the biomechanical measure directly obtained from the orientation sensor measurements is based on the peak trunk angle and this measure is used to evaluate adherence of the STS rise to the MT strategy (discussed in Sections 2.2 and 2.3 and applied in Chapter 6). Scarborough et al. [25] distinguished the MT strategy from the DVR and ETF strategies by the peak trunk flexion: 51° (SD 3.8°) for the MT strategy rise, and 35° (SD 4.6°) and 64° (SD 5.4°) for the DVR and ETF strategies, respectively. Because there is at least a 13° mean difference between the MT strategy and another rise strategy, a difference much larger than the 2° angular dynamic accuracy range in the Xsens sensor, sensor accuracy should not cause an error in determining the rise strategy based on the trunk flexion angle. Thus the Xsens sensors are sufficiently accurate for measuring trunk flexion.

3.3.6 Conclusion

In conclusion, the completed study presents a method of analyzing STS motion and has provided results for reaction forces, joint angles, and joint moments during the STS movement. The similarities between study and literature reaction forces and joint angle time history graph shapes validated the accuracy of data collection. Also the similarity between the study and literature values of normalized joint torques validated the accuracy of the model. The similarities in results between this study and other studies that analyze the biomechanics of STS have validated the use of this method for STS motion characterization and joint moment calculations. In addition, the accuracies of the force plate and the motion sensors have been shown to be sufficient for the purposes of this

experiment and further experiments. Therefore the method of data collection and analysis used in this study can be used in all subsequent experiments that will occur in the thesis research.

Based on this experiment, some recommendations for future STS studies using this approach are to: use a more stable adjustable stool for chair rise, consider asking subjects to rise using a rhythmic beat so that rise speeds will be consistent across trials, and use a method which enables faster and more repeatable attachment/detachment of orientation sensors to the subjects than the tensor bandages used in this experiment.

The next chapter presents a simulation study which examined different locations on the body to provide STS assistance. This study was based on a simulated biomechanical model of a person rising from a chair. The kinematic data obtained from the validation experiment detailed in this chapter were used as reference data for this simulated model.

Chapter 4 Simulation Study

4.1 Simulation introduction

In the previous chapter a method of characterizing the joint motions and joint torques in unassisted STS was established. The next stage in the thesis was to conduct a preliminary study on different assist modes to see if there is an easily identifiable single best mode of STS assist. A biomechanical model of a person performing STS was developed in simulation to test and analyze different modes of assist. Results of this analysis helped direct the design of the test bed by identifying the modes of assist that merit further investigation. The validity of these modes of assist was discussed with physiotherapists. Based on the simulation results and discussion with physiotherapists the locations of assist to be provided by the test bed were selected.

4.2 Simulation model

The STS task was modeled using a modified three-link inverted pendulum model. The inverted pendulum structure for modeling human sagittal plane tasks has been validated by Barin [48] and used by Prinz et al. [49] in STS modeling. The model consists of three rigid body linked segments representing the lower legs (shank), upper legs (thighs) and Head/Arms/Trunk (HAT). The HAT segment of the model was modified such that the forearm and upper arm are extended to allow for assistance application at the forearm and upper arm. The mass of the HAT segment was distributed among the trunk, upper arm, and forearm. The model is shown in Figure 4.1. This simplified model is an inherently unstable system that requires suitable control to maintain balance. Revolute joint actuators were modeled at the ankle, knee, and hip, and angular position and velocity feedback was used to implement closed loop balance control.

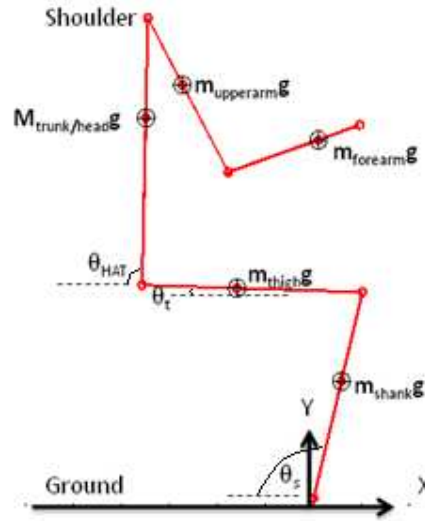


Figure 4.1: Simulation model. θ_s is trunk angle, θ_t is thigh angle, θ_{HAT} is head/arm/trunk angle. Body segment angles are measured with respect to the horizontal plane. Gravity loads are labeled for each body segment.

4.3 Control of model

The control of the STS transfer was modeled using a feedforward and feedback controller that guided the motion along a desired angular position and angular velocity trajectory. The simulated closed loop system is shown in Figure 4.2.

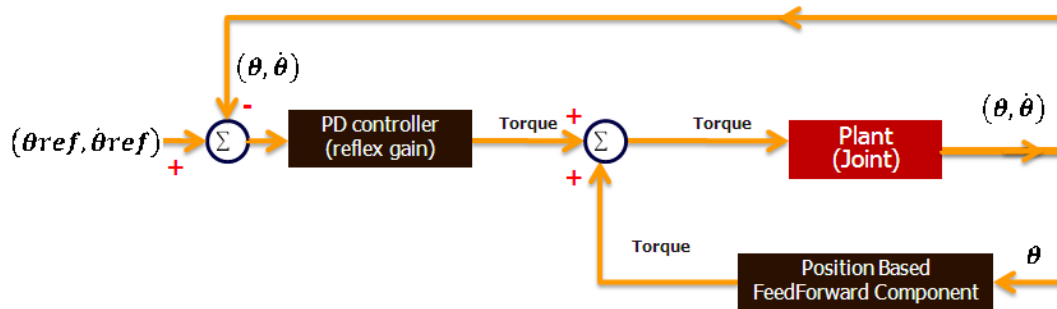


Figure 4.2: Control system of joints. $(\theta, \dot{\theta})$ represent the joint angle and joint angular velocity $(\theta_{ref}, \dot{\theta}_{ref})$ represent the reference joint angle and joint angular velocity obtained from a representative trial of the validation study in the previous chapter.

4.3.1 Feedforward component

The feedforward component of joint torque was used provide the torque required to maintain each body segment of the model in equilibrium according to the current joint angle. The control law for this component is shown in Equation 4.1.

$$\vec{T} = D(\theta)\ddot{\theta} + H(\theta, \dot{\theta})\dot{\theta} + G(\theta) \quad (4.1)$$

In this equation, $D(\theta)$ represents the matrix defining the inertial components of joint moments, $H(\theta, \dot{\theta})$ represents the Coriolis component, and $G(\theta)$ represents the gravitational component of the body segments. The predominant torque component in this equation is due to the static gravity component $G(\theta)$, which is dependant solely on the current joint angles of the model. Also, it has been shown that the dynamic component of the equation ($D(\theta)\ddot{\theta} + H(\theta, \dot{\theta})\dot{\theta}$) accounts for less than 10% of the torque required for standing [43]. Thus the input to this controller was limited to the current angle (θ) of the model. A time based prediction of the angular velocity and acceleration ($\dot{\theta}, \ddot{\theta}$) using results from the validation study was used for the angular velocity and acceleration components of the control law equation.

4.3.2 Feedback component

Joint torques in human motion are produced in part by muscle contractions and muscle viscoelastic passive properties. Fitzpatrick et al. [50] has shown that joint stiffness is partially linked to feedback reflex gain based on studying the effect of sensory feedback on small perturbations during quiet standing. This feedback reflex gain was used in modeling human postural control by Bonnet et al. [51], who modeled the reflex gain as a spring damping system at each joint.

Using this representation of reflex gain, a feedback PD controller was implemented in the model, with the proportional and derivative gains representing the stiffness and viscosity of the spring damping system. Ankle stiffness and viscosity values were obtained from Loram et al. [52], knee stiffness and viscosity were obtained from Zhang et al. [53] and hip stiffness and viscosity were obtained from Cholewicki et al. [54]. All of these studies characterized these parameters in the respective joints as a function of joint position. This enabled a more accurate representation of joint stiffness than if a single average stiffness value was used for each joint. The inputs to the PD controller consisted of the current simulation joint angle and angular velocity and the reference angular position and angular

velocity. The reference angle and angular velocity trajectories were used to drive the model according to the kinematics of a representative human unassisted STS trial obtained from the validation study of the previous chapter.

4.3.3 Simulation model with weakness

To test the different modes of assistance, weakness was simulated in the model by saturating the maximum allowable applied knee torque. Hughes et al. [15] showed that knee extensor strength is a limiting factor for STS in older adults, and a study on failed STS by Riley et al. [27] showed that the maximum knee torque that functionally impaired older adults were able to generate during a failed STS attempt was 95 Nm. Thus, weakness was modeled by saturating the maximum applied torque to the knee joint of the model at 95 Nm.

The weakened model was enabled to rise by an external assist applied to the model. Various locations of assistance were tested to determine if there was a particular best mode. The assist modes, i.e., the locations to test STS assistance, were chosen based on a review of the modes of assist employed by existing STS assistive devices as discussed in Chapter 2 and through a review of manual patient lifting techniques. The literature has shown that existing STS assistive devices predominantly assist users at the buttocks [20] [22] [37] and the arms [19] [16] [17] [18]. A compilation of patient handling techniques by Hollins [55] describing manual STS lifting techniques showed that there are four different locations where assistance is applied to help patients with STS transfer: buttocks, waist, elbows, and upper arms. Based on this information, the buttocks, upper arm, and forearm were chosen as the locations to apply assistance force in simulation (Figure 4.3).

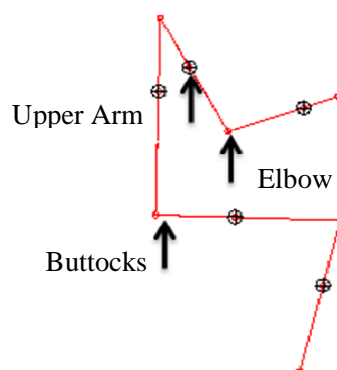


Figure 4.3: Locations of applied assistance on weakened model. Assistance is applied at the buttocks, upper arm and elbow.

4.3.4 Control of weakened model

The previous control scheme of the model was modified to allow for the testing of different modes of STS assistance. A weakness and an assistance component were added to the control scheme as shown in Figure 4.4.

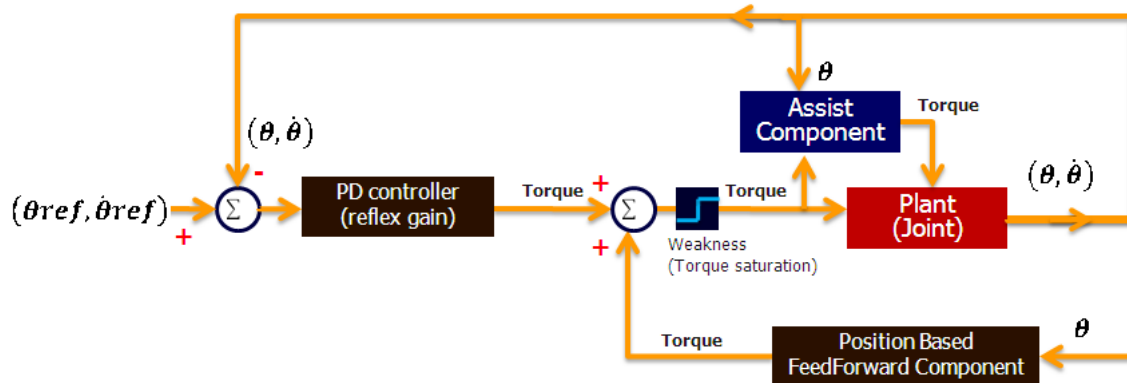


Figure 4.4: Control system of joints for weakened model.

4.3.5 Weakness component

Weakness in the subject was modeled as torque saturation to the knee. The maximum torque command to the knee joint was limited to 95 Nm. Ankle and hip torques were not saturated as they typically are not limiting factors for elders who experience difficulty with STS.

4.3.6 Assist component

The assist force was applied as an external load on the body at the buttocks, elbow, or upper arm (Figure 4.3), and was used to compensate for the weakness imposed through knee torque saturation. The inputs to this component were the current joint angle and current knee torque command after saturation. The assist component predicted the amount of assist required to compensate for the knee torque saturation and applied assistance to the joint accordingly. The control law for this component is the same as control law for the feedforward controller except the control equation was used to compute the assist component in place of the knee torque. Since the saturated knee torque was a known input in the equation, the assist force was substituted as an unknown into the $\vec{T}(\theta)$ matrix of

the feedforward control law in place of the knee torque. Based on the current knee angle and current saturated knee torque, the controller computed the assist force required to compensate for the knee torque saturation and calculated the equivalent joint torque based on this assist force.

4.4 Simulation experiments and cost function

4.4.1 Simulation validation experiment

The first experiment in simulation involved the model performing unassisted STS transfer without weakness imposed through knee torque saturation. This experiment was completed to validate the simulation model by comparing the simulation body segment trajectories and joint torques to reference body segment trajectories and joint torques obtained from a representative trial of the validation study described in the previous chapter. Once the model was validated as an accurate representation of human body segment motions and joint torques, it was used to evaluate different modes of STS assistance.

4.4.2 STS assist modes experiment

STS assistance was investigated by simulating STS transfer on a weakened model and applying assistance force individually at the buttocks, upper arm, and elbow of the model. A cost function was developed to determine which of the three assist modes provided the best assistance. The cost function consisted of three components: a stability component, an assistance component, and a joint torque component.

4.4.3 Stability cost

The stability component evaluated the stability of a particular mode of assist by examining the Center of Pressure (CoP) trajectory of the foot force during the rise. Following the convention given in Schultz et al. [21] where maximum stability during STS was characterized to be when the floor reaction force is centered between the heels and toes, the deviation of the CoP from the foot center was used as the measure of stability. The ankle reaction force (F_{ay}) and reaction moment (M_a) from each simulated mode of STS assisted transfer were used in Equations 4.2 and 4.3 to calculate the CoP of the foot force. Figure 4.5 shows a diagram of the foot with the forces and moments included.

$$F_{foot} = F_{ay} \quad (4.2)$$

$$X_{cop} = (M_a - F_{ay}(\frac{L_f}{2}))/F_{foot} \quad (4.3)$$

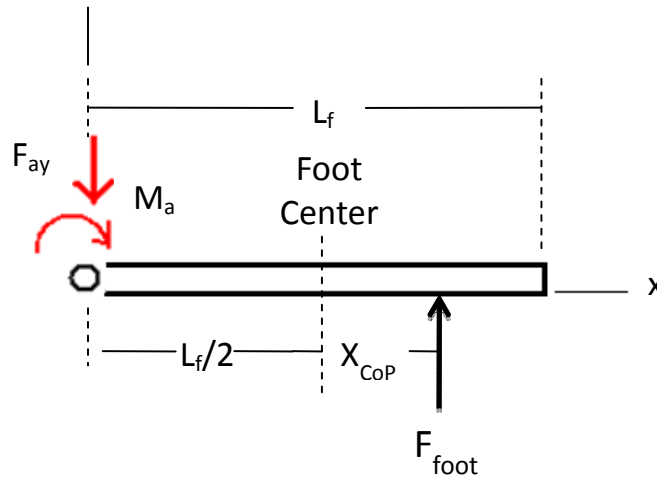


Figure 4.5: Diagram of foot with reaction force locations.

Assist modes were penalized in proportion to the distance between the center of the foot and maximum foot force center of pressure. Equation 4.4 represents the stability cost and Figure 4.6 shows the cost function for stability evaluation.

$$C_{stability} = X_{copmax} / \left(\frac{L_f}{2}\right) \quad (4.4)$$

4.4.4 Assistance cost

The assistance component evaluated the amount of work and time put into assisting the model to a standing position. The assist force (F_{assist}), distance travelled by the assist (d), and the assist time (t_{assist}) were calculated for each mode of assisted STS performed by the model and used as inputs to the cost function. The force and distance was multiplied to obtain the assist work. The maximum assist work in all the simulations was less than 100 Nm and the maximum assist time in all the simulations was less than one second. Thus, the assist work was normalized to a maximum work of 100 Nm and the assist time was normalized over a maximum assist time of one second. Cost function penalties were incurred in proportion to how close the assist work and the assist time was to the

normalized values of work and time for a particular mode of assist. Equation 4.5 shows the assist cost equation, and

Figure 4.6 shows the cost function for assistance evaluation.

$$C_{assist} = 0.5(F_{assist}d)/100Nm + 0.5t_{assist}/1s \quad (4.5)$$

4.4.5 Joint torque cost

The joint torque component evaluated the effects of each mode of assistance on the ankle and hip joints. The inputs to this cost function were the maximum ankle and hip torques from each simulated mode of STS assisted transfer. Assist modes that resulted in an increase in maximum ankle and hip torques ($T_{max_assisted}$) from the maximum unassisted ankle and knee torque ($T_{max_unassisted}$) were penalized. Cost function penalties were incurred in proportion to how close the ankle and hip torques in the assisted motion were to the maximum available torque for the particular joint (T_{max_joint}). The maximum values of joint torques were chosen according to the maximum available ankle and hip joint torques in elderly adults [21]. If the assisted maximum ankle and hip torques were less than the unassisted maximum torques, no cost penalty was incurred. Equation 4.6 shows the torque cost equation and Figure 4.6 shows the cost function for joint torque evaluation.

$$C_{torque} = (T_{max_assisted} - T_{max_unassisted})/T_{max_joint} \quad (4.6)$$

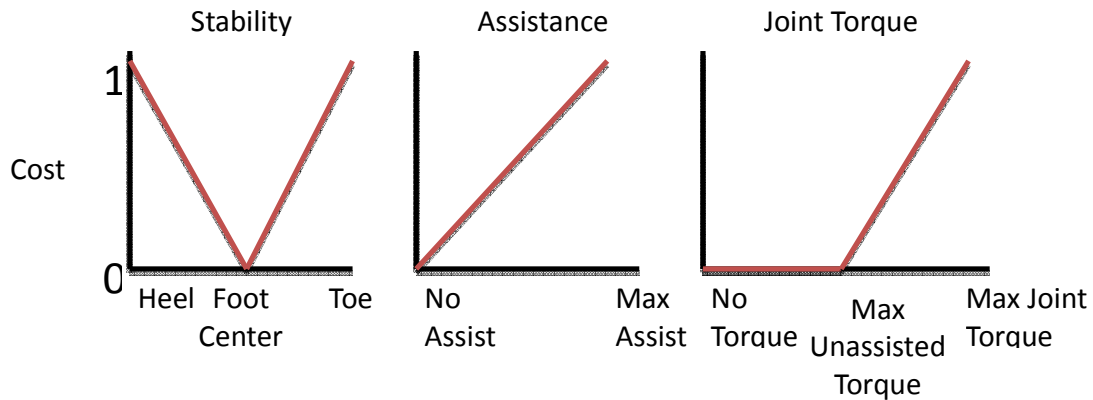


Figure 4.6: Cost functions for stability, assistance, and torque evaluation.

4.4.6 Total cost

The three components of the cost function were combined according to Equation 4.7. Each component of the cost function was given equal importance and therefore weighted equally in the equation. The effectiveness of a particular mode of assist was determined by how close its cost function value was to zero. A comparison of the cost function results of each assist gave a preliminary indication of the best mode of assist for STS assistance.

$$C_{total} = \frac{1}{3}C_{stability} + \frac{1}{3}C_{assist} + \frac{1}{3}C_{torque} \quad (4.7)$$

4.5 Results

Figure 4.7 and Figure 4.8 show the results of the simulation validation experiment. In Figure 4.7, the body segment angles during an unassisted simulated STS transfer were plotted together with the body segment angles of the reference unassisted STS trial. Similarly, Figure 4.8 shows a plot of the simulated joint torque trajectory during an unassisted simulated STS transfer along with the joint torques of the reference unassisted STS trial. The reference values are representative of actual human body segment trajectories and joint torques obtained from the validation study described in the previous chapter.

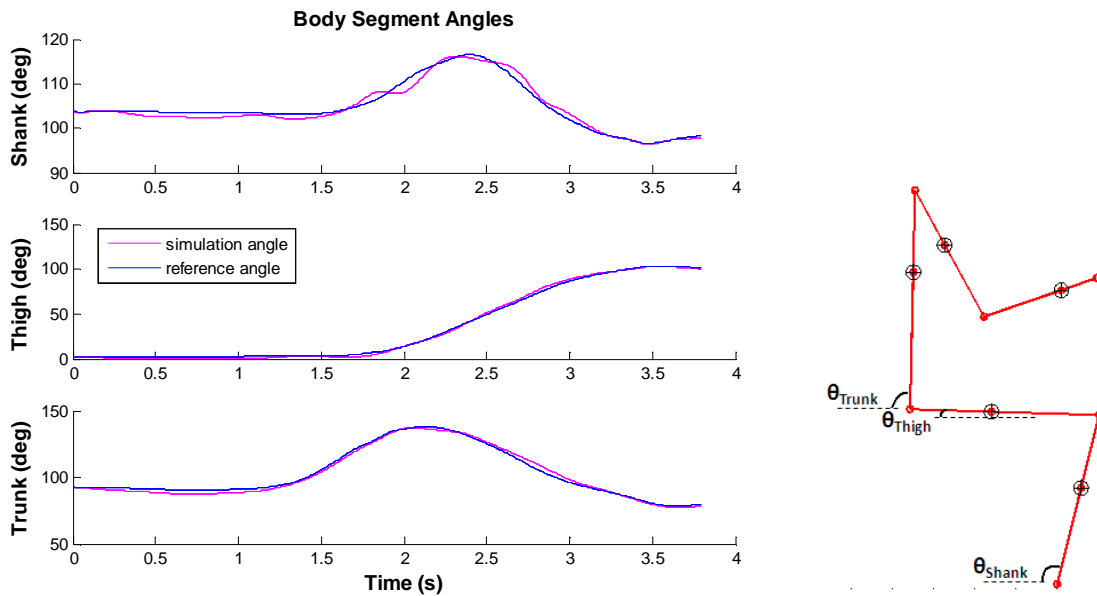


Figure 4.7: Comparison of body segment angles between simulation and reference trajectories for an unassisted STS trial.

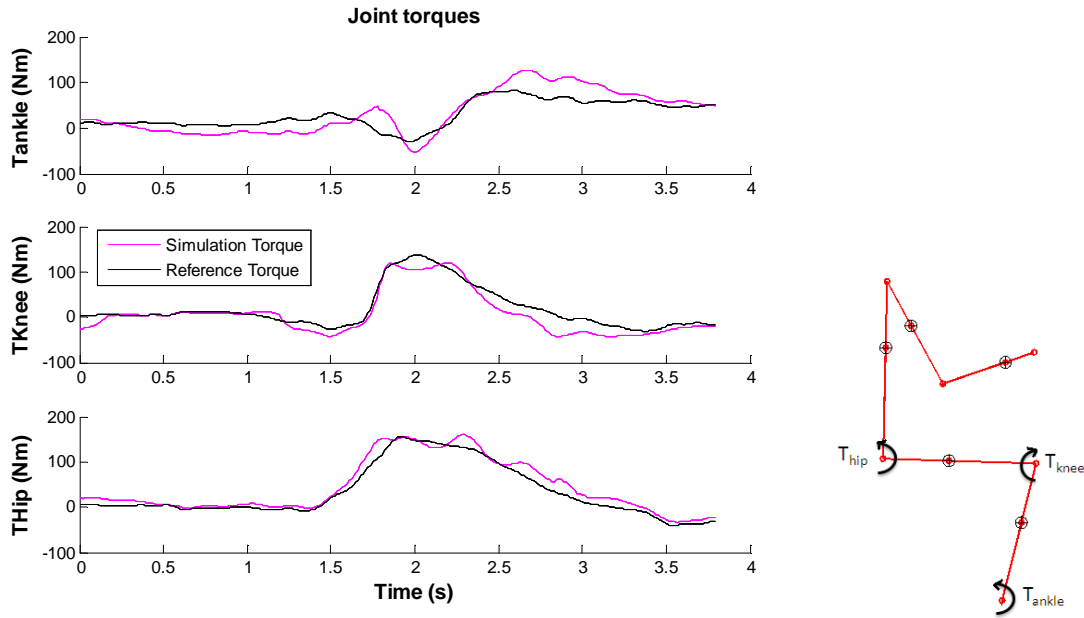


Figure 4.8: Comparison of joint torque trajectories between simulation and reference trajectories for an unassisted STS trial.

The body segment angle trajectory plot shows that the motion of the simulated model closely followed the reference motion for all joint segments as indicated by the low Root Mean Squared Error (RMSE) (Table 4.1), indicating that the PD controller was able to accurately output joint torque reflex gains to track the reference angle input to the controller.

Table 4.1: Root Mean Squared Error of Body Segment Angle Trajectory.

	Shank	Thigh	Trunk
RMSE	0.86	0.97	1.48

The joint torque trajectory plot shows that the torques generated by the model had some deviation from the reference joint torque trajectory as indicated by the RMSE values (Table 4.2). Each of the simulation torque curves is the sum of the feedforward gravity compensation input and the PD reflex input (discussed in Sections 4.3.1 and 4.3.2). Errors in the PD reflex input are due to the use of

generalized PD gains based on average joint stiffness and damping instead of subject specific joint stiffness and damping. Errors in the feedforward gravity compensation input are due to the use of a time based prediction of the angular velocity and acceleration instead of actual model velocity and acceleration in feedforward torque input computations. The combination of these errors results in the deviation of the simulation torque from the reference torque.

Table 4.2: Root Mean Squared Error of Joint Torque Trajectory.

	Ankle	Knee	Hip
RMSE	24.3	16.8	18.43

Although the RMSE values for joint torque trajectory was comparatively higher than the RMSE values for the body segment angle trajectory, the model was considered to be suitable to perform further experiments investigating assisted STS. The reasoning behind this is twofold. First, the cost function only contains one component directly related to the joint torques of the simulation; the other two components are primarily dependent on the joint angle of the simulation, which has been shown to be accurate. Secondly, the purpose of the assisted STS simulation experiments is to compare the merits of the three modes of assist to each other rather than to an absolute standard, thus joint torque inaccuracies should not prevent a valid comparison of the cost function results.

Figure 4.9 shows the results of the cost function analysis that analyzed the effectiveness of the three modes of STS assistance. The overall results of the cost function show that there is little difference in the effectiveness of the three modes of STS assistance. The cost function values of stability were similar for each mode of assist, indicating that all three modes of assisted transfer had similar maximum center of pressure values about the foot. The torque component of the buttocks assist was higher than the upper arm and elbow assist. This was due to the fact that the buttocks assisted rise resulted in a maximum ankle torque higher than the maximum ankle torques during the upper arm and elbow assisted transfers. Conversely, the assist force component of the buttocks assist cost was lower than that of the other two assists since the elbow and upper arm assists required a greater force than the buttocks assist to raise the person to a standing position.

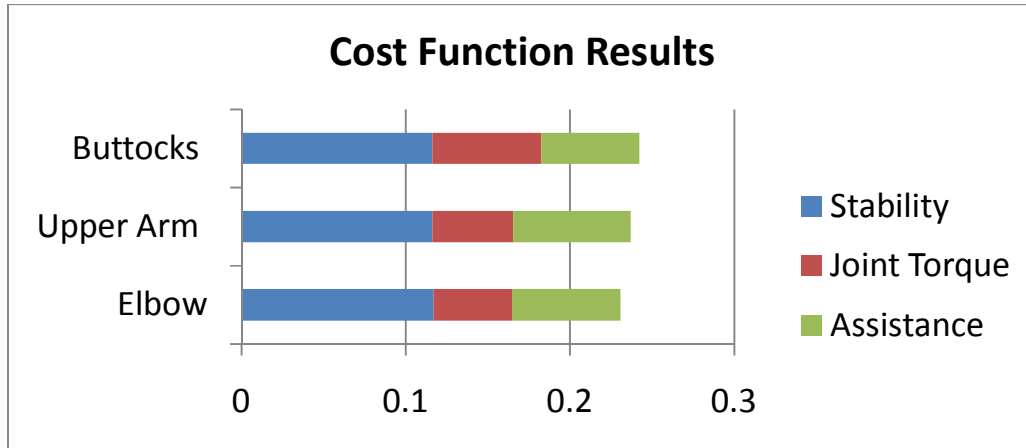


Figure 4.9: Cost function results for three modes of STS assisted transfer.

4.6 Discussion

4.6.1 Simulation results

The most important result of this study was the comparison of the effectiveness of the three different modes of assistance. The experiments investigating different modes of STS assistance showed that there is minimal difference in overall effectiveness of the three locations of assist based on the similarities in the cost function results. This indicates that all three locations are viable for further investigation through a test bed that examines assistance at these locations. Furthermore, the cost function results for the upper arm and elbow assists are very similar except for a slight difference in the assistance cost. This suggests that it may be an option to combine these two assist modes into a single mode of assist for the arms.

4.6.2 Expert opinion

4.6.2.1 Buttocks and waist assist

Advice from physiotherapists in the University of British Columbia Hospital (Joey Lijauco) and Vancouver General Hospital (Joanna Lawrence, Helen Bolton, and Diane Cook) was obtained to corroborate the results of the STS assistance simulation. These experts advised that load assistance for STS should be provided directly to the muscles that are primarily used in the STS transfer, namely the lower back and thigh muscles. Goulart [56] analyzed the electromyographic activity of muscles

activated during STS transfer and showed that the muscles engaged in the execution of STS movement are the quadriceps, hamstrings, and lumbar paraspinal (lower back) muscles. Force applied to the buttocks will directly help reduce quadriceps and thigh muscle requirements, thus it was confirmed that the buttocks is a good location for assist. It was also suggested that the waist be used as an assist location because assistance at the waist can help reduce the lower back muscle requirements as well as quadriceps and thigh muscle requirements. In addition, the waist is used as an assist location in commercially available patient standing assist devices [35].

4.6.2.2 Arm assist

The maximum load that can be applied at the shoulders in humans is significantly lower than loads that can be applied at the hip or knee [21]. Load bearing assistance applied at the arms is fully transferred through the shoulders and can harm elders with frailty in the shoulders if excessive assist forces are applied. Schultz et al. [21] also suggested that inadequate shoulder strength can limit STS ability in some frail people when rising with arm rest assistance. Thus, it was suggested by the physiotherapist that the arm assist be used primarily to guide the STS trajectory instead of providing force assistance.

4.7 Conclusion

A simulation model was developed to perform a preliminary investigation of different STS assist modes to determine if there exists an easily identifiable best mode of STS assistance. The results of the cost function analysis of the assisted STS simulations showed that there was no obvious best mode of assist. Similarities in the cost function results for the upper arm and forearm assists have validated the option of combining these assist modes into a single arm assist. Since the effectiveness of both the buttocks and arm assists have been shown to be comparable, the test bed will be developed to include both of these assist to further investigate their effectiveness in assisting elders with STS. Discussions with physiotherapists to supplement the simulation study confirmed the buttocks as a viable location for providing STS assistance. The functional purpose of the arm assist has been modified to assist primarily with trajectory guidance rather than force assistance. In addition, the waist has been added as a location to test assistance in the Test Bed. The assist modes to be examined by the Test Bed are summarized in the following list.

1. **Seat assist:** Assist force will be applied at the buttocks and assistance will be used primarily to help reduce the joint loads required for standing.
2. **Waist assist:** Assist force will be applied at the waist and assistance will be used primarily to help reduce the joint loads required for standing.
3. **Arm assist:** Assistance at the upper arm and lower arm will be combined and the assistance will be used primarily to guide the STS trajectory.

The next chapter (Chapter 5) presents the design process and detailed design of test bed, including a description of the seat, waist, and arm assist mechanisms developed in accordance with their identification in this chapter as the locations to provide STS assistance.

Chapter 5 Test Bed Design

5.1 Introduction

The literature review, consultation with clinical experts, analysis and simulation presented in the preceding chapters led to the identification of the seat, waist, and arms as key assistance locations to be empirically evaluated in a STS test bed. Furthermore, based on the work reported in the previous chapters, the seat and waist assists were selected for evaluation in a force assistance mode, while the arm assist was selected for evaluation in a trajectory guidance mode. The next step to achieving the thesis objective of providing an empirical quantification of different modes of load-sharing STS was to design and build a test bed to provide assistance at these three locations. The design and development of the test bed involved four main stages, illustrated in Figure 5.1. This chapter describes the four test bed design stages: the specification of functional design requirements; experiments with a critical function prototype to help quantify the force and trajectory specifications listed in the functional design requirements; the design of the test bed; and the validation of the functional design requirements based on pilot studies with the test bed.

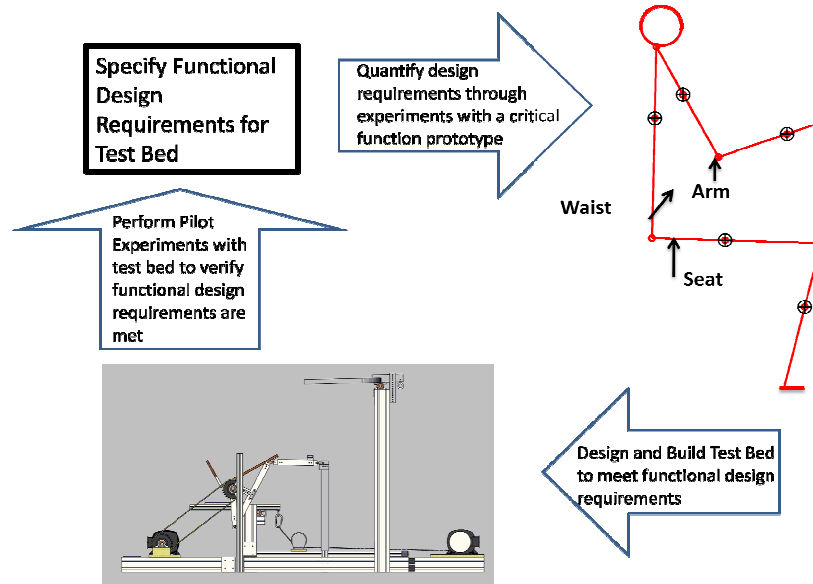


Figure 5.1: Schematic of the test bed design process. The design process is initiated by specifying target functional design requirements (top left corner of schematic).

5.2 Test bed functional design requirements

Based on the research reported in the preceding chapters, the test bed must be able to provide assistance with STS to older adult subjects at the seat, waist, and arms. Assistance at the seat and waist should primarily provide load-sharing knee torque reduction, and assistance at the arms should primarily provide trajectory guidance. These test bed assistance requirements were translated into four specific functional design requirements, presented as follows:

- i. Provide assistance at the waist and seat such that a user can rise from a normal chair height (thighs parallel to the ground) to a standing position, while ensuring that the user provides a knee torque greater than 35% of the knee torque required to rise unassisted.
 - The knee torque range was chosen based on a study on knee torques during STS in young and functionally impaired older adults [15]. The young healthy adults in this study used 35% of their available knee strength to rise whereas the functionally impaired older adults used up to 97% of their available knee strength to rise. Because functionally impaired older adults may use close to 100% of available knee strength to rise, the seat and waist assists should reduce the knee strength required to rise. Additionally, to help maintain strength, the assists should also ensure that users contribute at least the same amount of knee strength to rise as a young healthy adult. Therefore, to ensure load sharing between user and assist, it was decided that the waist and seat assist should be designed such that users are required to contribute at least 35% of the knee torque required for them to rise without assistance (assuming that when rising without assistance users employ close to 100% of their available knee strength).
- ii. Provide an arm assist trajectory such that when guided by the arm assist, users employ a MT STS strategy characterized by a peak trunk flexion of 51°.
 - As discussed in the literature review, Scarborough et al. [25] concluded that a MT strategy is the safest and most preferred for STS because of stability and success in rising. The goal of the arm assist, therefore, is to guide the trajectory of the arms such that a MT strategy is employed. Scarborough et al. also classified the strategies for STS according to the maximum trunk flexion achieved during the rise. The MT strategy was associated with a mean peak trunk flexion of 51° (SD 3.8°), the DVR and ETF strategies were associated with mean peak trunk flexions of 35° (SD 4.6°) and 64° (SD 5.4), respectively [25] (refer back to Section 2.2).
- iii. Assist users to rise to a standing position with a rise time of two to four seconds.
 - This requirement is based on natural STS speeds in older persons [57].
- iv. Accommodate users with a height range of 150 cm to 185 cm and mass up to 90 kg.

- This requirement is based on the maximum range of heights among men between the ages of 65 and 69 [58] and the 75% percentile mass of a 70 yr. old male [59].

5.3 Critical function prototype experiment

5.3.1 Introduction

An experimental critical function prototype was developed to quantify the functional design requirements related to user weight and trajectory. The prototype provided manual assistance at the seat, waist, and arms. Experiments with the prototype were completed and the following force and kinematic data were collected to help determine the maximum required assist load for the load bearing seat and waist assists as well as the required trajectories for the trajectory guiding arm assist. This information was used in the design of test bed actuation and the design of the arm guidance assist mechanism. The two specific objectives for the critical function prototype experiment (illustrated in Figure 5.2) were to:

- Provide manual load bearing assistive forces at the seat and waist of subjects using the prototype and quantify the amount of force necessary to assist a 90 kg person at the seat and waist.
- Provide a force at the arms of subjects to direct the trajectory of subjects during the STS motion and quantify the trajectory through which the arms pass as subjects rise to a standing position.

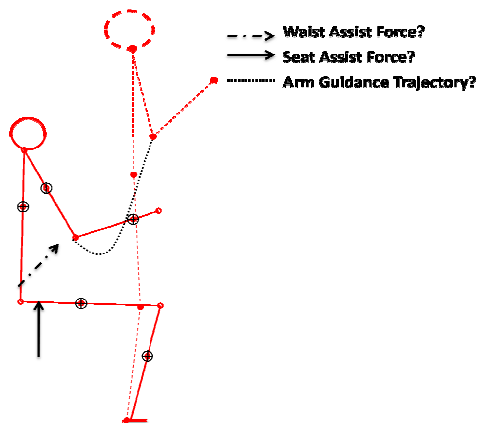


Figure 5.2: Locations at which test bed must provide assistance. Before developing the test bed, the maximum assist force for waist and seat assistance and the trajectory for arm guidance assistance must be quantified.

5.3.2 Experimental procedure

5.3.2.1 Test subjects

Three healthy male subjects between the ages of 22 and 32 were used in the critical function prototype experiments. The average mass was 71 kg (SD 12 kg, range 61-89 kg) and the average height was 1.75 m (SD 0.09 m, range 1.65 m-1.85 m)

5.3.2.2 Test equipment

The prototype consisted of two components: a force transmitting cradle and a test frame (Figure 5.3). The force transmitting cradle was used to manually assist subjects to a standing position at the seat, waist, or arms. The cradle consisted of 3 segments: a lifting structure, a six-axis AMTI (Advanced Medical Technology Incorporated) load cell, and an interface support. To perform manually assisted rises, forces and torques were applied by the experimenter to the subject via the force transmitting cradle. The location of the load cell between the lifting structure (held by the experimenter) and the interface support (interfaced to the subject) allowed for measurement of the forces and torques applied to the subject during the assisted rise.

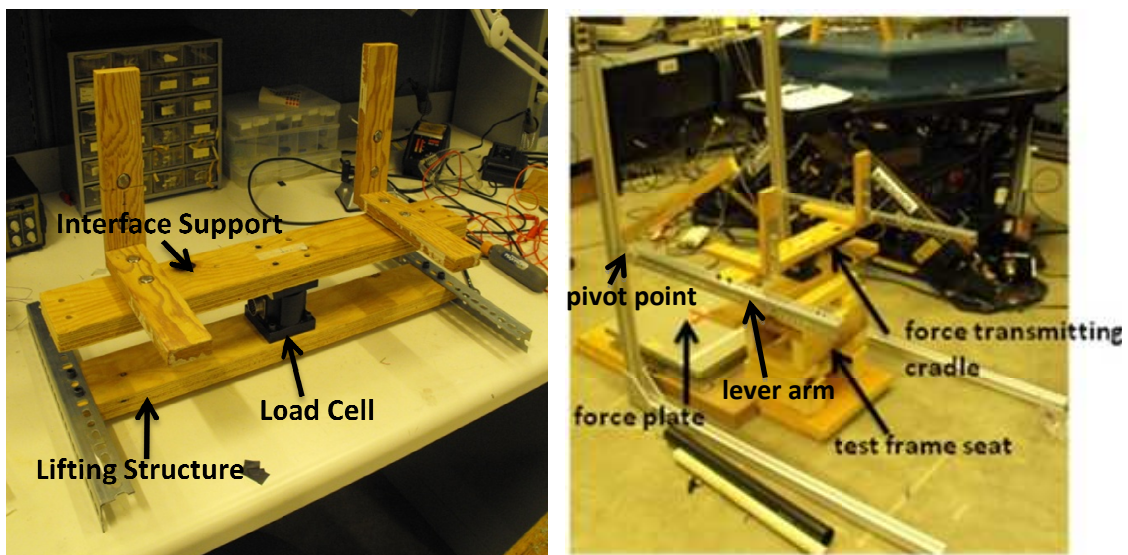


Figure 5.3: Left image: force transmitting cradle. Right Image: test frame with force transmitting cradle attached and configured for seat assist.

The test frame was used to constrain the motion of the force transmitting cradle to a one degree of freedom rotation for the waist and seat assists. Lever arms on the frame were attached to the force transmitting cradle and rotated about a pivot point on the frame. The height of the lever arms was adjusted to provide either waist assistance or seat assistance. Subjects were seated on a height adjustable seat within the test frame. An AMTI 6-axis foot force plate was placed in the test frame to collect the ground reaction force data for each STS experiment. Figure 5.3 shows a picture of the test frame with the force transmitting cradle attached and configured to provide assistance at the seat. In addition to the prototype apparatus and force sensors, four orientation sensors (Xsens Motion Technologies), were used in experiments. Three sensors were attached to the subject's shank, thigh and trunk to collect kinematic data from the motion of the subjects and one orientation sensor was attached to the force transmitting cradle to measure the rotation of the cradle (Figure 5.4).

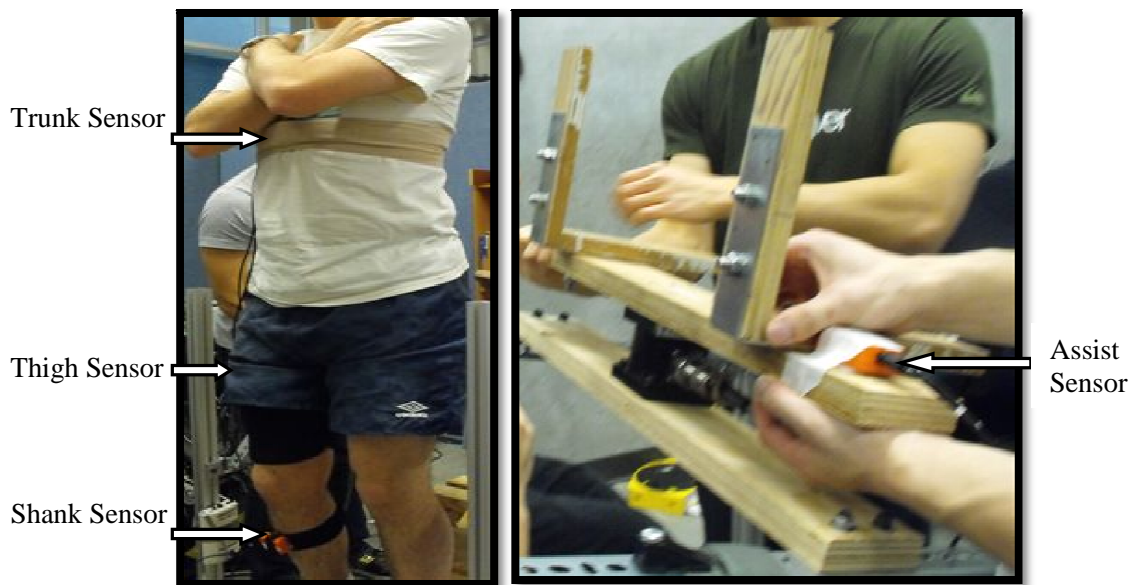


Figure 5.4: Left image: Orientation sensor locations on subject. Sensors attached to shank, thigh and trunk (thigh and trunk sensors not visible). Right Image: Orientation sensor on force transmitting cradle.

5.3.2.3 Experimental setup and STS modes

The critical function prototype was built to provide four modes of STS namely: unassisted, seat-assisted, waist-assisted and arm-assisted STS rises. A lead experimenter supervised the motion of each mode of assist, and the manual assistance (lifting) for each of the assisted STS modes was provided by two experiment assistants.

Unassisted STS mode: The unassisted STS mode was configured by attaching the force transmitting cradle to the test frame lever arms. The subject was seated onto the interface support of the force transmitting cradle and rose to a standing position without any manual assistance from the experiment assistants (Figure 5.5).

Seat-assisted STS mode: The seat assisted STS mode was configured by attaching the force transmitting cradle to the test frame lever arms. The subject was seated on the interface support of the force transmitting cradle and assistance was provided through a normal force applied to the lifting structure of the cradle by the experiment assistants. The lever arms rotated about the pivot point on the test frame and moved the subject in a forward and upward motion to a standing position (Figure 5.5).

Waist-assisted STS mode: The waist-assisted STS mode was configured by attaching the force transmitting cradle to the lever arms and raising the lever arms to the top of the frame. The subject was seated on the test frame seat, and straps were attached from the waist of the subject to the lifting structure of the force transmitting cradle. Assistance was provided through a normal force applied to the interface support of the cradle by the experiment assistants. The resulting rotation of the lever arm about the pivot point transmitted force through the waist strap and assisted the subject to a standing position (Figure 5.5).

Arm-assisted STS mode: The arm assist STS mode was configured by seating the subject on the test frame seat and placing the interface support of the force transmitting cradle under the subject's elbows. A forward and upward force was applied to the lifting structure of the cradle by the experiment assistants and the subject was raised to a standing position (Figure 5.5).

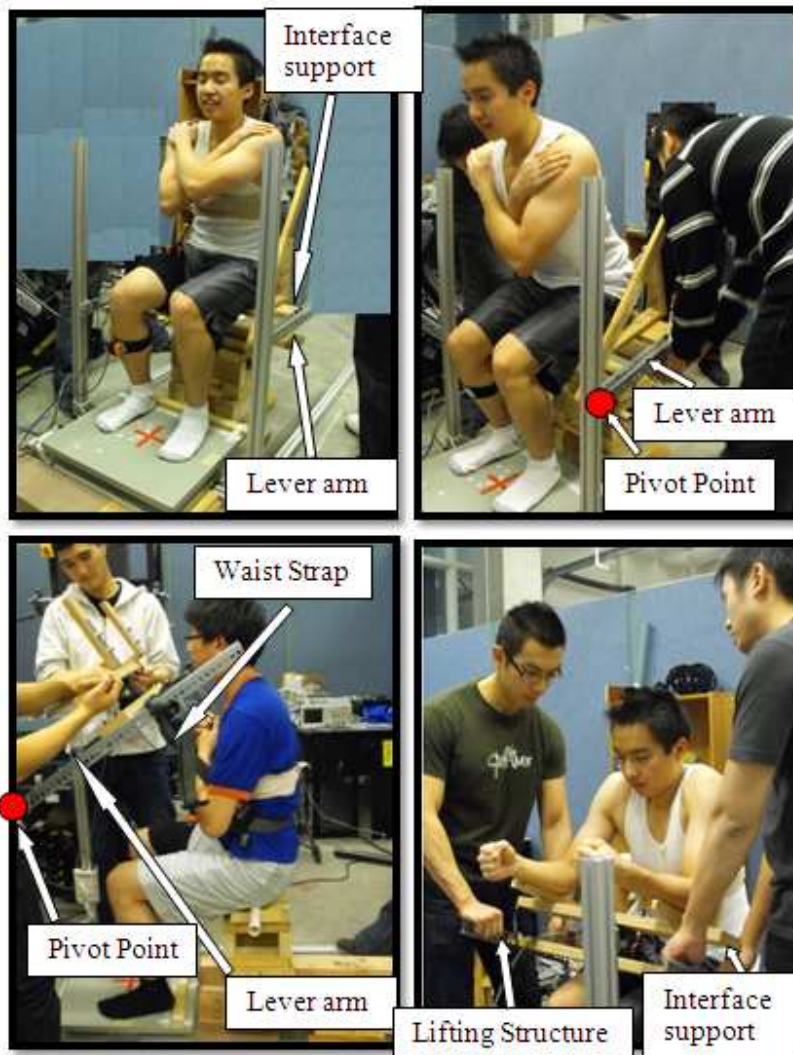


Figure 5.5: Four modes of STS. Clockwise from top left corner: unassisted, seat-assisted, arm-assisted and waist-assisted STS.

5.3.2.4 Set-up and procedure

At the beginning of the experimental procedure, the force plate and load cell were zeroed to correct for drift. Also, orientation sensor measurements were referenced to a predefined world coordinate frame by aligning the sensors with the world frame and then zeroing the sensors. Subject anthropometric data were then measured and recorded as described in Section 5.3.2.5 (see below).

Next, the Xsens orientation sensors were attached to a standing subject using adjustable straps, Figure 5.4. Sensors were attached to the shank, thigh, and chest at the CoM of each segment. The CoM location was determined using approximate anthropometric coefficients based on segment lengths [46]. A sensor was also attached to the force transmitting cradle, Figure 5.4. The subjects were then seated in the test frame with their feet positioned on the force plate. The position of the feet was adjusted to be similar for all subjects by using a wooden block attached to the force plate to locate the heel position of each subject. Foot position was also symmetrical about the longitudinal force plate axis.

Table 5.1: STS trials and modes.

	STS Mode			
	Unassisted	Seat Assist	Waist Assist	Arm Assist
Number of normal seat height trials	5	5	5	5
Number of lowered seat height trials	-	2	2	-

Experiments were conducted using each of the four STS modes: unassisted, seat-assisted, waist-assisted, and arm-assisted. Table 5.1 provides an overview of the total number of experiment trials performed. A trial was defined as a single STS motion performed under the conditions for the particular mode of STS rise (conditions for each mode of STS were detailed in Section 5.3.2.3). For the seat-assisted and waist-assisted STS modes, trials were conducted with chair height adjusted to a normal seat height (subject thighs parallel to the ground) and a lowered seat height (normal seat height lowered by three inches) to compare the amount of force required to provide assistance at each chair height.

Five unassisted reference STS trials were conducted at the start of the experiment. Each subject sat with trunk erect and waited for a verbal cue from the lead experimenter before starting the STS movement. After the verbal cue, the subject stood at a self-selected speed and, once standing, maintained a balanced upright position until asked to be seated again.

For the seat and waist assistance modes, subjects performed seven assisted trials in which force assistance was provided by the experiment assistants to lift the subject to a standing position. Five trials were completed with the chair height adjusted to a normal seat height, and two trials were

completed at a lowered seat height. The subject sat with trunk erect, and assistants stood on both sides of the subject with their hands on the lifting structure of the force transmitting cradle. Upon a verbal cue from the experiment leader, the experiment assistants raised the force transmitting cradle to assist the subject to a standing position.

For the arm assist mode, each subject performed five trials while a force was provided by the experiment assistants at the arms of the subject to direct their trajectory during the STS motion. Five trials were completed at the normal seat height. Subjects sat with trunk erect and experiment assistants stood on both sides of the subject with their hands on the lifting structure of the force transmitting cradle. Upon a verbal cue from the experiment leader the experiment assistants guided the force transmitting cradle and directed the trajectory of the subject to a standing position through a forward and upward motion.

5.3.2.5 Data collection and post processing

Anthropometric data were collected prior to experiments (Table 5.2). Body segment lengths were found by palpation at joints to find the point of rotation. The seat assist force location was measured prior to the seat-assisted rise, and the waist assist force location was measured prior to the waist-assisted rise. The subject weight and shank length, thigh length and head/arm/torso length were fed into a spreadsheet to calculate body segment masses, CoM locations, and moments of inertia.

Table 5.2: Measured anthropometric data.

Anthropometric Data	Measurement
Weight	vertical force on force plate
Height	heel to crown of head
Shank Length	femoral condyles / medial malleolus
Thigh Length	greater trochanter / femoral condyles
Head/arms/torso length	greater trochanter/ glenohumeral joint
seat assist force location	center of force transmitting cradle/femoral condyles
waist assist force location	greater trochanter/connection point of waist assist straps to waist

The force and orientation sensor data collection was initiated two seconds before the verbal rise cue and lasted approximately five seconds for each trial. Data collected from the force plate, load cells, and orientation sensors are listed in (Table 5.3). Reaction forces were collected from the force plate

and the six-axis force sensor at a frequency of 50 Hz and were digitally filtered with a zero-phase lag, bi-directional, fourth-order, low pass Butterworth filter with a cut-off frequency of five Hz. Orientation sensor data were also collected at a frequency of 50Hz and filtered in the same way as the force plate data. The accelerometer data were gravity compensated using angular position data from the orientation sensors to negate the gravity force readings on the sensors. All data filtering and gravity compensation were computed offline in Matlab after the trials were completed.

Table 5.3: Measured orientation sensor and force plate data. The force plate, load cell and orientation sensors each have their own coordinate frame, thus the subscripts x,y,z represent the individual axes of these coordinate frames.

Force plate measures	6-axis load cell measures	Orientation Sensor Measurements
F_x	F_x	Linear Acceleration (a_x, a_y, a_z)
F_y	F_y	Angular Velocity ($\omega_x, \omega_y, \omega_z$)
F_z	F_z	Angular Position ($\theta_x, \theta_y, \theta_z$)
M_x	M_x	
M_y	M_y	
M_z	M_z	

5.3.2.6 Data analysis

The data were analyzed to determine the maximum loads required to assist subjects at the seat and waist and to determine the trajectory of the elbows in each of the four STS modes.

5.3.2.6.1 Waist and seat force data averaging

For the waist-assisted and seat-assisted rises, the assistance force was applied normal to the force transmitting cradle. Thus, all of the assist force was transmitted through the z-axis of the 6-axis load cell. The peak assist force was measured for each of the five normal seat height seat-assisted and waist-assisted trials (F_{z_s} & F_{z_w}) and the two lowered seat height seat-assisted and waist-assisted trials ($F_{z_{sl}}$ & $F_{z_{wl}}$). The average of these forces was calculated as shown in Table 5.4.

Table 5.4: Measured maximum assist forces for each of the waist-assisted and seat-assisted trials.

	Trial 1	Trial 2	Trial 3	Trial 4	Trial 5	Average
Max Assist Force <small>Normal Seat-Assisted Trial</small>	$F_{z_{s1}}$	$F_{z_{s2}}$	$F_{z_{s3}}$	$F_{z_{s4}}$	$F_{z_{s5}}$	$\Sigma F_{z_s}/5$
Max Assist Force <small>Lowered Seat-Assisted Trial</small>	$F_{z_{sl1}}$	$F_{z_{sl2}}$				$\Sigma F_{z_{sl}}/2$
Max Assist Force <small>Normal Waist-Assisted Trial</small>	$F_{z_{w1}}$	$F_{z_{w2}}$	$F_{z_{w3}}$	$F_{z_{w4}}$	$F_{z_{w5}}$	$\Sigma F_{z_w}/5$
Max Assist Force <small>Lowered Waist-Assisted Trial</small>	$F_{z_{wl1}}$	$F_{z_{wl2}}$				$\Sigma F_{z_{wl}}/2$

5.3.2.6.2 Waist and seat force data scaling

After averaging the maximum assist forces for each of the four conditions shown in Table 5.4, the average forces were then scaled according to Equation 5.1 to represent the required assist load for a subject with a 90 kg mass. This scaled force was then averaged between the three subjects and multiplied by a design factor of 1.2 according to Equation 5.2 to represent the maximum assist force required by a 90 kg subject.

$$F_{scaled} = (Max\ Assist\ Force) \left(\frac{90}{subject\ mass} \right) \quad (5.1)$$

$$F_{scaledavg} = (1.2) \Sigma F_{scaled} / 3 \quad (5.2)$$

5.3.2.6.3 Elbow trajectory calculation

To calculate the elbow assist trajectory for each of the assists, the kinematic data obtained from the Xsens sensors for each set of experiments was put into the three-link simulation model developed in Chapter 4. An inverse dynamics analysis was run in simulation so that the model was constrained to follow the exact reference kinematics provided by the Xsens sensors, and the profile of the elbow joint trajectory was recorded.

5.3.3 Results

5.3.3.1 Assist force results

The average maximum assist force of the five normal seat and two lowered seat heights for the seat and waist assist assists are shown in Table 5.5 and Table 5.6. The maximum of these two forces is underlined for each subject and this maximum force has been scaled to represent the assistance force

required by a 90 kg person (based on Equation 5.1). The average scaled force for each assist is also shown (based on Equation 5.2).

Table 5.5: Maximum assist forces required for seat-assisted STS.

Seat Assist: Max Assist Forces

Seat Assist	Subject 1	Subject 2	Subject 3
Subject Mass (kg)	62	66	86
Normal Seat Height Maximum Force (N)	390	<u>465</u>	<u>520</u>
Lowered Seat Height Maximum Force (N)	<u>415</u>	420	325
Scaled Max Force (N)	600	636	545
Average Scaled Force (N)	715		

Table 5.6: Maximum assist forces required for waist-assisted STS.

Waist Assist: Max Assist Forces

Waist Assist	Subject 1	Subject 2	Subject 3
Subject Mass (kg)	62	66	86
Normal Seat Height Maximum Force (N)	170	165	190
Lowered Seat Height Maximum Force (N)	<u>235</u>	<u>250</u>	<u>280</u>
Scaled Max Force (N)	340	342	293
Average Scaled Force (N)	390		

5.3.3.2 Assist trajectory results

The elbow joint trajectory for the arm-assisted STS was calculated for each subject. In addition, elbow trajectories for the unassisted, seat-assisted, and waist-assisted rises were also calculated for each subject. Arm-assisted STS results were only obtained for Subjects 1 and 2. Subject 3 did not complete the arm-assisted rise, due to reported discomfort when rising with assistance. The elbow trajectories of a representative subject performing each of the four modes of STS are shown in Figure 5.6. Note that x-y plane used in the following plots of arm trajectories (Figure 5.6, Figure 5.12, Appendix A, and Appendix B) map to the y-z plane in the test bed coordinate frame described in test bed experiments (Chapter 3 and Chapter 6).

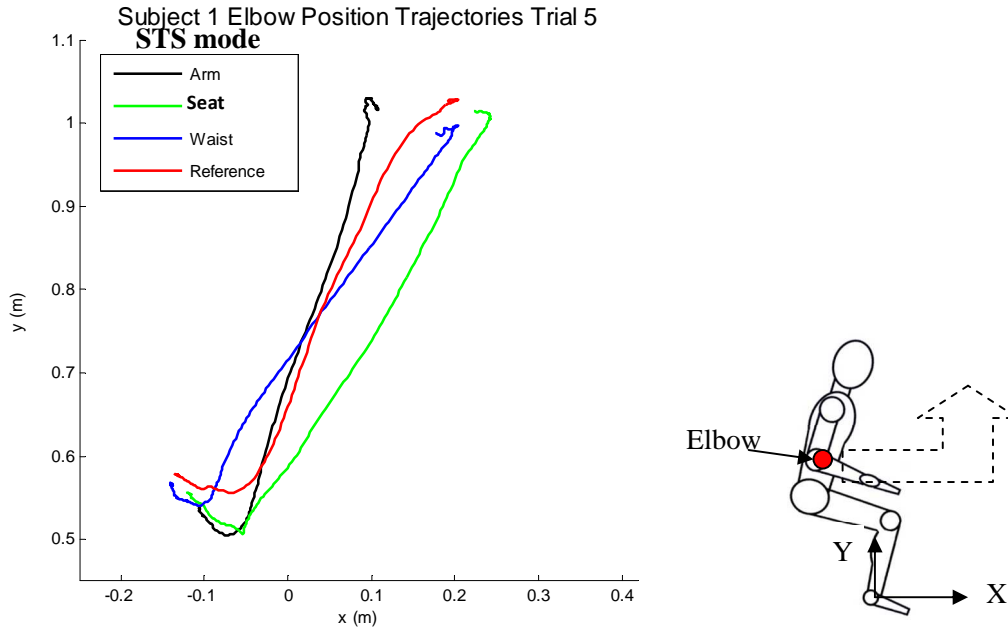


Figure 5.6: Trajectory of the elbow as the subject rises to a standing position for each assisted motion. The x-y coordinate frame origin of the graph is located at the ankle of the subject as shown on the human model diagram to the right of the plot.

5.3.4 Discussion and outcomes

Tables 5.5 and 5.6 show that the average scaled assist force, representing the maximum assist force that the test bed should provide, is 715 N for the seat assist and 390 N for the waist assist. These values will be used to design the actuator that will provide the seat and waist assistance.

Figure 5.6 shows four representative curves of the elbow trajectory during STS. The test bed arm guidance mechanism should be able to follow these trajectories to help guide the trajectory of the subject during assisted STS. The ability to follow the elbow trajectory of the seat-assisted and waist-assisted motion will increase the functional ability of the test bed to test a combination of the arm assist with one of the other two assists in addition to testing assists individually.

5.4 Initial test bed design

Utilizing the information provided by the critical function prototype experiments discussed in the previous section, a test bed was developed by a team of undergraduate students as a senior design project, with the author in the role of client representing the sponsor, the CARIS Lab. The test bed developed by the students consisted of a test frame with three integrated subsystems providing the seat, waist and arm assists. A diagram of their design is shown in Figure 5.7. The students built the framework of the test bed, including each of the assist mechanisms and wrote a detailed design report of their work [60]. Upon completion, the author then evaluated, extensively tested, and substantially revised the test bed to meet the safety, reliability, reconfiguration, data collection and control requirements for the proposed experiments. This section reviews the main components of the test bed as designed by the student team. The follow sections cover the additions and revisions made to the test bed design.

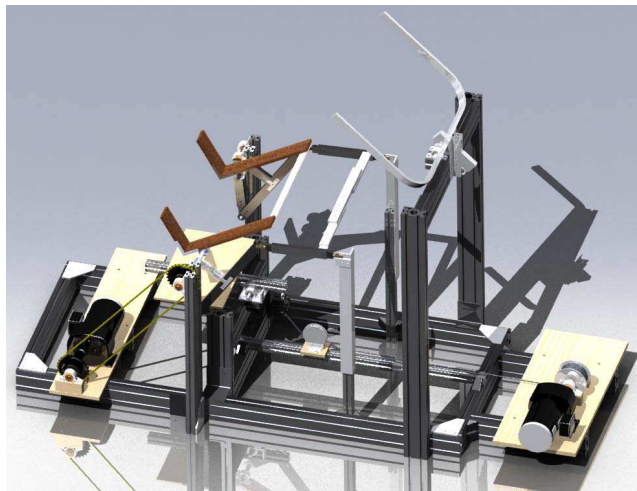


Figure 5.7: Initial sit-to-stand test bed design [60].

5.4.1 Test bed frame

The test bed frame was constructed using 4x4 cm and 5x10 cm slotted aluminum struts obtained from Item® [61]. The test bed consists of a seat platform and three assist mechanisms to provide STS assistance: a seat assist a waist assist, and an arm assist. Each of the individual assists was attached

to the frame in the configuration shown in Figure 5.8. The seat platform of the test bed had the dual functionality of serving as the seat assist as well as the user support for the starting position of the other assists. The design included two motors for actuation, the rear motor for actuation of the arm assist and the front motor for actuation of the seat and waist assist.

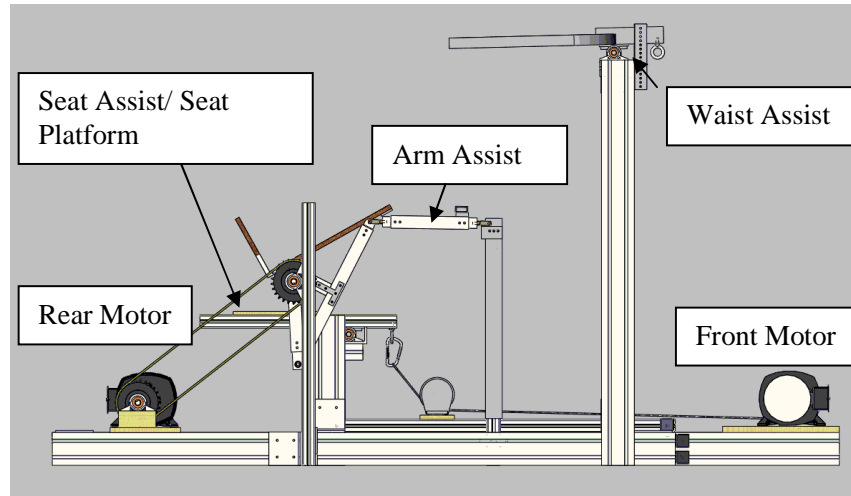


Figure 5.8: Side view of original test bed solution [60].

5.4.2 Seat assist mechanism

The seat assist mechanism developed by the students, representative of chair-mounted lifting aids [38], consists of a lever arm rotating about a pivot (Figure 5.9). A wooden seat is attached to one end of the lever arm and a cable is attached to the opposite end of the arm. The cable passes under a pulley and is wound up by a motor onto a spool. Actuation of the motor pulls the cable, rotating the lever arm about the pivot. This rotates the seat forward, raising the user to a standing position. The seat position is adjustable to allow for users within the height range of 150 cm to 185 cm to be seated. Calculations were completed to ensure that the maximum seat force of 715 N can be applied by the motor and the motor rotation speed allows the user to rise to a standing position in the time range of two to four seconds as specified in the functional requirements. These calculations can be found in the appendix of the student report [60], Appendix A.

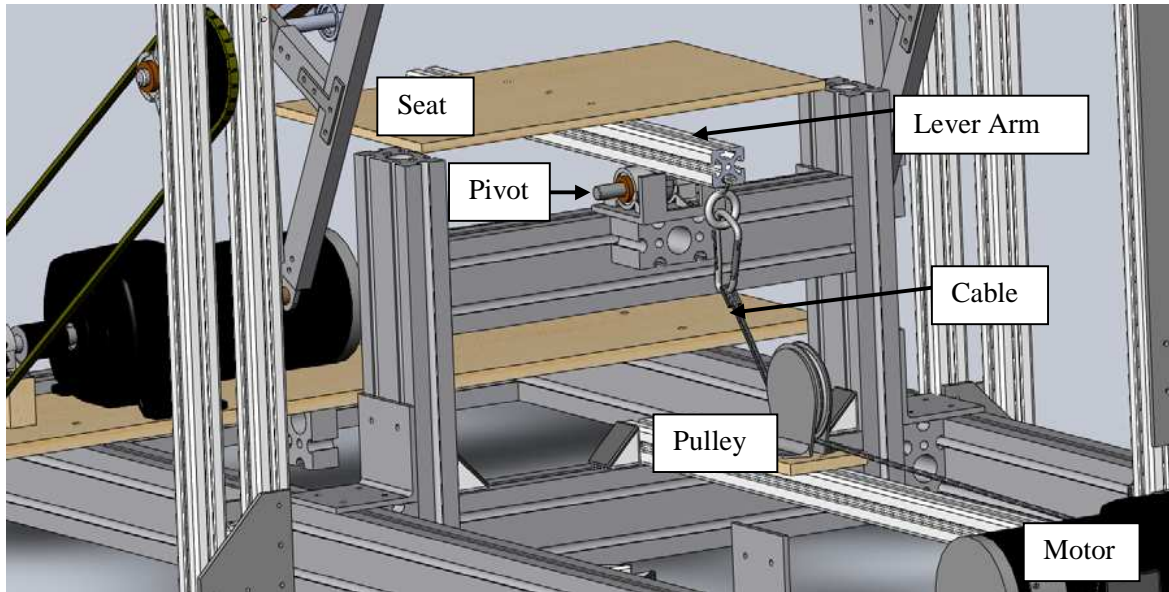


Figure 5.9: Diagram of seat assist mechanism [60].

5.4.3 Waist assist mechanism

The waist assist mechanism developed by the students, representative of many institutional lifts [35], also consists of a lever arm rotating about a pivot (Figure 5.10). A U-bar is attached to one end of the lever arm and a cable is attached to the opposite end of the arm. The cable is actuated by a motor, and tension in the cable rotates the arm about the pivot and raises the U-bar to a vertical position. A padded medical transfer belt (Lancaster Medical Supplies - not shown in diagram) is fastened about the user's waist and attached to waist straps connected to the U-bar. As the U-bar is raised to a vertical position, the user is transferred from a seated to standing position. Adjustability of the waist strap length allows for users within the height range of 150 cm to 185 cm to be assisted. Calculations were completed to ensure both that the maximum waist force of 390 N can be applied by the motor and that the motor rotation speed allows the user to rise to a standing position in the time range of two to four seconds as specified in the functional requirements. These calculations can be found in the appendix of the student report [60], Appendix A.

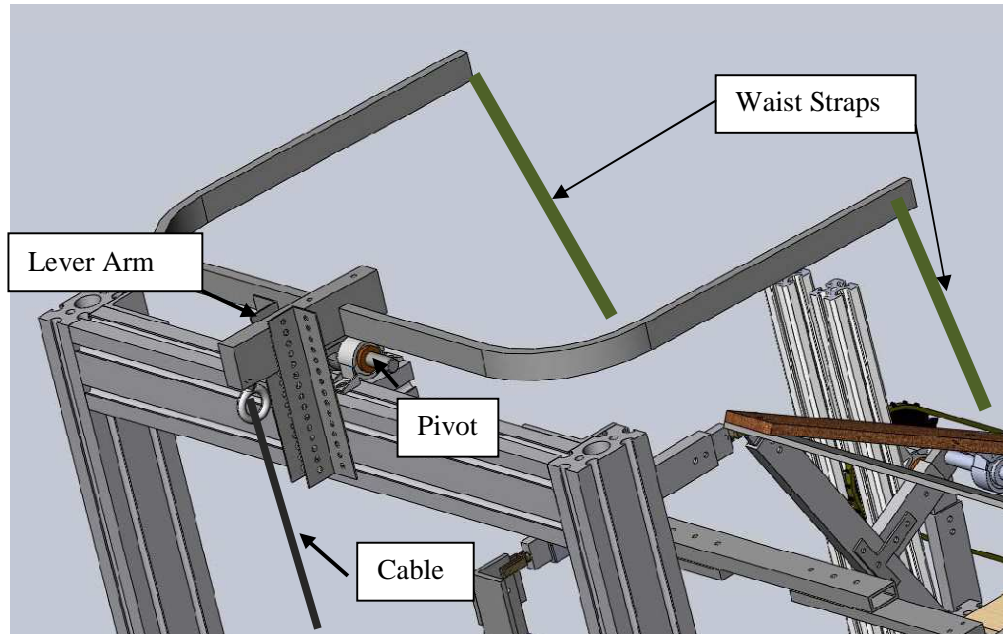


Figure 5.10: Diagram of waist assist mechanism [60].

5.4.4 Arm assist mechanism

The purpose of the arm assist is to guide the trajectory of the users as they rise. The arm assist mechanism developed by the students, based on assistive devices in research and development that provide assistance at the arms [16] [62], is composed of a 4-bar linkage and an arm cradle (Figure 5.11). The 4-bar linkage guides the arms of a user based on the trajectories of arm motion determined in the critical function prototype; the arm cradle is the interface between the user's arms and the 4-bar linkage.

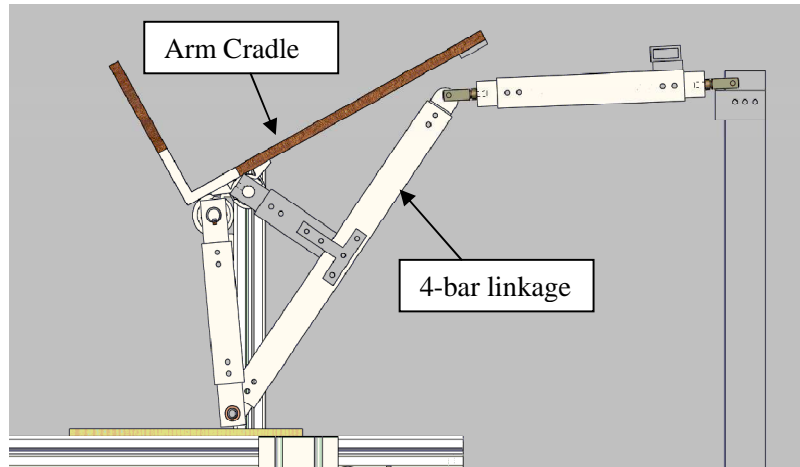


Figure 5.11: Diagram of arm assist mechanism [60].

5.4.4.1 Four-bar linkage

The 4-bar linkage was designed to guide the trajectory of the user through the STS motion. The linkage lengths of the 4-bar linkage were selected such that the trajectory provided by the 4-bar linkage would match the elbow trajectories of each of the four modes of STS carried out in the prototype experiments (Figure 5.6). These linkage lengths were determined by generating 4-bar linkage trajectories in Matlab and matching the trajectories to the trajectories obtained in the critical function prototype experiment. The linkage lengths and 4-bar linkage trajectory plots are in the student design report [60], and can be viewed in Appendix A and Appendix B.

The linkages were designed to have adjustable lengths to allow for the arm guidance mechanism to follow the arm trajectories of any of the 4 modes of STS rise. This enables the arm assist to be combined with the seat and waist assist in addition to providing assistance by itself. Linkage R2 is the driver linkage. As it rotates, the user is guided into a standing position through a trajectory determined by the linkage lengths. Figure 5.12 shows the 4-bar linkage trajectory and a table of the corresponding link lengths to obtain an elbow trajectory similar to one of the reference unassisted trajectories in the prototype experiment. The student report [60] contains trajectory plots and link length tables for the 4-bar linkage trajectory matching each of the other three elbow trajectories shown in Figure 5.12 (Appendix A and Appendix B).

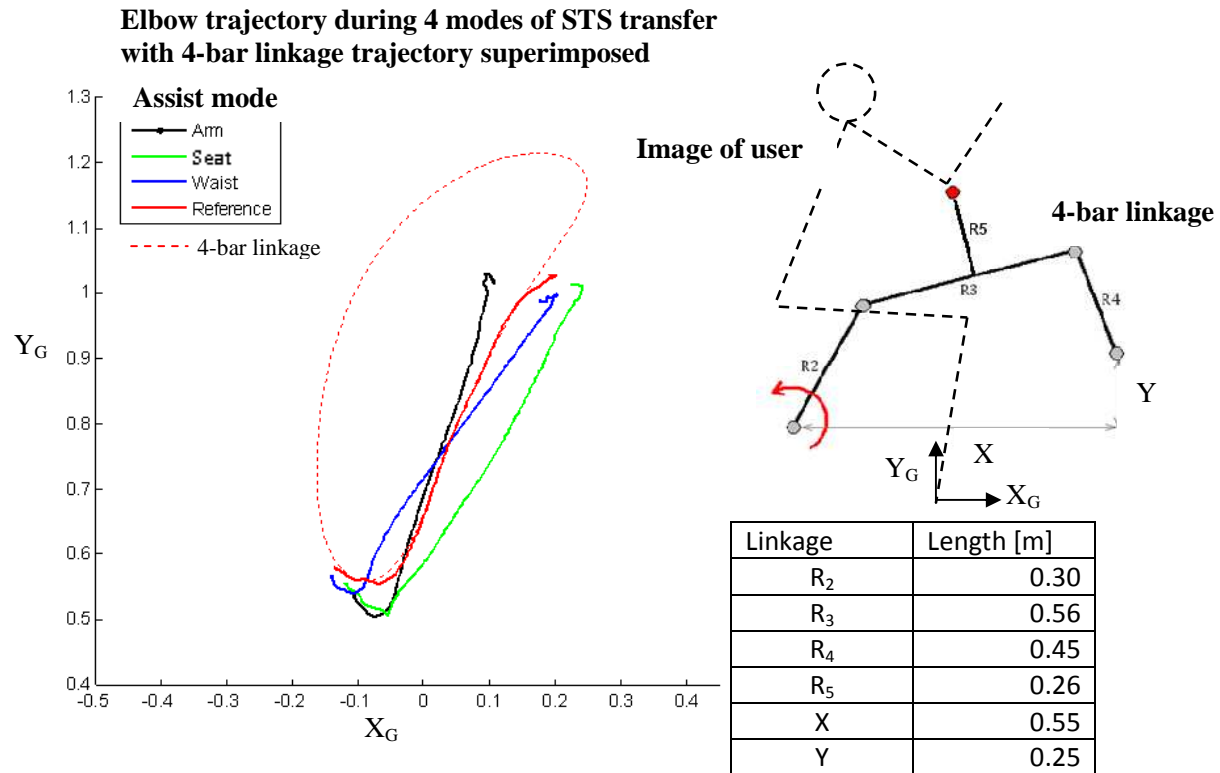


Figure 5.12: Trajectory of 4-bar linkage mechanism. The plot on the left shows the 4-bar linkage trajectory superimposed onto the reference unassisted trajectory of Figure 5.6. The figure on the top right shows the 4-bar linkage with a drawing of the user to show the point of contact between the linkage and the user. The table on the bottom right shows the linkage lengths required to obtain the 4-bar linkage trajectory shown in the plot [60].

5.4.4.2 Four-bar linkage adjustability

The arm assist mechanism linkages consist of aluminum square stock bearing blocks for the joints inserted into lengths of rectangular aluminum tubing. Holes in the tubing and square stock allow for length adjustability, and locking pins secure the square stock to the tubing as shown in Figure 5.13. The end linkages of the 4-bar mechanism can be adjusted in height as shown in Figure 5.14 to suit users in the height range of 150 cm to 185 cm.

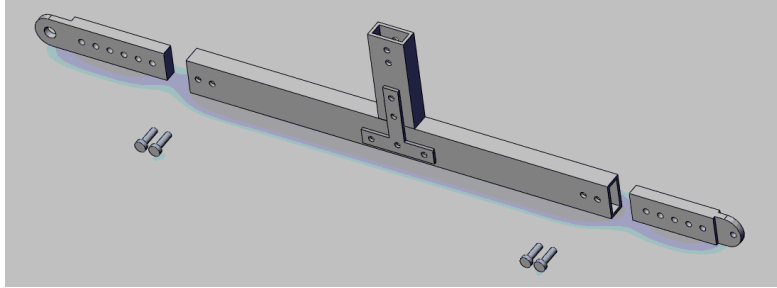


Figure 5.13: Length adjustable linkages and locking pins.

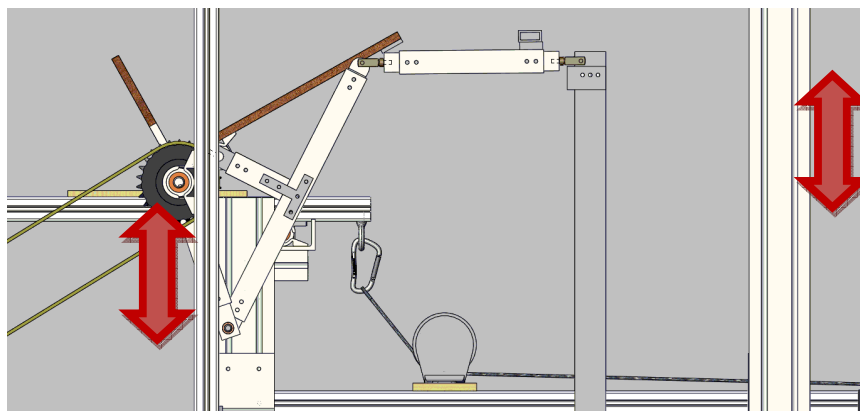


Figure 5.14: Adjustability of the mounting position of the linkage ends.

5.4.4.3 Arm cradles

The arm cradles are L-shaped plywood pieces designed to interface with the end of the 4-bar mechanism and support the upper arm and forearm of the user as the 4-bar mechanism guides the user into a standing position. The cradle is designed to rotate freely about an aluminum shaft that connects the cradle to the 4-bar mechanism on each side.

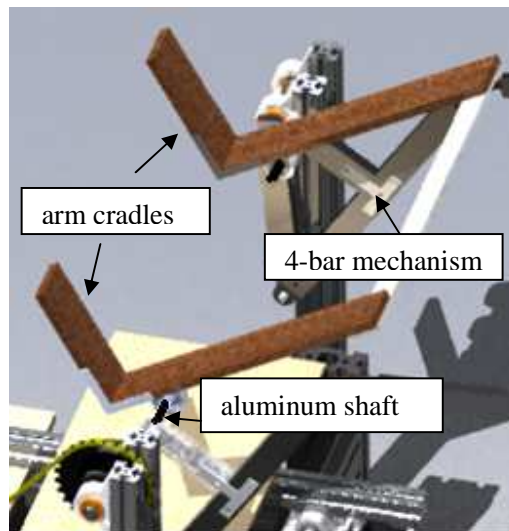


Figure 5.15: Arm cradle right and left side assemblies [60].

5.5 Test bed final design

The undergraduate team designed and built the test bed frame as well as the mechanisms to provide waist, seat, and arm assistance. The final test bed design was further developed through several additions and modifications. These include a test bed actuation system, a new adjustable arm cradle mechanism, a modified arm guidance mechanism trajectory setting, a test bed entry method, and force measurement sensors.

5.5.1 Test bed actuation system

The actuation system of the final test bed was changed from the student design such that all three assists are actuated by a single 90V permanent magnet DC geared motor instead of two motors. The motor shaft is coupled to a shaft containing a winch and a sprocket. The winch is used to transmit torque to the seat and waist assists and the sprocket is used to transmit torque to the arm assist (Figure 5.16).

Torque is transmitted to the seat and waist assist through a drive cable that is fixed to the winch and redirected by a rear-mounted pulley. A sling hook with latch serves as the connection point between the drive cable and the assist cables that actuate the seat and waist assists. Similar hooks on the ends

of the two assist cables allow either the seat assist cable or the waist assist cable to be connected to the drive cable by connecting the sling hooks together. The assist cables are redirected by pulleys to the seat and waist assist lever arms. When the seat or waist assist is not in use, the corresponding assist cable is disconnected from the drive cable. Figure 5.16 shows a cross-sectional view, highlighting the actuating mechanisms of the test bed.

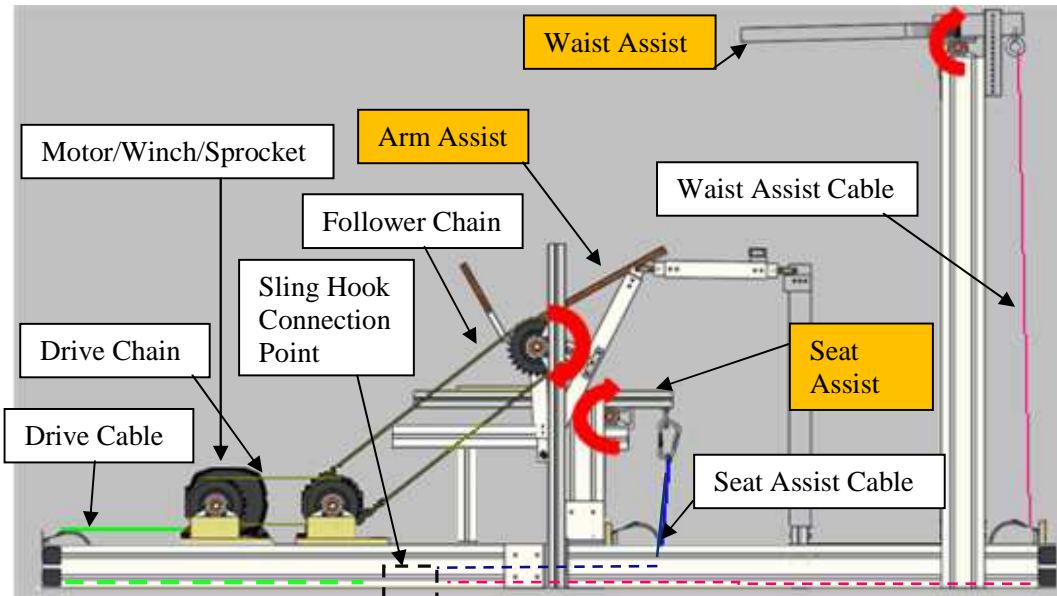


Figure 5.16: Test bed diagram showing actuation methods. The red arrows show the rotation points of each of the three assists.

Torque is transferred to the arm assist from the sprocket coupled to the motor shaft. A drive chain on the motor sprocket transmits torque to a jack shaft through a sprocket in the center of the jack shaft. As the shaft rotates, follower sprockets on the left and right ends of the shaft transmit torque through follower chains to sprockets connected to the two 4-bar linkage arm assist mechanisms. When the arm assist is not in use, the drive chain is removed from the motor sprocket by first loosening the motor mounting plate from the frame of the test bed and pushing it forward to slacken the drive chain, and then removing the chain from the sprocket. Figure 5.17 shows a rear view of the test-bed with the arm actuation system labeled.

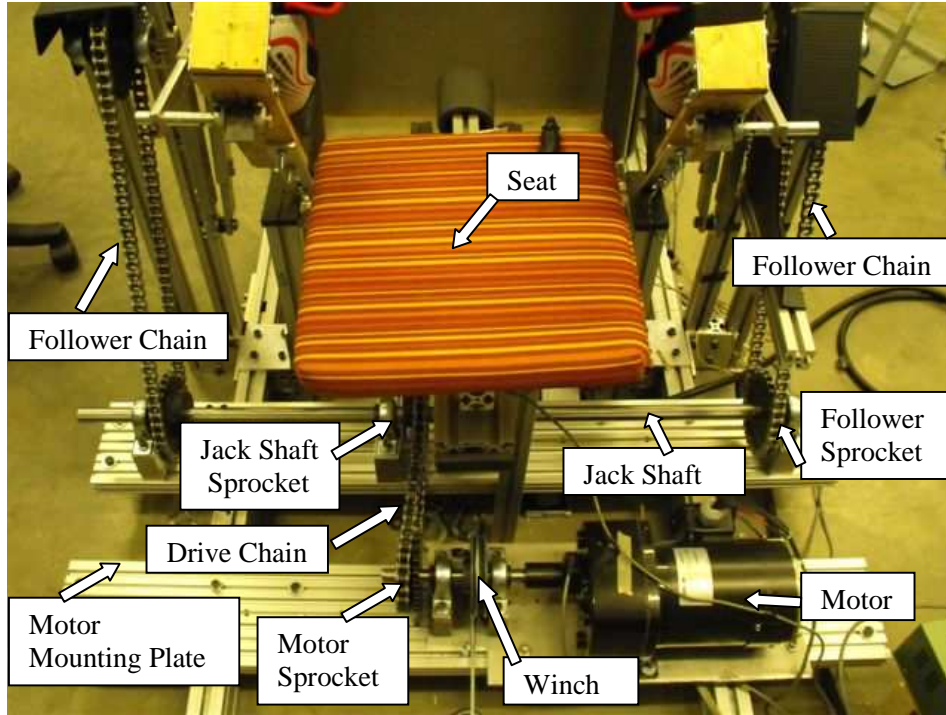


Figure 5.17: Rear view of test bed showing motor assembly and jack shaft system for arm assistance.

5.5.2 Test bed modified arm cradle

The arm cradles on the test bed were modified to provide added support and comfort to the user while rising. Modifications made include the addition of contoured elbow pads for comfort and adjustable handles for the user to grip for support during the assisted motion. In addition, the critical function prototype experiment showed that rotation of the arm cradle when rising with arm assistance is less than 90° , so a stopping mechanism consisting of a rigid angle bracket attached to the cradle shaft was added to limit the rotation of the arm cradle to 90° . Figure 5.18 shows a picture of the modified arm cradle.

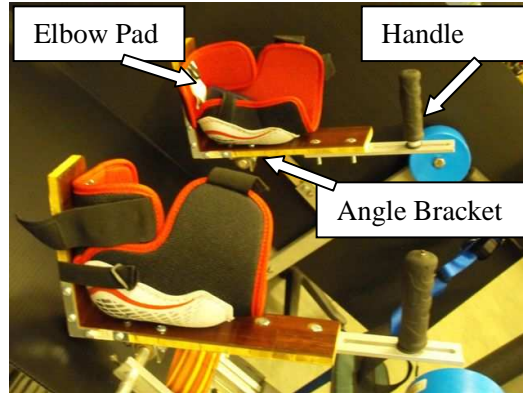


Figure 5.18: Modified arm cradle.

5.5.3 Modified arm guidance mechanism trajectory

The arm assist mechanism linkages were designed with aluminum square stock bearing blocks inserted into lengths of rectangular aluminum tubing. Holes in the tubing and square stock allow for length adjustability, and pins secure the square stock to the tubing (Figure 5.13). Locking pins were originally used instead of bolts for quick adjustment of the lengths of the links to change the generated trajectories to suit users of different heights. However, the locking pins resulted in considerable lateral wobble between the square stock and rectangular tubing, and had to be replaced with tightly fastened screws to pinch the tubing to the square stock. This significantly increased the time to adjust the arm linkages and thus made it impractical to modify the 4-bar trajectory to suit individual user heights. For this reason, the linkage lengths of the 4-bar linkage were set to provide a single representative trajectory.

Since the purpose of the arm assist mechanism is to guide users through a MT strategy rise, the arm assist trajectory was set using the elbow trajectory of the rise in the critical function experiment that resulted in a peak trunk flexion closest to 51° , which is the peak trunk flexion characteristic of a MT rise as determined by Scarborough et al. [25] (see trajectory functional requirements in Section 5.2). Table 5.7 shows the average peak trunk flexion for all the subjects in the critical function prototype experiment. Note that the reference trial of Subject 2 has an average peak trunk flexion of 46° , which is closest to the 51° trunk flexion characteristic of a MT rise. In addition, the height of Subject 2 is 172 cm, which is similar to the 173 cm average height of males in the age range of 65-69 yrs [58].

Table 5.7: Average peak trunk flexion during each mode of STS trial in the critical function prototype experiment (standard deviation).

Subject	Mass (kg)	Height (cm)	Reference (5 trials)	Seat Assist (5 trials)	Waist Assist (5 trials)	Arm Assist (5 trials)
			Avg. Peak Trunk Flexion (deg)			
S1	62	164	28 (2)	41 (4)	20 (4)	17 (4)
S2	66	172	46 (6)	37 (4)	15 (3)	27 (3)
S3	89	185	59 (1)	60 (3)	13(6)	-

Because of the close match in the peak trunk flexion of the unassisted rise of Subject 2 to the trunk flexion of a MT rise and the match in the height of Subject 2 to the average height of an older male adult (age range 65-69), a representative unassisted elbow trajectory from this subject was selected as the trajectory for the 4-bar linkage to match. The appendix of the student report [60]) includes arm linkage length data corresponding to the unassisted arm trajectory of this subject (Appendix A). The data used to set the arm linkage lengths are shown in Figure 5.19.

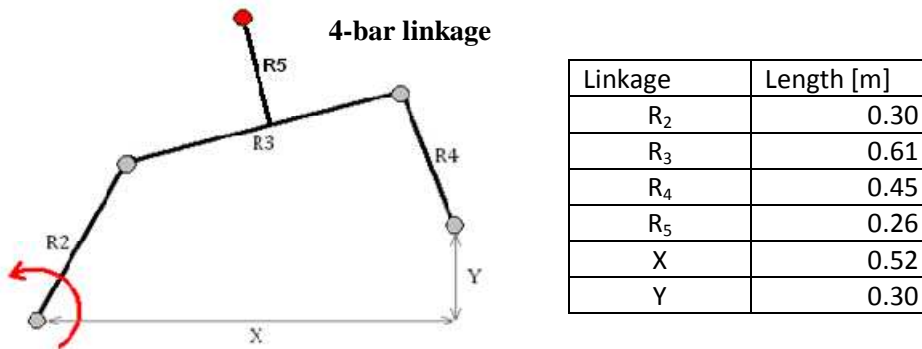


Figure 5.19: Test bed arm linkage lengths.

5.5.4 Test bed entry

The test bed has been designed to allow entrance from either side by disconnecting the end link of one of the 4-bar linkages from the support bar and retracting it to create an opening into the test bed (Figure 5.20). A grab bar in front of the test bed provides support during entry, and padding has been placed around sharp edges for user safety. In addition, clear plastic chain guards between the 4-bar linkages and the follower chains and circular disks at the linkage joints have been added to prevent users from coming in contact with pinch points while the arm assist is in motion. The end link of the 4-bar linkage is reconnected to the support bar when the test bed is in the arm assist mode.

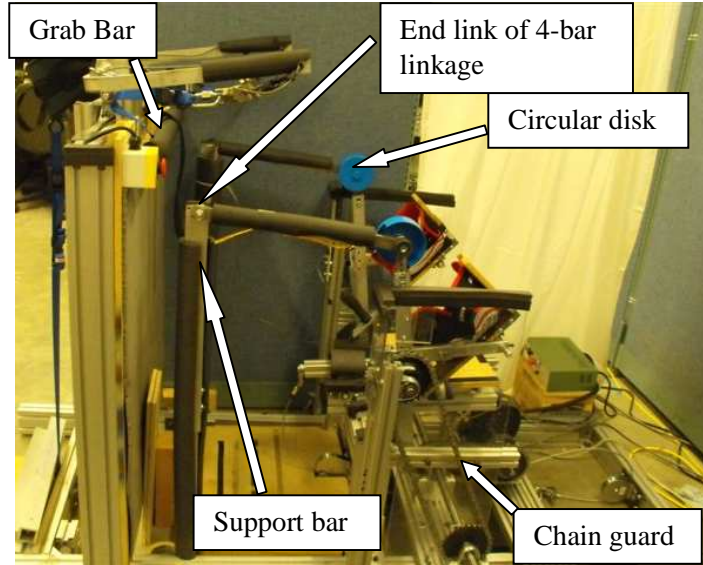


Figure 5.20: Test bed entry.

5.5.5 Test bed force measurement

Several load measuring devices have been implemented into the STS test bed to enable both the characterization of the forces applied by the user during the STS rises and characterization of the assist forces applied to the user during the assisted STS rises. The description of these load measuring devices is provided in Table 5.8 and their locations are shown in Figure 5.21.

Table 5.8: Description of load measuring devices in test bed.

Sensor	Location	Data Collected
Pressure Transducers Ltd. S-type 300 lb load cell (model PT4000-300lb)	Underneath the seat of the test bed	Vertical force applied by the user to the seat of the test bed prior to seat-off
Advanced Medical Technology 6-axis 1000 lb force plate (model OR6-7-1000-3985)	Underneath the feet of the user	Ground reaction forces and foot center of pressure location
Pressure Transducers Ltd. Two S-type 50lb load cells (model PT4000-50lb)	On both of the waist straps	Load applied by the waist assist to the waist of the user

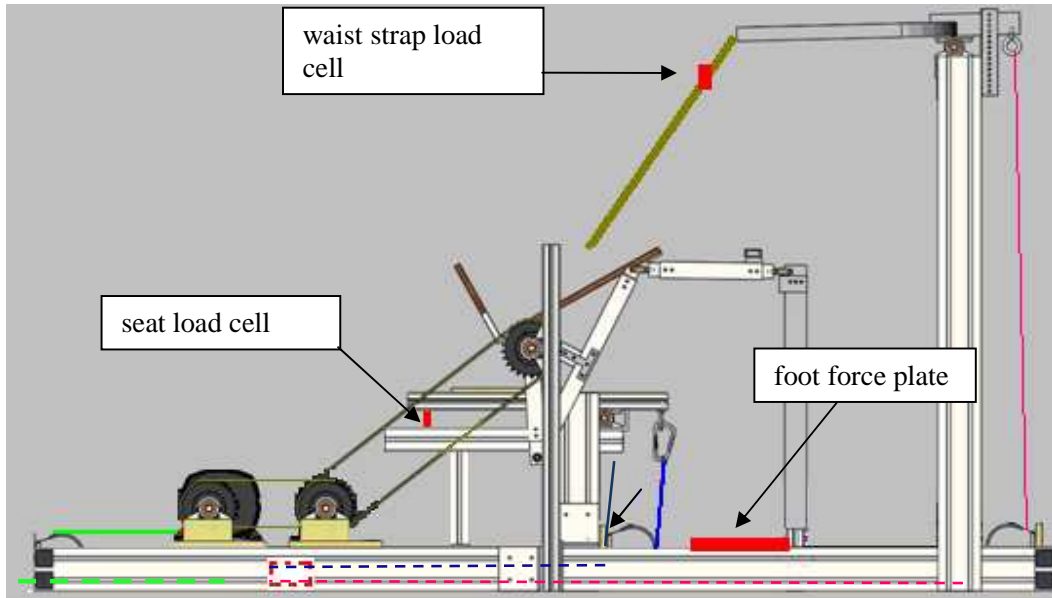


Figure 5.21: Load cell configuration.

5.6 Test bed control overview

This section provides an overview of the components engaged in controlling the motion of the test bed. Actuation for all three assist modes of the test bed is provided by a single motor. A test bed control system was developed to actuate and control each of the assist modes. Figure 5.22 shows a general diagram of the test bed control scheme. The following sections describe each component of the control scheme in detail.

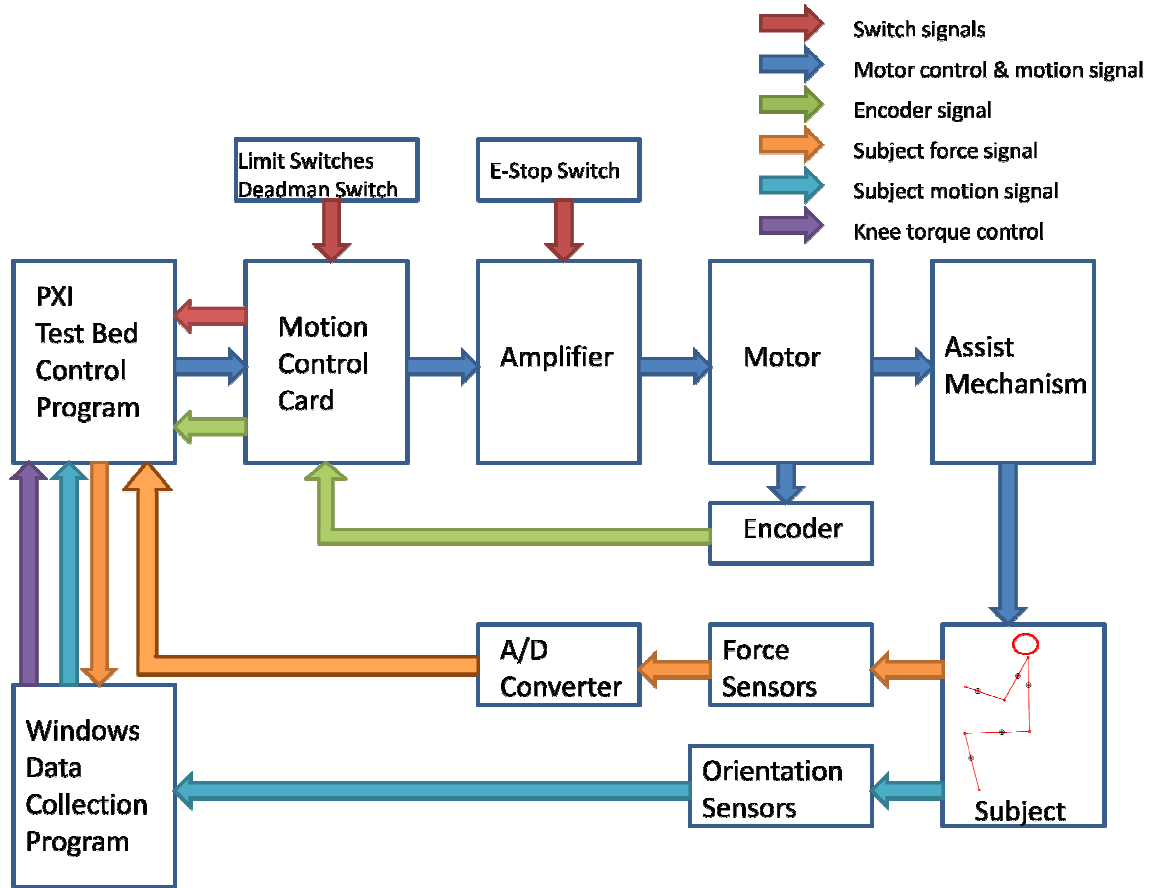


Figure 5.22: General diagram of test bed control scheme.

5.6.1 PXI Test Bed Control Program and Windows Data Collection Program

LabVIEW control programs in two computers are used to control the motion and mediate the data collection for the test bed. The PXI Test Bed Control Program is used to control the operation of the test bed and collect force sensor data, and the Windows Data Collection Program is used to collect and save data from the orientation sensors and perform calculations to determine the real time knee torque of users as they rise in the test bed.

5.6.1.1 PXI Test Bed Control Program

A National Instruments (NI) PXI 8196 Computer uses NI's real-time operating system to run the PXI Test Bed Control Program. The Test Bed Control Program graphical user interface (GUI) enables the

experimenter to control the motion of the test bed and visualize feedback from the limit switches, motor encoder, and motion and force sensors. The Test Bed Control Program also records the data sent from the force plate and load cells via coaxial cables to the NI PXI 6289 data acquisition card. These data are then also transmitted from the PXI Test Bed Control Program to the Windows Data Collection Program transmitted through a 100Base-T Ethernet connection using LabVIEW shared variables. LabVIEW shared variables are also used to transmit a knee torque control signal and orientation sensor signals from the Windows Data Collection program back to the PXI Test Bed Control Program. The use of the knee torque control signals and orientation sensor signals in controlling the motion of the motor is described in detail in Section 5.6.5. A detailed operation manual for the PXI Test Bed Control Program can be found in Appendix C.

5.6.1.2 Windows Data Collection Program

A Windows computer is used as the operating system for the Windows Data Collection Program. The Windows Data Collection Program is used to directly record and save the orientation sensor readings, which quantify user kinematics and assist forces during the assisted STS transfer. The Windows Data Collection Program also receives the load cell and force plate data from the PXI Test Bed Control Program via a LabVIEW shared variable and thus saves both the force and kinematic data on the Windows computer.

In addition, the Windows Data Collection Program performs knee torque computations, discussed in detail in Section 5.6.5, and outputs the results of these computations to the PXI Test Bed Control Program along with select orientation sensor measurements. The use of these knee torque computation signals and orientation sensor signals in the PXI Test Bed Control Program is described in detail in Section 5.6.5. The operation manual for the Windows Data Collection Program can be found in Appendix C.

5.6.2 Motion controller

The control of motor motion is implemented using a NI PXI-7344 motion card. The motion card and devices connected to the motion card are configured using the NI Measurement and Automation Explorer (MAX) software included with LabVIEW. The card manages the motor actuation through an output analog signal to the motor, and manages all of the switches and encoder inputs from the test bed. The NI UMI-7764 motion interface (Figure 5.23) is used to connect all wiring from the motion

card to actuators and sensors, and to provide auxiliary power to sensors and switches. The UMI-7764 data sheet is included in the appendix of the student report [60].

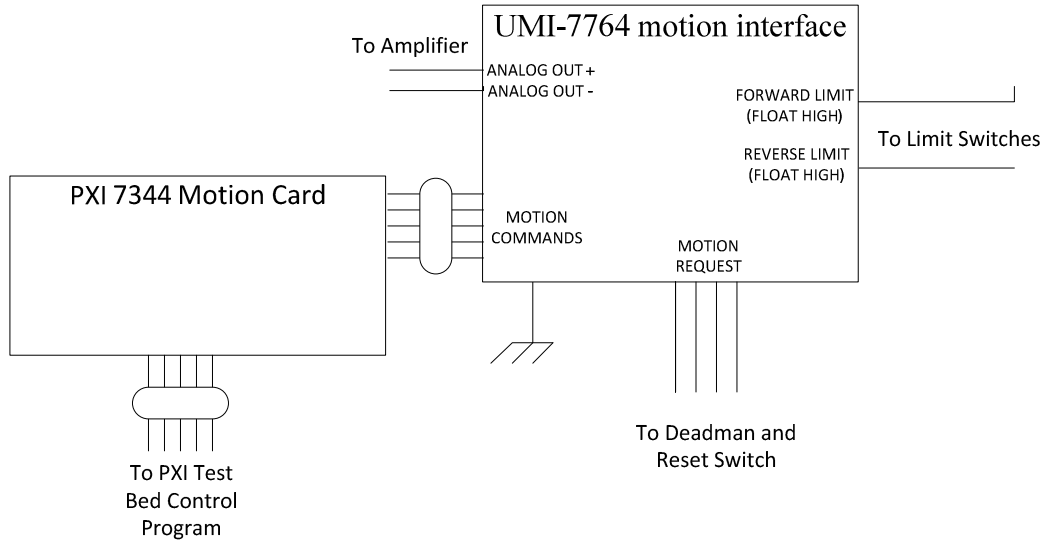


Figure 5.23: NI UMI-7764 motion interface.

The control of motor actuation is managed internally in the motion card. Figure 5.24 shows the general control diagram for the test bed motor control scheme. A servo-tune feature in the MAX software is used to automatically optimize Proportional Integral Derivative (PID) control parameters and identify system parameters such as inertia and friction by oscillating the system through a range of frequencies. The desired final motor angle keyed by the experimenter into the LabVIEW GUI is sent to the motion control card as the goal angle, θ_{goal} . The trajectory generator module in the motion control card accepts the goal angle and generates a trajectory profile. Using this trajectory profile, a continuously updated reference position $\theta_{ref}(t)$ is sent to the PID controller, which drives the motor to the goal angle based on the difference between this reference angle and the current motor angle (θ) (Figure 5.24). The PID controller output is converted to an analog voltage by the motion card's D/A converter and sent to the PWM servo amplifier, which in turn provides the current required to drive the motor based on the voltage input into the amplifier.

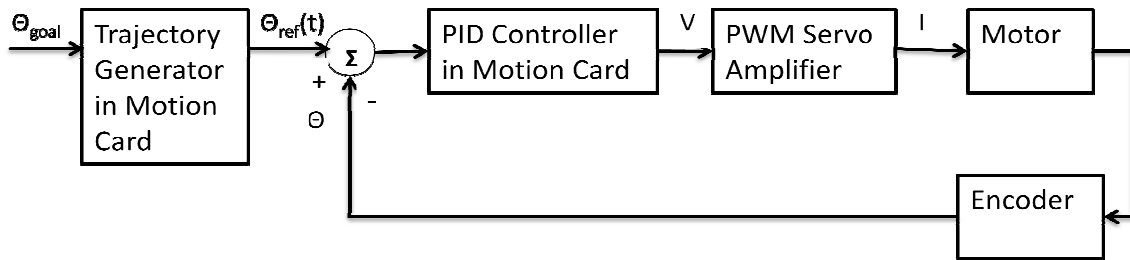


Figure 5.24: Motor position control diagram.

5.6.3 Amplifier and motor

The test bed is actuated using a ¼ hp DC brushless servomotor. The motor is powered through a AMC16A20AC servo amplifier, which includes a DC power supply. The motor is PWM driven, with a maximum voltage of 90V DC. Commands are sent through to the amplifier from the NI 7344 motion controller as +/-10V analog torque commands. Maximum and continuous motor currents are 8A and 3.8A, respectively. The amplifier and motor datasheets are included in the appendix of the student report [60].

5.6.4 Switches and encoder

5.6.4.1 Limit switches

For each mode of assist, a pair of limit switches sets bounds on the initial and final positions of the assist. Forward limit switches set the maximum final position of each assist and backward limit switches set the minimum initial position of each assist. The limit switches are all configured in a normally closed mode and wired to the motion control card such that motor motion is inhibited if a limit switch is opened (floats high) (Figure 5.25). The control box, shown in Figure 5.26, has two selector switches to define which pair of limit switches is active based on the current assist mode of the test bed. When the test bed is in a particular assist mode, only the limit switches for that particular mode are active. A two-position selector switch is used to activate or bypass the arm assist limit switch pair. A three-position selector switch is used to activate either the waist or seat assist limit switch pairs or bypass both of these limit switches. The separation of the arm assist selector switch from the seat/waist selector switch enables the test bed to operate the arm assist limit switches simultaneously with either of the waist or the seat assists. If an active limit switch is opened, the Motion Control Card halts the motion of the motor and displays to the user on the PXI Test Bed Control Program GUI that a limit switch has been opened.

5.6.4.2 Emergency stop switch

An emergency stop switch is wired directly to an inhibit pin on the motor amplifier. When the emergency stop switch is pressed, the inhibit pin is grounded and the motor drive is disabled (Figure 5.25). The emergency stop switch is situated on the control box along with the limit switch selector switches (Figure 5.26). Another emergency stop switch is located at the entrance of the test bed, where it can be accessed by test bed users, and is connected in series with the emergency stop switch on the control box.

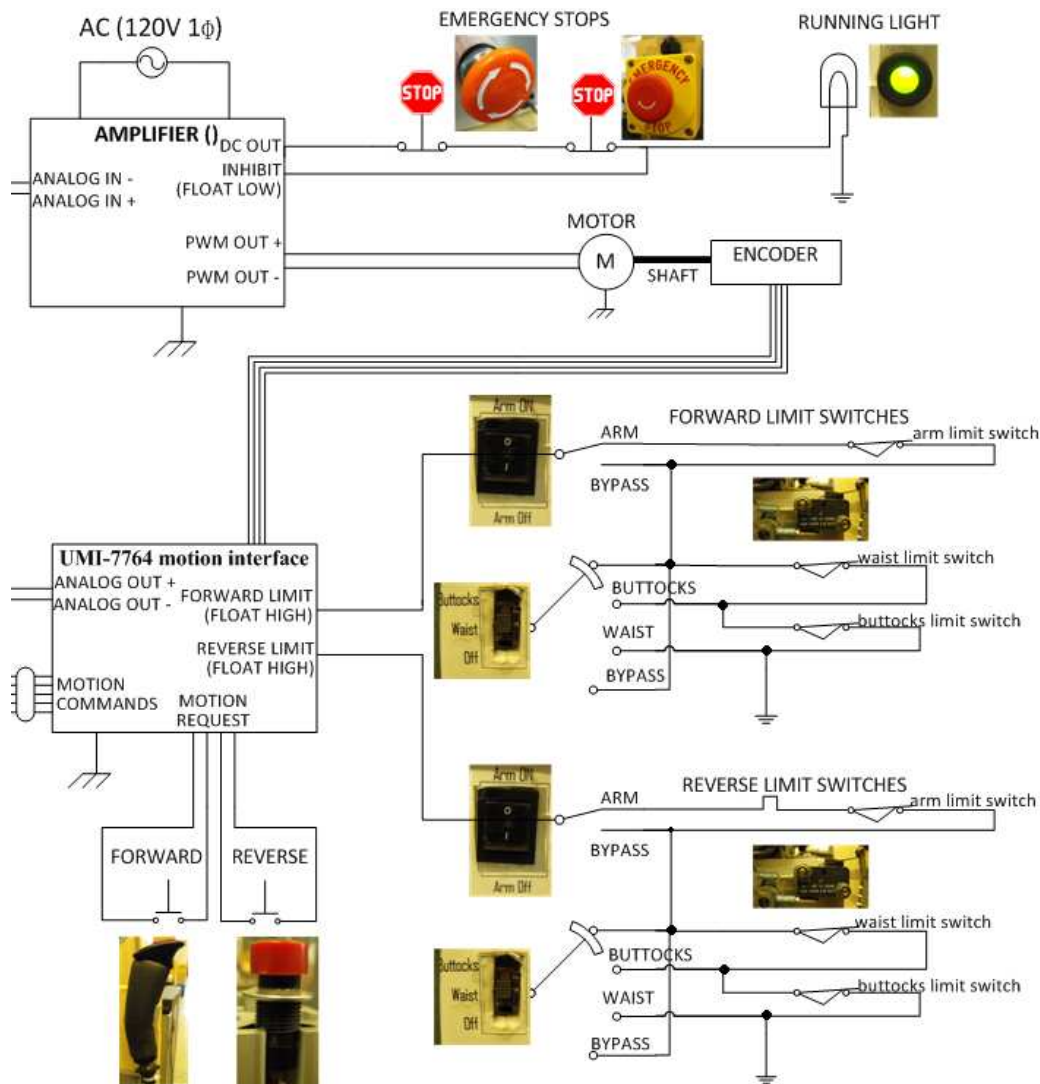


Figure 5.25: Electrical schematic showing e-stop, limit switch and motion switch wiring. Note that the references to “buttocks” in the schematic represent the seat assist.



Figure 5.26: Control box. Note that the label “buttocks” on the three position selector switch represents the seat assist.

5.6.4.3 Deadman and reset switches

A deadman switch and a reset switch operate the forward and reverse motion of the test bed. The deadman switch is held by the user and depressed to activate motion of the test bed. If the switch is released, the motor provides a holding torque to maintain the assist in the current position by setting the θ_{ref} in the controller (Figure 5.24) to be the current position of the motor. When the switch is depressed again, the θ_{ref} goes back to the original final position angle keyed into the LabVIEW GUI and the controller drives the motor to this final position. The deadman switch for the waist and seat assist is held in the hand of the user, but for the arm assist it is integrated as a button on top of the handle of the arm cradle. When the assist mode is switched to arm assist, the deadman switch wiring is disconnected from the waist/seat deadman switch and connected to the arm assist deadman switch. A bayonet connector is used at waist/seat and arm assist deadman switches to allow easy connect and disconnect between switches.

A reset switch located beside the upper sprocket on the right side of the test bed is used to rotate the motor in the reverse direction and reset the assist to the initial position. The reset switch operates in the same way as the deadman switch in that the motor is only actuated when the switch is depressed. Figure 5.25 shows the circuit diagram for the deadman and reset switches and Figure 5.27 shows pictures of the switches in the test bed.

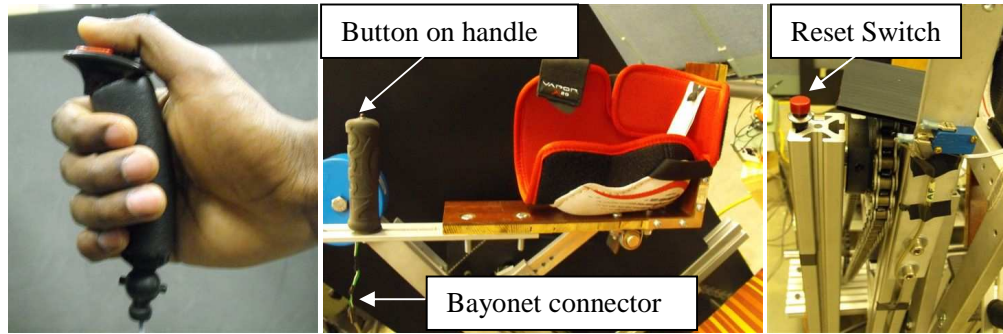


Figure 5.27: From left to right: Seat/waist deadman switch, arm cradle deadman switch, reset switch.

5.6.4.4 Encoder

The encoder used in the system is mounted to the motor shaft and has 1800 counts per revolution. The encoder is indexed to allow zeroing of the motor position. The encoder reading is sent directly to the motion control card to enable closed loop position control. The encoder datasheet can be found in the appendix of the student report [60].

5.6.4.5 Assist mechanism and sensor measurements

The three assist mechanisms used to provide assistance at the seat, waist, and arms have been described in detail in Section 5.4. Torque applied by the motor enables motion of the assist mechanism, which in turn provides the STS assistance force. As the user rises, the forces applied by the assist mechanism to the user and the reaction forces applied by the user are measured by the test bed load cells and force plates. All of the force measurement signals, as described in Section 5.5.5, are collected by the PXI Test Bed Control Program. The kinematics of the user (angular position, angular velocity, linear acceleration) are measured by three orientation sensors (Xsens Motion Technologies) that are attached to the user at the approximate center of mass of the shank, thigh, and chest. A fourth orientation sensor is attached to the biceps of the user to measure arm kinematics during arm-assisted STS rises. Kinematic measurements are directly sent to the Windows Data Collection Program.

5.6.5 Torque regulation control scheme

One of the functional requirements of the test bed is to provide load-sharing assistance such that during the seat and waist-assisted rise, the user provides at least 35% of the knee torque required to rise without assistance. The motor control system (described in Section 5.6.2) was augmented by a real-time knee torque monitor and a velocity limiter to encourage the user to apply a knee torque above the 35% threshold during the assisted rise. Figure 5.28 shows a diagram of the augmented motor control scheme.

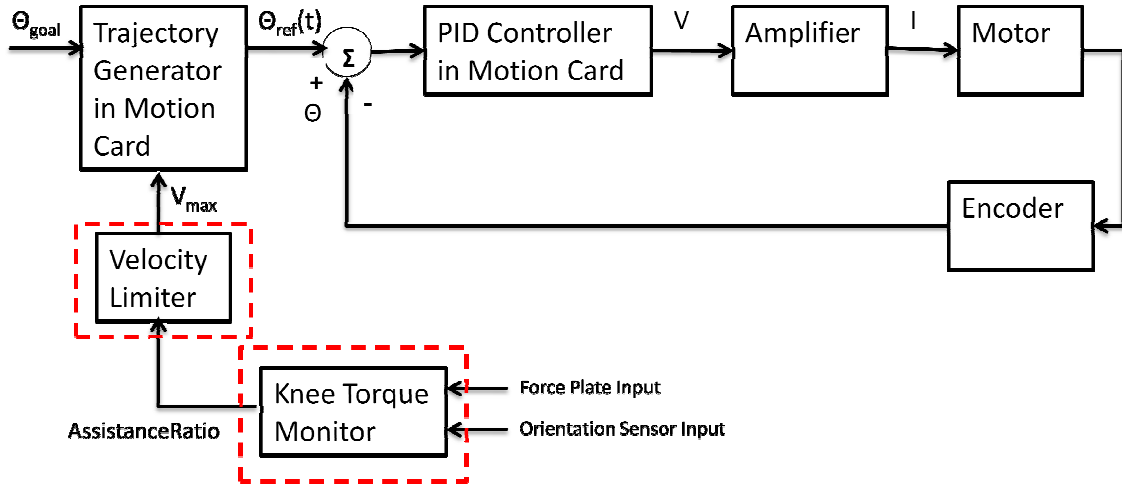


Figure 5.28: Augmented motor control system.

5.6.5.1 Knee torque monitor

The knee torque monitor uses anthropometric measurements and inputs from the force plate and body segment orientation sensors to compute a real-time estimate of the knee torque as the user rises. Knee torque is obtained by recursively applying the Newton-Euler equations to a three-link biomechanical model (described in Ch 2), starting at the feet [43]. The force plate inputs (CoP , F_{yfp} , F_{zfp}) are used to calculate the ankle torque and forces according to Equations 5.3 and 5.4. The knee torque is computed using Equation 5.5.

$$T_{ankle} = -(m_{foot}gl_{foot}) + (CoPF_{zfp}) - (h_{ankle}F_{yfp}) \quad (5.3)$$

$$F_{yankle} = F_{yfp} \quad F_{zankle} = F_{zfp} - m_{foot}g \quad (5.4)$$

$$T_{knee} = (L_d F_a) + (L_p F_s) + T_a - I_s \alpha_s \quad (5.5)$$

In the experimental procedure, the user first rises without assistance and the torque monitor computes unassisted knee torque as a function of thigh angle, generating a reference curve for subsequent use. As the user rises with assistance, the actual knee torque is computed in real time at 50 Hz and compared to the reference unassisted knee torque at the corresponding thigh angle. The monitor computes a knee torque ratio according to Equation 5.6:

$$AssistanceRatio = (T_{unassisted}(\theta_{knee})/T_{assisted}(\theta_{knee}))100\% \quad (5.6)$$

The torque monitor computations take place in the Windows Data Collection Program and the output of Equation 5.6 is sent to the velocity limiter in the PXI Test Bed Control Program via a LabVIEW shared variable. For a successful assisted rise the output of Equation 5.6 is a value above 35%, indicating that the user is providing at least 35% of the knee torque required for rising without assistance.

5.6.5.2 Velocity limiter

The velocity limiter is part of the PXI Test Bed Control Program and is used to set the maximum velocity at which the trajectory generator in the motion card runs the motor. This maximum velocity is varied according to the *AssistanceRatio* input received from the knee torque monitor. If *AssistanceRatio* is below 35% this indicates that the user is applying insufficient knee torque and the *Vmax* output of the velocity limiter is lowered, slowing down the motor and assist mechanism and providing a cue to users that they need to put more effort into the rise. The velocity limiter outputs (into the trajectory generator) a *Vmax* velocity proportional to the maximum motor velocity according to the following logic.

Velocity Limiter Logic

1. *If AssistanceRatio > 35%*

$$Vmax = 100\%(Maximum\ Motor\ Velocity)$$

2. *If AssistanceRatio < 35%.*

$$Vmax = (AssistanceRatio/35\%)\ Maximum\ Motor\ Velocity$$

The *AssistanceRatio* value updates continuously at 50 Hz as the user rises with assistance. According to the velocity limiter logic, if *AssistanceRatio* is greater than 35% the motor runs at a constant velocity equal to the maximum motor velocity, and if it is below 35% the motor velocity is ramped down from the maximum motor velocity in proportion to the current value of *AssistanceRatio*. If the user provides additional torque to raise the *AssistanceRatio* value above 35%, the motor velocity rises back to the maximum motor velocity.

5.6.5.3 Initial non-load-sharing assistance phase

To ensure that the assist provides a reduction of peak knee torque, the torque regulation control scheme was modified to have an initial phase in which constant assistance is provided by the assist mechanism independent of the amount of knee torque applied by the user. It has been determined that the knee torque required to rise is maximal either at seat-off or shortly thereafter [63]. A biomechanical analysis of STS in older adults showed that the thigh extends by 15° prior to seat-off [64]. Based on this, the initial phase for providing constant assistance was set to be during the first 15° of thigh rotation.

During an assisted rise, the thigh angle of the user is sent to the PXI Test Bed Control Program from the Windows Data Collection Program via a LabVIEW shared variable. The PXI Test Bed Control Program monitors this thigh angle and during the first 15° of thigh rotation, the seat and waist assist mechanisms provide constant assistance by rotating the assist mechanism at a constant speed during this time regardless of the amount of knee torque applied by the user. As soon as the thigh has rotated by 15°, the control scheme switches such that the assist mechanism motion is controlled by the velocity limiter described in the preceding section (Section 5.6.5.2), i.e., the mechanism only continues to move at 100% speed if the user provides knee torque greater than 35% of the knee torque required to rise without assistance. The modified control scheme is summarized as follows:

Logic for torque regulation control scheme with initial non-load-sharing assistance phase

1. *If thigh rotation < 15°*

$$V_{max} = 100\%$$

2. *If thigh rotation > 15°.*

- a. *If AssistanceRatio > 35%*

$$V_{max} = 100\%(\text{Maximum Motor Velocity})$$

b. If $\text{AssistanceRatio} < 35\%$.

$$V_{max} = (\text{AssistanceRatio}/35\%) \text{ Maximum Motor Velocity}$$

5.7 Data synchronization

5.7.1 Data collection overview

As described in Section 5.6.1, two computers are used to collect data from the test bed during experiments. The PXI Test Bed Control Program collects force plate data at a frequency of 50 Hz and continuously writes the data into a LabVIEW shared variable at that rate. The Windows Data Collection Program continuously reads the latest input into the LabVIEW shared variable at a frequency of 50 Hz and saves it along with the orientation data, also collected at a frequency of 50 Hz (Figure 5.29). The saved data from the Windows Data Collection Program, which include both force plate and orientation sensor data, are then post processed according to the procedure detailed in Section 6.2.4.

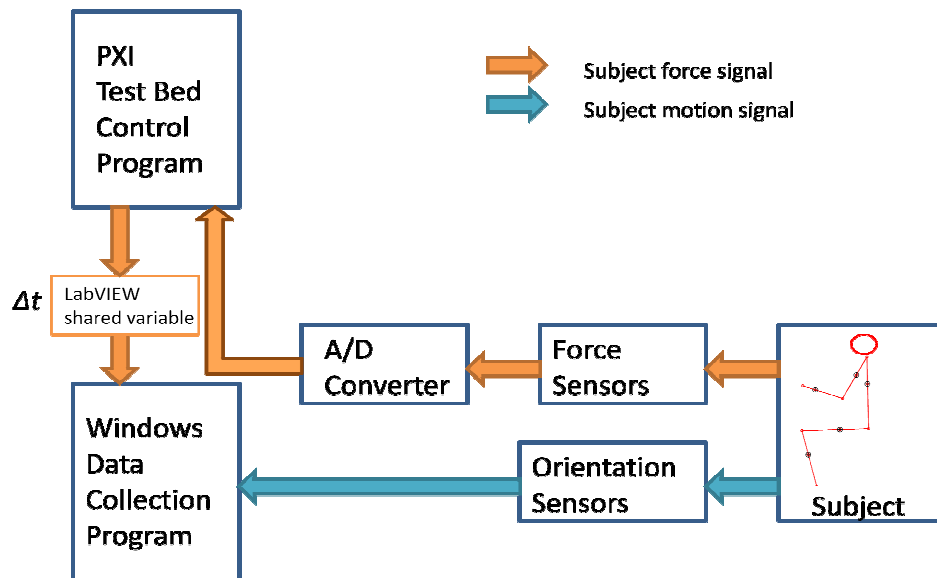


Figure 5.29: Data collection diagram. In the diagram, Δt indicates the delay in transmission of the force sensor data from the PXI Test Bed Control Program to the Windows Data Collection Program.

5.7.2 Synchronization problem and experiment

Because the force plate data are collected on the PXI Computer and transferred at a frequency of 50 Hz via an Ethernet link to the computer collecting the Xsens data, there is a delay in force sensor data transfer from the PXI to the Windows computer (illustrated as Δt in Figure 5.29). An experiment was conducted to characterize the data transfer delay by taping an orientation sensor to the back of the test bed seat lever arm, rotating the lever arm and dropping it onto a load cell (Figure 5.30). This lever arm drop experiment allowed for the characterization of delay by determining the instant in time at which the lever arm hit the load cell. Load cell and orientation sensor data were simultaneously collected on the PXI and Windows computers, respectively. A total of five lever arm drops were completed and the delay was characterized in each experiment.

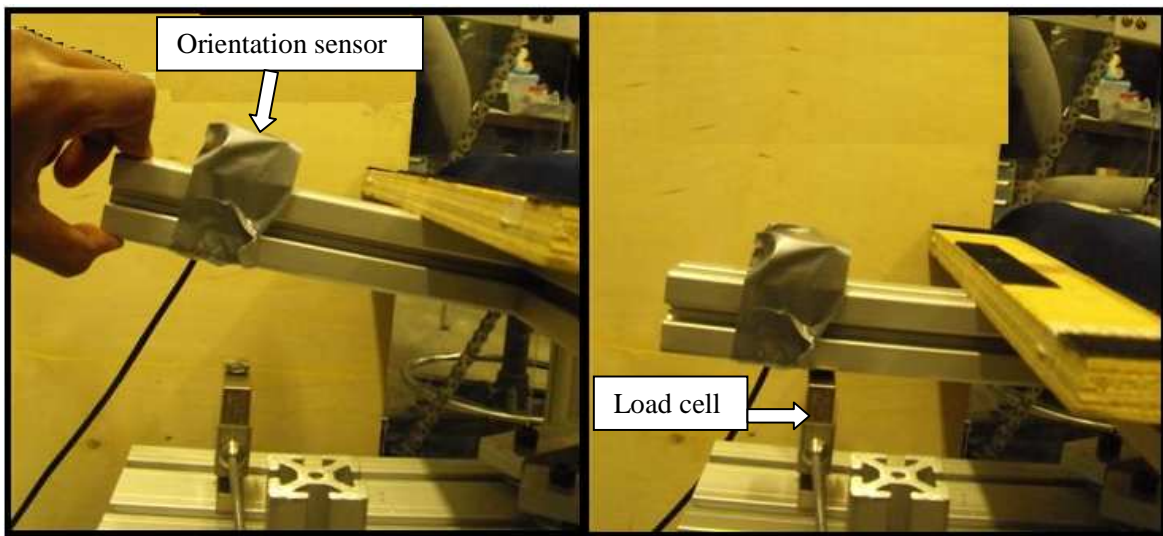


Figure 5.30: Synchronization experiment. The left picture shows the raised lever arm with orientation sensor attached (orientation sensor covered in tape). The right picture shows the dropped orientation sensor resting on the load cell.

5.7.3 Synchronization results and analysis

The delay was characterized using the data from the experiment saved on the Windows computer (force sensor measurements transferred from PXI computer and orientation sensor measurements captured directly on the Windows computer). At the instant the lever arm contacted the load cell, the

load cell had a marked decrease (compression force) in the force output and the orientation sensor velocity peaked (Figure 5.31). A load cell contact time was defined as the timestep after which the load cell force reading decreased more than 2N in a single timestep. An orientation sensor contact time was defined as the timestep of peak sensor rotation speed. The delay was characterized according to Equation 5.7.

$$\Delta t = \text{load cell contact time} - \text{orientation sensor contact time} \quad (5.7)$$

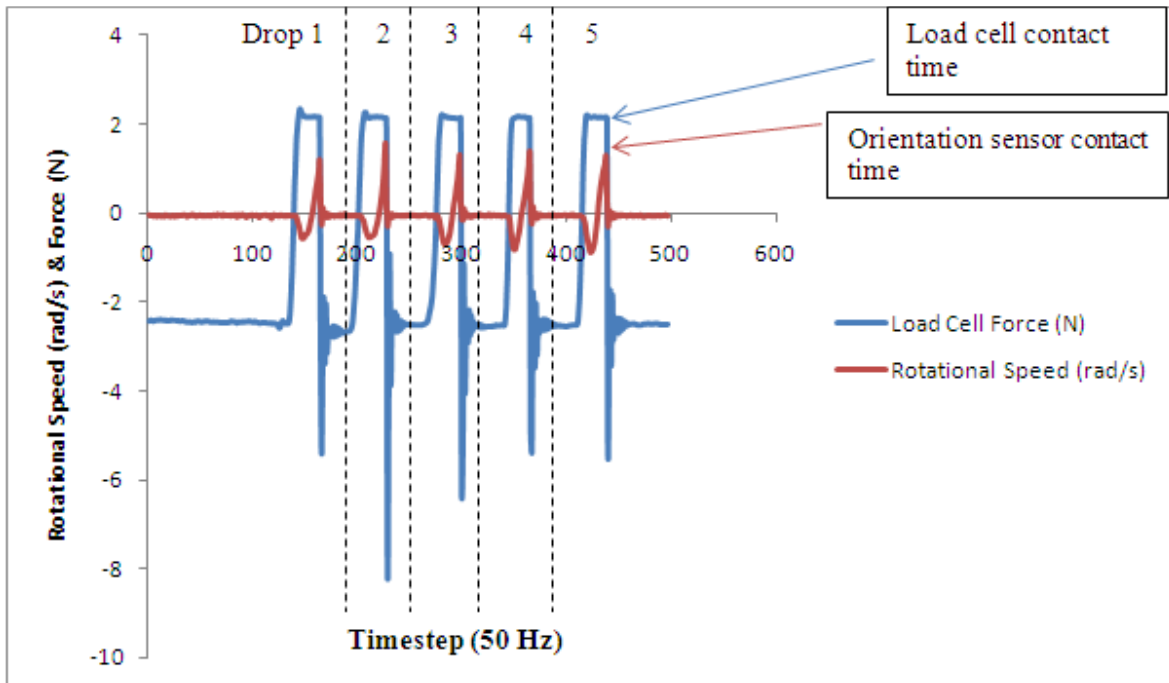


Figure 5.31: Graph showing five lever arm drops onto load cell (drop number indicated on top of graph). The blue curve indicates the load cell force reading; the red curve indicates the orientation sensor rotational speed reading. At the beginning of experiment lever arm is resting on load cell (load cell force $\sim -2\text{N}$, rotation speed = 0 rad/s). The lever arm is then raised (load cell force increases to $\sim +2$, rotation speed of orientation sensor has negative slope). The lever arm is then dropped (rotation speed of orientation sensor has positive slope until the lever arm hits the load cell). The lever arm hits the load cell (rotation speed slope changes and load cell force drops back down to $\sim -2\text{N}$, after oscillations). The process is repeated 4 times as shown on the graph.

Table 5.9 shows that in two of the trials the delay was less than one timestep (0 – 20 ms) and in three of the trials the delay was between one and two timesteps (i.e., 20 – 40 ms). From these results it was decided that the delay in the data collection would be corrected by shifting all of the force data saved onto the Windows computer backward by one timestep in relation to the orientation sensor data.

Table 5.9: Force delay characterization. The forces used to characterize the load cell contact time and the rotation speeds used to characterize the orientation sensor contact time are highlighted in bold. The timesteps corresponding to these contact times are also in bold.

Lever arm drop number	Timestep	Force (N)	Rotation speed (rad/s)	Δt
1	163	2.15	0.94	0
	164	2.15	1.19	
	165	-3.34	0.12	
2	226	2.14	1.19	1
	227	2.14	1.56	
	228	2.13	0.29	
	229	-8.03	-0.28	
3	297	2.11	1.01	1
	298	2.12	1.30	
	299	2.14	0.26	
	300	-6.32	-0.12	
4	364	2.13	1.08	0
	365	2.14	1.38	
	366	-4.99	0.01	
5	437	2.15	1.12	1
	438	2.16	1.29	
	439	2.13	0.34	
	440	-5.40	-0.29	

5.8 FMEA based on safety review

A Failure Modes and Effects Analysis (FMEA) was completed on the final test bed (Appendix D). Based on the FMEA a number of safety features were added to the test bed. These features include the following:

- a) Padding on all the sharp corners of the test bed and on hard surfaces that users may potentially contact.
- b) An additional emergency stop button located at the entrance of the test bed that can be accessed by users in the test bed.
- c) A clear plastic chain guard to prevent the user from coming in contact with the follower chains used in the arm assist mechanism.
- d) A test bed operational checklist to be completed before conducting experiments with users to verify that the test bed is in safe working condition (Appendix E).

5.9 Test bed functional design requirements validation

5.9.1 Pilot test results

Pilot tests were conducted on 6 healthy young adults to determine if the functional requirements were achieved by the assist mechanisms. The data collection and analysis procedure was the same as that described in Chapter 3. Subjects first performed STS rises in the test bed without assistance using a MT strategy, and then with assistance from each of the three modes of STS assistance. Table 5.10 shows the results of maximum trunk flexion and normalized knee torques for each of the four modes of STS.

Table 5.10: Trunk flexion and knee torque results from pilot tests with six subjects.

Combined Normalized Results (N=6)	Unassisted ^a	Arm	Waist	Seat
Max Trunk Flexion (deg)	43 (14)	33 (5)	12 (5)	26 (3)
Normalized Knee Max Torque (Nm/(BM*BH))	1.38 (0.25)	1.19 (0.21)	1.13 (0.27)	1.19 (0.26)
% unassisted peak knee torque	n/a	86%	81%	86%
Rise time ^b	1.9 (0.3)	3.2 (0.5)	2.6 (0.4)	2.3 (0.4)

^a Five trials for each STS mode of rise, results reported as means (standard deviation)

^b Rise time is defined from initiation of hip flexion to full extension of thigh.

5.9.2 Validation of design requirements

Four main functional design requirements were set regarding the design of the test bed. The following paragraphs reiterate the functional design requirements (outlined in Section 5.2) and describe, based on the results of the pilot studies, if the requirements were achieved.

- i. Ensure that the user provides a knee torque greater than 35% of the unassisted torque
 - a. Results from the pilot tests (Table 5.10) show that for each of the assisted modes of STS, the normalized maximum knee torque was greater than 35% of the normalized maximum knee torques of the unassisted STS. Thus the functional design requirement of ensuring that the user provides a knee torque greater than 35% of the unassisted torque was met.
- ii. Guide the trajectory of the arm assist such that the user employs a MT STS strategy
 - a. Results from the pilot tests (Table 5.10) show that for the arm assist the average maximum trunk flexion angle was 33°. This trunk flexion angle did not match the peak trunk flexion of the MT strategy (51°) as described by Scarborough et al. [25]; rather, it matched the 35° peak trunk flexion angle characteristic of DVR strategy.
- iii. The test bed assist should be able to help the user rise to a standing position with a rise time of two to four seconds.
 - a. Results from the pilot tests (Table 5.10) show that for all of the assisted STS rises, the rise time was between two and four seconds.
- iv. The test bed should be able to assist users with a height range of 150 cm to 185 cm and mass up to 90 kg.
 - a. The design calculations completed in appendix of the student report [60] (Appendix A) sized the dimensions of the test bed as well as the motor power such that users with a height range between 150cm and 185cm and mass up to 90 kg can be tested.

Results from the pilot tests indicate that the assist mechanisms on the test bed achieved all of the design requirements except for the requirement regarding the motion of the arm mechanism.

However, the arm-assisted STS rise resulted in an average peak trunk flexion of 33°, which was closer to the average unassisted peak trunk flexion of 44° than the waist assist (12° trunk flexion) and seat

assist (26° trunk flexion). Because of this, it was decided that the arm assist promoted sufficient transfer of momentum to merit a further investigation of the assist without further modifying the trajectory of the mechanism.

The test bed described in this chapter was developed to experimentally evaluate the biomechanics of different modes of assisted STS. This experimental evaluation is detailed in the next chapter (Chapter 6). Because the focus of this thesis is on biomechanical response in subjects induced by the different assist modes, and not specifically on the biomechanics of older adults with STS weakness, healthy older adults were recruited for experiments. Upon identification of the best assist based on the biomechanics of healthy older adults, further experiments with older adults who have weakness with STS can be performed to determine the effectiveness of this assist in the target population of older adults who have difficulty with STS.

Chapter 6 Test Bed Experiment

6.1 Introduction

As described in Chapter 5, the STS test bed was developed to characterize the biomechanical forces and motions arising from STS assistance at the waist, seat, and arms. In Chapter 2, three criteria, based on STS weakness in older adults, were established to evaluate the effectiveness of different modes of STS assistance. These criteria, i.e. stability, knee extensor effort reduction, and MT strategy adherence, were used to define five questions through which the test bed experiment detailed in this chapter characterizes each mode of assist: **a)** Which assist provides the greatest amount of static stability to the subject? **b)** Which assist provides the greatest amount of dynamic stability to the subject? **c)** Which mode of assist results in the greatest reduction in knee extensor effort required to rise while still sharing with the subject part of the knee load required to rise? **d)** Which mode of assist enables a subject to follow the clinically preferred MT STS strategy? and **e)** Which mode of assist do the subjects prefer to use? The answers to these questions will help determine the best mode/modes of assist and provide guidance for the development and deployment of institutional and consumer load-sharing STS assistive devices.

6.2 Experiment procedure

6.2.1 Subjects

A total of 17 community dwelling healthy elderly subjects (above the age of 60) were recruited for the study. Subjects were selected if they were able to rise unassisted from a chair and did not have any of the following contraindications: known musculoskeletal or neuromuscular conditions that would limit their ability to rise from a chair, balance disorders, osteoporosis, recent significant injury or treatment, recent hip or knee replacement, current rehabilitation care, or current fainting or dizzy spells [65]. Subject-reported level of mobility, assistive device use, and difficulty with STS were collected in a pre-experiment questionnaire (Appendix F). Informed consent was obtained from all subjects and consent was obtained conditional on the subject passing the above described selection criteria. This research was approved by the University of British Columbia Research Ethics Board (UBC Clinical Research Ethics Board number H10-00563).

The gender, age, mass and height were collected for each subject along with anthropometric data. These data are listed in Table 6.1 for all 17 subjects. Data for Subject 3 were recorded but not used because of an equipment error in the data collection during trials (described further in Section 6.2.4.4). Anthropometric data included measurements of total foot length (heel / 2nd toe), foot length (lateral malleolus / head metatarsal II), shank length (femoral condyles / medial malleolus), thigh length (greater trochanter / femoral condyles), head/arms/torso length (greater trochanter/ glenohumeral joint), upper arm length (glenohumeral joint / elbow axis), and forearm length (elbow axis / ulnar styloid). Body segment lengths were found by palpation at joints to find the point of rotation. The test bed seat height was pre-adjusted to 80% of the knee height, measured as the distance to the floor from the left medial tibial plateau [25].

Table 6.1: Summary of data from 17 healthy older adult subjects.

No.	Gender	Age	Mass [kg]	Height [cm]	Total Foot [cm]	Shank [cm]	Thigh [cm]	Trunk [cm]	Upper Arm [cm]	Fore- arm [cm]	Seat Height [cm]
1	M	65	65.1	165	25	30	40	50	24	24	35.5
2	M	76	78.4	179	26.5	40	50	42	25	27	43
3 ¹	F	78	55.6	166	23.5	37	45	37	28	25	40
4	M	65	84.3	174	24	37	47	43	29	25	39.5
5	M	73	64	177	24	40	47	43	25	26	41
5	M	73	72.6	161	21	37	43	40	27	25	38
7	M	84	70.5	169	23	38	49	42	26	24	38.5
8	M	77	75.3	184	29	43	49	48	31	27	43
9	M	70	70.9	173	25.5	37	50	43	24	26	39.5
10	M	69	63.8	175	23.5	38	47	49	28	28	38.8
11	M	70	66.5	176	25	40	47	51	28	26	40.3
12	M	80	77	176	27	39	49	46	27	24	41.5
13	F	69	57.4	176	26	38	49	43	26	25	39.5
14	F	66	55.3	165	22.5	36	43	40	20	24	37.8
15	F	68	73.6	169	24	38	48	42	23	25	39.3
16	F	63	70.7	162	22	37	49	39	25	24	37
17	F	69	76.3	174	24.5	41	46	52	26	26	41
	Mean	71	70.1	172	24.5	38.1	47.1	44.6	25.9	25.4	39.6
	SD	5.79	7.74	6.43	2.01	2.82	2.84	4.18	2.58	1.26	2.04

Data for Subject 3 are reported here, but not used due to an error in data collection during STS trials. Data from Subject 3 are not included in the reported Mean and SD at the bottom of the table.

6.2.2 Experimental design

6.2.2.1 Test bed assists

As detailed in Chapter 5, a STS test bed has been built for the purpose of the STS experiments (Figure 6.1). The Test Bed consists of a seat platform and three dynamic assist mechanisms to provide STS assistance: a seat assist, a waist assist, and an arm assist. The primary function of the arm assist is to provide stability and trajectory guidance as the subject rises rather than providing knee torque assistance. The primary function of the waist and seat assists is to reduce the knee torque required to rise. The waist and seat assist mechanisms are governed by a two-part control scheme that enables reduction of peak knee torque and also encourages subjects to rise using their own available strength. All of the assist mechanism motions are triggered by the subject through a deadman switch. Depression of the switch allows motion of the assist, and if the switch is released, the motion will stop.

A grab bar in front of the test bed (Figure 6.1) is used as an additional assist to represent assistance from commercial static grab bar assists [35] and as a reference for comparison with the three dynamic assists.

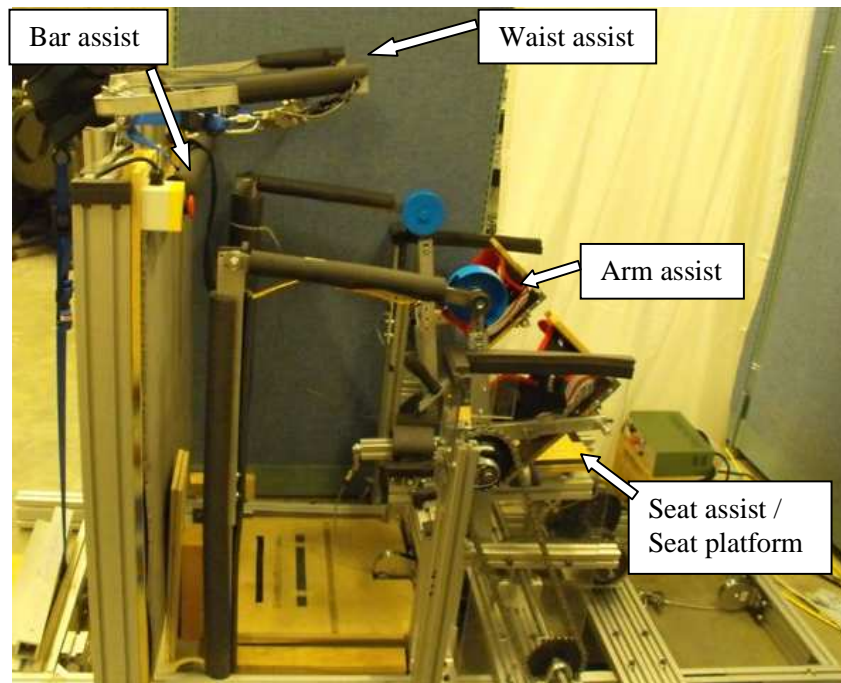


Figure 6.1: Sit-to-stand test bed.

6.2.2.2 Test bed data collection

A single-axis load cell and a six-axis force plate measure the forces applied by the subject during each STS rise. A Pressure Transducers Ltd. S-type 300 lb load cell (model PT4000-300lb) located underneath the seat of the test bed measures the force applied by the subject while seated. An Advanced Medical Technology 6-axis 1000 lb force plate (model OR6-7-1000-5571) underneath the feet of the subject measures the ground reaction forces and locates the center of pressure of the vertical foot force. A pair of Pressure Transducers Ltd. S-type 50 lb load cells (model PT4000-50lb) directly measure the load applied by the waist assist to the waist of the subject.

Kinematic data are collected using Xsens Technology Inc. Motion Sensors (Model MTx-49A53G25). The sensors measure three-dimensional linear acceleration and angular velocity of the body segment motions. The collection of the force and kinematic data during STS experiments enables the characterization of the biomechanical loads and motions arising from each STS rise.

6.2.2.3 Key biomechanical metrics

Experiments with the test bed involve subjects performing both unassisted STS and assisted STS using the four assists (which are referred to as assist modes or modes of assist hereafter) described in Section 6.2.2.1. Each mode of assist will be characterized through the five questions stated in the Introduction (Section 6.1).

Two separate hypotheses will be evaluated to answer the first four questions (a-d):

1. Each mode of assist offers a statistically significant improvement from the unassisted STS.
2. One mode of assist is statistically better than all of the other modes of assist.

These hypotheses will be evaluated using several key biomechanical metrics (listed below) obtained from STS biomechanics literature.

CoM Displacement: The displacement of the subject center of mass (CoM) relative to the ankle at seat-off will be used as the measure of static stability. A smaller absolute displacement indicates that the subject is in a position of greater static stability [31].

CoP Displacement: According to Schultz et al. [21], dynamic (postural) stability is maximized when the foot CoP is centred between heel and toes. Thus the measure for dynamic stability will be determined by the location of the foot CoP at seat-off with respect to the center of the foot.

Peak Knee Torque: To determine the knee extensor effort required to rise, peak knee torque during each of the modes of STS will be compared, with lower knee torques indicating less knee extensor effort required to rise [15].

Peak Knee Torque Ratio: The peak knee torque will also be used to verify partial engagement of subject knee strength (i.e., load sharing with the assist mechanism) by verifying that the peak knee torque during each assisted rise is greater than 35% of the peak knee torque during the unassisted rise. The justification for this metric is detailed in Section 5.2.

Peak Trunk Flexion: Finally, to determine adherence to the MT strategy, the peak trunk flexion for each of the assisted STS will be compared to the peak trunk flexion of the unassisted MT strategy STS [25]. A statistically significant difference between the assisted peak trunk flexion and unassisted peak trunk flexion would indicate a strategy different from the MT strategy.

To answer the fifth question (e), subjects will complete a post-experiment questionnaire (Table 6.2, Appendix G) reporting sense of stability, strength used, and rise strategy and confidence for all of the STS rises. The questionnaire contains 6 questions, listed in Table 6.2, and for each assist subjects will be asked to choose from a four-point Likert scale with a score of four indicating that they agree with the question and a score of one indicating that they disagree with the question and two and three indicating that they somewhat disagree or agree, respectively. The scores reported by subjects in the post-experiment questionnaire will be grouped for each assist mode and combined for all subjects. This will provide an overall qualitative sense of subjects’ reactions to each mode of assisted STS. The assisted STS mode/s that receives the highest average combined questionnaire score with a statistical difference from the next highest score will be considered as the assist mode most preferred by subjects.

Table 6.2: Post-experiment questionnaire.

1	I felt stable when using this assist
2	I was able to rise with this assist using the <u>same motion</u> as used during the unassisted rise
3	I was confident that I would not fall while rising using this assist
4	I was able to rise smoothly with this assist
5	I felt comfortable in terms of forces placed on my body while rising using this assist
6	I was able to rise with this assist using <u>less effort</u> than the effort required to rise unassisted

6.2.2.4 Experiments

Experiments with the test bed include a total of five different modes of STS. In the unassisted mode, subjects sit on the test bed seat and then rise to a standing position without any assistance. In the assisted modes, subjects sit on the test bed seat and then rise to a standing position using each of the four modes of assistance provided by the test bed (seat, waist, bar, and arm). A set of five trials (trial defined as a single STS rise) are recorded for each mode of STS and used in the data analysis. This number of trials is consistent with studies that analyzed both unassisted STS [42] and assisted STS [31]. During each trial, the seat force, ground reaction forces, and subject kinematics are recorded using the test bed data collection equipment described in Section 6.2.2.2.

For all subjects, trials involving the unassisted mode of STS are conducted first, followed by the four assisted modes of STS. The unassisted STS mode is performed first because data collected from this mode are used for the load-sharing control scheme of the seat-assisted and waist-assisted modes (see Section 5.6.5.1). However, a modified randomized block design is used to counterbalance the four assisted modes of STS. The modification to the randomized block design is the placement of the arm assist as either the first or last assisted STS, with this modification allowing for faster switching times between assist modes.

6.2.3 Protocol

At the commencement of the experimental procedure, orientation sensors (5 x 3.5 x 2 cm size) are attached to a seated subject using straps. Sensors are attached to the shank, thigh, and chest at the approximate center of mass (CoM) of each segment. The CoM location is determined using approximate anthropometric coefficients based on segment lengths [46]. Figure 6.2 shows the equipment and experiment setup.

The seat height is pre-adjusted to 80% of the subject's knee height using wooden blocks placed on top of the force plate to raise the floor height of the test bed. Before the start of the trials, the force plate is zeroed to correct for long-term drift and the weight of the wood on the force plate. Subjects are asked to sit sock-footed on a thin cushion (8 cm width x 3 cm height cross section) on the test bed seat. The cushion is used to isolate the force applied by the subject to the seat by leaving the thighs unsupported. The subjects are requested to locate their ischial tuberosities by palpation and sit such that the ischial tuberosities are centred on the cushion. A piece of medical tape is attached to the thigh in the plane of the ischial tuberosities so that the subjects can easily align their ischial tuberosities to

the center of the cushion in subsequent trials. Foot position is set such that the feet are placed parallel, fully on the force plate, shoulder-width apart. Each shank is positioned approximately in 18° flexion with respect to the vertical plane to approximate normal foot placement [11].

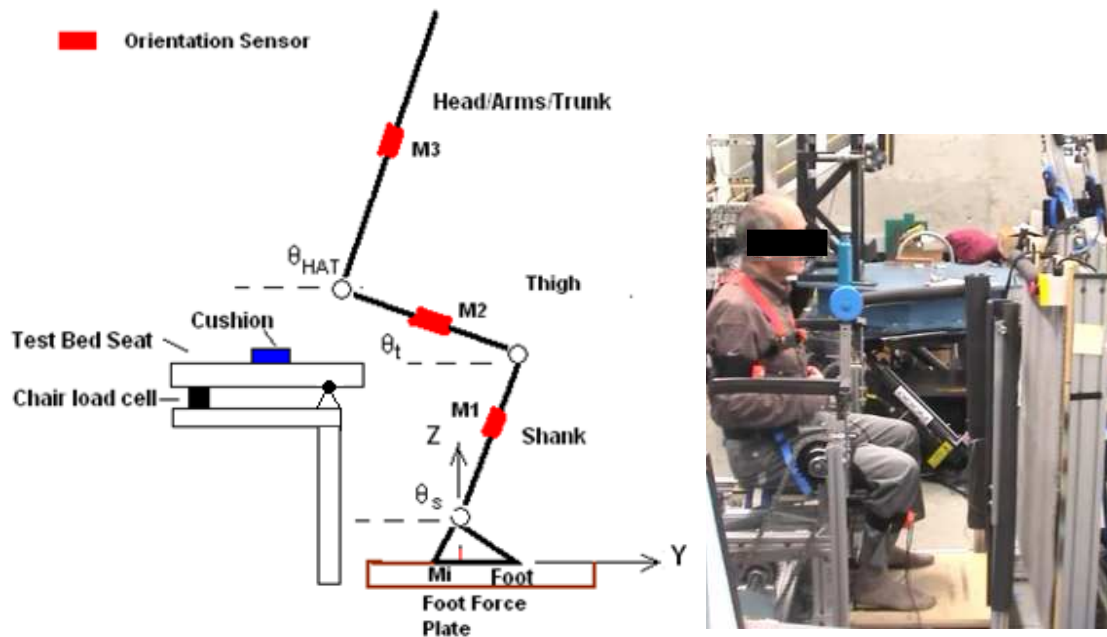


Figure 6.2: Experiment setup. θ_s is trunk angle, θ_t is thigh angle, θ_{HAT} is head/arm/trunk angle. Body segment angles are measured with respect to horizontal plane.

Subjects are first requested to sit down and maintain their trunk and head in an upright position. They are then asked to look straight ahead and rise to an erect position in five different manners: (a) five times with arms crossed across the stomach using a MT STS strategy as described in Hughes et al. [66] and demonstrated by the experimenter, (b) five times using the grab rail assist, (c) five times with the arm assist mechanism, (d) five times with the waist assist mechanism, and (e) five times with the seat assist mechanism (Figure 6.3 and Figure 6.4).

In case (a), subjects are asked to cross their arms in front of their stomach to prevent unmeasured forces from arm usage during the movement, and then asked to rise at a self-selected speed. In case (b), subjects are asked to rise at a self-selected speed and provide the required knee torque to stand up

by themselves, holding the grab rail for the duration of the rise to increase the stability of the motion (similar to the STS grab rail normal assist experiment described in Bahrami [31]). Subject position is normalized such that when seated with upright back and arms at full extension, subjects are able to hold onto the grab bar. In case (c), subjects are asked to provide the required knee torque to rise and use the assist mechanism to guide their trajectory as they rise to a standing position. Subjects are requested to hold onto the assist mechanism for the duration of the motion without putting their weight on the mechanism. In cases (d) and (e), subjects are asked to allow the force from the assist to guide them to a standing position. Subjects are also informed of the control scheme of the waist and seat assist, which slows the assist mechanism if they do not contribute sufficient effort, and are requested to use more of their own strength if they find that the assist mechanism is slowing down. Subjects are instructed on the operation of the deadman switch and motion of the assists and then given the opportunity to perform two to three practice trials for all the mechanically assisted modes of rise (cases (c), (d), and (e)). If a subject still has difficulty rising as instructed after the practice trials, additional practice trials are conducted until the subject reports confidence with the assist mechanism. The full experiment script is included in Appendix H and the experiment checklist is included in Appendix I.

For all trials, subjects are given the cue 'ready, go ahead' and subjects commence rising upon the instruction "go ahead". They remain standing as still as possible until data acquisition is completed, at which point they are asked to be seated again. An STS rise is considered successful if the feet remain still during the rise and if subjects maintain contact with the assists during the assisted rises. Upon completion of each set of assisted STS trials, subjects complete the post-experiment questionnaire for that set of trials.

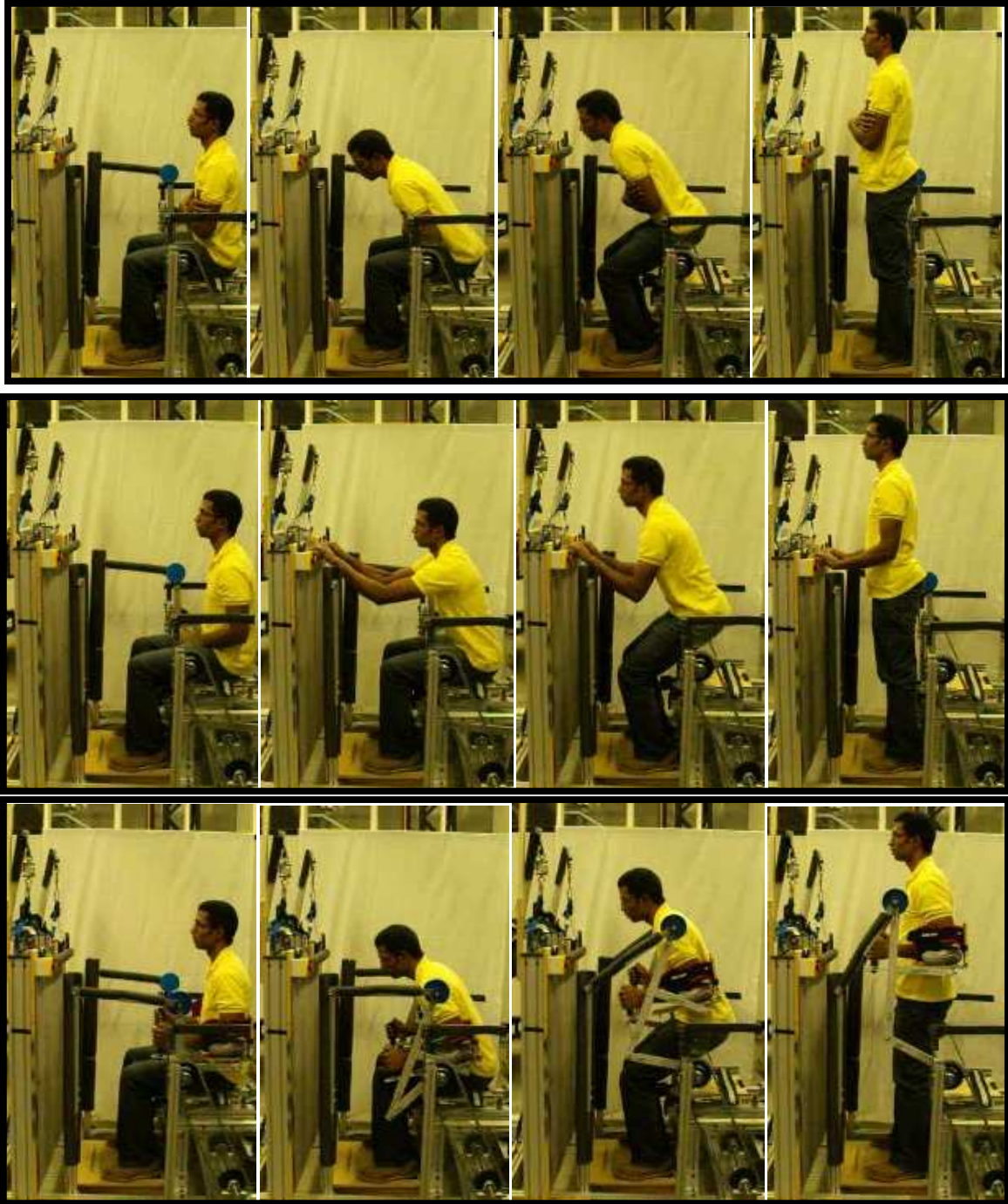


Figure 6.3: Still frame animation of three modes of STS. From top to bottom: unassisted, bar assist, arm assist. Each mode of STS has four still frames, representing approximately (from left to right): start of trunk flexion, start of thigh extension, maximum ankle dorsiflexion, and end of thigh extension.

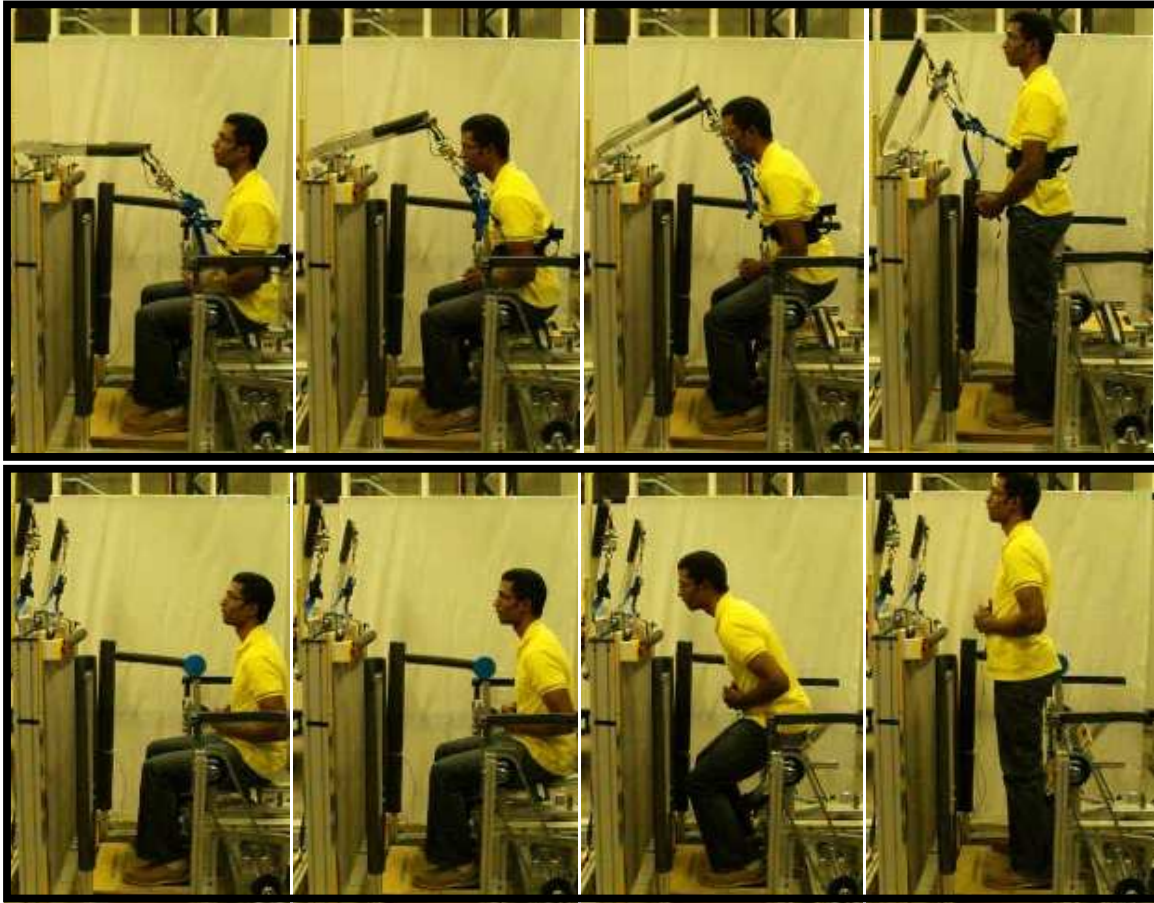


Figure 6.4: Still frame animation of two modes of STS. Top animation: waist assist. Bottom animation: seat assist. Each mode of STS has four still frames, representing approximately (from left to right): start of trunk flexion, start of thigh extension, maximum ankle dorsiflexion, and end of thigh extension.

6.2.3.1 Data collection procedure

The force and kinematic data collection is initiated on the ‘ready’ cue, one second before the ‘go’ cue and lasts ten seconds for each trial. Reaction and assist forces are collected from the force plate and load cells at a frequency of 50 Hz and are digitally filtered with a zero-delay, bidirectional, fourth-order, low pass, Butterworth filter at a cut-off frequency of five Hz [42]. Three-dimensional angular orientations and angular velocities as well as linear accelerations are obtained from the Xsens sensors. Xsens sensor data are collected at a frequency of 50 Hz and filtered in the same way as the force plate data.

Force plate data are collected on a National Instruments PXI Computer and transferred via an Ethernet link to the computer collecting the Xsens data. Data transfer delay is calculated as described in Section 5.7.3 and the force plate data is time shifted to synchronize force plate and Xsens data. The accelerometer data are gravity compensated, based on the estimated orientation of each sensor, to negate the gravity force readings on the sensors. All data filtering, time shifting, and gravity compensation are computed offline in Matlab after the trials are completed.

6.2.4 Data analysis

6.2.4.1 Model

A four-link rigid body biomechanical model, advocated in Mak et al. [42] and Kuo [44], was created to describe the kinematics and dynamics of the upper body and lower extremities during the STS motion. The model consists of four rigid body linked segments representing the feet, lower legs (shank), upper legs (thigh), and Head/Arms/Trunk (Figure 6.5). Using generalized anthropometric coefficients [46] the approximate body segment masses, CoM locations, and moments of inertia were calculated.

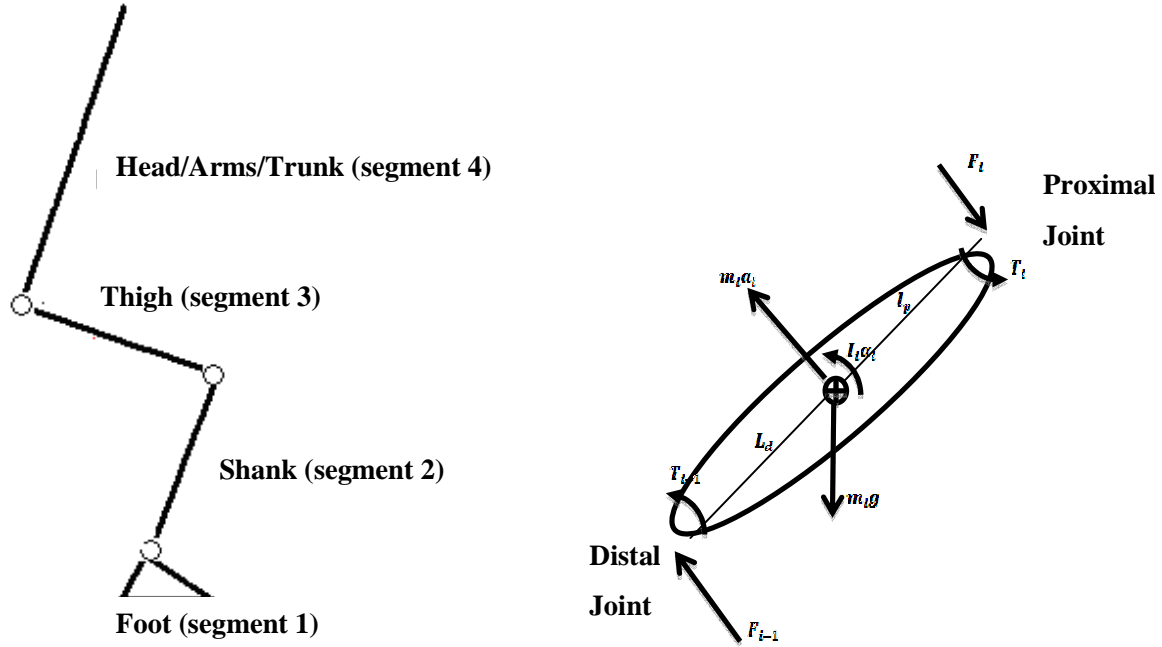


Figure 6.5: The 4-link rigid biomechanical model and a representative body segment used in the inverse dynamics model. The body consists of 4 segments connected by three joints. L_d is the distance to the distal joint from the CoM and L_p is the distance to the proximal joint from the CoM. T_{i-1} and F_{i-1} represent the joint torque and force acting on the distal joint of the current body segment (segment i) from the proximal joint of the previous body segment (segment $i-1$). Gravity force ($m_i g$) and acceleration force ($m_i a_i$) act at the CoM. T_i and F_i represent the joint torque and force acting on the proximal joint of the current body segment.

Symmetry across the sagittal plane was assumed [31], and therefore the model was created in a two dimensional plane. Using the body segment kinematic data, force plate dynamic data, and subject anthropometric data, the joint forces and torques were calculated recursively using Newton-Euler inverse dynamics analysis.

$$\sum Forces_i = m_i a_i \quad i = 1, \dots, 4 \quad (6.1)$$

$$\sum Moments_i = I_i \alpha_i \quad i = 1, \dots, 4 \quad (6.2)$$

$$T_{ankle} = -(m_{foot} g l_{foot}) + (CoPF_{zfp}) - (h_{ankle} F_{yfp}) \quad (6.3)$$

$$F_{yankle} = F_{yfp} \quad F_{zankle} = F_{zfp} - m_{foot} g \quad (6.4)$$

$$F_i = F_{i-1} - m_i g - m_i a_i \quad (6.5)$$

$$T_i = (L_d \times F_{i-1}) + (L_p \times F_i) + T_{i-1} - I_i \alpha_i \quad (6.6)$$

This analysis computes the dynamic equilibrium of body segments using the Newton-Euler equations of translation and angular motion (Equations 6.1 and 6.2). Figure 6.5 shows a representative segment of the biomechanical model used in the study with forces and torques labeled. The force plate inputs (CoP , F_{yfp} , F_{zfp}) are used to calculate the ankle torque and forces according to Equations 6.3 and 6.4. Working upwards, the remainder of the joint forces and torques are calculated using Equations 6.5 and 6.6. Linear accelerations of each segment are obtained directly from orientation sensors, and the angular acceleration is obtained by applying the central difference formula to differentiate the angular velocity measurements obtained from the orientation sensors. The sensor program automatically integrates angular velocity to provide sensor orientation data in the form of roll-pitch-yaw angles with rotations relative to the inertial frame of the sensor. Sensor drift is assumed to be negligible.

In all assist modes, except for the seat assist, seat reaction force (F_{seat}) is calculated using the seat load cell force and the horizontal ground reaction force. The seat reaction force is assumed to be applied to the ischial tuberosities. For calculation of hip torque prior to seat-off, the seat reaction forces (F_{seat}) and distance from the thigh CoM to ischial tuberosities (L_t) are included in the biomechanical model (Equations 6.7 and 6.8). For the seat assist, the rotation of the seat provides a seat force to subjects as they rise to a standing position. Therefore, for seat-assisted STS, the seat reaction force is determined using a whole body equilibrium equation (Equation 6.9), in which a_{ybody} and a_{zbody} are obtained from Equations 6.10 and 6.11, respectively.

$$F_{hip} = F_{knee} - m_{thigh}g - m_{thigh}a_{thigh} + F_{seat} \quad (6.7)$$

$$T_{hip} = (L_d \times F_{knee}) + (L_p \times F_{hip}) + T_{knee} - I_{thigh}\alpha_{thigh} + F_{seat}L_t \quad (6.8)$$

$$F_{yseat} = F_{yfp} + m_{body}a_{ybody} \quad F_{zseat} = -F_{zfp} + m_{body}g + m_{body}a_{zbody} \quad (6.9)$$

$$a_{ybody} = \frac{m_{foot}a_{yfoot} + m_{shank}a_{yshank} + m_{thigh}a_{ythigh} + m_{HAT}a_{yHAT}}{m_{foot} + m_{shank} + m_{thigh} + m_{HAT}} \quad (6.10)$$

$$a_{zbody} = \frac{m_{foot}a_{zfoot} + m_{shank}a_{zshank} + m_{thigh}a_{zthigh} + m_{HAT}a_{zHAT}}{m_{foot} + m_{shank} + m_{thigh} + m_{HAT}} \quad (6.11)$$

6.2.4.2 Extended model

For the bar-assisted and arm-assisted motions, the 4-link biomechanical model is extended to a 6-link model by separating the head/arms/trunk segment into 3 segments consisting of the head/trunk, upper arm, and forearm.

6.2.4.3 Treatment of data

Using the kinematic and kinetic data from the force plate, load cells, and orientation sensors in the 4-link biomechanical model, several biomechanical parameters are then calculated. The body segment angles with respect to the horizontal plane are determined directly from orientation sensor measurements of the joint angles. The maximum trunk flexion is determined as the difference between the initial trunk angle reading and the peak trunk angle reading.

Because it was found to be difficult to attach the trunk sensor exactly parallel with the torso, an offset is introduced into the trunk sensor reading to compensate for the discrepancy between the true trunk angle and the reading from the trunk angle sensor. During the last two seconds of data collection, while the subject is in an erect standing position, the average trunk sensor reading is computed and offset such that the sensor reads a value of approximately 90° during this phase of quiet standing.

The horizontal projection of the whole body center of mass is determined from segmental masses and their estimated approximate CoM locations [46]. Foot center of pressure location is calculated from force plate data and referenced to the foot position on the force plate. The CoM and CoP locations are measured at the time at which the subject loses contact with the test bed. For the unassisted, bar and arm-assisted trials, this is the instant at which the subject loses contact with the seat, referred to as the seat-off time and determined as the point at which the seat load cell force reaches zero. For the waist-assisted and seat-assisted trials this is the instant at which the subject loses contact with the assist mechanism, referred to as the assist-end time and defined as the time at which the assist force or a related force reaches a specified value. For the waist assist this occurs when the waist assist load cell force is within 5 N of the final value achieved after the subject is fully standing (approximately 0 N). For the seat assist, this occurs when the force plate vertical ground reaction force reaches 100% of body weight [67].

The hip, knee, and ankle torques are determined using the 4-link biomechanical model. The movement time is also measured (defined as the interval between the start of motion and the end of motion). The start of motion is defined as the initiation of trunk flexion (the time at which trunk

angular velocity exceeds 0.1 rad/s [65]), and the end of motion is defined as the time at which thigh extension ceases (the time at which thigh extension angular velocity reduces below 0.1 rad/s).

The peak knee torque is obtained from the knee torque measurements for all of the STS modes. The peak knee torque ratio is calculated for all of the assisted STS modes according to Equation 6.12, where $T_{k-assisted}$ is the assisted peak knee torque and $T_{k-unassisted}$ is the unassisted peak knee torque.

$$Peak\ Knee\ Torque\ Ratio = T_{k-assisted}/T_{k-unassisted} \quad (6.12)$$

To enable comparison of the data across subjects, the calculated data are normalized according to the following procedure. Knee torque is normalized by the product of body segment height and mass, and foot CoP and body horizontal CoM are normalized by total foot length. The duration of the motion, i.e., the movement time, is given a normalized value of 1.0 [31]. Subjects perform five trials using the five modes of STS, and the average values of the biomechanical metrics are computed for each set of five trials. For the post-experiment questionnaire, the scores reported by subjects for all six questions are grouped for each assist mode and combined for the 16 subjects.

To determine statistical differences, a repeated measures ANOVA is conducted on the data obtained for each of biomechanical metrics, excluding the peak knee torque ratio. The peak knee torque ratio is excluded from the ANOVA because the purpose of this metric is only to verify load sharing by ensuring that the average assisted knee torque is greater than 35% of the average unassisted knee torque. After each ANOVA, a *post-hoc* Bonferroni test is conducted to determine if there are significant differences between individual assist modes for each biomechanical metric and for the combined questionnaire scores. There are a total of 44 statistical tests; thus the significance level is set at $\alpha = 0.05/44 = 0.001$ for both the quantitative and qualitative data.

For the peak knee torque ratio, a one sample t-test is conducted to determine if the peak knee torque ratio for each mode of assisted STS has a value significantly greater than 35%. This t-test is performed by first computing the ratio margin according to Equation 6.13, and then testing the null hypothesis that the ratio margin is equal to zero. If the calculated ratio margin is greater than zero and the null hypothesis is proved false, then the peak knee torque ratio has a value significantly greater than 35%. T-tests are also conducted at a significance level of $\alpha = 0.001$.

$$\text{Ratio Margin} = (\text{Peak Knee Torque Ratio})100\% - 35\% \quad (6.13)$$

Because the post-experiment questionnaire contains ordinal data, a non-parametric repeated measures analysis is conducted (the Friedman test) to determine if there are statistical differences between assists in the results of the post-experiment questionnaire. This analysis is followed by *post-hoc* Wilcoxon Signed-Rank tests to individually characterize the statistical differences in scores between each of the assist modes.

6.2.4.4 Data anomalies

For one of the subjects, an error occurred in the data collection due to the force plate amplifier being accidentally turned off during the experiment. All of the data for this subject were discarded because the analysis of the biomechanical metrics could not be completed for all assists due to the missing force plate data. For the balance of this thesis, the phrase “all subjects” refers to all subjects for whom a complete set of data was acquired.

For another subject in one of the seat-assisted trials, the seat force sensor became loose, resulting in an error in the seat force sensor reading; thus a total of four trials instead of five trials were used for the calculation of the average seat-assist biomechanical metrics for this subject.

Finally, one of the subjects only had four valid waist-assisted trials. The fifth trial was discarded because the subject rose faster than the assist mechanism and did not use the assist to aid with the STS. Thus, for this subject a total of 4 trials were used instead of five trials for the calculation of the average waist-assisted biomechanical metrics.

6.3 Results

The data were analysed to obtain results for each of the five questions described in Section 6.1 and quantified in Section 6.2.2.3. Analyses were performed for each of the results to determine statistical differences from the unassisted mode and statistical differences from each of the other assisted STS modes. Table 6.3 presents a summary of the results.

Table 6.3: Summary of results from key biomechanical metrics and post-experiment questionnaire from all subjects for the five modes of STS (standard deviation). For each metric the statistically best result(s) are highlighted in bold. All of the results are highlighted for the peak knee torque ratio because each assisted mode of STS had a peak knee torque ratio significantly greater than 35% of the unassisted peak knee torque.

	Unassisted	Bar	Arm	Waist	Seat
CoM - Xank [%Length Foot]	-0.43 (0.11)	-0.52 (0.17)	-0.53 (0.18)	0.05 (0.12)	-0.25 (0.12)
CoP - Xfootcenter [%Length Foot]	-0.34 (0.07)	-0.31 (0.06)	-0.36 (0.08)	-0.13 (0.15)	-0.11 (0.11)
Peak Knee Torque [%Body Mass * Body Height]	1.39 (0.22)	1.25 (0.16)	1.31 (0.20)	1.07 (0.22)	1.13 (0.22)
Peak Knee Torque Ratio [% unassisted peak knee torque]	n/a	90 (8.6)	94 (11.1)	77 (14.1)	81 (12.7)
Peak Trunk Flexion (degrees)	37.25 (6.65)	22.18 (5.60)	24.49 (7.79)	8.83 (3.97)	19.30 (5.42)
Mean Post-Experiment Questionnaire Score	n/a	3.7 (0.5)	3.4 (0.9)	3.4 (0.9)	3.9 (0.3)

6.3.1 Static stability

A significant difference was detected between the CoM displacement at seat-off for the unassisted and seat-assisted STS ($p < 0.001$), and for the unassisted and waist-assisted STS ($p < 0.001$). No significance was detected between the unassisted and arm-assisted STS ($p = 0.009$) and the unassisted and bar-assisted STS ($p = 0.009$).

A significant difference was noted between the seat and waist ($p < 0.001$), the seat and bar ($p < 0.001$) and the seat and arm ($p < 0.001$) assisted STS rises. In addition, a significant difference was detected between the waist and bar ($p < 0.001$) and waist and arm ($p < 0.001$) assisted STS rises. The full results of the CoM displacement from the ankle at seat-off for each subject and the results of the CoM displacement ANOVA are included in Appendix J.

Figure 6.6 shows the average values of the CoM displacement at seat-off for each of the five modes of STS. Figure 6.7 shows the trajectory of the horizontal projection of the CoM for a representative subject performing each of the five modes of STS. Differences in the CoM displacement at Movement Start and Movement End in Figure 6.7 are due to variance in the initial and final position of the subject between modes of STS.

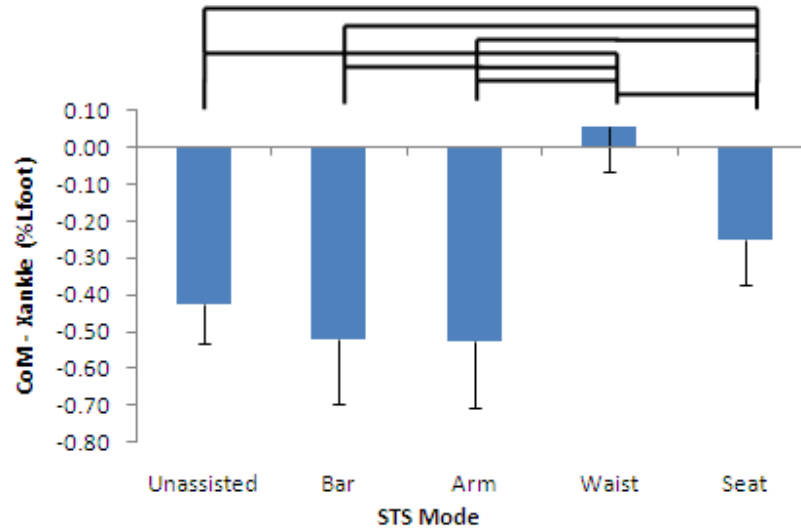


Figure 6.6: Average distance of the horizontal projection of the total CoM from the ankle at seat-off. Error bars indicate standard deviation. Note that for the seat-assisted and waist-assisted STS rises, seat-off is the point at which the user loses contact with the assist mechanism. CoM displacement is normalized to subject foot length. The horizontal lines connect pairs of STS modes for which there is a significant difference.

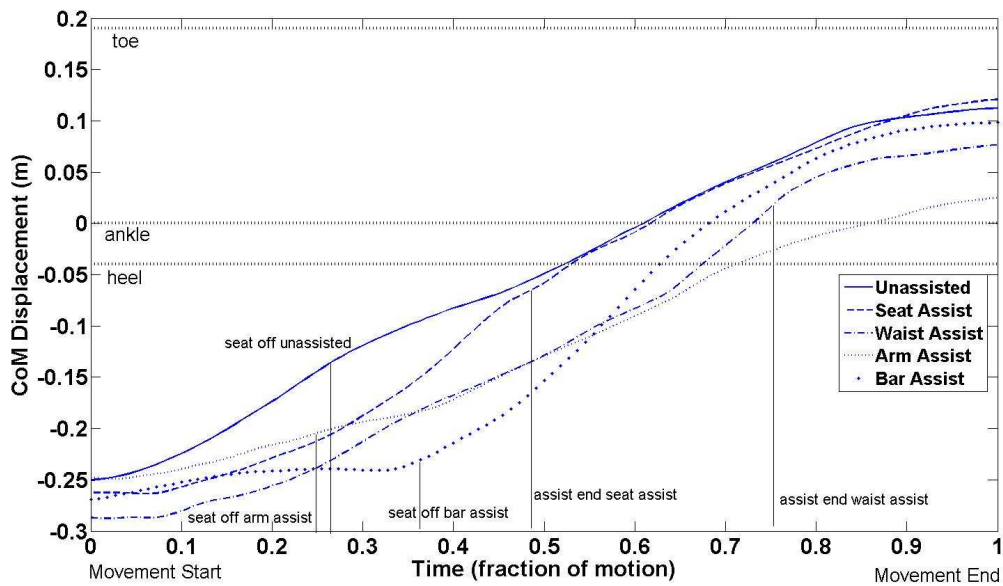


Figure 6.7: Trajectory of the horizontal projection of the total body CoM of a representative subject for five modes of STS. The vertical lines indicate the times at which the CoM displacement from the ankle is measured for each assist. For unassisted, arm, and bar assisted STS rises, the CoM displacement is measured at seat-off time. For the seat and waist assist, the CoM displacement is measured at the assist-end time.

6.3.2 Dynamic stability results

A significant difference was detected between the CoP location at seat-off for the unassisted and seat-assisted STS ($p < 0.001$) and the unassisted and waist-assisted STS ($p < 0.001$). No significance was detected between the unassisted and arm-assisted STS ($p = 0.043$) and the unassisted and bar-assisted STS ($p = 0.124$).

No significant difference was noted between the seat-assisted and waist-assisted STS ($p = 0.669$) but there was a significant difference between the seat and bar ($p < 0.001$) and seat and arm ($p < 0.001$), as well as the waist and bar ($p < 0.001$) and waist and arm ($p < 0.001$) assisted STS rises. The full results of the CoP displacement from the foot center at seat-off for each subject and the results of the CoP displacement ANOVA are included in Appendix K.

Figure 6.8 shows the average values of the CoP displacement at seat-off for each of the five modes of STS. Figure 6.9 shows the trajectory of the horizontal projection of the CoP for a representative subject performing each of the five modes of STS. Differences in the CoP displacement at Movement Start and Movement End in Figure 6.9 are due to variance in the initial and final position of the subject between modes of STS.

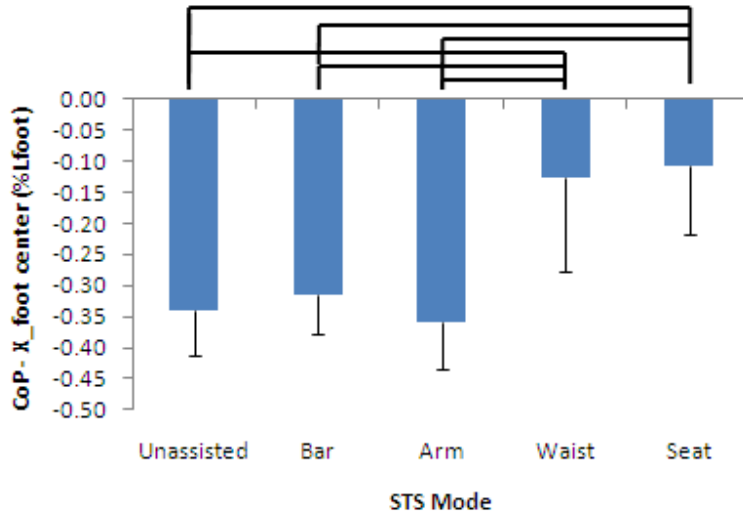


Figure 6.8: Average displacement of the foot CoP from the foot center at seat-off. Error bars indicate standard deviation. Note that for the seat-assisted and waist-assisted STS rises, seat-off is the point at which the subject loses contact with the assist mechanism. Distance is normalized to subject foot length. The horizontal lines connect pairs of STS modes for which there is a significant difference.

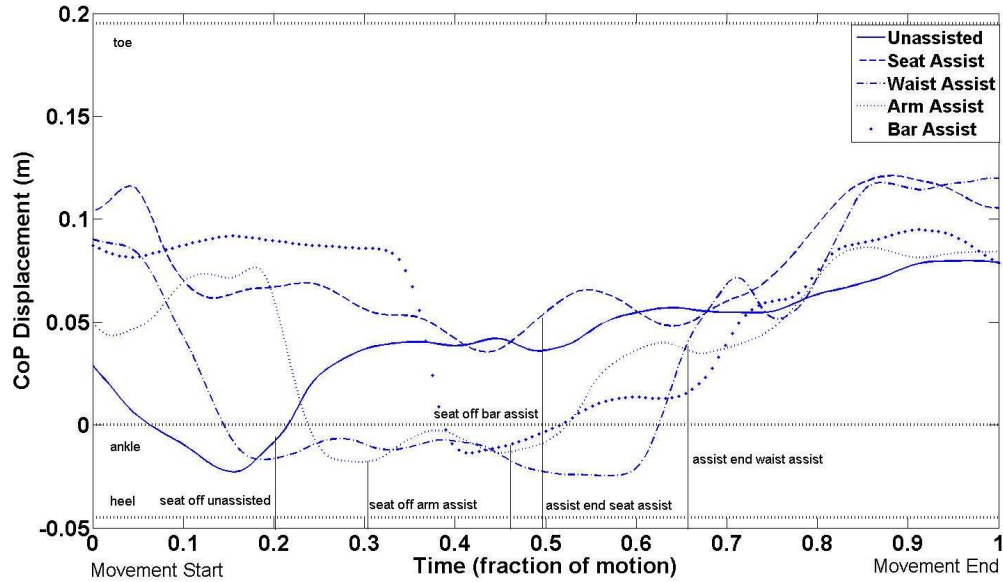


Figure 6.9: Trajectory of the foot CoP of a representative subject for five modes of STS. The vertical lines indicate the key points at which the CoP displacement from the foot center is measured for each assist. For unassisted, arm, and bar assisted STS rises, the CoP displacement is measured at seat-off time. For the seat and waist assist, the CoP displacement is measured at the assist-end time.

6.3.3 Knee extensor effort results

A significant difference was detected between the peak knee torque for the unassisted and seat-assisted STS ($p < 0.001$) and between the unassisted and waist-assisted STS ($p < 0.001$). No significance was detected between the unassisted and arm-assisted STS ($p = 0.141$) and between the unassisted and bar-assisted STS ($p = 0.001$).

No significant difference was detected between the seat-assisted and waist-assisted STS rises ($p = 0.095$), but the waist-assisted STS was significantly different from the arm-assisted STS ($p < 0.001$). The full results of the peak knee torque for each subject and the results of the peak knee torque ANOVA are included in Appendix L.

Figure 6.10 shows the average values of the peak knee torques for each of the five modes of STS. Figure 6.11 shows the trajectory of the knee torque for a representative subject during each of the five modes of STS. In Figure 6.11, the knee torque of the arm and bar assist at the Movement End is 50 N. This is greater than the knee torques for the other modes of STS, which reduce to approximately 0 N at the Movement End. These dissimilarities in knee torques are due to differences in the foot CoP of the subject at the Movement End time for these modes of STS, which in turn affects the ankle and knee torque at the Movement End time according to Equations 6.3 and 6.6. This CoP difference may be the result of a difference in the end position of the subject for these modes of STS. The experiment protocol required that the subject's hands remain in contact with the assist mechanism for the duration of the bar-assisted and arm-assisted STS rises whereas for the other modes of STS, the protocol required that the arms be crossed across the stomach for the duration of the rise.

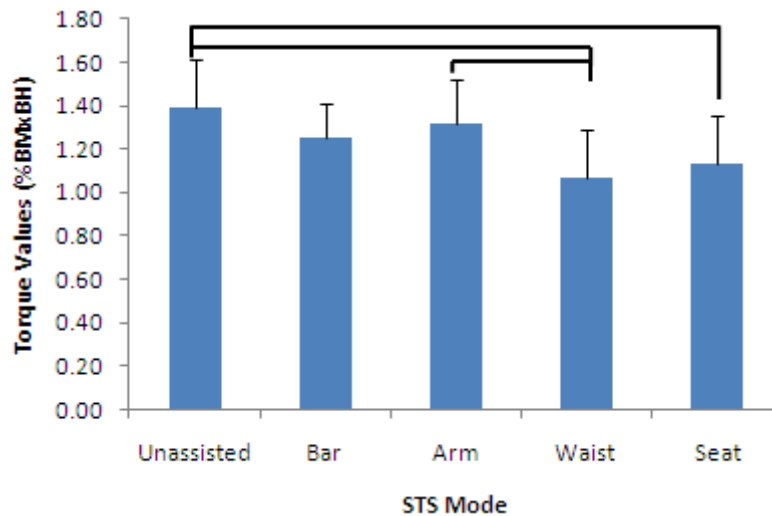


Figure 6.10: Average peak knee torque for each of the five modes of STS. Error bars indicate standard deviation. Torques are normalized to (body mass x body height). The horizontal lines connect pairs of STS modes for which there is a significant difference.

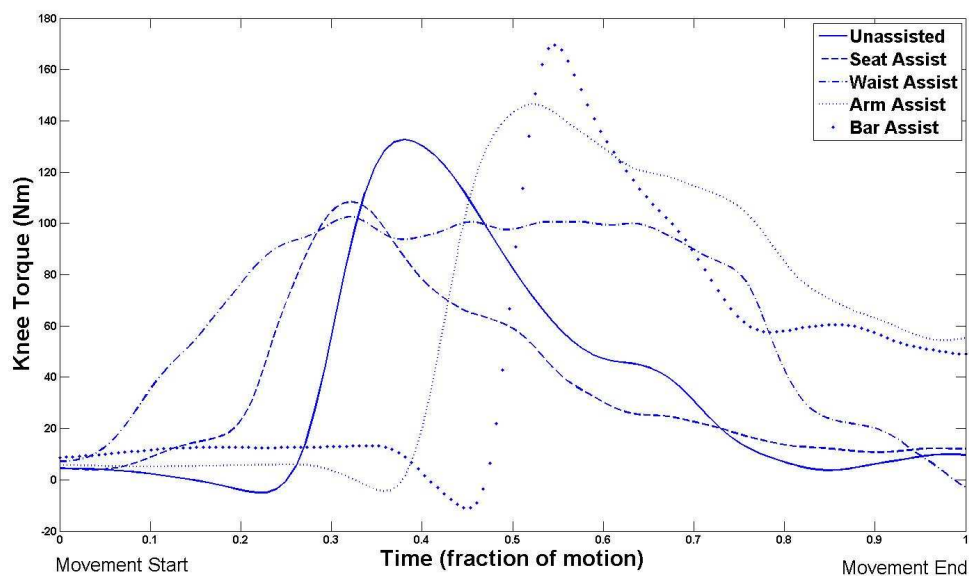


Figure 6.11: Knee torque trajectories of a representative subject for five modes of STS.

In accordance with the criterion that the assist mechanism should share the knee load required to rise with the subject, all of the assist mechanisms achieved the peak knee torque ratio requirement. The average peak knee torques generated in all four of the assisted STS rises were greater than 35% of average peak knee torque for the unassisted rise (Figure 6.12) with the waist assist providing the lowest torque ratio, at 77% of the peak unassisted knee torque, and the arm assist providing the highest torque ratio, at 94% of the peak unassisted knee torque. The full results of the peak knee torque ratio for each subject and the results of the peak knee torque t-tests are included in Appendix M.

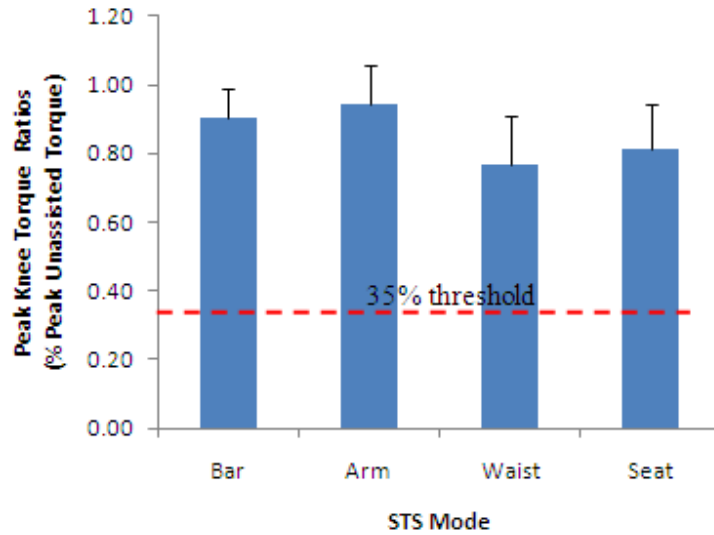


Figure 6.12: Ratio of average peak knee torque of each of the assisted rises to the average peak torque of the unassisted rise. Error bars indicate standard deviation.

6.3.4 Momentum transfer strategy adherence results

Significant differences in peak trunk flexion were detected between the unassisted STS and all of the assisted STS rises at identical significance levels ($p < 0.001$).

No significant difference was detected between the peak trunk flexion for the bar, arm and seat assisted rises, but significant differences did exist between the waist and bar ($p < 0.001$), waist and arm ($p < 0.001$), and waist and seat assisted STS rises ($p < 0.001$). The full results of the peak trunk flexion measure for each subject and the results of the peak trunk flexion ANOVA are included in Appendix N.

Figure 6.13 shows the average values of the peak trunk flexion for each of the five modes of STS.

Figure 6.14 shows the trajectory of the trunk angle for a representative subject performing each of the five modes of STS.

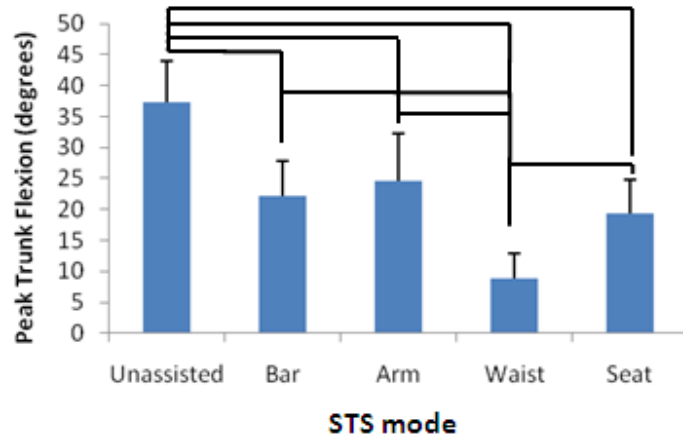


Figure 6.13: Average peak trunk flexion for each of the five modes of STS. Error bars indicate standard deviation. The horizontal lines connect pairs of STS modes for which there is a significant difference.

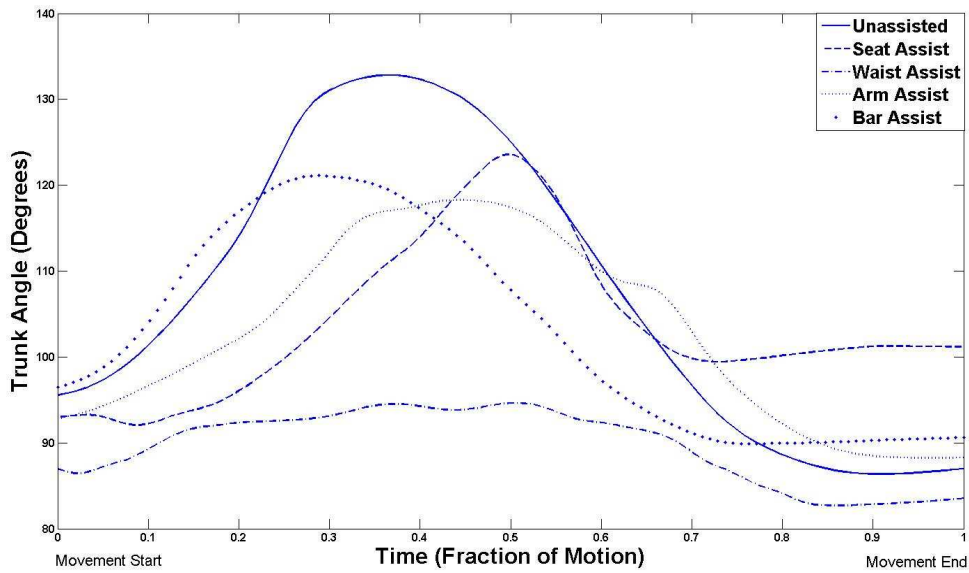


Figure 6.14: Trunk angle trajectories of a representative subject for five modes of STS.

6.3.5 Questionnaire results

6.3.5.1 Pre-experiment questionnaire results

The pre-experiment questionnaire results indicate that none of the subjects used assistive devices to help them with STS, and none of the subjects had difficulty rising out of a chair. Two subjects reported having difficulty with mobility; one subject had cartilage out of his right knee and the other subject reported having stiffness, arthritis and muscle weakness. The full results of the pre-experiment questionnaire are included in Appendix O.

6.3.5.2 Post-experiment questionnaire results

Significant differences in the scores for the post-experiment questionnaire were detected between the seat and waist ($p < 0.001$) and between the seat and arm ($p < 0.001$) assisted STS rises. Significant differences were also detected between the bar and waist ($p < 0.001$) and between bar and arm ($p < 0.001$) assisted STS rises. No difference was detected between the bar-assisted and seat-assisted STS rises ($p = 0.005$). Figure 6.15 shows the average scores for each assist in the post-experiment questionnaire. The full results of the post-experiment questionnaire and the combined post-experiment questionnaire ANOVA are included in Appendix P.

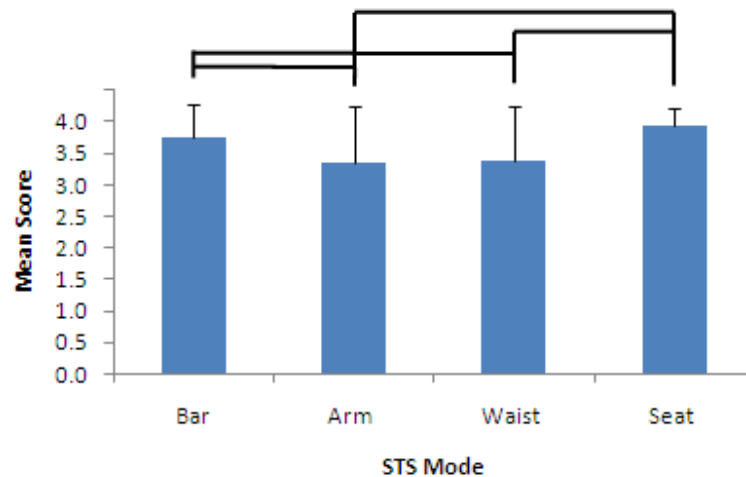


Figure 6.15: Average scores for each assist in the post-experiment questionnaire. Error bars indicate standard deviation. Note that maximum mean score is 4.0. The horizontal lines connect pairs of STS modes for which there is a significant difference.

6.4 Discussion

6.4.1 Static stability discussion

Both the waist and seat assists provided significant static stability improvements relative to the unassisted STS. The static stability results for the bar and arm assists did not reveal any statistical differences from the unassisted STS. The static stability as measured by the CoM for waist-assisted STS was also significantly better than the seat-assisted STS; thus, the waist assist is the most statically stable mode. Figure 6.7 shows that for all of the assists, the total body CoM is monotonically increasing. Because the assist-end time for the waist-assisted and seat-assisted STS rises occurred closer to the end of the motion than the seat-off time of the bar and arm assist, the waist and seat assists provide greater static stability than the other assists.

On average the thigh angle at the end of assist for the seat assist was 30.3° (SD 6.6°) and for the waist assist was 76.9° (SD 8.5°) with respect to the horizontal. During a STS rise, the thigh angle increases to approximately 90° at the end of the rise, thus for the waist assist, the thigh angle at assist-end was very close to the angle of a fully standing subject. Based on this analysis and the statistical comparison with the other assists, of the assists tested, the waist assist was determined to provide the best static stability during STS.

Although the static stability result for the bar assist was not significantly different from the unassisted rise, the bar-assisted rise did have a larger CoM displacement from the ankle position at seat-off than the CoM displacement of the unassisted rise. This is consistent with Bahrami et al. [31], who showed that when rising with bar support, subjects did not try to transfer their body CoM from the chair to the support base of the feet before leaving the chair, resulting in a larger CoM displacement from the ankle at seat-off during the bar-assisted rise compared to the unassisted rise.

6.4.2 Dynamic stability discussion

Both the waist and seat assists provided significant dynamic stability improvements over the unassisted STS. The dynamic stability results for the bar and arm assists did not reveal any statistical difference from the unassisted STS. Also, there was no statistical difference between the waist and seat assists with regards to the dynamic stability measures. Thus, of the assists tested, the waist and seat assists are considered to be equally the most dynamically stable modes of assisted STS.

6.4.3 Knee extensor effort discussion

Both the waist and the seat assist provided a significant reduction in the knee torque required to rise compared to the unassisted STS. The bar and arm assists did not significantly reduce the knee torque from the unassisted STS. This is in accordance with the STS experimental protocol, which requested that subjects use the bar and arm assists for guidance and stability but not to reduce knee torque (Section 6.2.3), and to use the waist and seat assists to reduce the knee torque required to rise. There was no statistical difference between the waist and seat assists in terms of torque reduction, thus the waist and seat assists are equally effective with respect to reducing the knee extensor effort required to rise.

In addition to assisting with STS knee extensor effort reduction, the seat-assisted and waist-assisted STS rises share the knee load with subjects as evident from the peak knee torque ratios, which were significantly greater than the threshold of 35% of the unassisted peak knee torque: 77% for the waist assist and 81% for the seat assist.

The knee torque reduction by the seat assist is consistent with Wretenberg et al. [22], who reported a significant mean peak knee torque reduction, when using a spring loaded flap seat, from 73 Nm to 41 Nm ($p < 0.001$). This is equivalent to a peak knee torque at 56% of the unassisted peak knee torque. In the present study, the peak knee torque when rising with the seat assist was only reduced to 81% of the unassisted peak knee torque.

6.4.4 Momentum transfer strategy adherence discussion

According to the criterion for MT Strategy adherence, for an assisted STS to follow the MT strategy, the peak trunk flexion of the assisted STS must not be significantly different from the peak trunk flexion of the unassisted STS. All of the assisted STS rise modes generated significantly lower peak trunk flexion angles compared to the unassisted STS. Thus no assist was able to adequately replicate the MT strategy as characterized by this measure. The low trunk flexion peak angles suggest that all of the assisted STS rises promote a dominant vertical rise [25]. The waist assist had a peak trunk flexion angle that was significantly lower than that for all of the other assisted rises ($p < 0.001$). This indicates that the waist assist provided the least amount of momentum transfer with subjects flexing their trunk very little during the STS motion.

The arm assist mechanism was designed to promote a MT strategy. Subjects expressed difficulty in learning and following the motion of the mechanism and were unable to rise with a MT strategy using

this assist. In addition, the use of a single trajectory for subjects of different heights and body segment lengths resulted in a wide variance of motions generated by the assist as indicated by the standard deviation of the peak trunk angle (7.8°), which was larger than the standard deviation of the peak trunk angle of all of the other assisted STS rises (refer back to Table 6.3).

The peak trunk flexion in the seat-assisted rise was 18° less than the peak trunk flexion in the unassisted rise. This smaller peak trunk flexion in the seat-assisted rise is consistent with Bashford et al. [37], who found that the ejector mechanism resulted in a peak trunk flexion 6.1° less than the peak trunk flexion when rising without an ejector mechanism. However, Bashford et al. did not present statistical results and the results were averaged over a small sample size (five subjects).

6.4.5 Hypothesis discussion

The comparisons of each assisted STS mode with the unassisted STS and with the other assisted STS modes were completed to answer the questions stated in the Introduction (Section 6.1) by evaluating the two hypotheses stated in Section 6.2.2.3.

With respect to the first hypothesis (each mode of assist offers a statistically significant improvement from the unassisted STS), results show that the arm and bar assists did not offer significant improvements from the unassisted STS. However the seat and waist assists did offer significant improvements with respect to static and dynamic stability and knee extensor effort reduction.

With respect to the second hypothesis (one mode of assist is statistically better than all of the other modes of assist), results showed that the waist assist was significantly better than all the other assists in terms of the static stability metric. In terms of dynamic stability and knee extensor effort reduction, the waist and seat assists were equally better than the arm and bar assists.

6.4.6 Post-experiment questionnaire discussion

The seat and bar assists both received scores in the post-experiment questionnaire that were significantly higher than the scores received for the waist and arm assists (refer back to Figure 6.15). No significant difference was detected between the questionnaire scores for the seat and bar assists, thus both of these assists were the modes of assisted STS most preferred by the subjects of the modes tested.

Subjects recorded comments for some of the assists on the post-experiment questionnaire. A general summary of the subject comments is listed below (full set of comments is included in Appendix Q):

- **Bar assist:** assist helped with stability but did not help with reducing the effort to rise.
- **Arm assist:** assist was not natural or smooth and required more effort than rising without assistance.
- **Waist assist:** effort was reduced but the assist was not very smooth or natural in the force and motion it provided.
- **Seat Assist:** assist reduced the effort required to rise and allowed for a smooth rising motion.

6.5 Summary

Experiments with the STS test bed examined five different modes of STS in terms of key biomechanical metrics and subject feedback on each mode of assist. Summary plots for subjects performing each mode of STS are included in Appendix R and Appendix S. Results from the experiment show that the waist and seat assist both provide improvements in the static and dynamic stability of subjects from the unassisted STS and that the waist assist provides the greatest amount of static stability improvement. Both the seat and waist assist reduce the knee extensor effort required to rise from the unassisted STS rise while engaging subjects' available strength. None of the assists are able to adequately reproduce the unassisted MT STS strategy.

Thus, with respect to the key biomechanical metrics of static stability, dynamic stability, knee extensor strength reduction and load sharing, and MT strategy adherence, the waist and seat assists offer improvements in all areas, except for promoting a MT strategy.

The results of the post-experiment questionnaire show that the most preferred STS assists reported by subjects are the seat and bar assist, with significantly lower preference being given to the waist and arm assists.

Although the results from the static and dynamic stability and knee extensor effort biomechanical metrics are very similar for the seat and waist assists, there were statistically significant differences between these assists with respect to MT strategy adherence and subject qualitative feedback. Results show that the waist assist promoted very little momentum transfer as seen by the peak trunk flexion during the waist-assisted rise, which was significantly lower than the peak trunk flexion during all other assisted rises. In addition, questionnaire results show that subject preference was given to the seat assist over the waist assist. These results suggest that, of the modes tested, the seat assist is the best mode of STS assist.

Chapter 7 Conclusions and Recommendations

7.1 Conclusions

The objective of this work was to provide an empirical quantification of different modes of load-sharing sit to stand (STS) to determine the best mode/s of assisted STS. This empirical quantification will increase knowledge into the biomechanics of different modes of assisted STS and help direct the design of new and improved STS assistive devices.

The review of the literature, presented in Chapter 2, characterized STS in older adults and identified the target areas of STS assistance required by older persons, namely: maintaining stability while rising, reducing the knee extensor effort required to rise, and providing guidance with a momentum transfer STS strategy. In addition, Chapter 2 developed the importance of assistive devices that incorporate users' available strength by sharing the effort required to rise and identified that there is a lack of such load-sharing devices. Finally, the chapter described the existing STS assistive devices available commercially and in research and development and identified the need for a biomechanical and qualitative comparison of the different modes of STS assistance to determine which is the most appropriate for older adults with STS difficulties.

Based on the issues related to STS assistive devices identified in the literature review, the guiding research question that led to the development of the test bed was: What is the best mode of assisting a person with STS in the context of a device that provides load-sharing STS assistance? The load-sharing capability was included in the guiding research question to help advance the development of load-sharing assistive STS devices, a need also identified in the literature review.

A STS test bed with load-sharing capabilities that tested multiple assist locations was developed to study the assistive STS process. Through simulation work and discussions with physiotherapists, the key STS assist locations for the test bed were selected: the arms, waist, and seat. The arms were identified as a location to provide trajectory guidance and stability assistance, and the waist and seat were identified as locations at which to provide load-sharing force assistance.

The test bed was built with three mechanical assists and one static assist. The mechanical assists consisted of an arm assist, seat assist, and waist assist, and the static assist consisted of a bar assist. A critical function prototype experiment was conducted to help quantify the force and trajectory design requirements for the test bed mechanical assists. Results from the experiment defined the force requirements for the waist and seat assists and defined the trajectory for the arm assist mechanism.

The test bed assist mechanisms were designed and built to achieve these requirements. In addition, the assists were designed such that they were representative of existing STS devices. This enables the results of test bed analysis to be transferrable to existing STS devices. The seat assist was designed similar to chair mounted lifting aids, the waist assist designed similar to institutional waist-assisted lifts, and the arm assist designed similar to arm guided devices in research and development. The bar assist was added to compare the mechanically assisted STS modes with a static mode of assist similar to commercially available grab bar type assists. A load-sharing control scheme was designed to slow down the assist mechanism if the user was not applying sufficient knee torque during the assisted STS motion. To implement this control scheme, anthropometric, force plate, and motion sensor measures were used to calculate a real time estimate of the subject's knee torque, and this estimate was used to control the speed of the waist and seat assist mechanisms.

To determine the best STS assist mode, a STS experiment was developed to answer two main experimental questions: does each mode of assisted STS provide a statistically significant improvement from the unassisted rise? Furthermore, which mode of assist provides a statistically significant improvement from all the other assists? Experiments were then completed with 17 healthy older adult subjects (6 female and 11 male) performing five modes of STS: one unassisted momentum transfer mode and four assisted modes. Kinematic and kinetic measures were gathered during the STS rises using force plate and orientation sensor measurements. These measures were used as inputs to a rigid-link biomechanical model of each subject performing STS, and biomechanical metrics were extracted from this model. In addition, a questionnaire was completed by each subject reporting perceived stability, effort, and motion guidance of each assisted STS.

Biomechanical metrics were selected to evaluate each mode of STS assist based on the three key areas of assistance required by older adults described in Section 2.3: stability, knee extensor effort reduction, and adherence to the momentum transfer rise strategy. These metrics, obtained from the literature (Section 6.2.2.3), include measuring the foot CoM and total body CoP at seat-off to evaluate static and dynamic stability respectively, measuring knee torque to evaluate knee extensor effort reduction and load-sharing, and measuring peak trunk flexion angle to measure adherence to the momentum transfer strategy. The biomechanical metrics were extracted from the model developed in Section 6.2.4.1 and used in statistical tests to determine which, if any, assists offered improvements from the unassisted STS. Both the biomechanical metrics and the questionnaire results were used in statistical tests to determine which assists offered improvements from all other assists.

Results from the statistical analysis on the biomechanical metrics showed that with regard to the first experimental question (Which assists offer improvements from the unassisted rise?), none of the biomechanical metrics recorded for the arm and bar assists showed statistically significant improvements from the corresponding metrics recorded for the unassisted rise. However the static and dynamic stability metrics and the knee extensor effort reduction metric for the waist and seat assists did show significant improvement from the corresponding metrics for the unassisted STS rise. With respect to the momentum transfer strategy metric, all of the assisted STS modes had peak trunk flexion angles significantly lower than the peak trunk flexion for the unassisted STS. This indicated that none of the assists provided guidance according to a momentum transfer STS strategy; instead, they all promoted a dominant vertical rise STS strategy.

With respect to the second experimental question (Which assist is better than all of the other assists?), the waist assist was significantly better than all of the other assists in terms of the static stability metric. For the dynamic stability metric and the knee extensor effort reduction metric, the waist and seat assists were significantly better than both the arm and bar assists, but no significant difference was detected between the waist and seat assists. Thus, in terms of static stability, the waist assist is the best assist, and in terms of dynamic stability and knee extensor effort reduction, both the waist and seat assist are equally the best assists. Statistical analysis of the questionnaire indicated that the seat and bar assists received significantly higher scores than the arm and waist assists but no significant difference was detected between the seat and bar assists. Thus with respect to overall subject feedback, the seat and bar are the assists equally preferred by subjects.

Reflecting back to the guiding research question (What is the best mode of assisting a person with STS in the context of a device that provides load-sharing STS assistance?), results from statistical analysis of the biomechanical metrics show a similarity between the seat and waist assist. However, the seat assist provides a greater amount of trunk flexion angle than the waist assist and thus has more potential to train an individual to rise using a momentum transfer strategy (although neither the seat nor the waist assist promoted a true momentum transfer strategy in the experiments). Also, the seat assist received a more favourable rating than the waist assist with respect to subject qualitative feedback. For these reason, of the modes tested, the seat assist has been selected as the best mode of assisting a person with STS in the context of a device that provides load-sharing STS assistance.

The waist assist provides assistive force up to the point that the subject is very close to a fully standing position. For this reason, it is the most statically stable assist. Thus, the waist assist is recommended for a clinical setting in which patient safety and stability are of high importance.

The goal of having subjects provide part of the knee torque required to rise during the waist-assisted and seat-assisted STS was achieved for both the waist and seat assists. The load-sharing criterion entailed that, during assisted rises, subjects must provide a peak assisted knee torque greater than 35% of the peak knee torque required to rise without assistance (Section 6.2.2.3). Both the waist and seat assists had peak knee torques considerably higher than 35% of the unassisted knee torque with the waist-assisted STS rise resulting in a peak knee torque of 77% of the peak unassisted knee torque and the seat-assisted rise resulting in a peak knee torque of 81% of the peak unassisted knee torque.

7.2 Recommendations

7.2.1 Test bed design recommendations

7.2.1.1 Load sharing

The load-sharing control scheme was designed with the intent of encouraging subjects to engage their own knee extensor effort by slowing down the assist mechanism in the case of insufficient contribution of knee torque during the STS rise. However, the load-sharing control scheme did not encourage subjects to engage their own knee extensor effort, because even when subjects relied fully on the assist mechanism during the entire assisted part of the rise, the mechanism provided assistance at a constant speed. The reason for the minimal effect of load sharing was the conservative nature of the control scheme. The control scheme provided constant speed assistance (no load sharing) for the first 15° of thigh rotation; for the remainder of the STS, lowered speed assistance was provided by the assist mechanism only if subjects applied less than 35% of the knee torque required to rise without assistance. Experiments with varying thresholds of thigh angles, different from the 15° used in the present study, should be completed to determine the best thigh angle at which to initiate the load-sharing control scheme. In addition, changing the load sharing percentage to a higher value from the 35% used in this study would require subjects to use more knee extensor effort in the STS rise. Thus, there are two aspects of the control scheme that can be modified to determine how best to promote load sharing for both the waist and seat assists.

Different methods of determining subject knee extensor effort should also be investigated. Munroe et al. [39] examined knee muscle activation through EMG signals when rising using a seat base assist. A comparison of the knee torque approach used in this thesis should be made with the EMG based approach to see which is best for determining subject knee extensor activation.

7.2.1.2 Arm guidance mechanism

The arm guidance mechanism was designed with the intent of guiding the trajectory of subjects through a momentum transfer STS rise. However, results from the experiment showed that the mechanism did not promote a momentum transfer rise as originally desired. Because the final design of the mechanism was not reconfigurable to provide different rise trajectories, subjects with varying heights had to conform to a single rise trajectory that did not feel natural for many of them. A recommendation for the arm assist mechanism is to investigate different STS rise trajectories to determine if others might better promote a momentum transfer STS strategy. In addition, a reworking of the arm assist mechanism is recommended to allow for easier reconfiguration to suit subjects of different heights and to be able to customize the arm trajectory for each subject.

7.2.2 Recommendations for further research

7.2.2.1 Experiments with older adults who have STS difficulties

The experiment described in Chapter 6 was performed with healthy older adults. Since the target population for which to provide STS assistance is older adults who have difficulty with STS, further experiments should be performed with older adults who have functional limitations pertaining to STS. Because the seat assist has been identified as the best mode of assist based on subject biomechanics and preference, experiments should focus on the effectiveness of this mode of assistance in specifically compensating for the difficulties with STS experienced by experiment participants. The experiments could be conducted using the procedure and analysis methods of the experiment detailed in Chapter 6.

7.2.2.2 Commercial STS assistive device

Results from the experimental analysis in Chapter 6 determined that the seat assist is the best mode of assisting people with STS. If further experiments with older adults who have difficulties with STS confirm these results, then the natural next step in this research is to focus on the development and commercialization of a new load-sharing seat-based assistive STS device.

This future avenue of research should commence by investigating how the load-sharing control scheme of the test bed can be incorporated into a seat based assistive device. This investigation could be pursued by first performing background research work on existing seat based assistive devices and conducting an experimental study on the different types of seat based devices to evaluate them in terms of the biomechanical metrics defined in Chapter 6 of this thesis. This would help identify the limitations of existing devices and drive the design requirements of a new seat based assistive device. Furthermore, an investigation into generalizing the load-sharing control scheme would have to be completed so that load sharing can be maintained without the need for a force plate and motion sensors as required in the current control scheme. Using this generalized load-sharing control scheme and the identified weaknesses in existing seat based assistive STS devices, an improved load-sharing seat based assistive device could be developed.

7.2.2.3 Rehabilitation applications

In addition to assessing the biomechanics of assisted STS, the test bed has the potential to be used as an apparatus for restoring STS functionality in older adults who have difficulty rising out of a chair. Because the load-sharing settings can be varied, the test bed has potential to be used in the rehabilitation of patients relearning to use their leg muscles for STS. Repetitions of assistance with the seat and waist mechanisms while gradually reducing the amount of assist force provided can help train people with STS and strengthen their leg muscles at a level of difficulty according to their strength and ability. In addition, if the arm assist mechanism is refined to promote a momentum transfer strategy, then repeated rises in this mechanism can help people learn to coordinate their motion to rise using a momentum transfer strategy. The assessment of stability, knee extensor strength used and adherence to the momentum transfer rise strategy through data collected from the test bed can be used to track the progress of rehabilitation.

Therefore, a future avenue for research using the STS test bed is to determine how the test bed can be used as a tool to help with STS rehabilitation. This investigation could be pursued by first performing background research work that investigates how rehabilitation efforts are currently used to mitigate the subject-related contributing factors to STS failure described in Chapter 2 of this thesis. The next step would be to identify how the test bed could be used to provide the same results as obtained from current STS rehabilitation efforts. This identification could take place by demonstrating the capabilities of the test bed to rehabilitation experts, such as the ones who generously contributed their time in consulting on the development of the test bed and the assist motions, and asking them to

generate ideas in which the test bed could now help with STS rehabilitation. Finally, after identifying how the test bed can be used as a tool to help with STS rehabilitation, experiments with the test bed should be performed in a rehabilitation context and results should be analyzed to determine the effectiveness of the test bed in helping with STS rehabilitation.

Bibliography

- [1] C. Williams, "The sandwich generation," *Canadian Social Trends*, vol. 11, Jan. 2005, pp. 16-21.
- [2] Statistics Canada, *Canada Year Book 2009 Catalog no. 11-402-X*, Ministry of Industry, 2009.
- [3] K. Cranswick and D. Dosman, "Eldercare: What we know today," *Canadian Social Trends*, vol. 86, 2008, p. 48-56.
- [4] M.J. Gibson, M. Freiman, S. Gregory, E. Kassner, A. Kochera, F. Mullen, S. Pandya, D. Redfoot, A. Straight, and B. Wright, "Beyond 50.03: A report to the nation on independent living and disability," *Washington, DC: AARP*, 2003.
- [5] H. Hoenig, D.H. Taylor, and F.A. Sloan, "Does assistive technology substitute for personal assistance among the disabled elderly?," *American Journal of Public Health*, vol. 93, Feb. 2003, pp. 330-7.
- [6] E.M. Agree and V.A. Freedman, "A comparison of assistive technology and personal care in alleviating disability and unmet need.," *The Gerontologist*, vol. 43, Jun. 2003, pp. 335-44.
- [7] L.M. Verbrugge, C. Rennert, and J.H. Madans, "The great efficacy of personal and equipment assistance in reducing disability.," *American Journal of Public Health*, vol. 87, Mar. 1997, pp. 384-92.
- [8] M.M. Desai, H.R. Lentzner, and J.D. Weeks, "Unmet need for personal assistance with activities of daily living among older adults.," *The Gerontologist*, vol. 41, Feb. 2001, pp. 82-8.
- [9] T. Leon, J; Lair, "Functional Status of the Noninstitutionalized Elderly Estimates of ADL and IADL Difficulties," *DHHS Publication*, vol. 90, 1990.
- [10] D.R. Mehr, B.E. Fries, and B.C. Williams, "How different are VA nursing home residents?," *Journal of the American Geriatrics Society*, vol. 41, Oct. 1993, pp. 1095-101.
- [11] P.O. Riley, M.L. Schenkman, R.W. Mann, and W.A. Hodge, "Mechanics of a constrained chair-rise," *Journal of Biomechanics*, vol. 24, Jan. 1991, pp. 77-85.
- [12] M.H. Edlich, R.F.; Heather, C.L.; Galumbeck, "Revolutionary Advances in Adaptive Seating Systems for the Elderly and Persons with Disabilities that Assist Sit-to-Stand Transfers," *Journal of Long Term Effects of Medical Implants*, 2003, pp. 31-9.
- [13] M.E. Tinetti, M. Speechley, and S.F. Ginter, "Risk factors for falls among elderly persons living in the community.," *The New England Journal of Medicine*, vol. 319, Dec. 1988, pp. 1701-7.

- [14] S.R. Cummings, M.C. Nevitt, W.S. Browner, K. Stone, K.M. Fox, K.E. Ensrud, J. Cauley, D. Black, and T.M. Vogt, "Risk factors for hip fracture in white women. Study of Osteoporotic Fractures Research Group," *The New England Journal of Medicine*, vol. 332, Mar. 1995, pp. 767-73.
- [15] M.A. Hughes, B.S. Myers, and M.L. Schenkman, "The role of strength in rising from a chair in the functionally impaired elderly," *Journal of Biomechanics*, vol. 29, Dec. 1996, pp. 1509-1513.
- [16] P. Médéric, V. Pasqui, F. Plumet, and P. Bidaud, "Design of a walking-aid and sit to stand transfer assisting device for elderly people," *7th Int. Conf. Climbing Walking Robots, Madrid, Spain*, 2004.
- [17] O. Chuy, Y. Hirat, Z. Wang, and K. Kosuge, *Approach in Assisting a Sit-to-Stand Movement Using Robotic Walking Support System*, IEEE, 2006.
- [18] D. Chugo, T. Kitamura, J. Songmin, and K. Takase, "Steady standing assistance using active walker function," *SICE Annual Conference 2007*, IEEE, 2007, pp. 3060-3063.
- [19] Y. Takahashi, O. Nitta, K. Tomuro, and T. Komeda, "Development of a Sit-to-Stand Assistance System," *11th international conference on Computers Helping People with Special Needs*, 2008, pp. 1277-1284.
- [20] D. Chugo, H. Kaetsu, N. Miyake, K. Kawabata, H. Asama, and K. Kosuge, "Force Assistance System for Standing-Up Motion," *2006 International Conference on Mechatronics and Automation*, IEEE, 2006, pp. 1103-1108.
- [21] A.B. Schultz, N.B. Alexander, and J.A. Ashton-Miller, "Biomechanical analyses of rising from a chair," *Journal of Biomechanics*, vol. 25, Dec. 1992, pp. 1383-1391.
- [22] P. Wretenberg, U.P. Arborelius, L. Weidenhielm, and F. Lindberg, "Rising from a chair by a spring-loaded flap seat: a biomechanical analysis," *Scandinavian Journal of Rehabilitation Medicine*, vol. 25, Dec. 1993, pp. 153-9.
- [23] M. Hirvensalo, T. Rantanen, and E. Heikkinen, "Mobility difficulties and physical activity as predictors of mortality and loss of independence in the community-living older population," *Journal of the American Geriatrics Society*, vol. 48, pp. 493-498.
- [24] M. Schenkman, R.A. Berger, P.O. Riley, R.W. Mann, and W.A. Hodge, "Whole-body movements during rising to standing from sitting," *Physical Therapy*, vol. 70, Oct. 1990, pp. 638-48; discussion 648-51.
- [25] D.M. Scarborough, C.A. McGibbon, and D.E. Krebs, "Chair rise strategies in older adults with functional limitations," *Journal of Rehabilitation Research and Development*, vol. 44, Jan. 2007, pp. 33-42.

- [26] M. Bernardi, A. Rosponi, V. Castellano, A. Rodio, M. Trallesi, A.S. Delussu, and M. Marchetti, "Determinants of sit-to-stand capability in the motor impaired elderly," *Journal of Electromyography and Kinesiology : official journal of the International Society of Electrophysiological Kinesiology*, vol. 14, Jun. 2004, pp. 401-10.
- [27] P.O. Riley, D.E. Krebs, and R.A. Papat, "Biomechanical analysis of failed sit-to-stand," *IEEE Transactions on Rehabilitation Engineering : a publication of the IEEE Engineering in Medicine and Biology Society*, vol. 5, Dec. 1997, pp. 353-9.
- [28] M.A. Hughes and M.L. Schenkman, "Chair rise strategy in the functionally impaired elderly," *Journal of Rehabilitation Research and Development*, vol. 33, Oct. 1996, pp. 409-12.
- [29] N. Deshpande, E.J. Metter, S. Bandinelli, F. Lauretani, B.G. Windham, and L. Ferrucci, "Psychological, physical, and sensory correlates of fear of falling and consequent activity restriction in the elderly: the InCHIANTI study," *American Journal of Physical Medicine & Rehabilitation / Association of Academic Physiatrists*, vol. 87, May. 2008, pp. 354-62.
- [30] M. Schenkman, M.A. Hughes, G. Samsa, and S. Studenski, "The relative importance of strength and balance in chair rise by functionally impaired older individuals," *Journal of the American Geriatrics Society*, vol. 44, Dec. 1996, pp. 1441-6.
- [31] F. Bahrami, "Biomechanical analysis of sit-to-stand transfer in healthy and paraplegic subjects," *Clinical Biomechanics*, vol. 15, Feb. 2000, pp. 123-133.
- [32] D.K. Weiner, R. Long, M.A. Hughes, J. Chandler, and S. Studenski, "When older adults face the chair-rise challenge. A study of chair height availability and height-modified chair-rise performance in the elderly," *Journal of the American Geriatrics Society*, vol. 41, Jan. 1993, pp. 6-10.
- [33] J. Rosie and D. Taylor, "Sit-to-stand as home exercise for mobility-limited adults over 80 years of age : GrandStand System™ may keep you standing?," *Age and Ageing*, vol. 36, pp. 555-562.
- [34] K. Berg, S. Wood-Dauphinee, and J.I. Williams, "The Balance Scale: reliability assessment with elderly residents and patients with an acute stroke," *Scandinavian Journal of Rehabilitation Medicine*, vol. 27, Mar. 1995, pp. 27-36.
- [35] *Technology for Long Term Care - Lifting and Transferring* (n.d.) [Online]. Available: <http://www.techforltc.org/producttype.aspx?id=2057,1892>.
- [36] D.M. O'Meara and R.M. Smith, "The effects of unilateral grab rail assistance on the sit-to-stand performance of older aged adults," *Human Movement Science*, vol. 25, Apr. 2006, pp. 257-74.
- [37] G.M. Bashford, J.R. Steele, B.J. Munro, G.; Westcott, and M.E. Jones, "Ejector chairs: Do they work and are they safe?," *Australian Occupational Therapy Journal*, vol. 45, 1998, pp. 99-106.

- [38] B. Munro, "A kinematic and kinetic analysis of the sit-to-stand transfer using an ejector chair implications for elderly rheumatoid arthritic patients," *Journal of Biomechanics*, vol. 31, Dec. 1997, pp. 263-271.
- [39] B. Munro, "Does using an ejector chair affect muscle activation patterns in rheumatoid arthritic patients? A preliminary investigation," *Journal of Electromyography and Kinesiology*, vol. 10, Feb. 2000, pp. 25-32.
- [40] S. Ruzsala and I. Musa, "An evaluation of equipment to assist patient sit-to-stand activities in physiotherapy," *Physiotherapy*, vol. 91, Mar. 2005, pp. 35-41.
- [41] D. Chugo, K. Kawabata, H. Kaetsu, N. Miyake, K. Kosuge, H. Asama, and E. Okada, "Force Assistance Control for Standing-Up Motion," *The First IEEE/RAS-EMBS International Conference on Biomedical Robotics and Biomechatronics, 2006. BioRob 2006.*, IEEE, , pp. 135-140.
- [42] M. Mak, O. Levin, J. Mizrahi, and C.W.Y. Hui-Chan, "Joint torques during sit-to-stand in healthy subjects and people with Parkinson's disease," *Clinical Biomechanics*, vol. 18, Mar. 2003, pp. 197-206.
- [43] E.B. Hutchinson, P.O. Riley, and D.E. Krebs, "A dynamic analysis of the joint forces and torques during rising from a chair," *IEEE Transactions on Rehabilitation Engineering*, vol. 2, Jun. 1994, pp. 49-56.
- [44] A.D. Kuo, "A Least-Squares Estimation Approach to Improving the Precision of Inverse Dynamics Computations," *Journal of Biomechanical Engineering*, vol. 120, Feb. 1998, pp. 148-159.
- [45] W.G.M. Janssen, H.B.J. Bussmann, and H.J. Stam, "Determinants of the sit-to-stand movement: a review," *Physical Therapy*, vol. 82, Sep. 2002, pp. 866-79.
- [46] D.A. Winter, *Biomechanics and Motor Control of Human Movement*, Hoboken, NJ, USA: John Wiley & Sons, Inc., 2005.
- [47] T. Lundin, "On the assumption of bilateral lower extremity joint moment symmetry during the sit-to-stand task," *Journal of Biomechanics*, vol. 28, Jan. 1995, pp. 109-112.
- [48] K. Barin, "Evaluation of a generalized model of human postural dynamics and control in the sagittal plane," *Biological Cybernetics*, vol. 61, May. 1989, pp. 37-50-50.
- [49] R. Prinz, S. Neville, and N.J. Livingston, "Development of a Fuzzy-Based Sit-to-Stand Controller," *Electrical and Computer Engineering, 2007. CCECE 2007. Canadian Conference on*, pp. 1631-1634.

- [50] R.C. Fitzpatrick, R.B. Gorman, D. Burke, and S.C. Gandevia, "Postural proprioceptive reflexes in standing human subjects: bandwidth of response and transmission characteristics," *The Journal of Physiology*, vol. 458, Dec. 1992, pp. 69-83.
- [51] V. Bonnet, P. Fraisse, N. Ramdani, J. Lagarde, S. Ramdani, and B.G. Bardy, "A robotic closed-loop scheme to model human postural coordination," *2009 IEEE/RSJ International Conference on Intelligent Robots and Systems*, IEEE, 2009, pp. 2525-2530.
- [52] I.D. Loram and M. Lakie, "Direct measurement of human ankle stiffness during quiet standing: the intrinsic mechanical stiffness is insufficient for stability.," *The Journal of Physiology*, vol. 545, Dec. 2002, pp. 1041-53.
- [53] L.-Q. Zhang, G. Nuber, J. Butler, M. Bowen, and W.Z. Rymer, "In vivo human knee joint dynamic properties as functions of muscle contraction and joint position," *Journal of Biomechanics*, vol. 31, Nov. 1997, pp. 71-76.
- [54] J. Cholewicki, A.P. Simons, and A. Radebold, "Effects of external trunk loads on lumbar spine stability," *Journal of Biomechanics*, vol. 33, Nov. 2000, pp. 1377-85.
- [55] M. Hollins, *Safer Lifting for Patient Care*, Blackwell Scientific Publications, 1991.
- [56] F. Rodrigues-de-Paula Goulart, "Patterned electromyographic activity in the sit-to-stand movement," *Clinical Neurophysiology*, vol. 110, Sep. 1999, pp. 1634-1640.
- [57] Y.-C. Pai, B. Naughton, R. Chang, and M. Rogers, "Control of body centre of mass momentum during sit-to-stand among young and elderly adults," *Gait & Posture*, vol. 2, Jun. 1994, pp. 109-116.
- [58] A.M. Master, R.P. Lasser, and G. Beckman, "Tables of average weight and height of Americans aged 65 to 94 years: relationship of weight and height to survival," *Journal of the American Medical Association*, vol. 172, Feb. 1960, pp. 658-62.
- [59] Centers For Disease Control And Prevention, *The Third National Health and Nutrition Examination Survey (NHANES III 1988-1994) Reference Manuals and Reports (CD-ROM)*, Bethesda, MD: Centers for Disease Control and Prevention;; .
- [60] T. Chen, D. Cho, J. Chu, M. Mak, S. Quan, and R. So, *Sit - To - Stand Project Final Report*, 2010.
- [61] *Item Products* (n.d.) [Online] Available: <http://www.item24.com/en>.
- [62] D. Chugo, W. Mastuoka, S. Jia, K. Takase, and H. Asama, "Rehabilitation walker with standing assistance," *2007 IEEE 10th International Conference on Rehabilitation Robotics*, IEEE, 2007, pp. 132-137.

- [63] E.R. Ikeda, M.L. Schenkman, P.O. Riley, and W.A. Hodge, "Influence of age on dynamics of rising from a chair," *Physical Therapy*, vol. 71, Jun. 1991, pp. 473-81.
- [64] N.B. Alexander, A.B. Schultz, and D.N. Warwick, "Rising from a chair: effects of age and functional ability on performance biomechanics," *Journal of Gerontology*, vol. 46, May. 1991, pp. M91-8.
- [65] M. Gross, "Effect of muscle strength and movement speed on the biomechanics of rising from a chair in healthy elderly and young women," *Gait & Posture*, vol. 8, Dec. 1998, pp. 175-185.
- [66] M.A. Hughes, D.K. Weiner, M.L. Schenkman, R.M. Long, and S.A. Studenski, "Chair rise strategies in the elderly," *Clinical Biomechanics*, vol. 9, May. 1994, pp. 187-192.
- [67] C.A. McGibbon, D. Goldvasser, D.E. Krebs, and D. Moxley Scarborough, "Instant of chair-rise lift-off can be predicted by foot-floor reaction forces," *Human Movement Science*, vol. 23, Sep. 2004, pp. 121-32.
- [68] I. McDowell and C. Newell, *Measuring Health: A Guide to Rating Scales and Questionnaires*, Oxford University Press, USA, 1996.

Appendix A: Appendix from Student Report – Design Calculations

Arm Guidance Simulations

Samples of reference curves matched by the 4-bar linkage mechanism. Curves matched by adjusting the linkage lengths to suit short, medium and tall subjects.

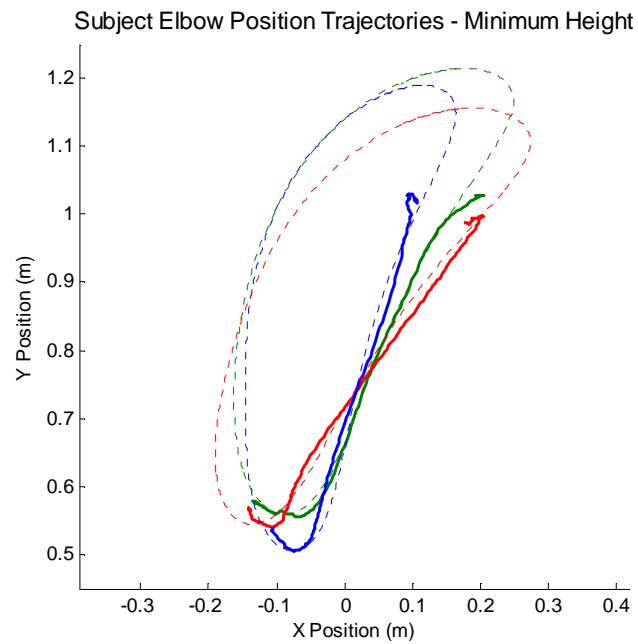


Figure A.1: Subject elbow position trajectories – minimum height.

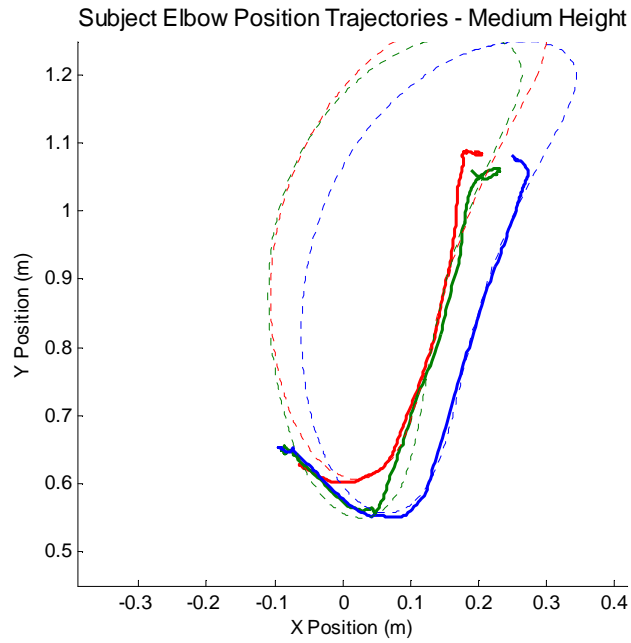


Figure A.2: Subject elbow position trajectories – medium height.

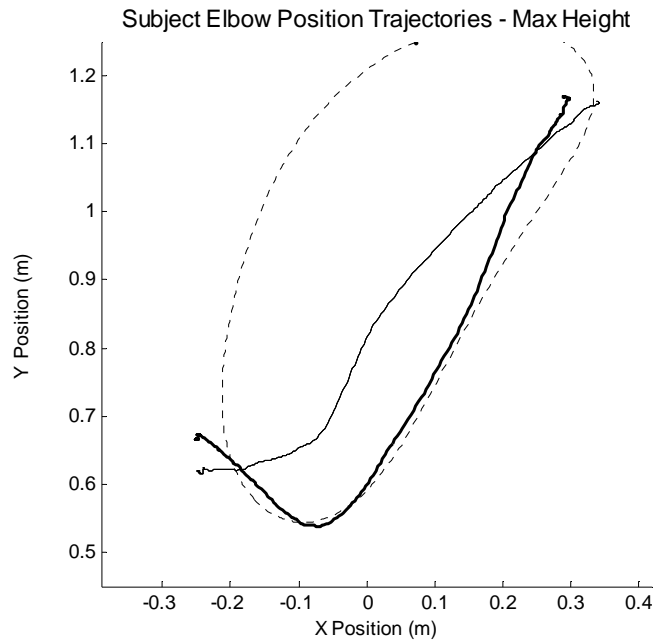


Figure A.3: Subject elbow position trajectories – maximum height.

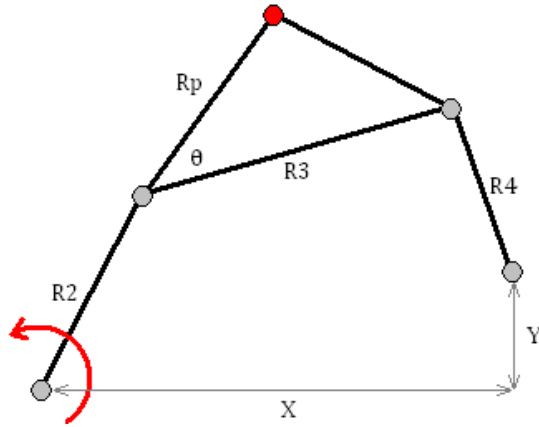
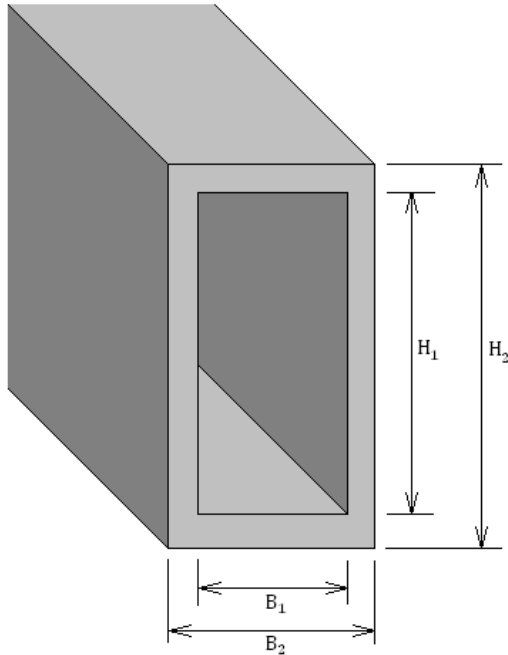


Figure A.4: 4-bar linkage mechanism and linkage naming references.

Table A.1: Linkage adjustment range corresponding to the trajectory graphs.

Test Subject	X	Y	R1	R2	R3	R4	Rp	θ (rad)
Minimum height	0.520	0.740	0.6	0.3	0.52	0.45	0.45	0.611
	0.548	0.719	0.6	0.3	0.56	0.45	0.45	0.611
	0.580	0.595	0.6	0.3	0.55	0.45	0.45	0.611
Medium height	0.491	0.894	0.6	0.3	0.61	0.45	0.45	0.611
	0.491	0.844	0.6	0.3	0.61	0.45	0.45	0.611
	0.460	0.896	0.6	0.3	0.59	0.4	0.45	0.698
Maximum Height	0.689	0.672	0.7	0.35	0.62	0.5	0.4	0.785

Linkage Housing Force Calculations (arm guidance mechanism linkages – outer aluminum tubing)



Bending:

$$\sigma_{yield} = 275MPa$$

$$H_2 = 1.5'' = 0.0381m$$

$$B_2 = 0.75'' = 0.01905m$$

$$\text{Thickness} = 1/8'' = 0.003175m$$

$$H_1 = 1.25'' = 0.03175m$$

$$B_1 = 0.5'' = 0.0127m$$

$$I = \frac{1}{12}(B_2H_2^3 - B_1H_1^3) = 6.4711 \cdot 10^{-7}m^4$$

$$M_{max} = 120Nm$$

$$c = 0.01905m$$

$$\sigma_{bend} = \frac{Mc}{I}$$

$$\sigma_{bend} = \frac{120Nm \cdot 0.01905m}{6.4711 \cdot 10^{-7}m^4} = 3.53MPa$$

$$\sigma_{bend} \ll \sigma_{yield} \checkmark$$

Torsion:

$$\tau_{shear} = 26GPa$$

$$T_{applied} = 183N \cdot 0.30m = 55Nm$$

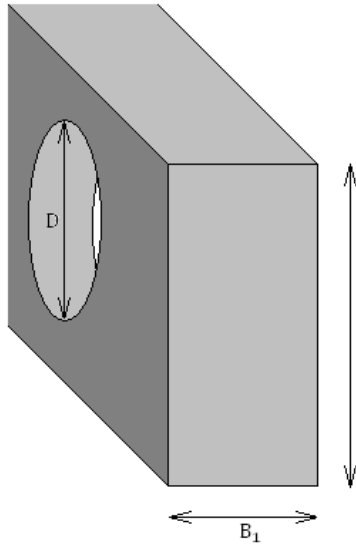
$$T_{max} = 2A_m t \cdot \tau_{shear}$$

$$T_{max} = 2 \cdot (0.0381 - 0.003175)(0.01905 - 0.003175) \cdot 0.003175 \cdot 26 \cdot 10^9$$

$$T_{max} = 91537Nm$$

$$T_{max} \gg T_{applied} \checkmark$$

**Linkage Extension Block Force Calculations (Arm guidance mechanism linkages
– aluminum square stock bearing blocks)²**



Bending:

$$\sigma_{yield} = 275MPa$$

$$H_1 = 1.25'' = 0.03175m$$

$$B_1 = 0.5'' = 0.0127m$$

$$I = \frac{1}{12} B_1 H_1^3 = 3.3873 \cdot 10^{-8} m^4$$

$$M_{max} = 120Nm$$

$$c = 0.01588m$$

$$\sigma_{bend} = \frac{Mc}{I}$$

$$\sigma_{bend} = \frac{120Nm \cdot 0.01588m}{3.3873 \cdot 10^{-8} m^4} = 56.24MPa$$

$$\sigma_{bend} \ll \sigma_{yield} \checkmark$$

Torsion:

$$\tau_{shear} = 26GPa$$

$$T_{applied} = 55Nm$$

$$\tau_{max} \cong \frac{T_{applied}}{H_1 B_1^2} \left(3 + \frac{1.8}{H_1/B_1} \right)$$

$$\tau_{max} \cong \frac{55}{(0.03175)(0.0127^2)} \left(3 + \frac{1.8}{0.03175/0.0127} \right)$$

² Note that in the final test bed the aluminum square stock bearing blocks were replaced with steel square stock bearing blocks

$$\tau_{max} = 39.95MPa$$

$$\tau_{shear} \gg \tau_{max} \checkmark$$

Stress Concentration:

$$D = 0.25'' = 0.00635m$$

$$K_t = 2.5$$

$$F_{axial} = 400N$$

$$A_{cross-section} = H_1 B_1 = 0.0004032 m^2$$

$$\sigma_{axial} = K_t \cdot \frac{F_{axial}}{A_{cross-section}} = 2.5 \cdot \frac{400N}{0.0004032 m^2}$$

$$\sigma_{axial} = 2.48MPa$$

$$\sigma_{axial} \ll \sigma_{yield} \checkmark$$

Arm Guidance - Motor Requirements

The torque and power requirements for the arm guidance mechanism were calculated with a quasi-static force analysis, which assumes that the acceleration of the device is near zero.

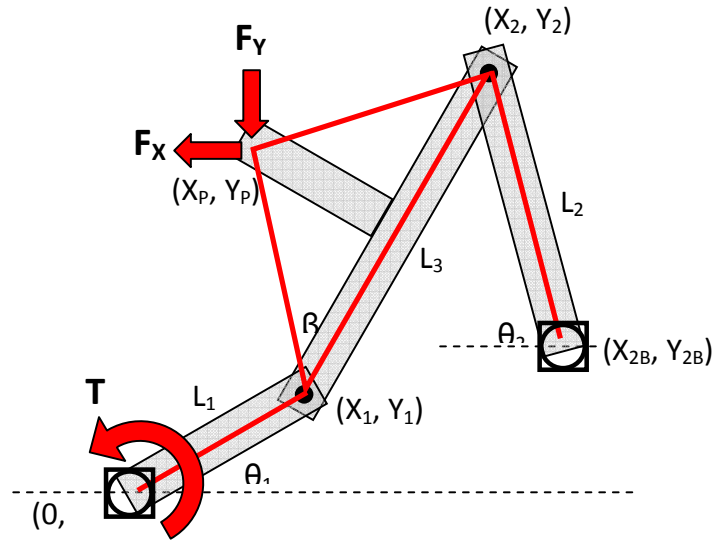


Figure A.5: 4-bar linkage force application.

From the mock-up experiments, the maximum user forces, F_X and F_Y were determined:

$$F_{X, \text{MAX}} = 130 \text{ N}$$

$$F_{Y, \text{MAX}} = 130 \text{ N}$$

From the kinematic analysis of the mechanism, using the SimMechanics model, the maximum dimensions were determined for L_1 , L_2 , L_3 , β , X_{2B} , Y_{2B} . Through geometry and trigonometry, the positions and coordinates of each linkage in the mechanism (X_1 , Y_1 , X_2 , Y_2 , X_P , Y_P , θ_2) were calculated relative to the Linkage 1 angle, θ_1 .

A free body diagram was drawn for each linkage, and a force balance analysis was performed.

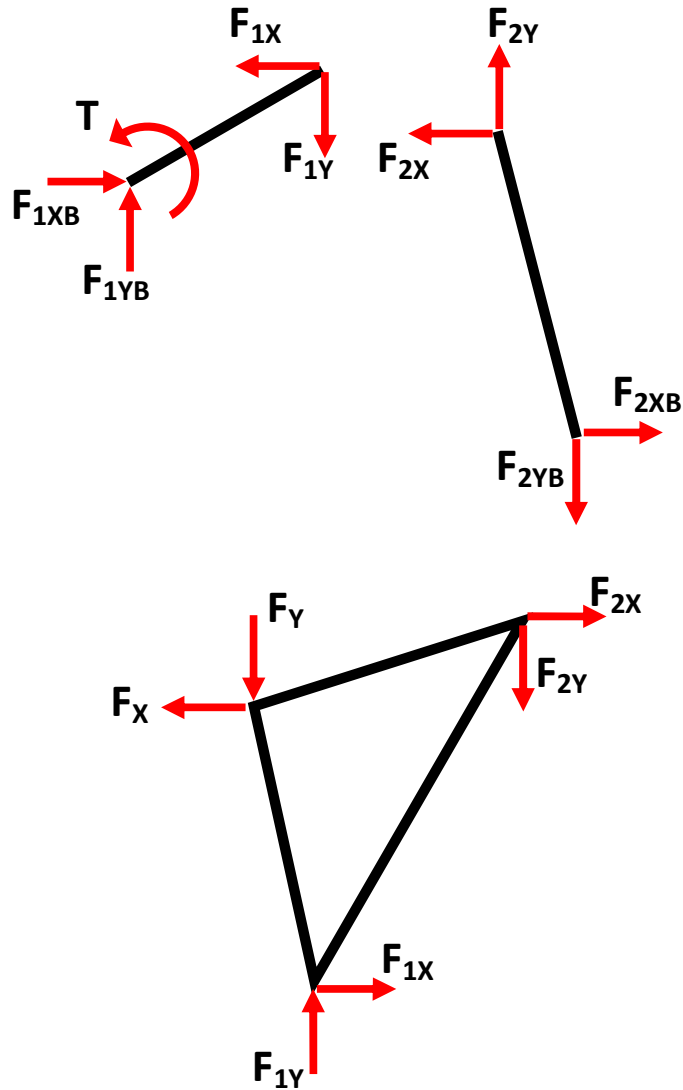


Figure A.6: Linkage free body diagrams.

There are 9 unknown forces or torques, and 9 equations of motion:

Linkage 1:

$$T = [F_{1X} \cdot \sin(\theta_1) + F_{1Y} \cdot \cos(\theta_1)] \cdot L_1$$

$$\Sigma F_{X1} = 0$$

$$\Sigma F_{Y1} = 0$$

Linkage 2:

$$\tan(\theta_2) = F_{2Y} / F_{2X}$$

$$\Sigma F_{X2} = 0$$

$$\Sigma F_{Y2} = 0$$

Linkage 3:

$$\Sigma M_{O3} = 0$$

$$\Sigma F_{X3} = 0$$

$$\Sigma F_{Y3} = 0$$

Through linear algebra, the driving torque, T, and the forces at each pivot were calculated, as functions of θ_1 . The maximum torque was determined:

$$T_{MAX} = 120 \text{ Nm}$$

The maximum pivot forces were used to specify the appropriate bearings for each pivot.

The Linkage 1 angular velocity as a function of angle, $\omega(\theta_1)$, was determined from the kinematic analysis of the mechanism. By multiplying the angular velocity and the torque at each angle, the power requirement at each angle was determined:

$$P(\theta_1) = T(\theta_1) \times \omega(\theta_1)$$

$$P_{MAX} = 90 \text{ W}$$

Waist Assist Arm Calculations

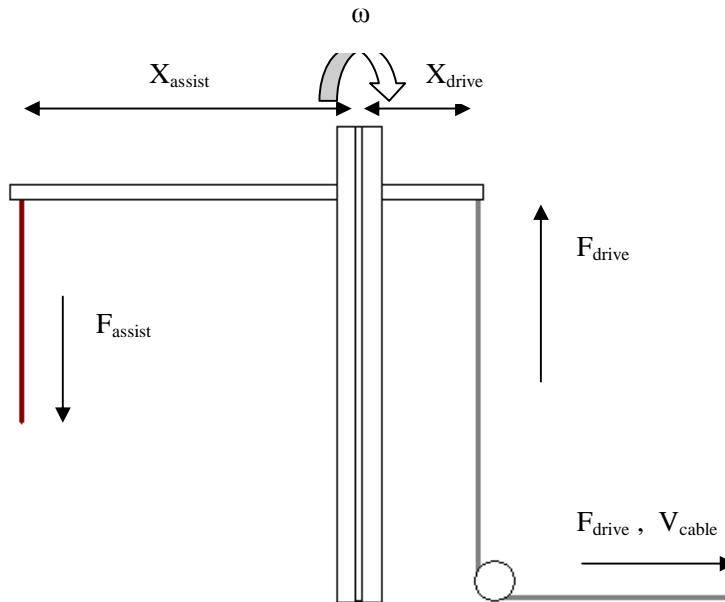


Figure A.7: Waist assist free body diagram.

$$X_{\text{assist}} = 0.45\text{m}$$

Force Analysis

$$F_{\text{drive}} = T_{\text{motor}} \div R_{\text{winch_spool}}$$

$$R_{\text{winch_spool}} = 2.0 \sim 3.0\text{cm}$$

$$T_{\text{motor}} = 123\text{Nm} \quad \mathbf{max}$$

$$\rightarrow F_{\text{drive}} = 4100\text{N}$$

The motor would pull the cable to provide **at least 4100N of force**

$\rightarrow X_{\text{drive}}$ can be as short as 0.043m; but we want it slightly longer, approx 0.10m.

Velocity Analysis

$$\omega_{\text{required}} = 50^\circ/3\text{s} = 0.291 \text{ rad/s}$$

$$\omega_{\text{motor}} = 8.7\text{rpm} = 0.911 \text{ rad/s} \quad \mathbf{max}$$

$$V_{\text{cable}} = 0.911\text{rad/s} * 0.02\text{m} = 0.1822\text{m/s}$$

$$\omega = 0.1822\text{m/s} \div X_{\text{drive}}$$

$$\rightarrow \text{Let } X_{\text{drive}} = 0.10 \text{ m}$$

$$\omega = 1.822\text{rad/s}$$

Therefore the system would be able to fulfill its speed and force requirements by utilizing a driving lever arm of approximately 10cm.

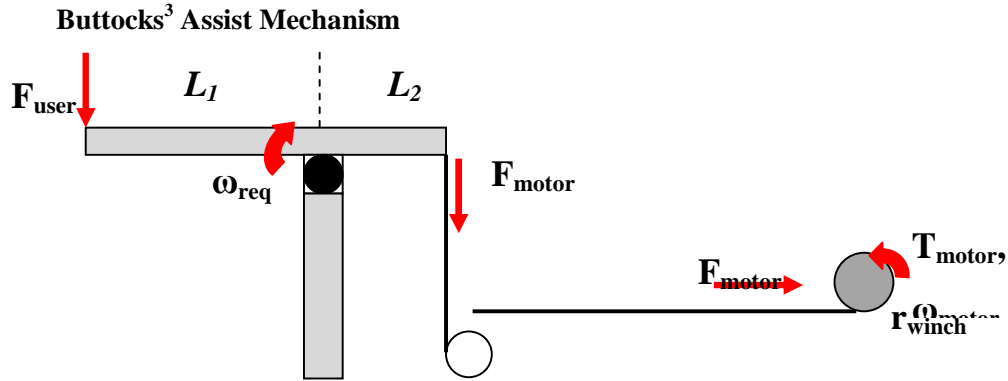


Figure A.8: Buttocks assist free body diagram.

From mock-up experiment:

$$\text{Power Required: } P_{req} = 245 \times L_1$$

$$F_{user,max} = 715 \text{ N}$$

$$L_1 = 0.45 \text{ m}$$

$$P = F \times L_1 \times \omega = 245 \times L_1 \rightarrow \omega_{req} = \frac{245}{715} = 0.343 \text{ rad/s}$$

Motor:

$$\text{Max. Torque: } T_{motor} = 1087 \text{ in-lb} = 123 \text{ Nm}$$

$$\text{Speed (90V): } \omega_{motor} = 8.7 \text{ RPM} = 0.911 \text{ rad/s}$$

$$\text{Winch Radius (Fully Wound): } r_{winch} = 0.044 \text{ m}$$

$$F_{motor} = \frac{T_{motor}}{r_{winch}} = \frac{123}{0.044} = 2795.5 \text{ N}$$

$$\sum M = 0: F_{motor} \times L_2 = F_{user} \times L_1$$

³ Note that the buttocks assist in the student report is the same assist as the seat assist in the thesis.

$$L_2 = \frac{F_{user}}{F_{motor}} \times L_1 = \frac{715}{2795.5} \times 0.45 = 0.115 \text{ m}$$

Check if angular velocity is sufficient:

$$\omega \times L_2 = \omega_{motor} \times r_{winch}$$

$$\omega = \frac{\omega_{motor} \times r_{winch}}{L_2} = \frac{0.911 \times 0.044}{0.115} = 0.349 \text{ rad/s} > \omega_{req} \checkmark$$

Appendix B: Student Report Excerpt – Arm Linkage Adjustability and Buttocks (Seat) and Waist Assist Descriptions

Trajectory guidance is provided by two sets of 4-bar linkages, as shown in Figure B.1.

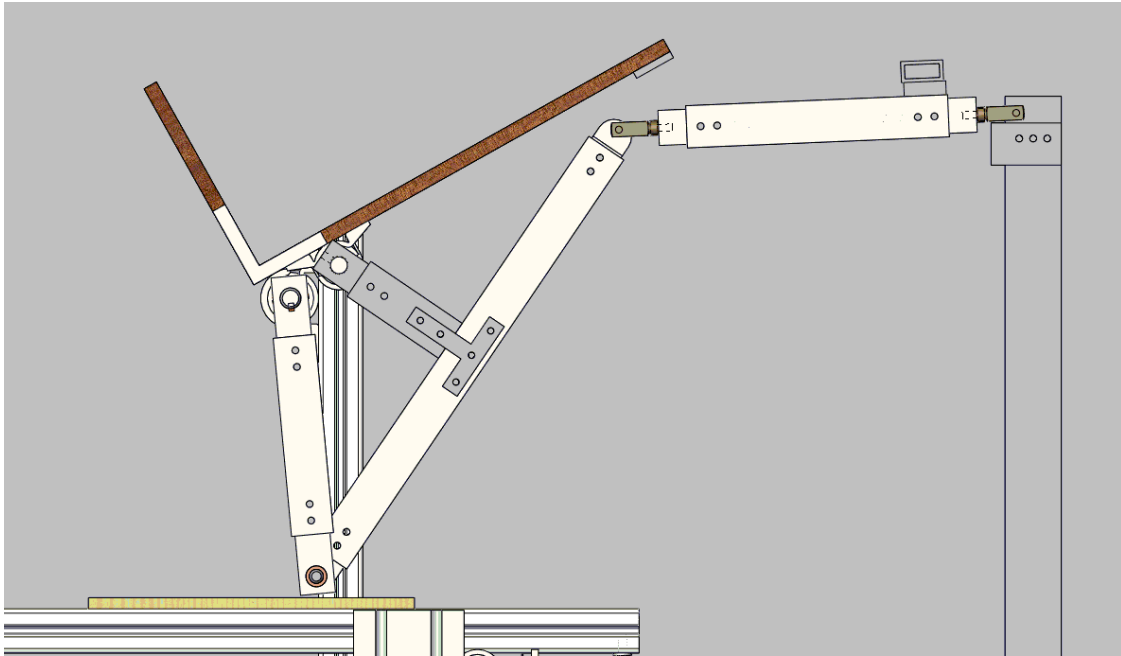


Figure B.1: Mechanical model of the 4-bar linkage system

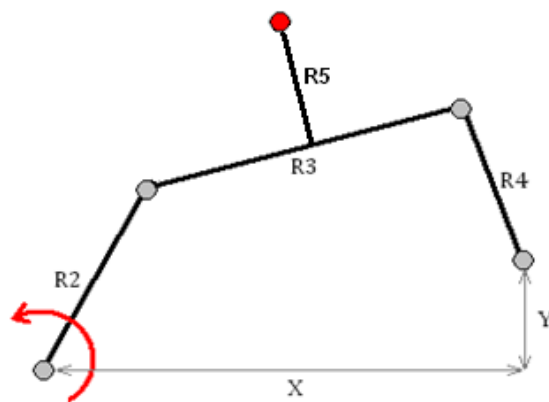


Figure B.2: Linkage layout and reference names

The user’s arms are connected to the linkage through two arm cradles at the top of link R5. The arm guidance mechanism is driven through a roller chain and sprocket transmission on one side. The two sets of linkages are coupled at two points: at linkage R4 and at the cradle.

As linkage R2 is driven by the motor and rotated, the user follows a trajectory path that is dependent on the orientation and the lengths of each of the linkages. By adjusting the length and orientation of the 4-bar linkage mechanism, the trajectory path can be modified to closely coincide with the desired user elbow trajectory (refer to Appendix F – User Manual).

The arm guidance linkages have maximum and minimum lengths as highlighted in the following Table. The arm linkage mechanism was designed based on a SimMechanics model of the 4-bar linkage (refer to Appendix A – Calculations).

Table B.1: Maximum and minimum linkage lengths.

Linkage/Position	Maximum [cm]	Minimum [cm]	Increment [cm]
R2	40	30	2
R3	60	50	2
R4	46	40	2
R5	20	18	2
Origin Height	74	35	n/a
X	67	n/a	n/a
Y	75	15	n/a

In the following figures (B.3 to B.7), the dotted lines illustrate some of the achievable trajectories with the 4-bar linkage. The linkage trajectories closely match the desired trajectories, based on the mock-up tests, with a maximum offset of 1 to 2 cm.

Reference vs. Achieved Elbow Position Trajectories

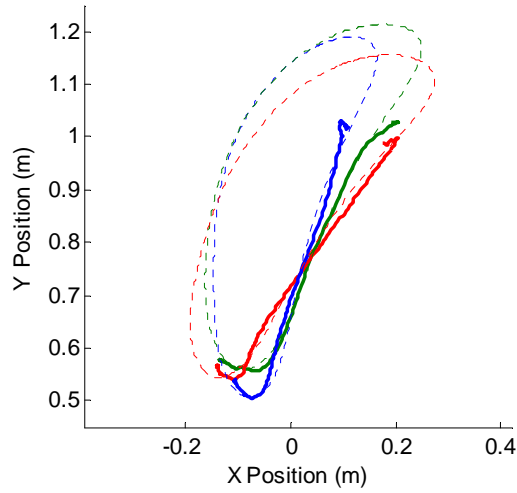


Figure B.3: Reference trajectories vs. achieved 4-bar linkage trajectories.

The linkage mechanism can be adjusted to very closely meet the 4 types of STS motion: arm-guided, buttocks-assisted, waist-assisted, and no-assist. This is illustrated in Figures B.4 to B.7. The dotted line is the trajectory followed by the linkage mechanism by setting it up to the corresponding orientation and lengths.

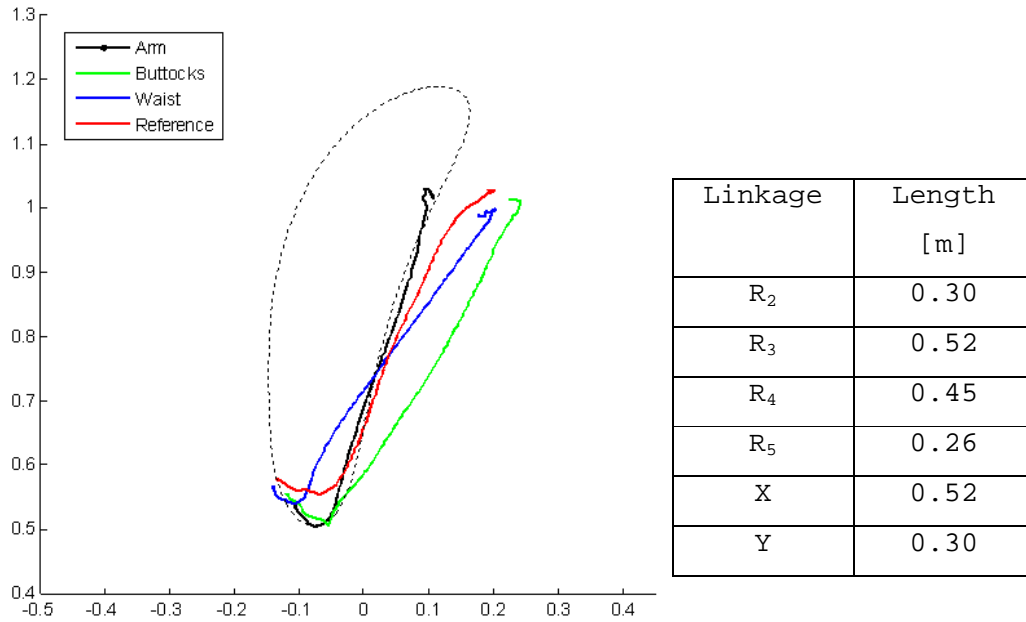
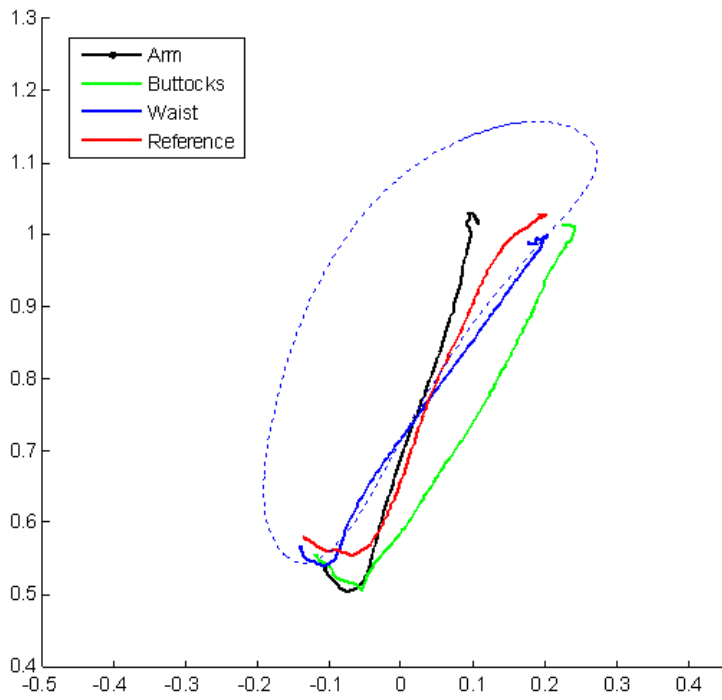
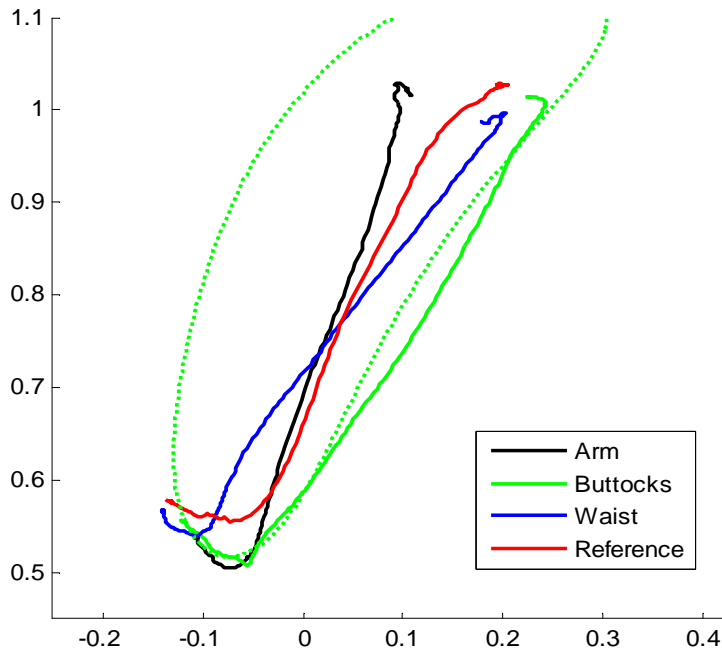


Figure B.4: Achieved trajectory for arm guidance.



Linkage	Length [m]
R_2	0.30
R_3	0.55
R_4	0.45
R_5	0.26
X	0.58
Y	0.16

Figure B.5: Achieved trajectory for waist assist.



Linkage	Length [m]
R_2	0.30
R_3	0.53
R_4	0.45
R_5	0.26
X	0.58
Y	0.16

Figure B.6: Achieved trajectory for buttocks guidance.

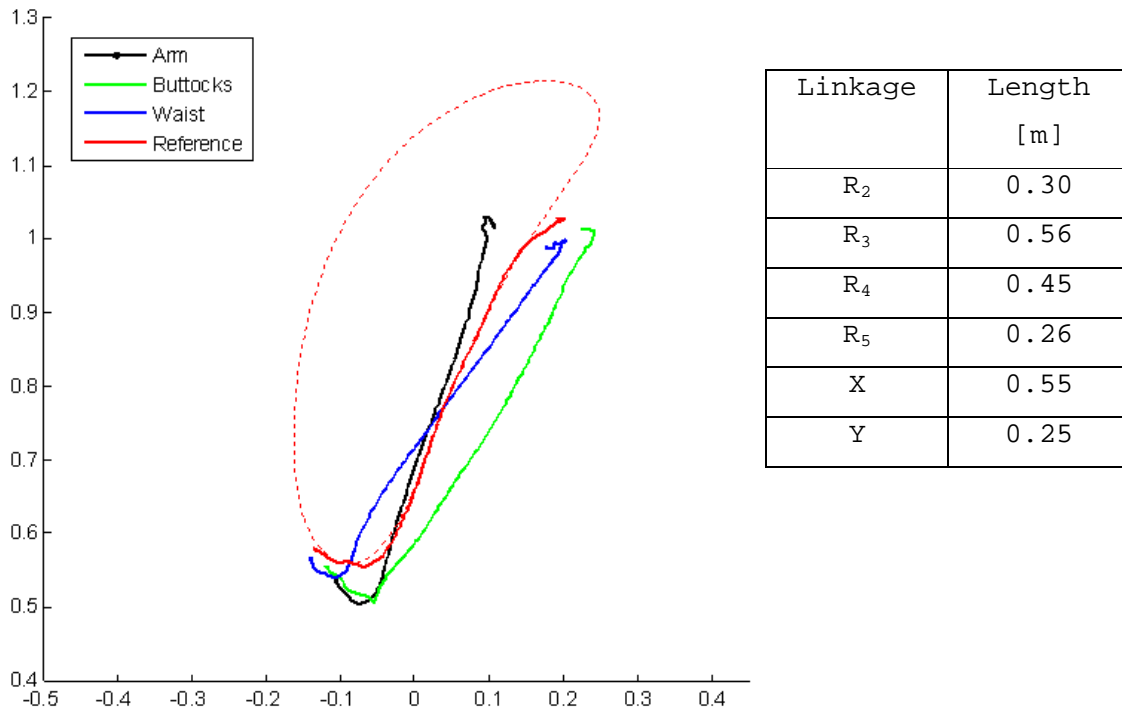


Figure B.7: Achieved trajectory for general sit-to-stand motion.

In the four setups shown, the linkage lengths are very close to each other; most of the variations are in the orientation and positioning of the overall device, which will determine how low or forward-leaning the STS motion will be.

Note that the linkage trajectories, shown by the dashed lines in the above figures, are oval-shaped. The reference trajectories are sufficient for test subjects taller than the mock-up test subjects, by having the user follow full length of the “oval trajectory” to get more movement range. The alternate option for accommodating taller test subjects is to increase each of the linkage lengths by one increment.

The linkages were fabricated from rectangular aluminum tubing. Aluminum rod is used as end pieces for each link, with either a clevis or a bushing for the pivot. The end pieces can slide in or out of the rectangular tubing to allow for length adjustment in 2 cm (approx 3/4") increments. Two locking pins are used to secure the end pieces rigidly at the desired lengths.

Buttocks and Waist Assist Mechanism

Moment Transfer Lever-Arm

In the original design, there are two lever arms for each of the waist and buttocks assist mechanisms, one on both sides of the user. The design was simplified based on consultation with the client and supervisor. The final design uses only one lever arm for each of the buttocks and waist assist mechanisms, as shown in Figure B.8 below:

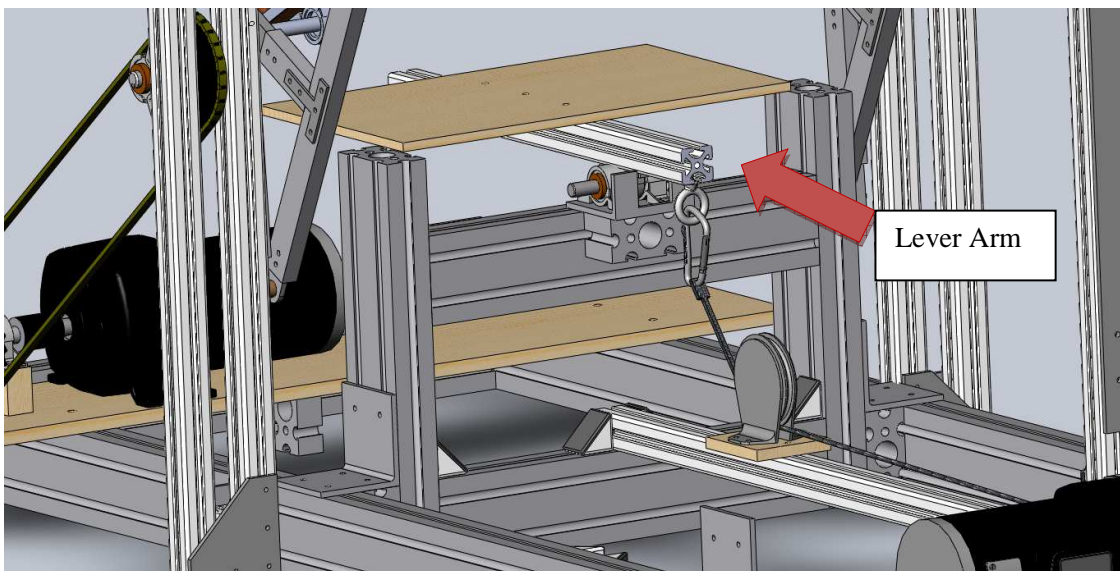


Figure B.8: Revised implementation for buttocks assist.

For the buttocks assist, the pivot of the lever arm is right beneath the knee of the user, so that the assistive motion is very close to the user's knee rotation. The range of motion is from 0° to approximately 60°. At 60°, the user is expected to be close to a fully standing position and no longer requiring assist force at the buttocks.

The assist arm, on which the subject is seated, is 45cm long. The lever arm, on the transmission side, is 15cm long, based on motor and transmission calculations. The lengths of the lever arm and assist arm are fully adjustable.

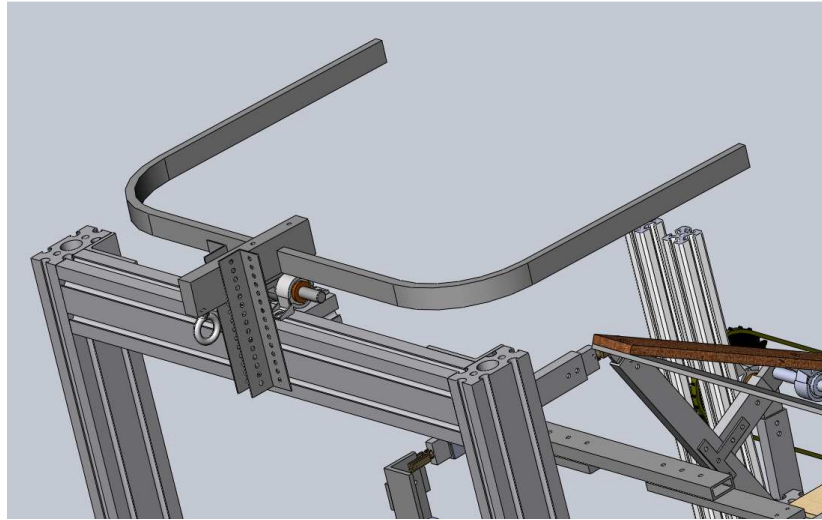


Figure B.9: Revised implementation for waist assist.

For the waist assist, the assist arms split from the middle and to both sides, helping lift the test subject by connecting a lifting chain from the assist arm to the user's waist as seen in Figure B.9. The user is secured with a padded transfer belt with loops on both sides, on which the chain can be connected. The chain is connected to the transfer belt and the assist arms using Karabiners.

The assist arm is fabricated from $\frac{1}{2}$ " x $1\frac{1}{4}$ " 6061-T6 aluminum, which was calculated to withstand the required moment with minimum deflection (refer to Appendix A – Calculations). The range of rotation is from 0° to approximately 50° . Rotation beyond this angle may cause excessive horizontal force assist to act on the user.

The assist arms, connected to the user, are 45cm long, while the lever arm, on the transmission side, is 10cm long. These dimensions are based on motor and transmission calculations (refer to Appendix A – Calculations). The assist arm is spaced 60cm apart to accommodate larger test subjects.

Motor and Transmission

The waist and buttocks assist share the same motor and transmission setup, to enable independent testing with each mechanism.

A 90V PMDC gear motor is secured rigidly on a platform at the front of the test bed, and coupled directly onto a shaft with a cold-rolled steel winch spool welded onto it. A $\frac{5}{16}$ " diameter steel cable is wound onto the winch spool. The free end of the cable has a hook, to enable connection to the transmission side of the lever arm for either the buttocks or waist assist. A pulley block is used to alter the direction of the winch cable, as well as the actuation force, from the horizontal to the vertical direction. This pulley can be shifted forward and backward to switch between buttocks and waist assist setups (refer to Appendix F – User Manual).

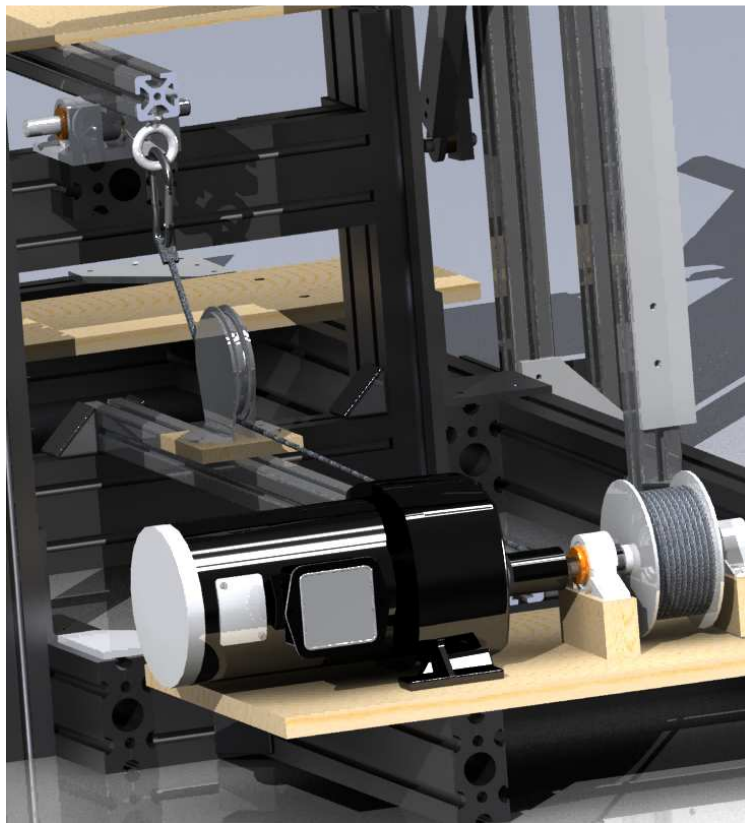


Figure B.10: Winch cable and lever arm.

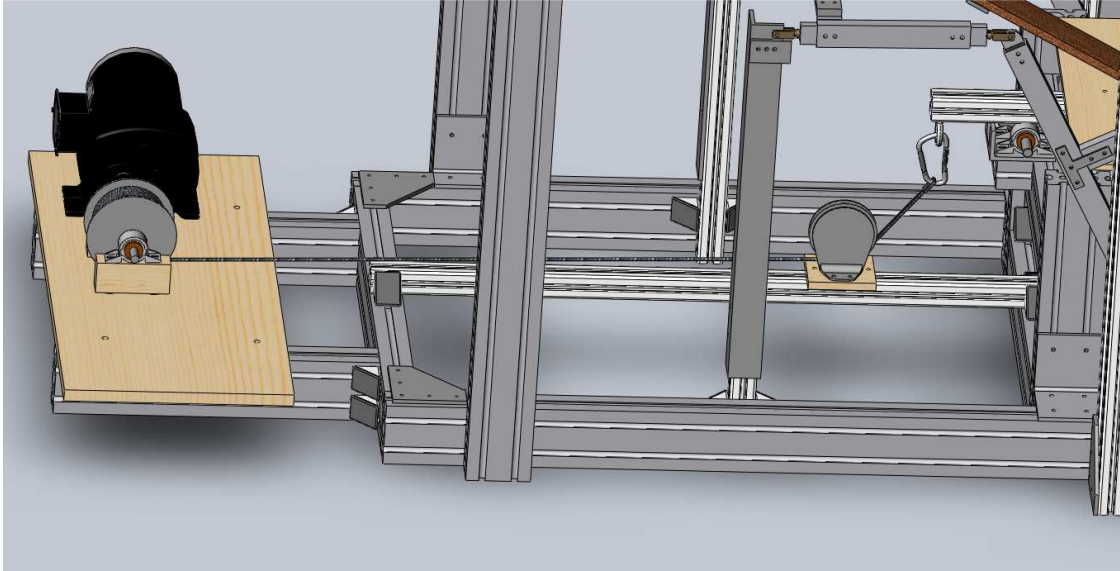


Figure B.11: Transmission - motor and winch setup.

This configuration enables a maximum of 390 N to be applied to the user during the buttocks assist and 715 N during waist assist.

Range of Adjustment

The following table highlights the range of adjustment for setting the pivot for waist and buttocks assist mechanisms to accommodate different users based on the final constructed prototype:

Table B.2: Adjustment range for waist and buttocks component – final.

Component	Maximum Height [m]	Required Max [cm]	Minimum Height [m]	Required Min [cm]
Buttocks assist pivot	50	47	25	25
Waist assist pivot	123	125	75	80

Appendix C: Test Bed Operation Manual

Sit to Stand Test Bed Operation Manual

April 15, 2011

The screenshot displays the software's main control panel. At the top, subject parameters are listed: Subject # 1, Subject Mass [kg] 3.61409, Shank Length [m] 0, Ankle Height [m] 0, and wood height [m] 0. Below these are foot length and heel position settings. The central area contains calibration controls, including 'Grab Orientation', 'Grab Mass', and 'Grab Initial HAT Angle' (98.0593). A 'Choose Calibration Method' section offers options like 'Get New Calibration Function' and 'Start Calibration Trial'. Assistance modes for Bar, Arm, Buttocks, and Waist are also configurable. On the right, a 'Rise' indicator and 'Current State' (Waiting for Initial Orientation) are shown. Two plots are visible: 'Knee Angle' (Plot 0) showing a step change from approximately -150 to -100 degrees, and 'Knee Torque' (Plot 0) showing a step change from approximately -150 to -100 Nm. A bar chart at the bottom shows 'Assisted Knee Torque' (0.30075) and 'Unassisted Knee Torque' (Inf).

This screenshot shows the 'INITIALIZATION/CALIBRATION' and 'MANUAL OVERRIDES AND DEBUGGING INFORMATION' sections. The left side includes buttons for 'Initialize', 'CALIBRATE CURRENT', 'GO HOME', and 'GO END'. A central 'RUN' button is accompanied by 'Test Mode' and 'Data Saving' indicators. The 'ACTIVE SENSORS' section includes 'RESET', 'DEAD-MAN', and 'Forward/Reverse Limit' buttons. The 'MANUAL POSITION LIMITS' section contains sliders for 'Arm Goal' (3286), 'Waist Goal' (3200), and 'Buttocks Goal' (1800). A 'CAUTION - JOGS' section features 'Forward' and 'Backward' buttons with a 'Jog Amt' of 10. The right side of the interface is filled with various numerical settings for 'Initial Ramp?', 'Upper/lower bound (100%)', 'Penalty Velocity', 'Mid Region/Ramp End Velocity', 'Lower Region Penalty Velocity', 'delta Angle' (15), 'Ramp Start Velocity' (100), 'Arm Assisted Speed' (100), 'CurrentKneeAngle' (0), 'threshold angle' (0), and 'InitialKneeAngle' (0).

Overview

This document details the operation of the test bed using the Windows and PXI LabVIEW programs as well as the mechanical configuration of the test bed. The PXI program is used to control the operation of the test bed, and the Windows program is used to collect data from the motion sensors and perform calculations to determine the real time knee torque of subjects as they stand up in the test bed.

Windows Program

A Windows computer is used as the operating system for the data collection program. The data collection program (**File Name: XsensRecordDec10PXITransfer**) is used to record and save the motion sensor readings, which quantify subject kinematics and assist forces during the assisted STS transfer. The data collection program also performs knee torque computations that are used to control the motion of the test bed according to the load sharing computations. A companion document called the Sit to Stand LabVIEW Program Document provides an in depth description of the operation of the Windows program. This document provides a general outline of the program.

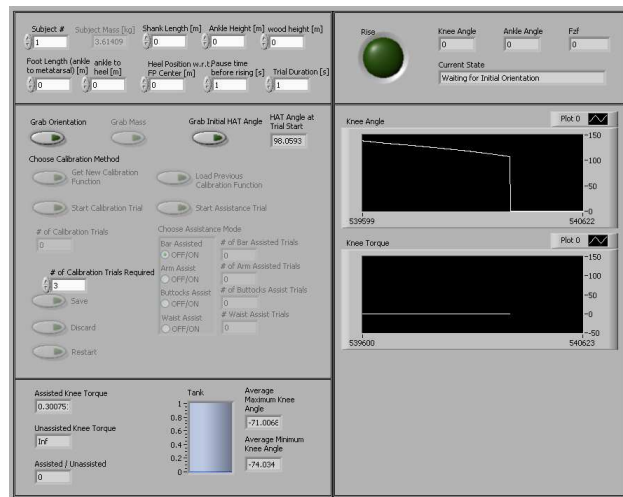


Figure C.1: Windows program.

PXI Program

A National Instruments PXI 8196 Computer is used as the operating system for the test bed control program. The test bed control program (**File Name: Sit to Stand Feb 4**) graphical user interface (GUI) enables the experimenter to control the motion of the test bed and visualize feedback from the limit switches, motor encoder, and motion and force sensors. At the commencement of an assisted STS transfer the experimenter presses the start button on the GUI. The experimenter then selects the mode of assist, either buttocks, waist or arm mode, and sets the encoder count position goals for the corresponding assist. These position goals are used to determine the start and end position of each of the test bed assist modes. Once the subject is seated and comfortable in the test bed, the experimenter selects the run buttons on the GUI. Motion of the test bed is then activated by the subject via a deadman switch, which enables the motor to run when depressed. The motor activates motion of the test bed and an encoder reads in the current position of the motor. Once the encoder count hits the end position goal, the motion of the motor ceases. Limit switches provide a hard limit on the start and endpoint of the assisted motion and a reset switch resets the assist back to the initial position when depressed. Switches are discussed in greater detail in the following section titled Test Bed Configuration. The GUI displays the currently active switch to the experimenter and the current position of the motor based on the encoder count from the motor encoder. The test bed control program also record the data from the force plate and load cells via a digital to analog converter (NI PXI 6289) which connects the BNC cables from the force plate and load cells to the National Instruments computer.

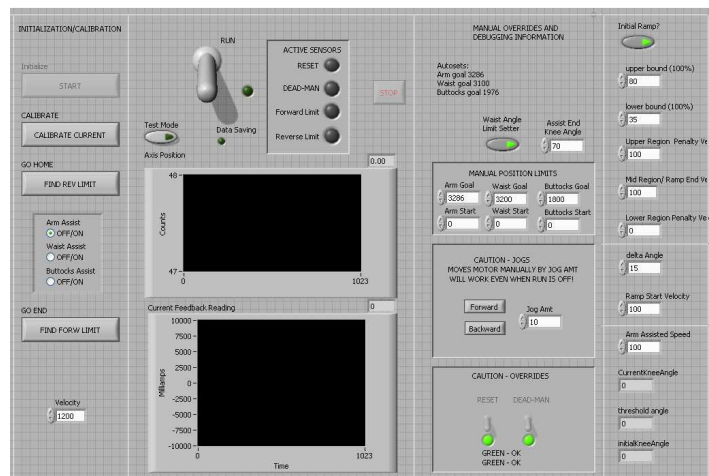


Figure C.2: PXI program.

Test Bed Operation

This section goes through the steps involved in performing experiments and collecting data from the test bed. The Windows program will be referred to as the Windows GUI and the PXI program will be referred to as the PXI GUI.

Data Entry

The first step is to input subject anthropometric measures into the Windows GUI.

Subject Number: This is the number of the subject and will correspond to the subject number in the filename of the saved subject data. Subject Data is saved on MNM computer, C:\Documents and Settings\caris\Desktop\XsensRecordData\

Anthropometric Measures: These measures (shank length, ankle height, foot length, ankle to heel) are inputs into an equation which calculates the real time knee torque of the subject. Details of the equation can be found in Sit to Stand LabVIEW Program Document.

Heel Position w.r.t. Force Plate Center: This measure is the distance between the heel and the center of the force plate. It is also used to calculate the knee torque of the subject

Wood Height: This is the height of the wooded plank placed on the force plate. The wood is used to adjust for users of different heights.

Pause Time Before Rising: When Start Calibration trial or Start Assistance Trial is clicked, the data collection program will start collecting data and wait this amount of seconds before the green Rise LED lights up.

Trial Duration: This is the length of time for which data will be collected during trials. Default is 10 seconds.

Subject #	Subject Mass [kg]	Shank Length [m]	Ankle Height [m]	wood height [m]
1	3.61409	0	0	0
Foot Length (ankle to metatarsal) [m]	ankle to heel [m]	Heel Position w.r.t. FP Center [m]	Pause time before rising [s]	Trial Duration [s]
0	0	0	1	1

Figure C.3: Data entry.

Calibration Trials

The next step is to perform the calibration trials. These trials are performed without assistance and are used to calculate the unassisted knee torque of subjects performing STS. The following steps are performed in obtaining calibration trials:

1. Enter in the number of calibration trials.
2. Before attaching the sensors onto the subject, place the sensors in a known orientation and click the Grab Orientation button.
3. Ask the subject to stand on the force plate and click the Grab Mass button.
4. Click Get New Calibration Function.
5. Click Start Calibration Trial and ask the subject to stand after the rise button lights up.
6. If the stand is satisfactory click save, otherwise click discard, the # of calibration trials will only increment if the save button has been clicked.
7. Once # of Calibration trials equals # of Calibration Trials Required, the calibration function will be calculated. Details of the calibration function can be found in Sit to Stand LabVIEW Program Document.
8. The restart button allows for calibration trials to be restarted.
9. The Load Previous calibration Function will load the previous calibration function if it exists in the folder C:\Documents and Settings\caris\Desktop\XsensRecordData\Previous Calibration Function.csv. More information of this is in the Sit to Stand LabVIEW Program Document.

The two graphs in the Windows GUI give a reading of the current knee angle of the subject and the current knee torque of the subject. A reading of the knee and ankle angle as well as the vertical force plate force is also provided as well as the current state of the state machine (more information on the states provided in the Sit to Stand LabVIEW Program Document).



Figure C.4: Calibration trials.

Assistance Trials

Assistance trials are started by clicking the Start Assistance Trial Button on the Windows GUI. Select the Assistance Mode for which assistance will be provided. The following steps are to be followed when performing assistance trials:

1. Choose Assistance Mode on the Windows GUI (either bar, arm, buttocks, or waist)
2. Make sure the test bed is physically set up for the selected assistance mode (see Test bed Configuration section)
3. Make sure that the PXI GUI is set correctly (more details in next section)
 - a. PXI program is turned on (click the start button in the PXI program)
 - b. The proper assist mode is selected (arm assist, waist assist, or buttocks assist)
 - c. Run button is toggled such that the toggle switch points upwards
 - d. Test mode button is off (i.e. green light off)
4. Click Start Assistance trial and ask subject to rise with assistance
5. If trial is satisfactory, click save otherwise click discard. The trial will increment only if the save button is clicked.
6. Once the desired number of trials is reached, select the next desired Assistance Mode and repeat steps 1-5.

The GUI also gives information on the Load Sharing of the Test Bed. (Load sharing described in detail in the Sit to Stand LabVIEW Program Document). The Bar Graph shows the real time knee torque ratio, i.e. a visual display of the reading of the Assisted/Unassisted Box. The Assisted Knee

Torque box is a real time reading of the knee torque while the person is rising with assistance, The Unassisted Knee Torque box is a real time reading of the calculated knee torque of the subject corresponding to the current knee angle if the subject were rising without assistance. This value is obtained from the calibration function, and is described in detail in the Sit to Stand LabVIEW Program Document.

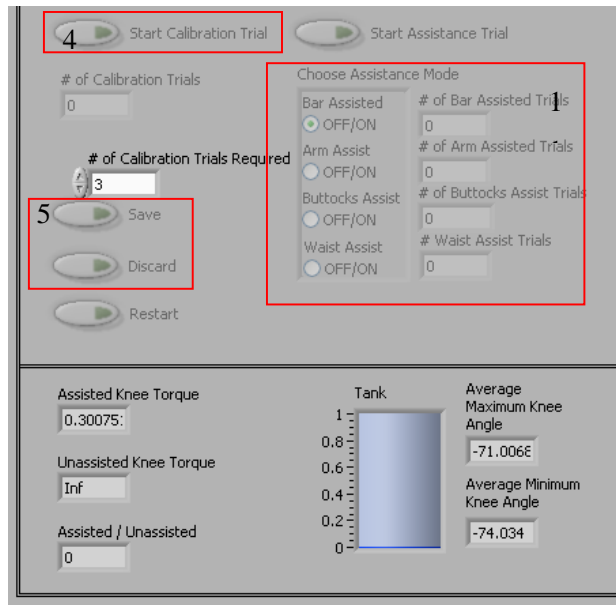


Figure C.5: Assistance trial Windows setting.

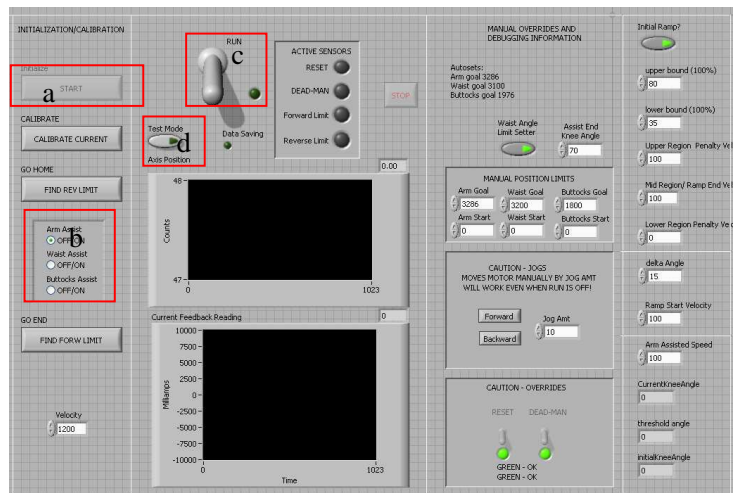


Figure C.6: Assistance trial PXI setting.

Detailed Description of PXI GUI

As described already, the PXI GUI is the control interface for the operation of the motion of the test bed. The PXI GUI enables the experimenter to control the motion of the test bed and visualize feedback from the limit switches, motor encoder, and motion and force sensors. The test bed control program also records the data from the force plate and load cells via a digital to analog converter (NI PXI 6289), which transmits signals from the force plate and load cells BNC cables to the National Instruments computer.

Initiation of the control program begins with pressing the start button. The program has two main operating states, the run “on” state and the run “off” state.

Run “Off” State

1. This state is active when the run toggle switch is off (pointing down). This state is used to set the software position limits of the test bed for the three assists, and also to select which assist mode is active.
2. Selecting the assist mode (Figure C.7) will activate the corresponding manual position limits. The Find Rev and Find Forw limit buttons will run the motor backwards and forwards respectively until the limit switch is hit. When the limit switch is hit the Manual Position Limit will automatically reset to the current encoder count.

*****Warning***:** when the Find Rev and Find Forw limit buttons are hit the motor will not stop running until the limit switch has been hit. Keep one hand close to the emergency stop button when running the Find Rev and Find Forw limit buttons.
3. The Manual Position limits are the soft limits at which the motor will halt when the encoder reaches the limit. These limits can be set for each of the 3 modes of assist. The active manual position limit is set by selecting the assist mode, see previous bullet point (point 2)
4. The current encoder count is displayed on the GUI and the time history of the encoder count is also shown on the graph with y axis labeled “Counts”. Rotation of the motor will increment or decrement the value of this count until either the physical limit switch is hit or the manual position limit is reached. More information on the physical limit switches is provided in the Test Bed Configuration section.
5. The time history of the motor current feedback reading is displayed on the graph with y axis labeled Milliamps.

6. A set of LEDs indicate which of 4 possible sensors is currently being activated. Details on each of the 4 sensors, which correspond to switches in the test bed are provided in the Test Bed Configuration section.
7. The Jog forward and Jog backward buttons enable motion of the motor incrementally either forward or backward when the program is in the run “off” state. The amount the motor jogs can be changed. The default jog amount is 10 counts.

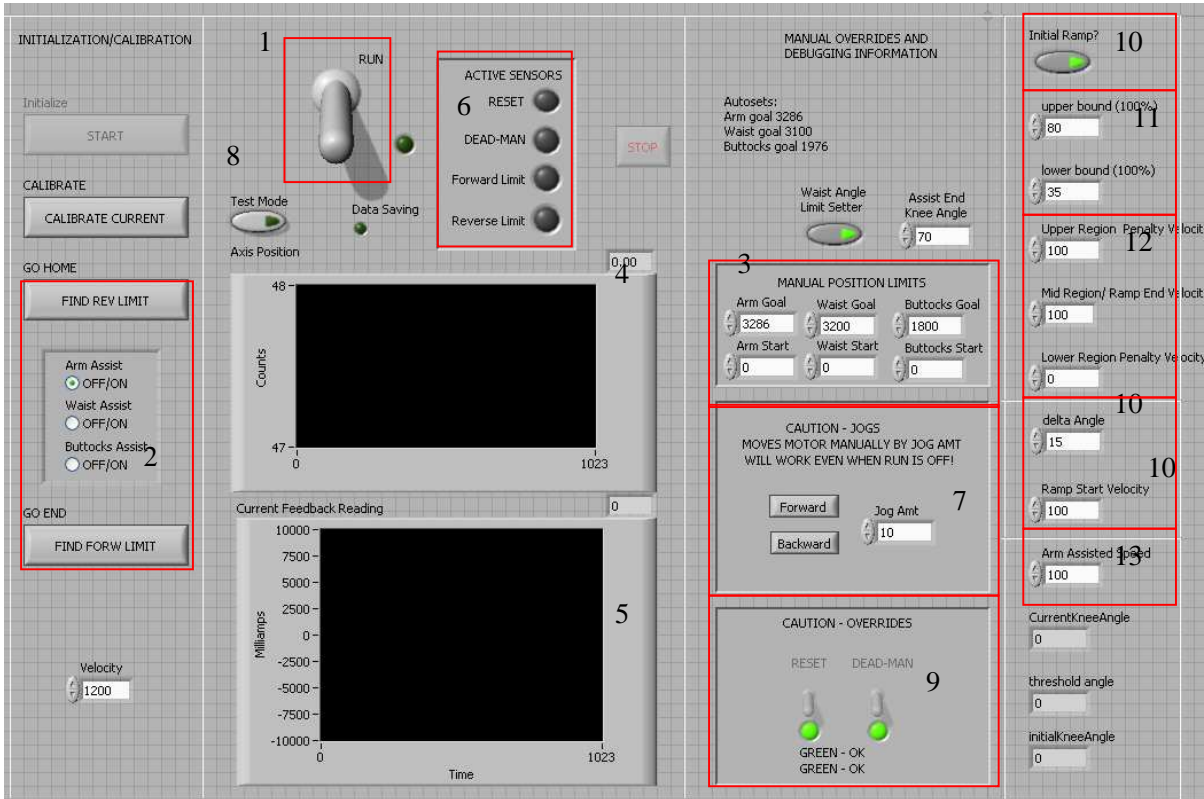


Figure C.7: PXI GUI details.

Run “On” State

When the test bed is being activated by the subject the PXI GUI must be in the Run “on” State.

This state is active when the run switch is toggled on (pointing up). When the run state is on, the test bed will run when either the deadman or reset switch is pressed. More information on the deadman and reset switch provided in the section on Test Bed Configuration.

8. When the test bed is in Test Mode (i.e. Test Mode button has been clicked and green light is on), the test bed will run without having to click start assistance trial on the windows GUI. If the test bed is not in test mode, it may only run when the start assistance trial has been clicked on the windows GUI.
9. The override switches allow the PXI GUI to run the motor either of forwards or backwards by toggling the reset or deadman switch.

Real Time Load Sharing/Speed Settings

A detailed description of the real time load sharing/ speed settings is given in the Sit to Stand LabVIEW Program Documentation. A brief overview of the functionality is provided in this section.

10. Initial Ramp: When this button is on, the initial velocity of the motor will ramp up from the ramp start velocity to the mid region/ramp end velocity at the beginning of the motion of the test bed. The duration of the ramp is according to the delta angle value inputted. This delta angle corresponds to the change in thigh angle for which the ramp function will be activated. E.g. if delta angle is 15, this means that the function will ramp up until the thigh/knee angle changes by 15°.
11. The upper and lower bound are the bounds for the load sharing function to be activated. When the knee torque ratio (described in detail in Ch. 5 of thesis and in the Sit to Stand windows documentation) is below the lower bound, the motor speed will ramp down to the lower region penalty velocity. When the torque ratio is between the lower and upper bound, the motor speed will rotate at the mid region/ ramp end velocity, and when the torque ratio is above the upper bound, the motor speed will ramp up to the upper region penalty velocity.
12. These are the three potential velocities at which the motor will run depending on if the torque ratio is below the lower bound, between the lower and upper bound, or above the upper bound. The velocity is a percentage of the maximum motor velocity (more details of this in the Sit to Stand LabVIEW Document) and thus can be set as number between 0 and 100%.
13. The arm assist mechanism does not incorporate load sharing and thus runs only at a single speed as set in the arm assist speed block.

Test Bed Configuration

Test Bed Entry

The test bed has been designed to allow entrance from either side by disconnecting the end link of one of the 4-bar linkages from the support bar and retracting it to create an opening into the test bed (Figure C.8).

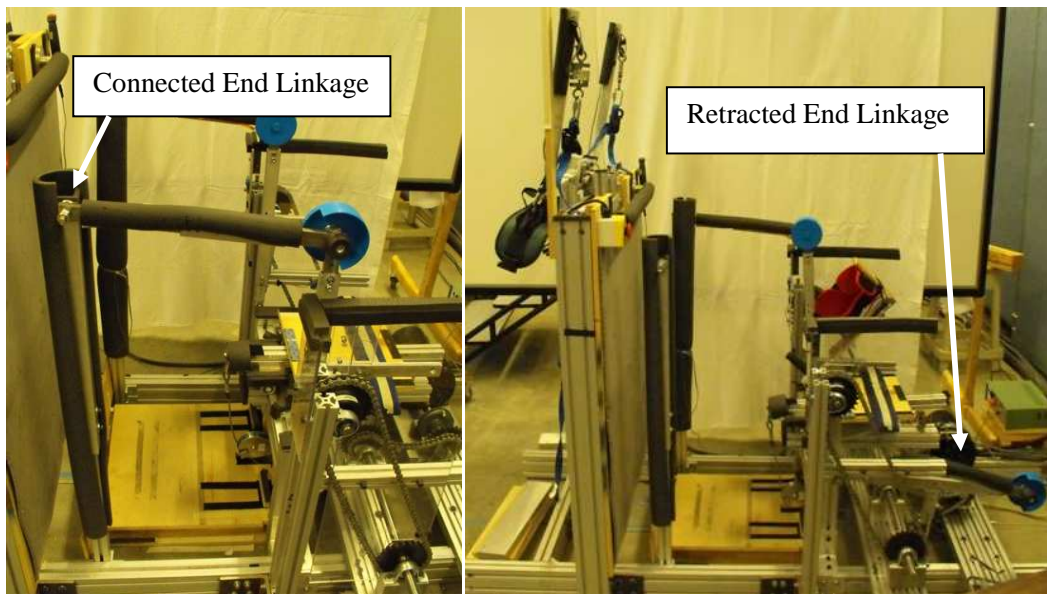


Figure C.8: Left image: End linkage connected. Right image: End linkage retracted.

Setting up For Arm Assist

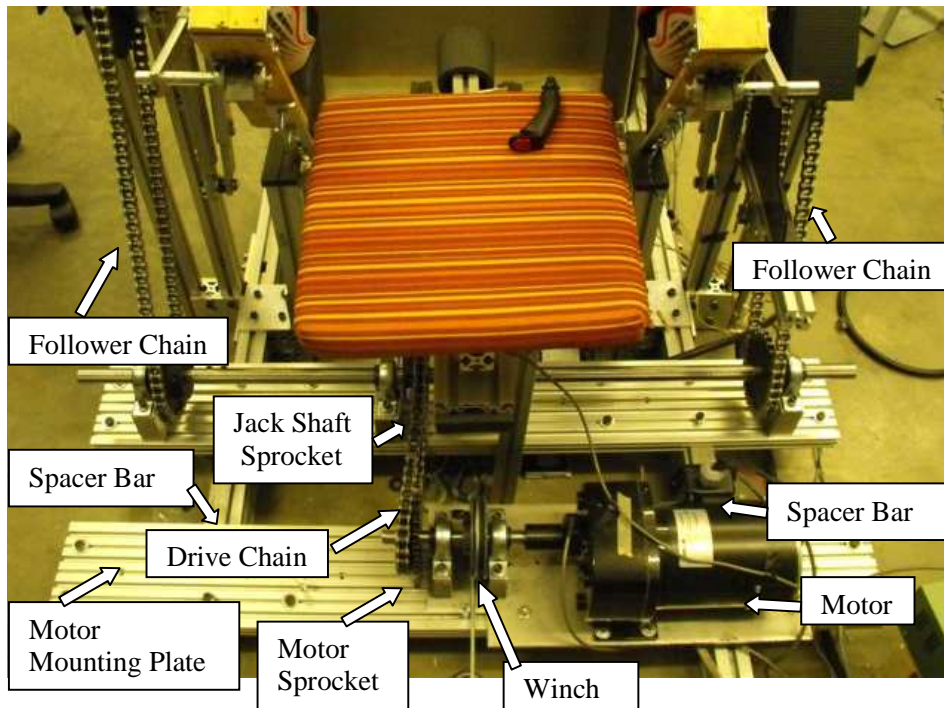


Figure C.9: Rear view of test bed showing labeled arm assist mechanism components.

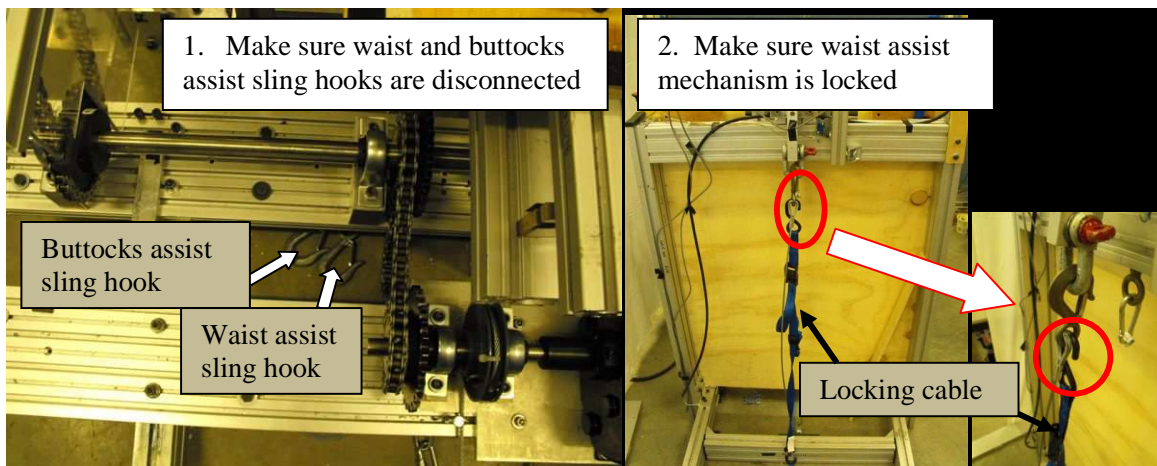


Figure C.10: Left image: Rear view of test bed showing disconnected waist and buttocks assist sling hooks. Center image: Front view of test bed showing locked waist assist. Right image: Close-up of waist assist locking cable.

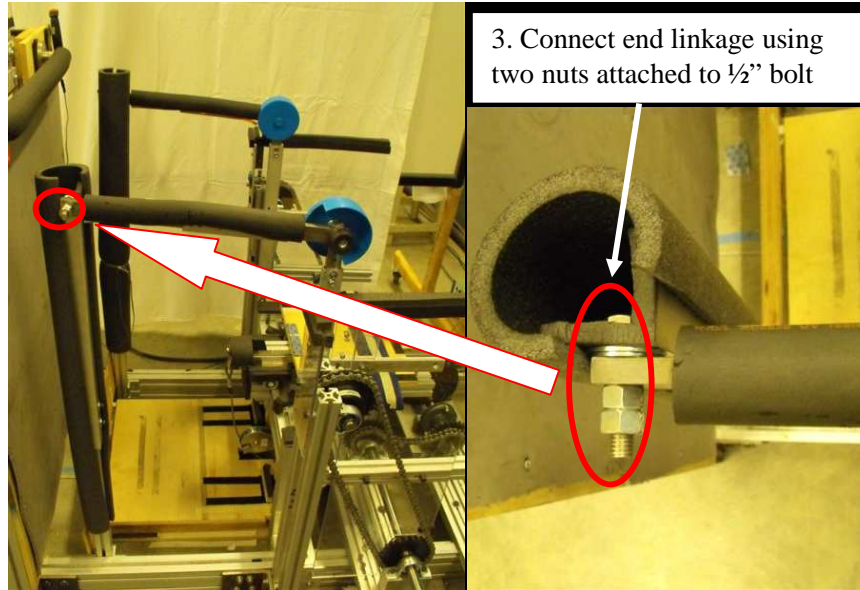


Figure C.11: Left image: Side view of test bed. Right image: Top view close-up of end linkage connection point.

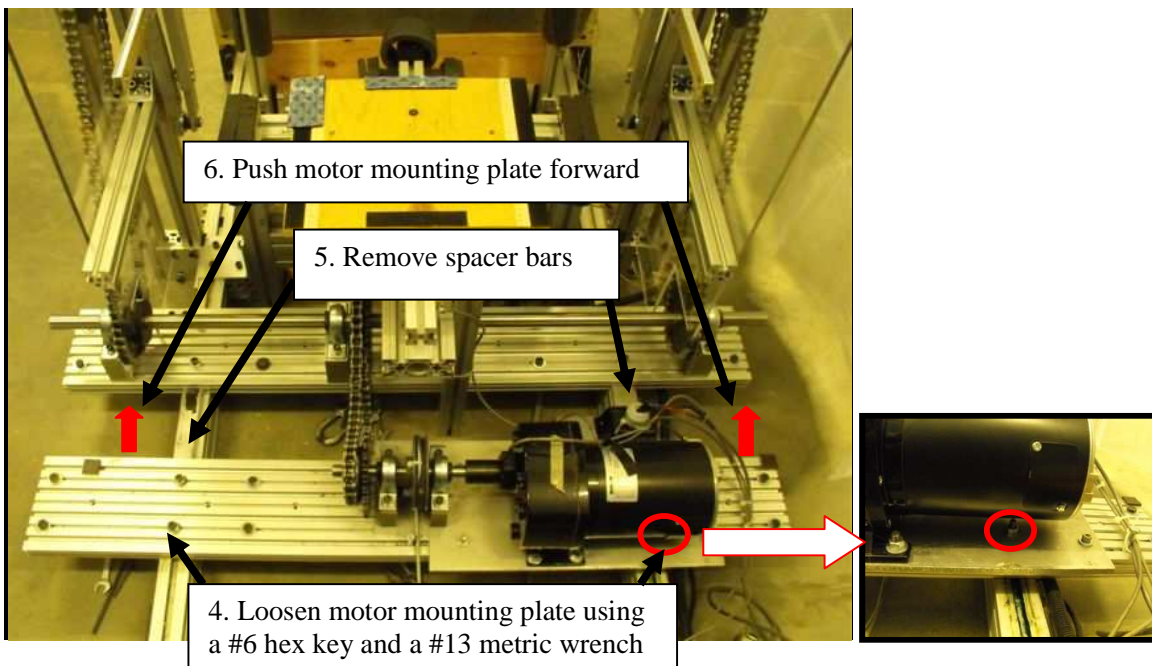


Figure C.12: Left image: rear view of test bed. Right image: Close-up of right side of motor mounting plate with connection bolt highlighted.

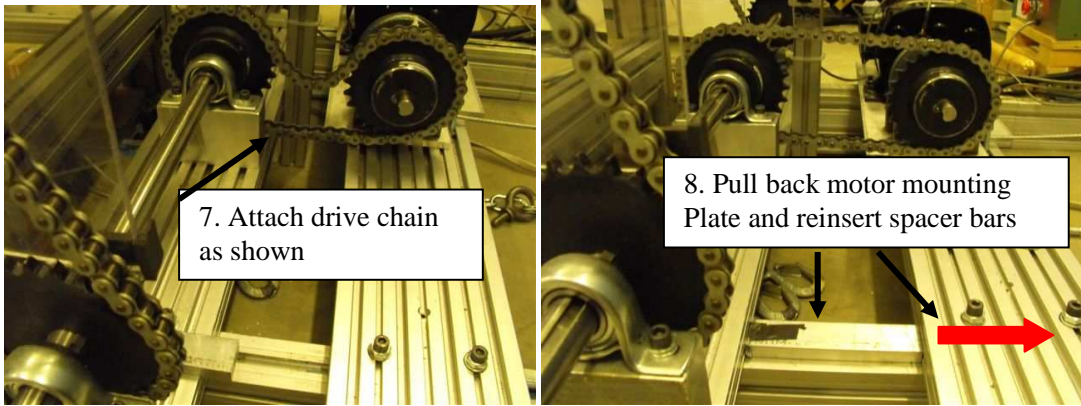


Figure C.13: Left image: Side view of test bed showing motor and jack shaft sprockets and loosened drive chain. Right image: Side view of test bed showing motor and jack shaft sprockets and tightened drive chain.

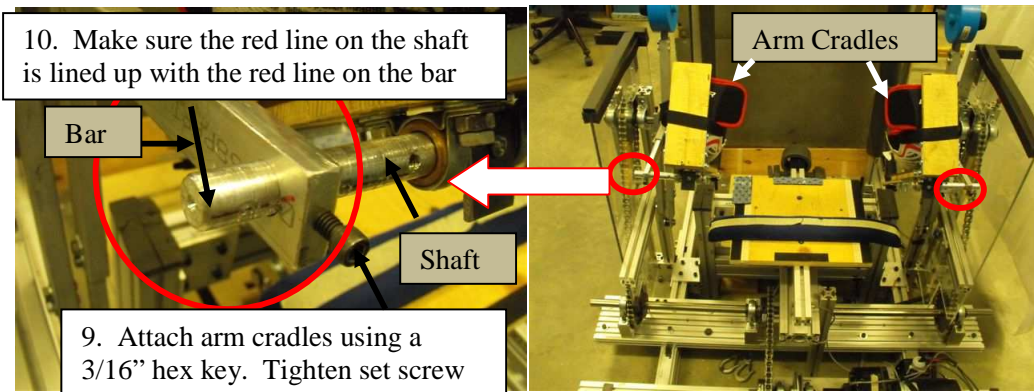


Figure C.14: Left image: Close-up of arm cradle attachment point. Right image: Rear view of test bed showing attached arm cradles.

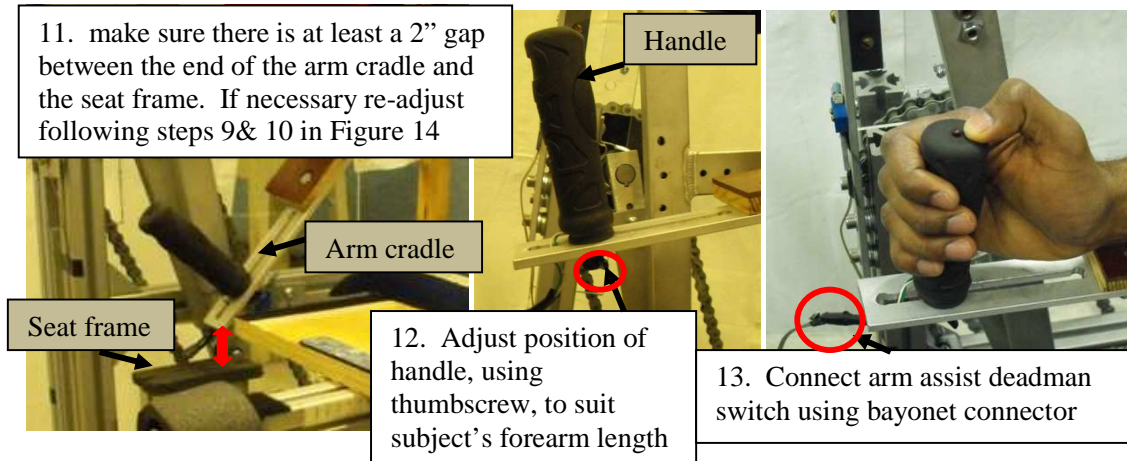


Figure C.15: Left image: Right arm cradle in rest position. Center image: Close-up of right arm cradle handle highlighting the adjustable thumbscrew. Right image: Close-up of right arm cradle highlighting deadman switch connection point.

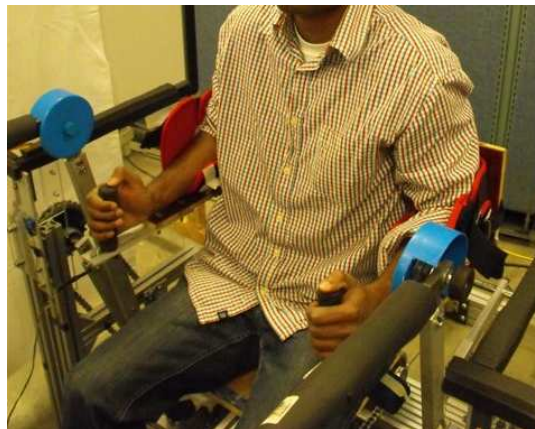


Figure C.16: Subject seated in test bed ready for arm assisted rise.

Setting up For Buttocks Assist

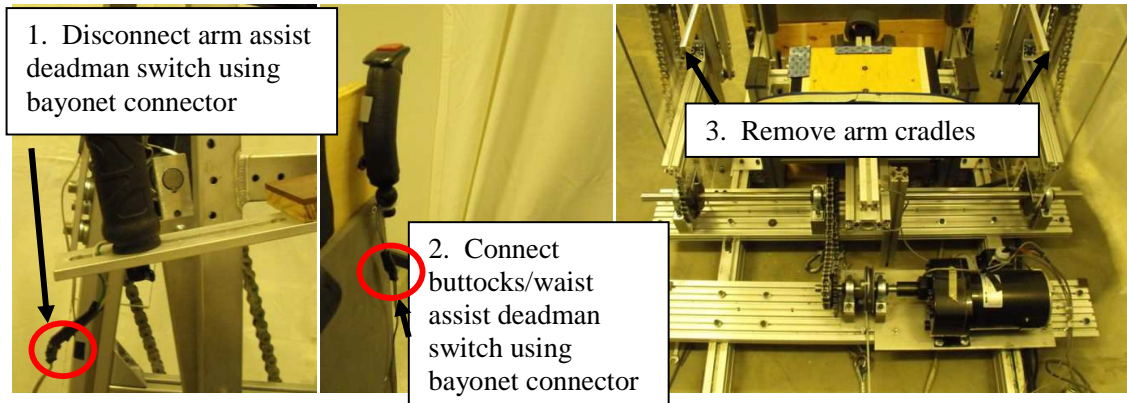


Figure C.17: Left image: Arm assist deadman switch. Center image: Buttocks/waist assist deadman switch. Right image: Rear view of test bed with arm cradles removed.

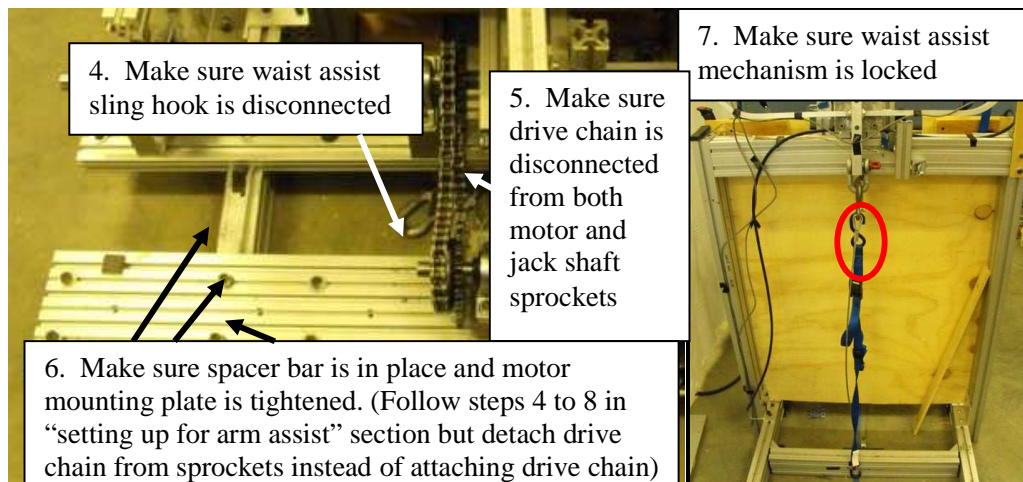


Figure C.18: Left image: Rear view of test bed showing disconnected waist assist sling hook and disconnected drive chain. Right image: Front view of test bed showing locked waist assist.

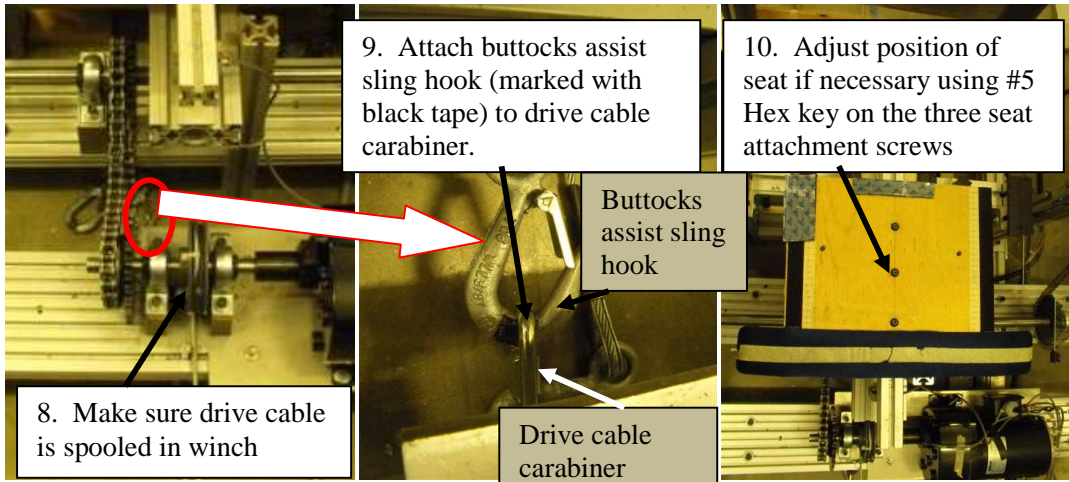


Figure C.19: Left image: Rear view of test bed highlighting buttocks assist cable attachment point. Center image: Close up of buttocks assist cable sling hook attachment point. Right image: Top view of test bed showing seat adjustability.



Figure C.20: Subject seated in test bed ready for buttocks assisted rise.

Setting up For Waist Assist

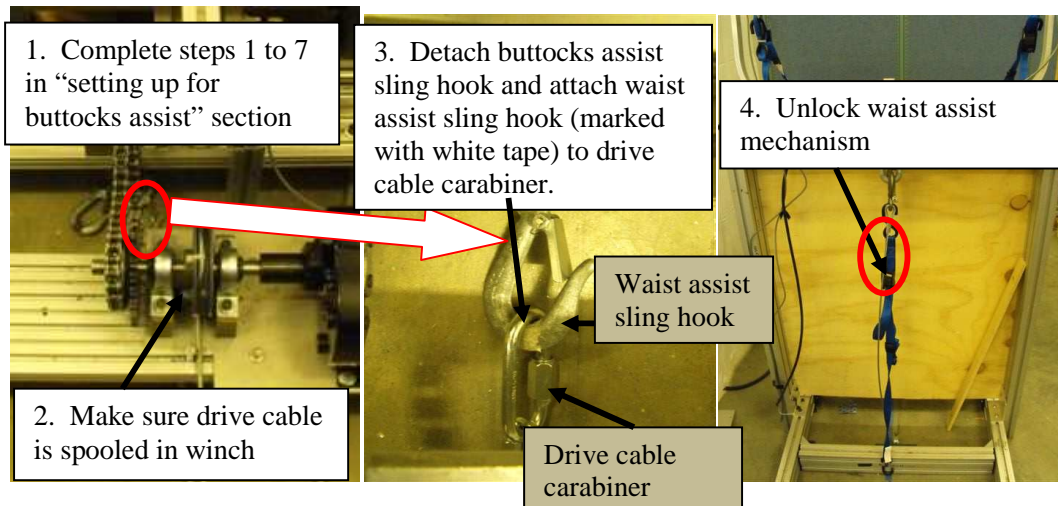


Figure C.21: Left image: Rear view of test bed highlighting waist assist cable attachment point. Center image: Close up of waist assist cable sling hook attachment point. Right image: Front view of test bed showing locked waist assist.

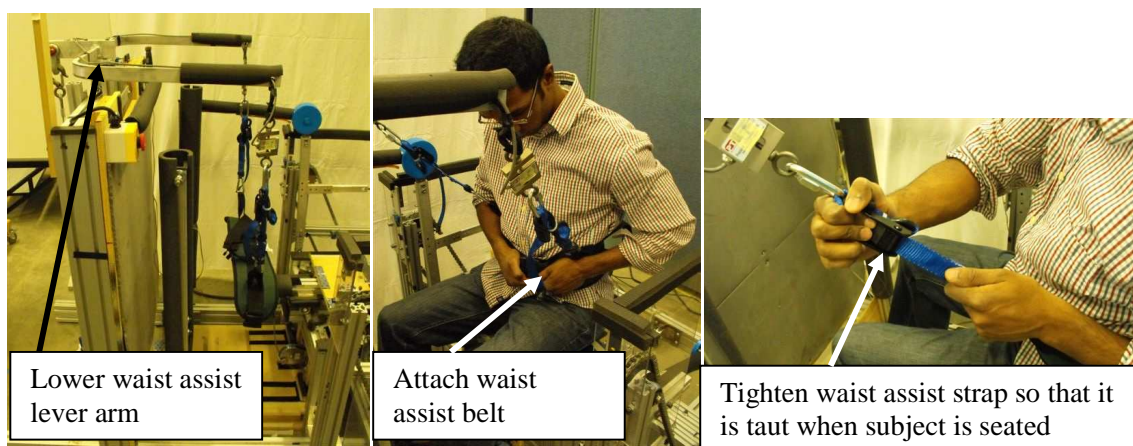


Figure C.22: Left image: Side view of test bed showing lowered waist assist lever arm. Center image: Image of subject attaching waist assist belt. Right image: image of subject tightening waist assist strap.



Figure C.23: Subject seated in test bed ready for waist assisted rise.

Switches

Figure C.24 shows the test bed control box. This box is used to activate the limit switches for each mode of assist. The three position selector switch is used to activate either the buttocks or waist assist limit switches or to turn both switches off, and the two position selector switch is used to activate the arm assist limit switches. An emergency stop button on the control box is used to halt motion of the test bed. An emergency stop button is also located at the entrance of the test bed and is within reach of the test bed user.



Figure C.24: Test bed control box. Use to activate the limit switches for the particular mode of rise.

The limit switches are used to constrain the beginning and end of the motion of the assist mechanisms. Figure C.25 shows the locations of each of the test bed limit switches.

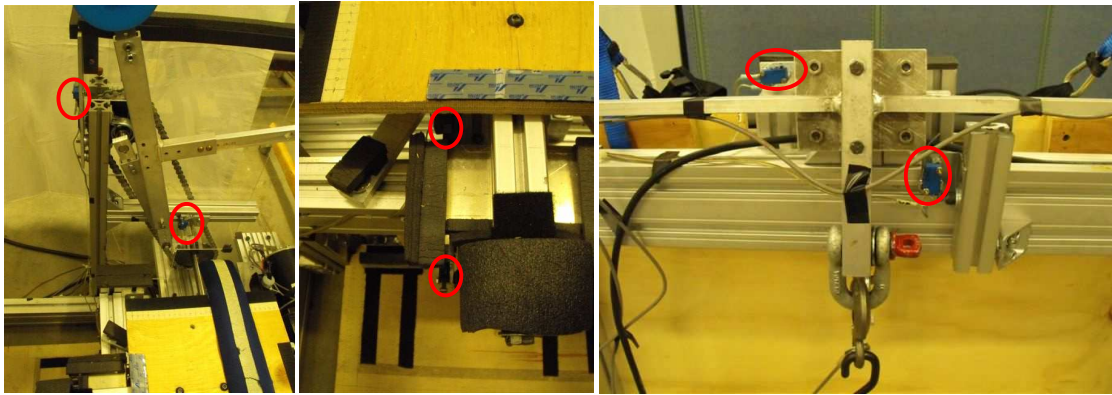


Figure C.25: Left image: Side view of test bed showing arm assist limit switches. Center image: Front view of test bed seat showing buttocks assist limit switches. Right image: Front view of test bed waist assist lever arm showing waist assist limit switches. In all images the limit switch locations are identified by the red circles.

The deadman switch, shown in Figure C.26, is used to activate forward motion of the test bed. A buttocks/waist deadman switch is used to activate motion of the buttocks and waist assists and an arm cradle deadman switch is used to activate motion of the arm assist. A reset switch is used to reverse the motion of the assists.

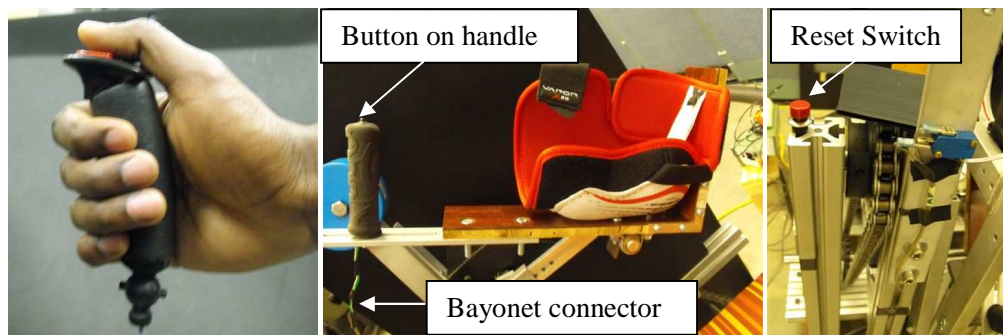


Figure C.26: Left image: Buttocks/waist deadman switch. Center image: Arm cradle deadman switch. The deadman switches are used to move the assists forward. Right image: Reset switch. The reset switch is used to move the assists backwards and is located on the right hand side of the test bed.

Checklists:

A detailed Failure Modes and Effects Analysis (FMEA) has been included in Appendix D of the Thesis (Biomechanical Analysis of Sit to Stand). A detailed safety check of the test bed should be completed using the safety checklist on this FMEA before commencing operation of the test bed. This checklist should be regularly consulted.

An experimental safety checklist has been included in Appendix E of the Thesis (Biomechanical Analysis of Sit to Stand). Before commencing experiments the operation condition of the test bed should be verified using this checklist.

Finally, an experiment checklist has been included in Appendix J of the Thesis. This checklist should be followed when operating each of the assist mechanisms.

Appendix D: Failure Modes and Effects Analysis

Waist assist

Part Name	Function	Failure Mode	Cause	Effect on User	Prevention	Action	Safety Checklist
Waist assist transfer straps	connection between belt and transfer bars	tangle	getting hooked up into the arm assist	cannot rise further	minimize snag points on strap and arm assist	cut excess strap to prevent tangle Look at arm assist snag points and fix	Do a manual lift of the waist assist bar to ensure strap won't snag
Waist assist limit switches	Stops the motion of the waist assist bar	switch is not hit Forward limit switch has to carry the weight of the bar	switch is knocked out of place Switch is lower than the rest bar limit switch bar gets bent Switch is not hitting the waist assist bar in a consistent location The rest bar on the left side is too low	User may get pulled further than intended	Ensure limit switch hits the waist assist bar in a place where it can hit consistently Ensure the rest bar is not so high that the limit switch is not depressed when the bar is hit. Ensure the rest bar is higher than the limit switch and ensure that the waist assist bar is resting on it	Ensure that the limit switches are rigidly placed	Perform a manual check on the rigidity of the limit switch Manually ensure that both limit switches are being hit Ensure that limit switches are not bent Ensure that the limit switch is depressed when the rest bar is hit Ensure the waist assist hits the rest bar and doesn't put all its weight on the limit switch
Waist assist rotation point	pivot point for waist assist	pivot is unable to rotate	obstruction in the rotation workspace	cannot pull user up	visual check to make sure area is clear	ensure all bolts are tightened Visual obstruction check	Visual obstruction check in rotation workspace
Waist assist rope connection	Pulls up the waist assist	connection points becomes disconnected	bolt unwinds	cannot pull user up	ensure bolt is tightened all the way	visual check	visually ensure that the red u-bolt is not becoming loose
Waist assist frame	supports the waist assist motion	frame gets bent	excessive force on frame	user is not pulled up correctly	Add structural support Visually ensure that crossbar is level and the vertical frame bars are level	Add structural support and do a visual check on the support bars to make sure they're level ensure bolts are tight	visually ensure that crossbar is level and the vertical frame bars are level
Waist assist locking mechanism	Holds the waist assist up and out of the way when it is not in use	improper connection of locking mechanism	Operator forgetting to lock mechanism	waist assist falls on user and injures them	always lock waist assist bar when not in use	checklist check	Ensure waist assist is locked out of the way when not in use
Waist assist pulley	redirects the motion of the waist assist to horizontal plane	rope comes off the pulley	improper attachment of pulley	not pulled up properly	visual check to make sure rope is on pulley Ensure bolts are tight	Ensure bolts are tight	Visual check to make sure rope is on pulley
Waist assist cable	Pull up the waist assist bar	rope or carabiner breaks	excessive load	User falls down	use swage fittings and rated carabiners	Use 3/16" rope swage fit the rope connection use rated carabiners	Perform a visual check of the rope and connections to make sure there are no visual failure points ensure that the carabiner is screwed tight

Buttocks Assist

Part Name	Function	Failure Mode	Cause	Effect on User	Prevention	Action	Safety Checklist
Buttocks assist seat	support the user	seat slides forward in attachment groove	excessive shear load	user falls down	ensure connection bolts are tight	tighten bolts	ensure seat bolts are fastened tightly
Buttocks assist rope connection	pull the buttocks assist seat up	carabiner becomes loose	carabiner bolt not tightened	user falls down	ensure carabiner bolt is connected tightly	tighten bolts	ensure carabiner is fastened well
Buttocks assist pulley	redirects motion of buttocks assist cable	cable slides off pulley	cable not wound properly	twisting loads may cause structural failure resulting in the user falling	ensure cable stays on pulley	add capturing mechanism to prevent rope from falling off the side ensure bolts are tight	visual check to make sure rope is on pulley
Buttocks assist initial position	keep the chair at a horizontal position	seat falls backwards	lack of cantilever support	user falls backwards	ensure the seat is supported properly in the zero position	add a cantilever support	
Buttocks assist rotation point	pivot point for waist assist	pivot is unable to rotate	obstruction in the rotation workspace	cannot pull user up	visual check to make sure area is clear	ensure all bolts are tightened Visual obstruction check	Visual obstruction check in rotation workspace
Buttocks assist frame	supports the buttocks assist motion	frame gets bent	excessive force on frame	user is not pulled up correctly	Add structural support Visually ensure that crossbar is level and the vertical frame bars are level	Add structural support and do a visual check on the support bars to make sure they're level ensure bolts are tightened	visually ensure that crossbar is level and the vertical frame bars are level
Buttocks assist limit switches	Stops the motion of the waist assist bar	switch is not hit	switch is knocked out of place limit switch bar gets bent Switch is not hitting the buttocks assist in a consistent location	User may get pulled further than intended	Ensure limit switch hits the waist assist bar in a place where it can hit consistently Ensure the limit switch is rigidly mounted and that there will not be any rotational motion of the switch	Ensure that the limit switches are rigidly placed	Perform a manual check on the rigidity of the limit switch Manually ensure that both limit switches are being hit Ensure that limit switches are not bent Ensure that the limit switch is depressed before any hard limits are hit
Buttocks assist cable	Pull up the waist assist bar	rope or carabiner breaks	excessive load	User falls down	use swage fittings and rated carabiners	Use 3/16" rope swage fit the rope connection use rated carabiners	Perform a visual check of the rope and connections to make sure there are no visual failure points ensure that the carabiner is screwed tight

Arm Assist

Part Name	Function	Failure Mode	Cause	Effect on User	Prevention	Action	Safety Checklist
Arm assist 4-bar mechanism	Support arms	clash preventing motion	bolt head clash clash with seat vertical supports clash with sprocket vertical bars	user cannot move forward	add space where necessary	perform a manual rotation of the 4-bar mechanism to ensure no clash	manually rotate mechanism to ensure no clash
		bars become loose	link connecting bolts not tight	user falls	ensure bolts are tightened	tighten bolts	ensure bolts are tightened on 4 bar linkage
Arm assist support bars	support the motion of 4 bar linkage	bars bend	excessive force on frame	user motion changes	add brackets for stability	add brackets for stability ensure all bolts are tightened	visual check to ensure bars are straight
Arm assist sprockets and chain	rotate chain for arm assist	sprockets are prevented from rotation	clash with side bars tangling of wires from limit switches interference in rotational workspace	user cannot move forward	ensure the workspace is clear and that the sprocket has clearance from the vertical support bars	perform a manual rotation of the 4-bar mechanism to ensure no clash	perform a visual check and ensure there is nothing that will interfere with chain and sprocket, ensure that limit switch cables are all out of the way
		Chain slip	chain is not properly tensioned	user falls	ensure chain is tight	pull shaft plate back and tighten bolts so that chain is tight tighten set screws on all sprockets	check that shaft plate bolts are tightened and pull chain. If chain can be easily pulled one inch it is tight
Arm assist sprocket mount	supports the arm assist as it moves up	if the bearings are not aligned the sprocket will clash with the side support bar	improper alignment	user cannot move forward	ensure bearings are aligned	tighten bearing bolts and check for alignment	make sure bearing bolts are tight and aligned Also ensure left and right side are at same height

Driving Mechanism

Part Name	Function	Failure Mode	Cause	Effect on User	Prevention	Action	Safety Checklist
Set screw couple from motor	couples motor to driving mechanism	keyway failure	excessive load	user falls or doesn't move	ensure coupling set screw is tight and that motor is bolted to plate properly	ensure motor is bolted to plate tightly ensure coupling set screw is tight	ensure motor is bolted to plate tightly ensure coupling set screw is tight
Drive Pulley	rotates buttocks and waist assist	rope slip from pulley	pulley is not centered	user will not be lifted	ensure that pulley is centered	align pulley and tighten set screw	ensure pulley is centered and ensure set screw is tight
Drive sprocket	rotates arm assist	chain slip	motor plate and shaft plate are not spaced far enough misalignment between two sprockets	user will not be lifted	use spacer bars align sprockets	ensure spacer bars are in place and sprockets are aligned and tightend with set screw	ensure spacer bars are in place and all plates are tightly mounted onto frame
Waist assist inteface pulley	redirects waist assist pulley motion	rope slip from pulley	rope is not tensioned underneath pulley pulley is not centered	user will not be lifted properly	use a bar underneath to capture the rope	make sure pulley screws are tight and make sure spacer bar is in place	ensure spacer bar is in place and do a visual inspection while the rope is tensioned

Electrical

Part Name	Function	Failure Mode	Cause	Effect on User	Prevention	Action	Safety Checklist
Limit switches	prevents overrotation of mechanism	Switch does not work	loose electrical connection	may potentially exceed motion limit	tighten connections	check all electrical connections	visual inspection of contact connections
			wires are not plugged in		visual check	check all electrical connections	check labview GUI to see that switches lights are turning on as the switch is hit
			loose mechanical connection		tighten screws	tighten mechanical contacts and make sure there is no chance for rotation	ensure that limit switch is on tight
			poor mechanical contact		ensure good contact surface	contact a consistent surface, e.g. plate surface instead of small screw surface	manual rotate assists and ensure that limit switches are being hit
Emergency stop	stops motor drive	switch does not work	connection to inhibit loosened	motor will not stop	check to ensure inhibit is in and that connection is tight	use stranded wire for E-stop and ensure tight connection	push e-stop and ensure red light comes on in the amp
Reset switch	resets assist to initial position	switch does not work	loose electrical connection	motor will not reset	ensure good electrical connections	ensure good electrical connections	do trial run with reset switch
Deadman switch	Go switch	switch does not work	loose electrical connection	user cannot control motor motion	ensure good electrical connections	ensure good electrical connections	do trial run with deadman switch

User failure

location	failure	action	safety checklist	Task
Testbed workspace	user hits the waist assist bar	waist assist locking mechanism	ensure waist assist bar is locked in the vertical position at all times that the waist assist is not in use	make locking mechanism
	user trips up on floor	ensure floor level using boards which are at even heights		cut 1/2" boards size of force plate
Entry into testbed	user falls as they get into testbed	grab bar for testbed entry		mount grab bar
	User hits sharp corner from arm assist bar or bolts	cover angles using pipe insulation and cover bolt ends cap ends of structural framing		cover all sharp corners
Sitting on chair	user falls as they try to sit into testbed chair	grab bar to hold as user sits down		design grab bar location and mount
Deadman switch	switch gets caught as user rises	make sure cable is in a space that is free from tangle with assist motion	check the deadman switch cable so that it doesn't clash before the user operates it	
buttocks assist	user falls forward from buttocks assist	add a board in front of assist with padding so that the user doesn't fall through testbed testbed entry handle can also be grabbed		install board and add foam padding to plywood board
	user falls sidewas from buttocks assist and grabs arm assist linkage	Ensure arm assist mechanism is locked Cover sharp edges of arm assist mechanism Make sure that the side grab bars are accessible cover chain on the inside		cover edges of arm mechanism design locking mechanism for arm assist Use wood to cover the inside of the chain to prevent access
	user falls backwards from buttocks assist	install a back board to the assist so that the user doesn't fall into the driving chain		design a back board behind the user
	User gets pinched by the rotation of the buttocks assist	cover pinch points		cover pinch points
	User gets caught in the buttocks assist rope	rope cover		rope cover
	User gets caught in the buttocks assist limit switch	move the limit switches away so that they don't contact the user		move the limit switches away so that they don't contact the user
Waist assist	Rope gets caught in arm assist mechanism	minimize snag points		
	Falling failures are same as buttocks assist			
Arm assist	user falls while arm assist is moving and gets hand caught in a pinch point	cover all pinch points		

Appendix E: Test Bed Safety Checklist

1. Ensure E-stop is on
2. Visual check of drive pulley to make sure the cable attached to the pulley is fastened and not frayed in any way.
3. Visual check of pulley cable travel range to make sure that there is nothing in the way that will snag
4. Visual check to ensure that buttocks cable is in pulley
5. Visual check of waist assist cable and buttocks assist cable fastening points
6. Visual check of limit switches
 - a. Ensure that switches are activated when the assist reaches end of motion
 - b. Ensure that switches are working by looking at LabVIEW and seeing that light comes on
 - c. Ensure that the switch is physically not loose
 - d. Ensure that the cables to the switch are not loose
7. Check the E-stop switches
8. Ensure buttocks and waist assist and arm assist frame bars are all level
9. Ensure the buttocks assist seat is tightly attached to the rail
10. Ensure that the load cells remain calibrated properly
11. Ensure that the arm assist rotation chains are tight
12. Ensure that the upper sprockets are not interfering with the side walls
13. Ensure that starting position of buttocks seat is at zero degrees and that limit switch is depressed
14. Ensure that starting position of waist assist does not have complete weight on the limit switch but on the rest bar
15. Make sure load cells are turned on
16. Run the find reverse limit and find forward limit switch in labview for each assist to set the assist start and finish encoder counts
17. Complete one trial run including reset for all the assists

Appendix G: Post-Experiment Questionnaire

**Please answer the following questions about the experiment.
The comment sections are optional.**

1. I felt stable while rising using this assist

	Disagree	Somewhat Disagree	Somewhat Agree	Agree	Comments
Grab Bar Assist	1	2	3	4	_____
Seat Assist	1	2	3	4	_____
Waist Assist	1	2	3	4	_____
Arm Assist	1	2	3	4	_____

2. I was confident that I would not fall while rising using this assist

	Disagree	Somewhat Disagree	Somewhat Agree	Agree	Comments
Grab Bar Assist	1	2	3	4	_____
Seat Assist	1	2	3	4	_____
Waist Assist	1	2	3	4	_____
Arm Assist	1	2	3	4	_____

3. I was able to rise with this assist using the same motion as used during the unassisted rise

	Disagree	Somewhat Disagree	Somewhat Agree	Agree	Comments
Grab Bar Assist	1	2	3	4	_____
Seat Assist	1	2	3	4	_____
Waist Assist	1	2	3	4	_____
Arm Assist	1	2	3	4	_____

4. I was able to rise smoothly with this assist

	Disagree	Somewhat Disagree	Somewhat Agree	Agree	Comments
Grab Bar Assist	1	2	3	4	_____
Seat Assist	1	2	3	4	_____
Waist Assist	1	2	3	4	_____
Arm Assist	1	2	3	4	_____

5. I felt comfortable in terms of forces placed on my body while rising using this assist

	Disagree	Somewhat Disagree	Somewhat Agree	Agree	Comments
Grab Bar Assist	1	2	3	4	_____
Seat Assist	1	2	3	4	_____
Waist Assist	1	2	3	4	_____
Arm Assist	1	2	3	4	_____

6. I was able to rise with this assist using less effort than the effort required to rise unassisted

	Disagree	Somewhat Disagree	Somewhat Agree	Agree	Comments
Grab Bar Assist	1	2	3	4	_____
Seat Assist	1	2	3	4	_____
Waist Assist	1	2	3	4	_____
Arm Assist	1	2	3	4	_____

Appendix H: Experiment Script

Safety Protocol Instructions:

We are doing four different types of assists which I will describe to you. There is an E-stop switch which you can push at any time during the assisted motion, but you will be in control of the motion of the test bed with a push button switch.

We have a grab bar to help you get in and out of the test bed and also to assist you sitting down. You can also use the side rails when you sit back down.

We will have to switch to different assists. When we do so, please keep your hands on your lap, or in front of you.

Experiment Instructions:

Initial Instructions:

We want you to have your feet shoulder width apart, back straight at the beginning, looking forward at the X target with your hands crossed on your lap. When I ask you to rise, please stand to an erect position and remain standing as still as possible until I indicate that you can sit back down.

We want you to have your heel against the pads and your seat lined up with the tape for each rise.

We are going to do a three phase standing procedure. When I say ready you say yes. When I say go you stand. When I say you may be seated please sit. When you sit you can use the bar or sides to help you sit back down.

We will be doing 5-7 trials of each assist

Unassisted STS:

Make sure when you rise your heels are back and your seat is lined up.

Sit with your hands crossed on your lap

I will demonstrate an MT strategy which consists of a continuous transition of forward to upward motion.

Stand up to an **erect position** and remain standing still until I indicate you may sit down.

Bar STS:

Start with your hands on your lap, lean forward and grab the assist bar and use it to stabilize you as you rise. Don't use the grab bar to pull you up, just to stabilize you.

Seat Assist:

First you need to learn the motion of the seat assist. Push the deadman switch, lean forward and as you lean forward the assist will help you rise. Please allow the force of the assist to guide your motion. The assist will stop helping you about half way up at which point you should continue to rise until you are standing still

When you push the switch the assist will move forward. Please let go of the switch at the end of the motion. Put your arms on your lap and push the deadman switch. At the end of the rise release the switch.

Try to maintain contact with the seat as you rise, i.e. don't rise faster than the seat. If you feel the seat slowing down then put more effort.

When we indicate that you may sit please sit down using the grab bar and side rails for help.

Waist Assist:

First you need to learn the motion of the waist assist. Lean forward, push the deadman switch, and the assist will help you rise. Please allow the force of the assist to guide your motion. The assist will stop helping you about $\frac{3}{4}$ of the way up at which point you should continue to rise until you are standing still

When you push the switch the assist will move forward. Please let go of the switch at the end of the motion. Put your arms on your lap and push the deadman switch. At the end of the rise release the switch.

Try to maintain contact with the assist as you rise, i.e. don't rise faster than the assist. If you feel the assist slowing down then put more effort.

When we indicate that you may sit please sit down using the grab bar and side rails for help.

Arm Assist:

We first need to set three things, start position, end position, and rise speed.

The purpose of this assist is to guide your motion as you stand up. Please don't lean on the assist, but rather use the assist to guide your upper body as you rise. When you push the switch it will go up.

Try to keep your arms in the same position beside your torso and move your whole upper body with the assist at the start

When you push the switch the assist will move forward. Please let go of the switch at the end of the motion.

When we indicate that we are going to lower the assist mechanism, please take your hands out of the cradle and put them on the grab bar.

When we indicate that you may sit please sit down using the grab bar and side rails for help.

Appendix I: Experiment Checklist

	Tasks in LabVIEW
	Spreadsheet Tasks
Pre subject arrival tasks	
Print off subject consent form and pre and post questionnaires and experiment log (Write assist order in log)	
Ensure that all the documents are identified by subject number	
Put a sticky note on the side of test bed with the subject number	
Conduct the “Test Bed Safety Checklist”	
Do a run of the test bed in the test mode (for all 3 assists)	
Set up test bed to the first assist mode	
Load cell calibration check	
Ensure Xsens is untangled	
Cut tape for thigh	
Set up video camera	
Second digital camera for pictures (check battery)	
make sure we have access for Xsens and moog (double check that the Xsens is working properly)	
make sure all our measuring supplies are present (tape, rulers, alan keys etc)	
make sure previous trial data are saved/backed up and cleaned from desktop	
Set up a computer folder with the spreadsheet with subject number and date	
Turn on Xsens	
Open XsensRecordDec10PXITransfer file & SitToStandDec 14-Addition from Eric file (LabVIEW 8.5)	
Enter the subject number in the LabVIEW Xsens Program	
check Xsens for drift on Windows VI	
Perform initial orientation grab	

Subject Setup Tasks

Lead Tasks	Assistant Tasks
Take consent form	
Ask subject to complete pre-experiment questionnaire	
Measure Subject Height & knee height	
Explain Safety features of the Testbed (E-stop, Grab bar, keeping arms in front of you)	Enter Subject height and Knee height into spreadsheet
Explain the different assists of the test bed and that we will be doing 5-7 trials	Put wood on and zero force plate (ENSURE WOOD IS AT THE EDGES OF F.P.)
Explain that we will be asking questions after each set of trials	
Measure Parameters	input into spreadsheet:
Put tape on segment CoM's	
Put the sensors on the person at approximate CoMs	
Ask the subject to stand in the test bed	Grab weight in Windows VI
Ensure HAT sensor fixed and ask the Subject to stand straight while a calibration grab is performed	record heel position in LabVIEW
Ask the subject to sit in the test bed and fix the heel location of the subject.	Enter their weight into spreadsheet
Put tape on thigh in plane with ischial tuberosities, Measure Knee to Ischial Tuberosities	Enter Knee to Ischial Tuberosities into spreadsheet
Adjust the location of the gel pad so that the subject is seated with ankle angle at 108° and with ischial tuberosities on the gel pad.	Verify that the ankle angle is at 108°
Measure the Distance from Gel Cushion center to pivot	Enter the Distance from Gel Cushion center to pivot into spreadsheet
	Enter the subject parameters from Excel Spreadsheet into LabVIEW
	Turn on Video

Switching Assist Tasks

Assistant Tasks	Lead Tasks
Ask questionnaire questions from previous assisted trials	Ask Assistant to attach the assist sensor in the correct place (on arm for bar and arm assists)
Attach the Assist Sensor in the correct place	
Use Velcro to eliminate loose wires	
Take off E-stop	
verify that sensors don't get tangled	
Measure the Heel position and record in log	Check ankle angle 108 and enter in heel position into LabVIEW. If we change the ankle and seat position for bar assist CHANGE IT BACK
Measure the Distance from Gel Cushion Back Edge to pivot and record in log	
Ensure all of the sensors on the subject are in a constant position with the x-axis parallel to the ground. Ensure the y-axis is in the sagittal plane, especially for bicep sensor	Ensure thigh angle is the same as the initial angle for the unassisted calibration trials
	Take the test bed out of Test Mode
During Trial Tasks (5x)	
Make sure heel and seat are lined up	Instruct the subject to stand using the above script.
Make sure sensors are aligned with y-axis in sagittal plane and x-axis parallel to ground	Verify that I am saving the right amount of data (i.e. 8-10 seconds)
Make sure cables will not get tangled	Press start data collecting button
	When the green light comes on, ask user to stand
	Wait till the indicator goes off which tells us that the trial is finished
	Save Data
	Instruct Tom to Reset System
Ask the subject to put their hands on the safety bar before resetting system	Ask the subject to sit down

Bar assist:

Attach the Assist sensor on the bicep of user	
Ask user to adjust sitting position such that when arms are fully extended they are holding the bar	Move cushion and heel position
Measure the Distance from Gel Cushion Back Edge to pivot and record in log	Check ankle angle 108 and then enter in heel position into LabVIEW
Measure the Heel position and record in log	

Seat assist:

Turn on E-stop	
Ask User to Stand	
Take off the arm cradles and connect the deadman cable to the deadman switch	
Lock the waist assist into the vertical position	
Remove the drive chain for arm assist from the drive and follower sprockets	
Ensure spacer bars are in place and that the motor plate is tight on side rails	
Disconnect the cable from the waist assist and connect it to the seat assist and move the waist assist cable out of the way	
Set the limit control switch to seat assist	Set the switch to seat assist in the LabVIEW Motor Control program
Ask user to sit	Set the switch to seat assist in the LabVIEW Data collection Program
attach assist sensor to seat bar	Ensure that starting position of seat assist is at zero degrees and that limit switch is depressed
	Check to make sure the drive cable is in the pulley.
	Check to make sure the follower cable is in the pulley.

Waist assist:

Turn on E-stop	
Ask User to Stand	
Take off the arm cradles and connect the deadman cable to the deadman switch	
Lock the waist assist into the vertical position	
Remove the drive chain for arm assist from the drive and follower sprockets	
Ensure spacer bars are in place and that the motor plate is tight on side rails	
Disconnect the cable from the seat assist and connect it to the waist assist and move the seat assist cable out of the way	
Check to make sure the drive cable is in the pulley.	
Set the limit control switch to waist assist	Set the switch to waist assist in the LabVIEW Motor Control Program
Sit the person down on the chair	Set the switch to waist assist in the LabVIEW Data collection Program
UNLOCK WAIST ASSIST FROM VERTICAL POSITION and have them attach the waist assist belt	
Attach the waist assist sensor on the left strap	
Adjust the length of the waist assist straps and attach it to the waist of the user. Ask about the tension on the waist straps. We want it taut while the person is sitting down with his back straight.	
Ask user to put their arms outside the waist assist straps	
Input location of waist assist force into Experiment Log	Measure location of waist assist force location and tell Assistant
Jog to end position such that thigh is at 70°	Record end goal and check that thigh is at 70°

Arm assist

E-stop the motor	
Unhook the waist or seat assist cables from the drive cable	
Ensure drive cable is underneath the motor plate	Lock the waist assist into the vertical position
Set the limit control switch to arm assist	Set the switch to arm assist in the LabVIEW Motor Control program
Remove spacer bars	Set the switch to arm assist in the LabVIEW Data collection Program
Attach the chain to the sprocket	
Put spacer bar back in and tighten motor plate bolts	
Put the arm cradles on and adjust so that the user is comfortable (changed location)	Ensure arm assist chains are tight
Make sure that arm cradle lower limit of rotation will not clash with side of seat frame	
Adjust the handle location of arm cradle	
connect the deadman switch	
Attach the assist sensor to the bicep	
	Put test bed in Test mode and inform subject about motor jogging
Jog to start position that is comfortable for user	Record start goal
Jog to end position that is comfortable for user	Record end goal
Ensure that the experiment log parameters have all been filled in	
Copy parameters from log to spreadsheet and ensure all the spreadsheet parameters have been filled in	Ask subject to remove tape and belt
Save the video into Jeswin folder on Mathesula	Give subject parking pass
Type up experiment log	Copy all data into a single folder and save a back up
Type up the pre and post-experiment questionnaires	Put consent form into a locked cabinet
Ensure that all the documents are identified by subject number	Organize the log, pre and post-experiment questionnaires

Appendix J: Static Stability Results and ANOVA

Subject	Xcom_seatoff - Xankle (%Lfoot)				
	Unassisted	Bar	Arm	Waist	Seat
1	-0.24	-0.22	-0.40	0.31	-0.04
2	-0.43	-0.54	-0.58	0.01	-0.27
3 ¹	-0.44	-0.57	-0.44	n/a ¹	-0.34
4	-0.52	-0.55	-0.55	0.10	-0.03
5	-0.45	-0.48	-0.74	-0.11	-0.43
6	-0.45	-0.56	-0.59	-0.18	-0.46
7	-0.58	-1.00	-0.88	0.08	-0.30
8	-0.30	-0.43	-0.52	0.05	-0.15
9	-0.49	-0.62	-0.68	0.02	-0.33
10	-0.34	-0.60	-0.55	0.26	-0.32
11	-0.35	-0.32	-0.15	0.14	-0.25
12	-0.42	-0.39	-0.42	0.04	-0.24
13	-0.49	-0.64	-0.51	-0.01	-0.25
14	-0.40	-0.40	-0.36	0.09	-0.19
15	-0.46	-0.63	-0.43	0.00	-0.37
16	-0.62	-0.52	-0.72	-0.02	-0.27
17	-0.27	-0.48	-0.34	0.10	-0.11
Mean	-0.425	-0.523	-0.526	0.054	-0.251

Data for subject 3 is reported here, but not used due to an error in data collection during their waist-assisted STS trials. Thus data is not included in the reported mean at the bottom of the table.

EZAnalyze Results Report - Repeated Measures ANOVA CoM Displacement from Foot Center

Repeated Measures ANOVA Variables

	Unassisted	Bar	Arm	Waist	Seat
N Valid:	16	16	16	16	16
N Missing:	0	0	0	0	0
Mean:	-.425	-.523	-.526	.054	-.251
Std. Dev:	.107	.172	.179	.121	.123

ANOVA Table

Source of Variance	SS	DF	MS	F
Factor A	3.809	4.000	.952	90.162
Factor S	.914	15.000	.061	
A x S	.634	60.000	.011	
Total	5.357	79.000		

	P
Eta Squared	.000
	.857

Case Processing Summary - N removed due to missing data

N Removed	1.000
------------------	-------

The ANOVA results indicate that at least two of the repeated measures differed significantly. Individual measures which differ significantly are highlighted in yellow

Post Hoc tests	Comparison	Mean Difference	T-Value	P - Unadjusted	Sig. Level
Unassisted	Unassisted and Bar	.098	3.011	0.009	0.001
	Unassisted and Arm	.100	3.011	0.009	0.001
	Unassisted and Waist	.479	17.282	0.000	0.001
	Unassisted and Seat	.174	5.454	0.000	0.001
Bar	Bar and Arm	.003	.080	0.937	0.001
	Bar and Waist	.577	12.757	0.000	0.001
	Bar and Seat	.272	6.514	0.000	0.001
Arm	Arm and Waist	.580	13.545	0.000	0.001
	Arm and Seat	.274	6.389	0.000	0.001
Waist	Waist and Seat	.305	12.195	0.000	0.001

Appendix K: Dynamic Stability Results and ANOVA

Subject	Xcop_seatoff - Xfootcenter (%Lfoot)				
	Unassisted	Bar	Arm	Waist	Seat
1	-0.32	-0.29	-0.26	0.16	0.09
2	-0.36	-0.30	-0.39	-0.15	0.00
3 ¹	-0.38	-0.30	-0.34	n/a ¹	-0.32
4	-0.40	-0.33	-0.42	-0.24	0.01
5	-0.34	-0.34	-0.38	-0.29	-0.09
6	-0.16	-0.21	-0.23	-0.35	-0.01
7	-0.40	-0.34	-0.44	-0.02	-0.14
8	-0.37	-0.41	-0.38	0.04	-0.15
9	-0.39	-0.35	-0.43	-0.14	-0.23
10	-0.33	-0.36	-0.38	0.11	-0.12
11	-0.38	-0.27	-0.38	-0.30	-0.26
12	-0.37	-0.37	-0.37	-0.26	-0.13
13	-0.26	-0.29	-0.32	-0.14	-0.05
14	-0.43	-0.40	-0.42	-0.11	-0.28
15	-0.36	-0.33	-0.40	-0.26	-0.25
16	-0.35	-0.18	-0.34	-0.07	0.01
17	-0.21	-0.26	-0.19	0.00	-0.12
Mean	-.339	-.314	-.359	-.125	-.107

Data for subject 3 is reported here, but not used due to an error in data collection during their waist-assisted STS trials. Thus data is not included in the reported mean at the bottom of the table.

EZAnalyze Results Report - Repeated Measures ANOVA CoP Displacement from Foot Center

Repeated Measures ANOVA Variables

	Unassisted	Bar	Arm	Waist	Seat
N Valid:	16	16	16	16	16
N Missing:	0	0	0	0	0
Mean:	-.339	-.314	-.359	-.125	-.107
Std. Dev:	.073	.064	.075	.153	.111

ANOVA Table

Source of Variance	SS	DF	MS	F
Factor A	.959	4.000	.240	30.951
Factor S	.297	15.000	.020	
A x S	.465	60.000	.008	
Total	1.720	79.000		

	P
Eta Squared	.674

Case Processing Summary - N removed due to missing data

N Removed	1.000
------------------	-------

The ANOVA results indicate that at least two of the repeated measures differed significantly. Individual measures which differ significantly are highlighted in yellow

Post Hoc tests	Comparison	Mean Difference	T-Value	P - Unadjusted	Sig. Level
Unassisted	Unassisted and Bar	.025	1.631	0.124	0.001
	Unassisted and Arm	.020	2.213	0.043	0.001
	Unassisted and Waist	.214	4.954	0.000	0.001
	Unassisted and Seat	.232	8.748	0.000	0.001
Bar	Bar and Arm	.045	2.863	0.012	0.001
	Bar and Waist	.189	4.269	0.001	0.001
	Bar and Seat	.207	8.655	0.000	0.001
Arm	Arm and Waist	.233	5.829	0.000	0.001
	Arm and Seat	.252	10.011	0.000	0.001
Waist	Waist and Seat	.018	0.436	0.669	0.001

Appendix L: STS Knee Extensor Effort Results and ANOVA

Subject	Peak Knee Torque (Nm/(BodyWeight*BodyHeight))				
	Unassisted	Bar	Arm	Waist	Seat
1	0.98	0.97	0.90	0.51	0.69
2	1.44	1.22	1.42	0.88	0.91
3 ¹	1.62	1.55	1.33	n/a ¹	1.49
4	1.21	1.07	1.27	0.77	0.77
5	1.29	1.25	1.25	1.12	0.98
6	1.19	1.27	1.24	0.99	0.96
7	1.60	1.16	1.65	1.17	1.25
8	1.90	1.55	1.21	1.17	1.28
9	1.60	1.32	1.67	1.38	1.42
10	1.48	1.32	1.27	0.86	1.29
11	1.42	1.21	1.29	1.32	1.35
12	1.66	1.57	1.52	1.22	1.19
13	1.28	1.19	1.12	1.11	1.37
14	1.37	1.37	1.52	1.14	1.31
15	1.31	1.30	1.30	1.29	1.26
16	1.26	1.10	1.15	1.14	1.02
17	1.25	1.18	1.25	1.02	1.04
Mean	1.39	1.25	1.31	1.07	1.13

Data for subject 3 is reported here, but not used due to an error in data collection during their waist-assisted STS trials. Thus data is not included in the reported mean at the bottom of the table.

EZAnalyze Results Report - Repeated Measures ANOVA Peak Knee Torque

Repeated Measures ANOVA Variables

	Unassisted	Bar	Arm	Waist	Seat
N Valid:	16	16	16	16	16
N Missing:	0	0	0	0	0
Mean:	1.390	1.254	1.315	1.067	1.131
Std. Dev:	.222	.157	.201	.225	.223

ANOVA Table

Source of Variance	SS	DF	MS	F
Factor A	1.115	4.000	.279	16.041
Factor S	2.183	15.000	.146	
A x S	1.043	60.000	.017	
Total	4.342	79.000		
	P	.000		
	Eta Squared	.517		

Case Processing Summary - N removed due to missing data

N Removed	1.000
------------------	-------

*The ANOVA results indicate that at least two of the repeated measures differed significantly
Individual measures which differ significantly are highlighted in yellow*

Post Hoc tests	Comparison	Mean Difference	T-Value	P - Unadjusted	Sig. Level
Unassisted	Unassisted and Bar	.136	3.945	.001	0.001
	Unassisted and Arm	.075	1.554	.141	0.001
	Unassisted and Waist	.323	6.210	.000	0.001
	Unassisted and Seat	.259	5.454	.000	0.001
Bar	Bar and Arm	.061	1.261	.226	0.001
	Bar and Waist	.187	3.888	.001	0.001
	Bar and Seat	.123	2.667	.018	0.001
Arm	Arm and Waist	.248	5.065	.000	0.001
	Arm and Seat	.184	3.475	.003	0.001
Waist	Waist and Seat	.064	1.782	.095	0.001

Appendix M: STS Torque Ratio Results and Paired T-Tests

Subject	Ratio Margin (Mean Knee Torque Ratio -35%)			
	Bar	Arm	Waist	Seat
1	0.65	0.57	0.17	0.36
2	0.50	0.64	0.26	0.29
3	0.96	0.82	n/a ¹	0.91
4	0.53	0.70	0.28	0.28
5	0.62	0.62	0.52	0.41
6	0.72	0.69	0.48	0.46
7	0.38	0.68	0.38	0.43
8	0.47	0.28	0.27	0.32
9	0.47	0.70	0.51	0.54
10	0.54	0.50	0.23	0.52
11	0.50	0.56	0.58	0.60
12	0.60	0.57	0.38	0.37
13	0.58	0.53	0.52	0.72
14	0.65	0.76	0.48	0.60
15	0.64	0.65	0.63	0.61
16	0.52	0.56	0.56	0.46
17	0.59	0.65	0.47	0.48
Mean	0.56	0.60	0.42	0.47

EZAnalyze Results Report - One Sample T-Test with Numeric Test value of Zero

	Bar	Test Value	Arm	Test Value	Waist	Test Value	Buttocs	Test Value
N Valid:	16		16		16		16	
N Missing:	1		1		1		1	
Mean:	.560	0	.604	0	.420	0	.466	0
Std. Dev:	.086		.111		.141		.127	
Mean Diff:	.560		.604		.420		.466	
T-Score:	25.978		21.743		11.93		14.670	
Eta Squared:	.978		.969		.905		.935	
P:	.000		.000		.000		.000	

The difference between the observed mean and the Numeric Test Value is significant in all cases

Appendix N: Momentum Transfer Results and ANOVA

Subject	Peak Trunk Flexion (degrees)				
	Unassisted	Bar	Arm	Waist	Seat
1	28.6	21.9	23.7	5.1	10.0
2	43.9	28.5	21.1	6.5	23.5
3 ¹	37.4	14.3	24.8	n/a ¹	17.3
4	34.2	24.8	28.6	5.2	23.2
5	37.4	31.4	21.2	10.0	18.1
6	41.5	23.8	36.9	17.0	24.5
7	30.5	17.3	11.0	10.3	9.8
8	28.0	25.2	8.6	3.2	11.1
9	35.8	16.5	18.6	14.1	22.5
10	45.3	13.6	24.2	6.9	20.5
11	45.6	29.7	38.3	12.0	25.6
12	31.5	23.3	29.9	8.1	17.6
13	27.6	11.0	27.4	5.1	13.7
14	36.5	22.2	27.7	4.2	24.1
15	45.9	21.1	26.3	12.0	21.3
16	40.5	24.9	22.9	9.2	19.4
17	43.2	19.8	25.5	12.6	24.0
Mean	37.25	22.18	24.49	8.83	19.30

¹Data for subject 3 is reported here, but not used due to an error in data collection during their waist-assisted STS trials. Thus data is not included in the reported mean at the bottom of the table.

EZAnalyze Results Report - Repeated Measures ANOVA Peak Trunk Flexion

Repeated Measures ANOVA Variables

	Unassisted	Bar	Arm	Waist	Seat
N Valid:	16	16	16	16	16
N Missing:	0	0	0	0	0
Mean:	37.253	22.184	24.490	8.834	19.301
Std. Dev:	6.647	5.602	7.791	3.967	5.422

ANOVA Table

Source of Variance	SS	DF	MS	F
Factor A	6698.462	4.000	1674.616	74.091
Factor S	1364.908	15.000	90.994	
A x S	1356.136	60.000	22.602	
Total	9419.506	79.000		
	P	.000		
	Eta Squared	.832		

Case Processing Summary - N removed due to missing data

N Removed	1.000
------------------	-------

The ANOVA results indicate that at least two of the repeated measures differed significantly. Individual measures which differ significantly are highlighted in yellow.

Post Hoc tests	Comparison	Mean Difference	T-Value	P - Unadjusted	Sig. Level
Unassisted	Unassisted and Bar	15.069	7.986	0.000	0.001
	Unassisted and Arm	12.762	6.619	0.000	0.001
	Unassisted and Waist	28.419	19.811	0.000	0.001
	Unassisted and Seat	17.952	17.348	0.000	0.001
Bar	Bar and Arm	2.306	1.043	0.314	0.001
	Bar and Waist	13.350	7.962	0.000	0.001
	Bar and Seat	2.883	1.736	0.103	0.001
Arm	Arm and Waist	15.656	8.388	0.000	0.001
	Arm and Seat	5.189	3.445	0.004	0.001
Waist	Waist and Seat	10.467	8.191	0.000	0.001

Appendix O: Pre-Experiment Questionnaire Results

Subject Number	How old are you?	What is your gender?	Have you been diagnosed with any known musculoskeletal or neuromuscular conditions which limit your mobility?	Do you have difficulty rising unassisted from a chair?	If so, can you identify these difficulties?	Do you use an assistive device to help you with rising from a chair or bed?	If so, what device?
1	65	M	No	No	-	No	-
2	76	M	No	No	-	No	-
3	78	F	No	No	-	No	-
4	65	M	No	No	-	No	-
5	73	M	No	No	-	No	-
6	73	M	Yes (Cartilage out of right knee)	No	-	No	-
7	84	M	No	No	-	No	-
8	77	M	No	No	-	No	-
9	70	M	No	No	-	No	-
10	69	M	No	No	-	No	-
11	70	M	No	No	-	No	-
12	80	M	No	No	-	No	-
13	69	F	No	No	-	No	-
14	66	F	No	No	-	No	-
15	68	F	No	No	-	No	-
16	63	F	No	No	-	No	-
17	69	F	Yes (stiffness, arthritis, muscle weakness)	No	-	No	-

Appendix P: Post-Experiment Questionnaire Results and Statistical Tests

Question	Subject	Grab Bar Assist	Arm Assist	Waist Assist	Seat Assist
I felt stable when using this assist	1	3	2	2	4
	2	4	4	4	4
	3 ¹	4	4	4	4
	4	4	3	4	4
	5	4	4	4	4
	6	4	4	4	4
	7	4	4	4	4
	8	4	3	4	4
	9	4	3	3	3
	10	4	4	4	4
	11	4	4	4	4
	12	3	4	3	4
	13	4	3	3	4
	14	3	4	4	4
	15	4	4	2	4
	16	4	4	2	4
	17	4	4	3	4
I was confident that I would not fall while rising using this assist	1	4	2	3	4
	2	4	4	4	4
	3 ¹	4	4	4	4
	4	4	4	4	4
	5	4	4	4	4
	6	4	4	4	4
	7	4	4	4	4
	8	4	4	4	4
	9	4	3	4	3
	10	4	4	4	4
	11	4	4	4	4
	12	4	4	4	4
	13	4	4	4	4
	14	4	4	4	4
	15	4	4	4	4
	16	4	4	3	4
	17	4	3	4	4
I was able to rise with this assist using the same motion as used during the unassisted rise	1	3	2	2	4
	2	4	3	3	4
	3 ¹	4	4	4	4
	4	4	2	3	4
	5	4	4	4	4
	6	4	4	3	4
	7	4	3	4	4
	8	4	1	1	4
	9	4	4	2	4
	10	4	4	4	4
	11	4	4	1	4
	12	4	3	3	4
	13	4	2	2	2
	14	3	4	3	4
	15	4	3	2	4
	16	3	3	2	4
	17	4	4	4	4

Question	Subject	Grab Bar Assist	Arm Assist	Waist Assist	Seat Assist
I was able to rise smoothly with this assist	1	3	2	2	4
	2	4	3	4	4
	3 ¹	4	4	4	4
	4	4	3	3	3
	5	4	4	4	4
	6	4	4	4	4
	7	4	3	4	4
	8	4	1	4	4
	9	4	2	3	3
	10	4	4	4	4
	11	4	4	3	4
	12	4	4	3	4
	13	4	3	2	4
	14	3	3	4	4
	15	4	1	3	4
	16	4	4	2	4
	17	4	4	4	4
I felt comfortable in terms of forces placed on my body while rising using this assist	1	3	3	3	4
	2	4	4	4	4
	3 ¹	4	4	4	4
	4	4	2	3	4
	5	4	4	4	4
	6	4	4	4	4
	7	4	4	4	4
	8	4	2	4	4
	9	4	3	3	3
	10	4	4	4	4
	11	4	4	4	4
	12	4	4	4	4
	13	4	4	4	4
	14	4	4	4	4
	15	4	4	3	4
	16	3	4	1	4
	17	3	4	4	4
I was able to rise with this assist using less effort than the effort required to rise unassisted	1	3	2	3	4
	2	4	4	4	4
	3 ¹	3	2	4	4
	4	2	1	4	4
	5	3	4	4	4
	6	4	3	4	4
	7	4	3	4	4
	8	4	1	4	4
	9	3	2	3	4
	10	4	4	4	4
	11	3	4	4	4
	12	3	4	3	4
	13	2	2	4	4
	14	2	2	4	4
	15	3	4	2	4
	16	2	4	1	4
	17	4	3	4	4
Mean		3.74	3.35	3.39	3.93

¹Data for subject 3 is reported here, but not used due to an error in data collection during their waist-assisted STS trials. Thus data is not included in the reported mean at the bottom of the table.

Statistical Package for the Social Sciences Version 8 (SPSS) **Friedman and Wilcoxon Sign Ranks tests**

Descriptive Statistics								
	N	Mean	Std. Deviation	Minimum	Maximum	Percentiles		
						25th	50th (Median)	75th
Bar	96	3.7396	.52805	2.00	4.00	4.0000	4.0000	4.0000
Arm	96	3.3542	.90588	1.00	4.00	3.0000	4.0000	4.0000
Waist	96	3.3854	.86292	1.00	4.00	3.0000	4.0000	4.0000
Seat	96	3.9271	.29894	2.00	4.00	4.0000	4.0000	4.0000

Friedman Test

Ranks	
	Mean Rank
Bar	2.68
Arm	2.18
Waist	2.22
Seat	2.93

Test Statistics ^a	
N	96
Chi-square	50.716
df	3
Asymp. Sig.	.000

a. Friedman Test

There was a statistically significant difference between the four assists in terms of subject preference, $\chi^2(3) = 50.72, P = 0.000$

Wilcoxon Signed Ranks Test

		Ranks		
		N	Mean Rank	Sum of Ranks
Arm - Bar	Negative Ranks	34 ^a	23.53	800
	Positive Ranks	10 ^b	19	190
	Ties	52 ^c		
	Total	96		
Waist - Bar	Negative Ranks	33 ^d	20.8	686.5
	Positive Ranks	8 ^e	21.81	174.5
	Ties	55 ^f		
	Total	96		
Seat - Bar	Negative Ranks	6 ^g	13.75	82.5
	Positive Ranks	21 ^h	14.07	295.5
	Ties	69 ⁱ		
	Total	96		
Waist - Arm	Negative Ranks	20 ^j	23.73	474.5
	Positive Ranks	24 ^k	21.48	515.5
	Ties	52 ^l		
	Total	96		
Seat - Arm	Negative Ranks	0 ^m	0	0
	Positive Ranks	34 ⁿ	17.5	595
	Ties	62 ^o		
	Total	96		
Seat - Waist	Negative Ranks	1 ^p	10.5	10.5
	Positive Ranks	34 ^q	18.22	619.5
	Ties	61 ^r		
	Total	96		

- a. Arm < Bar
- b. Arm > Bar
- c. Arm = Bar
- d. Waist < Bar
- e. Waist > Bar
- f. Waist = Bar
- g. Seat < Bar
- h. Seat > Bar
- i. Seat = Bar
- j. Waist < Arm
- k. Waist > Arm
- l. Waist = Arm
- m. Seat < Arm
- n. Seat > Arm
- o. Seat = Arm
- p. Seat < Waist
- q. Seat > Waist
- r. Seat = Waist

Test Statistics^c (statistically significant results highlighted in yellow)

	Arm - Bar	Waist - Bar	Seat - Bar	Waist - Arm	Seat - Arm	Seat - Waist
Z	-3.758 ^a	-3.461 ^a	-2.742 ^b	-.248 ^b	-5.202 ^b	-5.123 ^b
Asymp. Sig. (2-tailed)	.000	.001	.006	.804	.000	.000

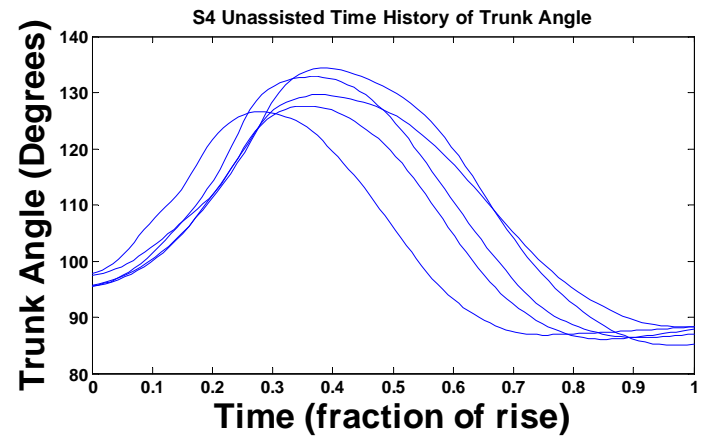
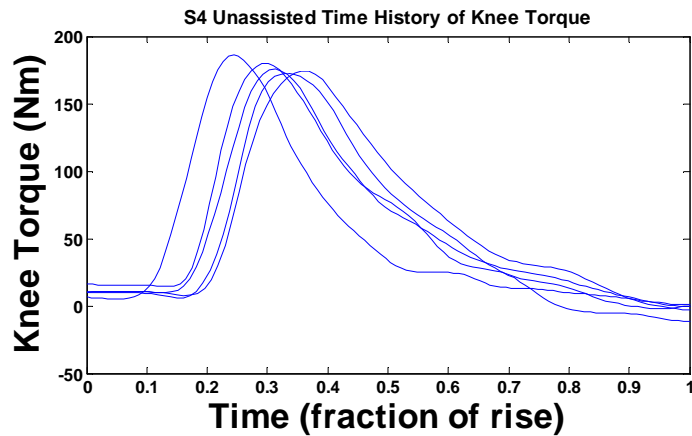
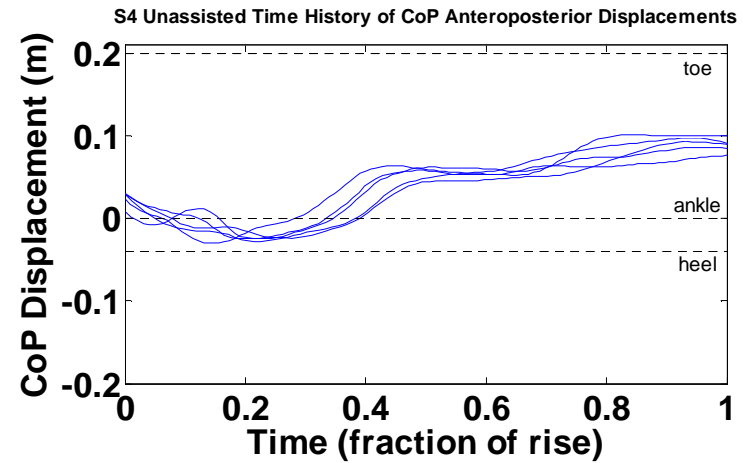
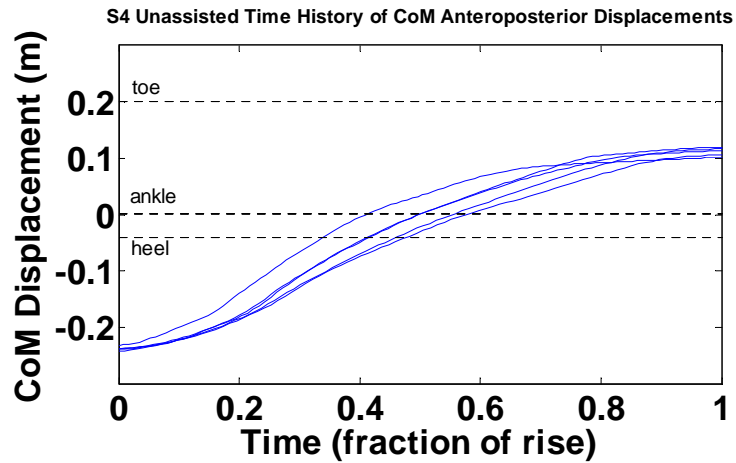
- a. Based on positive ranks.
- b. Based on negative ranks.
- c. Wilcoxon Signed Ranks Test

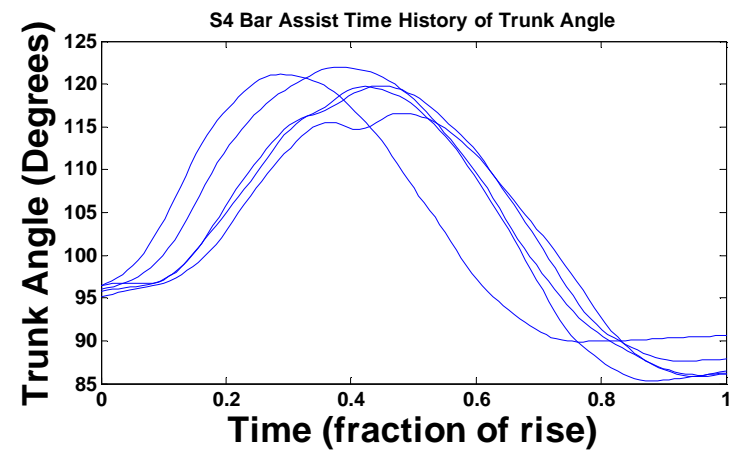
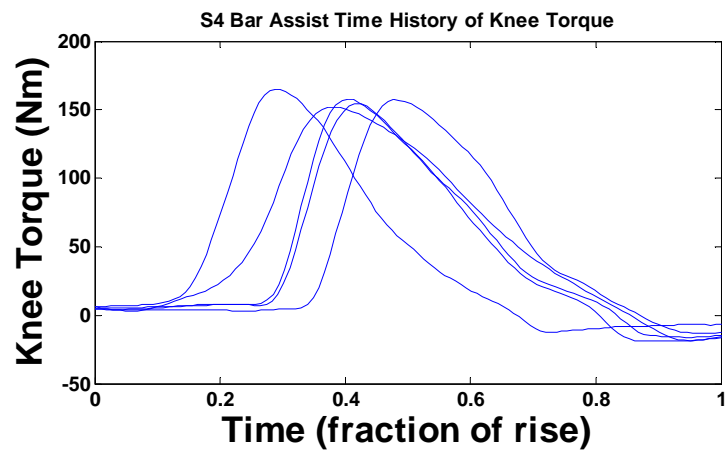
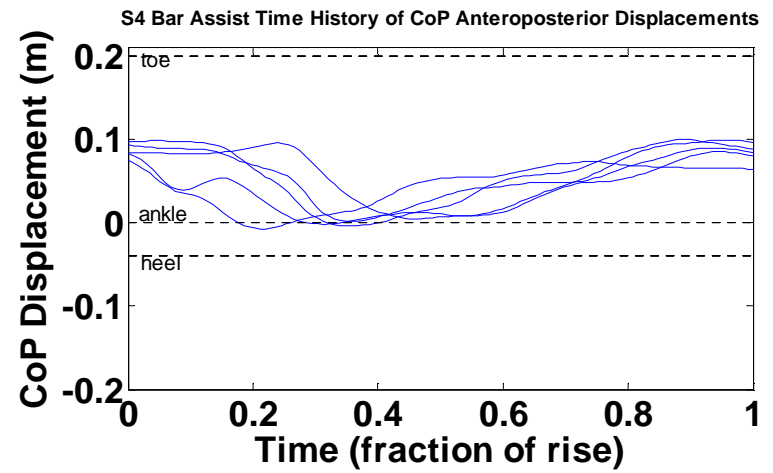
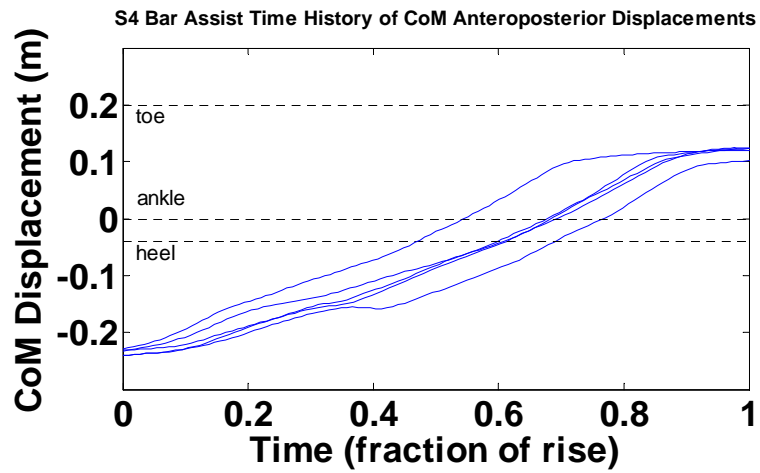
Appendix Q: Post-Experiment Questionnaire Comments

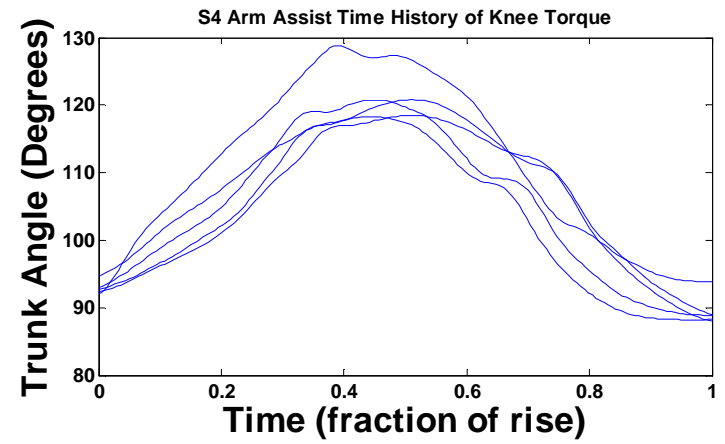
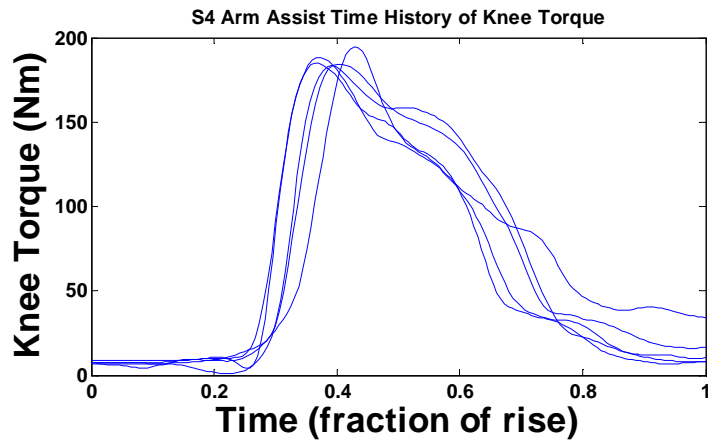
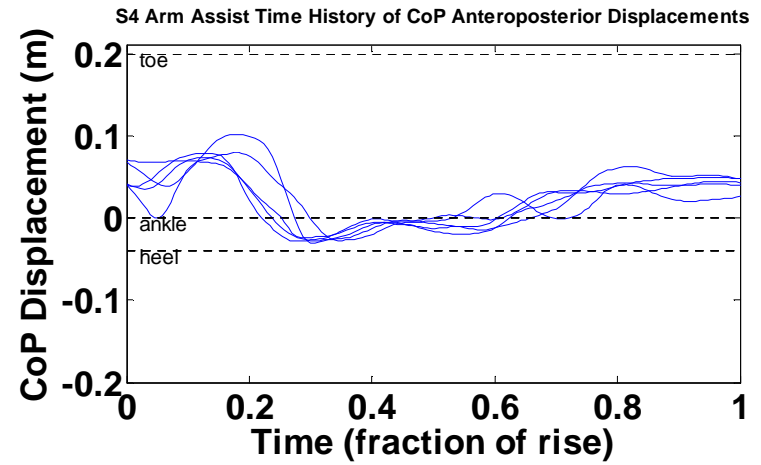
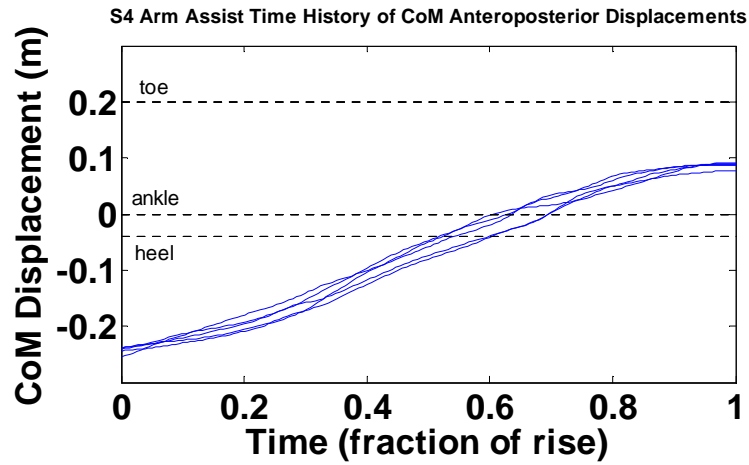
I felt stable when using this assist				I was confident that I would not fall while rising using this assist				I was able to rise with this assist using the same motion as during the unassisted rise			
Bar	Seat	Waist	Arm	Bar	Seat	Waist	Arm	Bar	Seat	Waist	Arm
felt good	after the first try		the arm rests could tip back too easily						used leg muscles slightly less than when unassisted	less effort - slightly different motion	not quite same motion
	I felt this was for my balance and my legs did the lifting		for the trials where I rose smoothly*						more "help" given with this smoother rhythm	less use of leg muscles than unassisted	I used my leg muscles more than in normal unassisted rising
			didn't feel "natural"							I tried to rely on the assist	spread arms a little
			movement of arm assist seemed slow							I felt I was jerking while standing up	

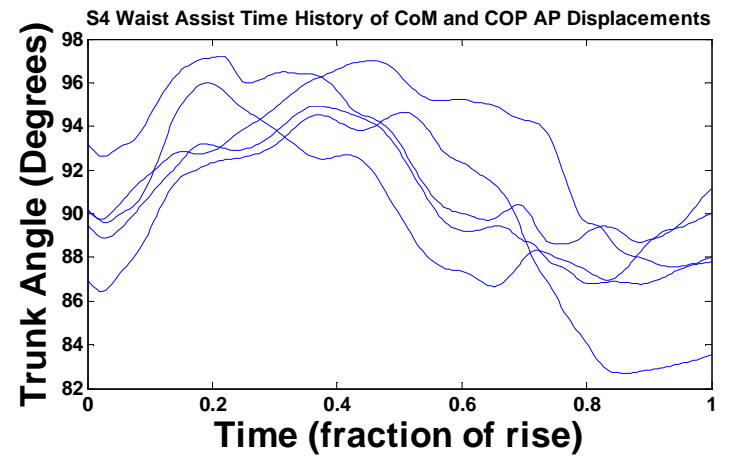
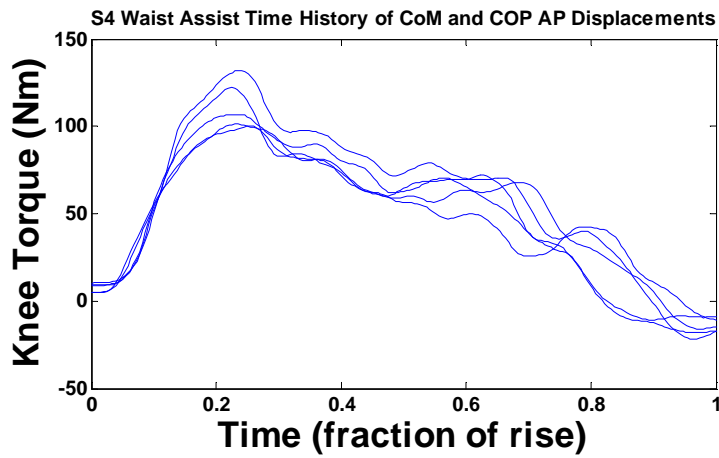
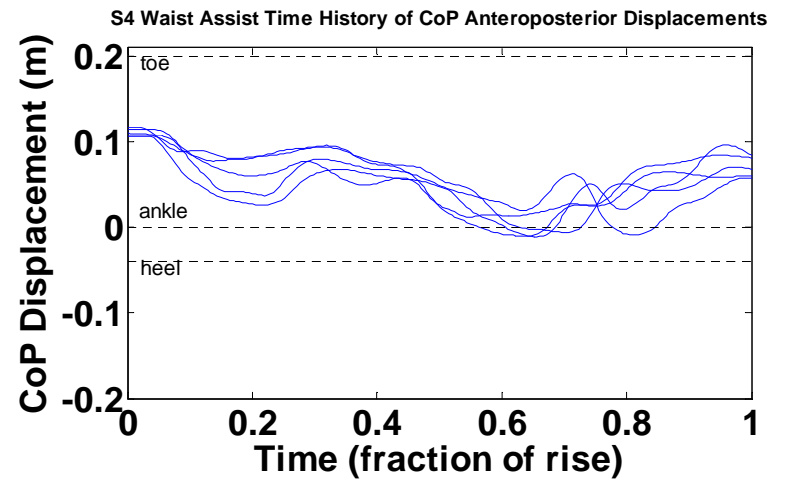
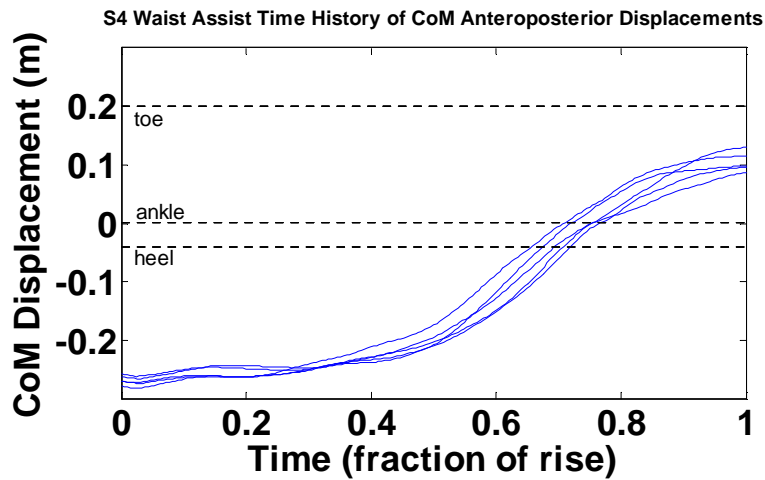
I was able to rise smoothly during this assist				I felt comfortable in terms of forces placed on my body while rising using this assist				I was able to rise with this assist using less effort than the effort required to rise unassisted			
Bar	Seat	Waist	Arm	Bar	Seat	Waist	Arm	Bar	Seat	Waist	Arm
	but a bit too fast	too fast	not quite as smooth	my knees hurt		my knees hurt	didn't feel natural	effort the same			no force from assist
		waiting for the initial help was a little destabilizing	at first not so smoothly	Did not feel an "assist" to lift other than a stabiliser			Did not feel a FORCE; mostly guidance for the motion	took about the same effort as unassisted			I was a little uncomfortable I think I could adjust
		felt unstable	Took a bit of practice!					It was a bit easier because of the balance the bar offered			I used my leg muscles more than in normal unassisted rising

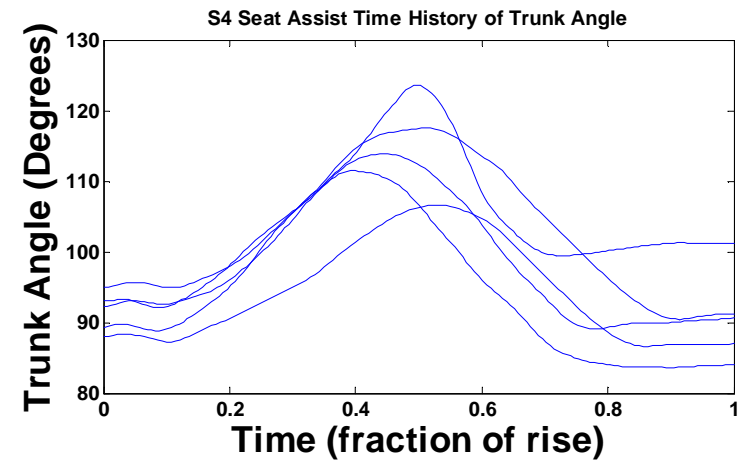
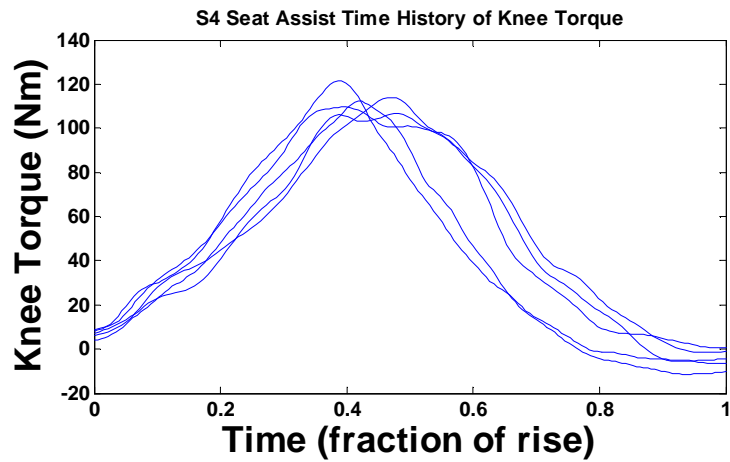
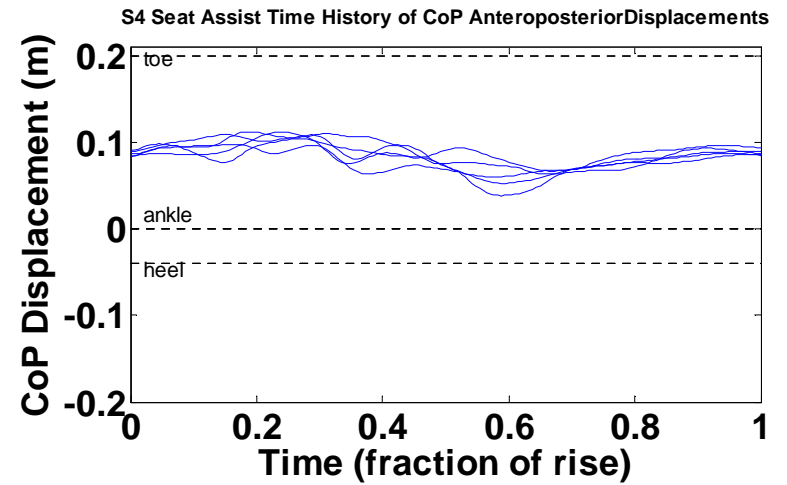
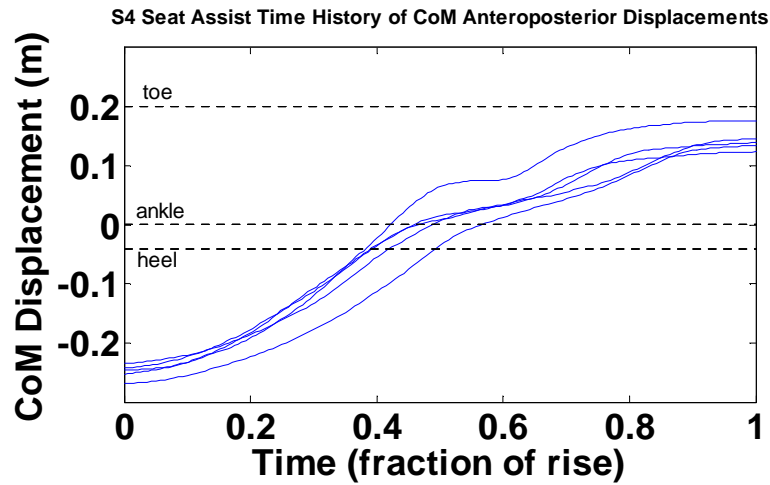
Appendix R: Single Subject (Subject 4) Multiple Trial Data Plots











Appendix S: Multiple Subjects (16 Subjects) Single Trial Data Plots

